PHD

Experimental and finite element analysis of cricket bats

Fisher, Sam

Award date:
2005

Awarding institution:
University of Bath

EXPERIMENTAL AND FINITE ELEMENT ANALYSIS OF CRICKET BATS.

Submitted by

SAM FISHER

For the degree of PhD of the University of Bath

2005

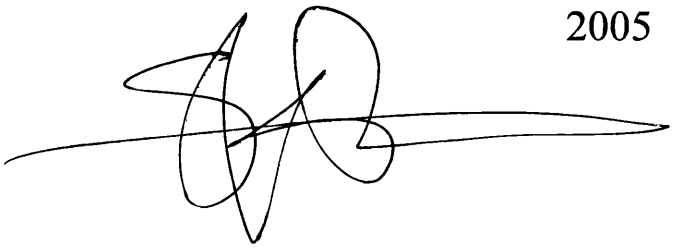

ProQuest LLC
789 East Eisenhower Parkway
P.O. Box 1346
Ann Arbor, MI 48106-1346

Abstract.

EXPERIMENTAL AND FINITE ELEMENT ANALYSIS OF CRICKET BATS.

SAM FISHER.

The purpose of this study was to develop a valid method for capturing and quantifying the post impact responses of cricket bats. There has been limited published work and those who had previously analysed cricket bats had not used high-speed camera systems. This investigation captured bat motion in two-dimensions at 2000Hz using a Photron 1280 PCI Fastcam-X. Five first class cricket bats each with different structural design were analysed using a drop test method. It was then possible to locate the three sweet spots positioned along the bat and discuss these in relation to changes in structural design, gripping type and location, ball impact speed and ball impact location. It was found that impact speed and the structural alterations made by manufacturers had little effect on the location of the sweet spots, although gripping type and location did influence their positions. To enable an accurate finite element analysis, the microstructure of cricket bat willow and handle cane were analysed. This data was entered into the Ansys Finite element analysis programme, where representative models of two of the experimentally analysed bats were constructed. Finite element analysis programmes allow the development and analysis of structures that would not necessarily be possible. Therefore, it was possible to establish the exact effect of major changes in dimensions on the location of the sweet spots of the bat without. Finally, structural alterations were suggested to maximise the performance of a cricket bat and improve comfort at the player's hands following impact.

Acknowledgements.

First and foremost, I would like to thank my parents who without them I would not have been able to complete this course. They have also given me unmitigated support and for that I am eternally grateful.

I would also like to thank the University of Bath staff for their help, in particular Prof. Alan Bramley and Dr. Martin Ansell for offering me this PhD project. Also my supervisor, Dr Jeff Vogwell, for his guidance throughout this study and having faith in my ability to complete it.

Thank you to Jon Gittings, Luke Nelson and Andy Perry who assisted me throughout my time at the University. Also, my test subjects whose participation during my experiments was essential to its completion.

To my friends who have undoubtedly helped, even if it was only to keep me laughing.

In particular, Kirstin and Aimee who in their own ways have been brilliant.

Thank you, it was much appreciated.

Table of contents.

Table of figures.

Table of tables.

1 INTRODUCTION.

Considerable research has been undertaken in the attempt to improve the performance of sporting equipment. This is particularly evident within tennis racket design and development, although, much of these improvements only make marginal improvements to the performance (Grant & Nixon, 1996a). However as with many sports, it is the marginal improvements that separate success from failure. Grant (1996) noted that it is now performance rather than cost that is the overriding consideration in the design and manufacture of modern sporting equipment. The extensive development and modernisation of equipment as with tennis rackets has not been so apparent in cricket bats, which often make cricket bats seem antiquated.

The main aim of much of this previous research has been to increase the size and effectiveness of the sweet spots. The definition of the sweet spot can vary, however most sportsmen identify the sweet spot of their striking implement in terms of the absence of shock, vibration and force on the hands (Cross, 2001c). The sweet spot is also associated with the maximum striking distance, as it is the location that maximum momentum is imparted into the ball (Grant, 1996). Each of the components that make up a sweet spot are suggested to be related to different contact points along the length of the bat or racket. The location of these points are affected by the structural design and material properties of the implement.

More recent research into this area has suggested that there may be up to three points or regions on a bat or racket that could be considered to be a sweet spot (eg. Brody, 1986 and Cross, 1998a). These are the centre of percussion, the nodal sweet spot and the power region. The nodal sweet spot and the centre of percussion are associated with the vibration and impulsive forces experienced by the player during the impact. The power region involves the point where the energy imparted into the ball is highest and the post impact ball velocity is maximised (Brody, 1981). The power region has been linked with the flexural stiffness of the striking implement and often the selection of an implement is based upon its rigidity due to the possible performance benefits. However, sweet spots are often located through trial and error, rather than through a better understanding of the striking implement (Noble & Eck, 1985).

When tennis rackets were originally constructed of wood, there was a trade off between frame rigidity and racket weight, due to the structural properties of wood (Brody, 1997). However with the advent of modern composites, a high Young's modulus can be achieved with no increase in the weight of the striking implement. This has caused the traditional wooden rackets to be almost completely replaced by composites with oversized dimensions that enable greater power, comfort and manoeuvrability.

The advance in equipment design has not occurred within cricket bat manufacturing. In fact innovations as in other sports is comparatively rare (Grant & Thethi, 1994). The traditional design of the bat has changed very little as many manufacturers pride themselves on their traditional techniques. This apparent lack of development may be due to the confinements of the rules, which limit manufacturers to using wood as the impacting surface. However, the rules do not specify that modifications cannot be made. Variations in the design have been limited to the back of the bat such as scallops, extended ridges or alterations in the weight (Grant, 1996). However, these modifications are accompanied with extravagant claims regarding their advantageous nature, although there is no scientific information supporting these claims.

1.1 Aim of the research.

The main aim of this study has been to establish and quantify the responses of some leading quality cricket bats following simulated and controlled cricket ball impacts. This includes the identification of the three main sweet spots and the influence of these sweet spots on cricket bat performance. This investigation has also established the effect of structural design and changes to the construction of the handle on implement performance. The effect of alterations to the dimensions and material properties of the cricket bat were also determined and it was discussed how performance and player comfort could be improved. Finally, this study has increased the limited literature that has been published in the area of cricket bat analysis.

1.2 Specific objectives.

Although research has been published regarding the analysis of cricket bats, it was the main purpose of this study to fully document cricket bat responses. In order to achieve this, three main objectives were outlined;

- Experimentally investigate the materials used and mechanical properties of cricket bats.
- Establish the location of the three main sweet spots and their effect on post impact responses using novel and conventional research techniques.
- Construct an accurate and reliable theoretical model of a cricket bat using a finite element computer package to establish the effects of structural design on cricket bat responses.

Once these have been completed, it will be possible to establish whether improvements to the post impact performance of cricket bats are attainable.

2 BACKGROUND.

The origin of cricket is still unclear as manuscripts showing two males playing with a bat and ball have been found during the 12th (Britannica, 2003) and 14th centuries (Wynne-Thomas, 1997) (Figure 2.1). However, it is speculated that cricket actually began in France in 1478, when a game of 'criquet' was played (Barty-King, 1979).

Figure 2.1: Early cricket (1340).

By the 17th century, cricket had become very popular throughout England, especially within the English gentry, although, it was not until 1744 that the first standardised rules of cricket were published (Grant, 1998b). Many of these laws (including the dimensions of the bat) and the customs, remain the same (more or less) to this day. This continuation of laws and traditions, have often caused non-players to believe cricket is a little obscure (Cricket information, 2001). However, regardless of the nature of the game, its popularity has continued to increase throughout the world (ICC, 2002).

2.1 The laws of Cricket – The bat.

The earliest bats were purely sticks, which gave way to clubs before a handled curved bat was introduced (Figure 2.2). The curved blade was constructed to incorporate the under-arm bowling of the ball along the ground (Grant, 1998a). In the late 18th century, over-arm bowling was introduced and the design of the bat was altered to accommodate the variability in the bounce of the ball (Grant, 1998a). The blades of the bats were straightened and constructed of a

single piece of wood also incorporating the handle (Gunn & Moore, 2001). It was not until 1853 that a cane handle was attached to the willow blade (Collyer, 1993). Cane is invariably used for the handle, interlaced with strips of rubber to provide protection against painful hand vibrations.

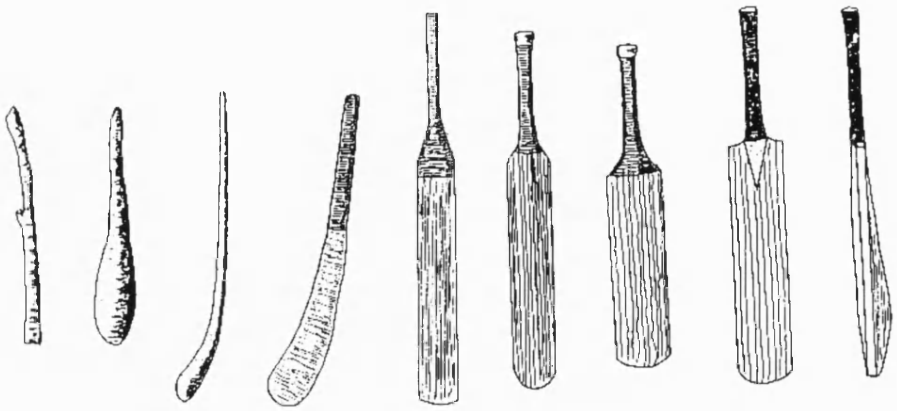

Figure 2.2: Cricket bat development (Collyer, 1993).

2.2 Cricket bat construction.

The construction of the bat begins when the willow trees are selected, felled and sawn into sections of 2ft 4inches (standard length for cricket bat construction) (Edlin, 1973). The sections are then cleft into wedge shaped segments, radiating from the centre (Figure 2.3).

Figure 2.3: Willow section cut into wedge shaped clefts (Edlin, 1973).

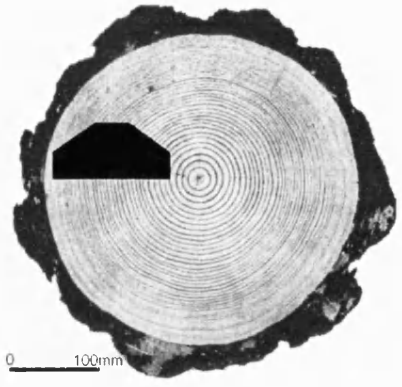

Figure 2.4: Orientation of a bat across the growth rings of a tree (modified Dinwoodie, 2000).

Each segment must be 4½ inches on the outer edge to ensure the maximum bat face width is possible. The face of the bat should lie along the radius of the tree with each of the annual rings

running down the face (Edlin, 1973) (Figure 2.4 & Figure 2.5). Before construction begins, each of the clefts are evaluated by assessing the rebound efficiency and weight (Fisher bats, 2001). The clefts can then be roughly shaped and stacked outdoors (Figure 2.6) to season (dry) for one year before being covered for a further three months (Edlin, 1973).

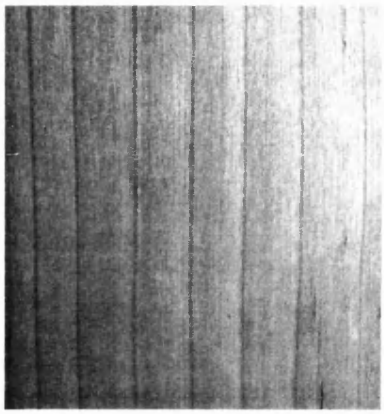

Figure 2.5: Growth rings across the face of a bat.

Figure 2.6: Stacks of wooden clefts (Edlin, 1973).

2.3 Cricket bat dimensions.

Most full sized bats are made to the limits of the MCC's rules regarding bat dimensions. Although, the dimensions of a bat can range significantly depending upon the needs of the individual player (Figure 2.7).

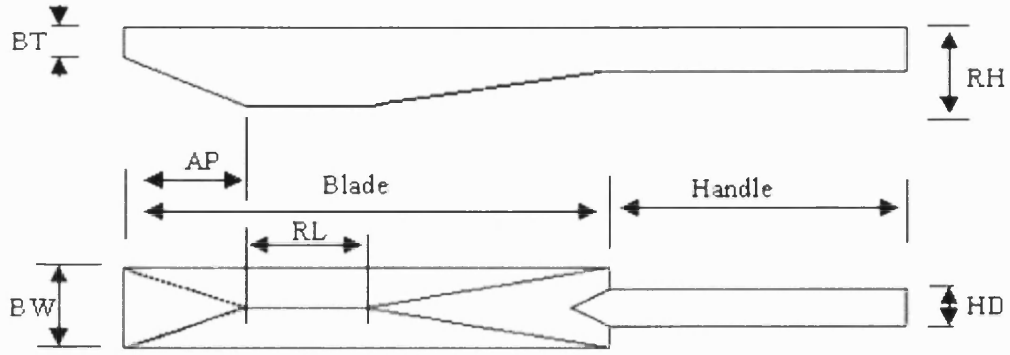

Parameter	Symbol	Range (mm)	Standard Value (mm)
Handle length	Handle	209-318	292
Blade length	Blade	432-600	575
Blade width	BW	89-110	110
Apex position	AP	55-385	165
Ridge length	RL	10-275	120
Ridge height	RH	20-80	50
Blade thickness	BT	5-35	20
Handle diameter	HD	20-50	30

Figure 2.7: Geometrical parameters of a cricket bat.

2.4 Pressing and knocking-in.

Following shaping, the clefts are pressed (up to 2000lb per square inch / 13789kN/m^2) to strengthen the timber sufficiently to withstand the impact of the ball (Salix, 2001). Sayers *et al.* (2000) reported that due to the soft and fibrous nature of the wood, pressing is imperative. Pressing is an important and delicate part of the bat manufacturing process as a balance must be reached between hardening the willow for strength and leaving the blade soft enough to play well (Salix, 2001). Grant & Nixon (1996a) noted that pressing during manufacture compresses a thin layer (up to 2mm) close to the surface, although this is not uniform. The density of the cells in this layer have been found to increase to 1500Kg/m^3, which increases the modal frequencies by up to 10% (Grant & Nixon, 1996a). Grant (1996) concluded that heavier pressing or knocking-in of the blade may offer some scope for improved bat performance. Although, over-pressing can deaden the bat, reducing the performance and increasing vibrations during impact (Edlin, 1973).

Once player's have purchased a bat, they are instructed to knock the bat in using either an old cricket ball or wooden mallet (Figure 2.8). This is to enhance the performance and prolong the life of the bat (Sportsmans Warehouse, 2001). It also further compresses the surface layer of the blade in an attempt to maximise bat performance.

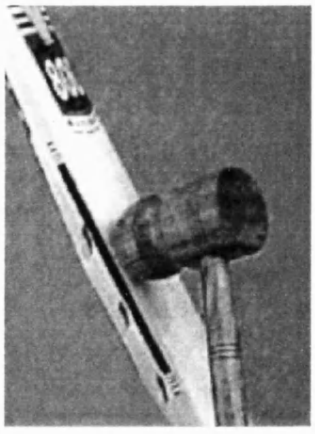

Figure 2.8: Knocking-in using a wooden mallet (Slazenger, 2001).

3 DEFINITIONS AND DYNAMIC THEORIES.

To aid understanding of the experimental results, it is important to relate them to basic engineering theories and principles. This chapter will identify the theory of impacts, bending and deflection along with vibrational aspects that are related to collisions. It was also the intention of this chapter to relate these principles to this study, highlighting the link to the responses of sporting equipment. It is the intention of this thesis to establish and analyse the sweet spots of cricket bats of varying structural design. As outlined in chapter 1, up to three locations have been found that were considered to represent a sweet spot (eg. Brody, 1986 and Cross, 1998a). Therefore, following an introduction to the mechanics of impacts and the theories relating to bending and deflection, this chapter will be divided into three parts identifying theories that are related to these sweet spots.

3.1 Impacts.

3.1.1 Introduction.

A physical impact is the process that involves the collision of two or more objects (Goldsmith, 1991). During most sports it could be suggested that impacts or collisions occur by definition of the game itself. Therefore, impacts and the resulting outcome are particularly important to this investigation. However, the theory of impacts is an extremely complex subject and this study does not intend to outline the specifics of every equation or theory. Therefore, this section intends to highlight particular aspects of impact theories that will aid the reader in their understanding of impacts related to sport.

3.1.2 Theory.

During sports like golf and cricket a beam is swung towards a ball, with the impact occurring away from the centre of mass and the axis of rotation of the implement. This type of impact can

be considered to be eccentric, as the contact point of the two colliding bodies are not located on the line connecting their centres of gravity (Goldsmith, 1991) (Figure 3.1). During cricket bat and ball impacts, eccentric impacts are most common as the centre of gravity is much higher from the bottom of the bat than the position of preferred impact.

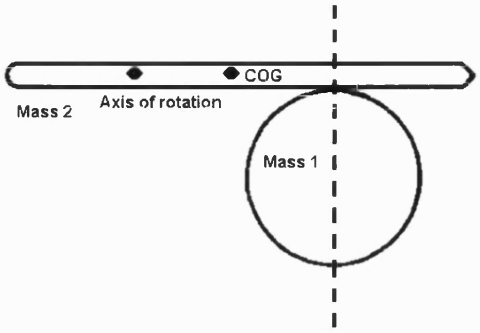

Figure 3.1: Eccentric impact (Goldsmith, 1991).

Impacts by their very nature involve the transference of energy following a short contact period. Casolo & Ruggieri (1991) and Kawazoe (1993) estimated that the impact phase lasts no longer than 100^{th} of a second (10ms). High-speed cameras operating at up to 4000 frames per second are often required to study the impact period accurately. Prior to impact, the striking implement is swung to create much of the energy that will be transferred to the ball. At the point of contact the ball will compress, while the implement will experience a backward or negative force. Daish (1972) noted that at this point the force gradually decelerates the implement and it is momentarily brought to rest relative to the ball. Following this point, the compressed ball begins to move forward at the same velocity as the swung implement. Finally, the elasticity in the ball causes it to reassert its original shape, which results in its forward motion relative to and away from the implement (Daish, 1972).

There are extensive equations that outline and establish the consequences of impacts between two bodies. However, mathematical investigations involving bats and balls often simplify the impacts to ease the calculation of the outcome. Thus, the mathematics that identify dynamic behaviour must be verified by suitable experiments (Goldsmith, 1991). Cross (1999b) noted that the simplest approach is to assume that the bat or racket is rigid and the handle is not subjected to any impulsive force during the collision. Therefore, the post impact ball velocity can be calculated and the coefficient of restitution (COR) established. During the impact period, intense forces are applied to and from the player's hands, forearm, elbow and shoulder,

which modifies the characteristics of the striking implement and impacting object. However, using simplified impact characteristics, any influence these factors may have on the impact conditions and ball responses are excluded. Equations often exclude the influence of the geometric shape, quality, material and state of the bat and ball on the performance of the striking implement (Penrose & Hose, 1998). Goldsmith (1991) also noted that the contact pressure between the impacting objects is often assumed to be uniform and that these surfaces are completely smooth. This does not occur during cricket ball and bat impacts as equal contact pressure will not be achieved as both of the surfaces are curved and there are considerable surface irregularities on both of the objects. The first theory to take into account both local deformation and irregularities in surface texture was the Hertz Law of contact, 1881 (Goldsmith, 1991). This theory takes into account the geometrical and elastic properties of the colliding bodies to establish deformation characteristics. This study does not intend to analyse the use of Hertz Law in relation to ball and bat impacts during cricket. A complete explanation and analysis of this law relative to impacting spherical objects can be found in Goldsmith (1991), Chapter *IV*.

3.2 Beam bending theory.

3.2.1 Introduction.

A cricket bat is a structural beam and so it is important to consider relevant theories regarding the deflection and bending of beams. Flexural stiffness and deflection relative to the performance of sporting equipment has received considerable interest (see Chapter 9 for literature review), as a greater flexural stiffness leads to an increased post impact ball velocity. Thus, the key principles will be highlighted during this chapter to enhance the understanding of this impact response.

3.2.2 Theory.

At impact, a cricket bat will deflect depending upon the properties of the bat. The magnitude of this deflection will influence the energy returned to the ball, the loads experienced at the hands and the frequency of vibration. A rigid bat will absorb and store less energy at impact and so

more energy is transferred to the ball, this maximises the post impact striking distance. However, a more rigid implement will have a higher natural frequency and this has been found to increase player discomfort (Bartlett, 2000).

If a cricket bat exhibited constant material properties, cross sectional area and was clamped at one end during the application of a load, it could be considered to be a cantilever beam (Figure 3.2).

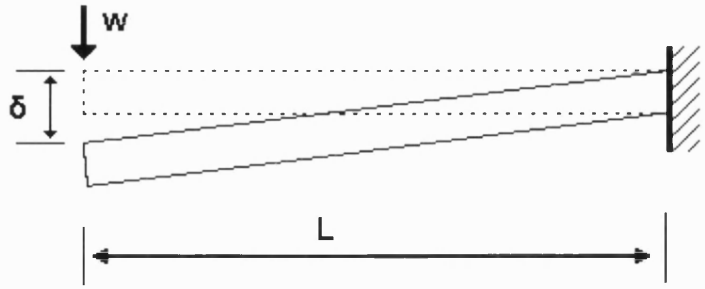

Figure 3.2: Cantilever beam with constant EI.

where, δ is the deflection, w is the applied load and L is the length of the beam.

When a load is applied to a cantilever, it will deflect to a magnitude relative to the load and the beams Young's modulus. A low modulus will mean a large deflection and a low natural vibrational frequency (Ashby & Jones, 1996). By assuming a bat is within these parameters, the magnitude of the end deflection can established using Equation 3.1 (Ashby & Jones, 1996).

$$\delta = -wL^3/3EI$$

Equation 3.1

where, E is the Young's modulus and I is the second moment of area of the beam.

As the stiffness of the bat (K) affects the magnitude of the impact load transferred to the hands and the vibrational frequencies, it is also important to establish this variable (Equation 3.2), (Ashby & Jones, 1996).

$$K = w/\delta = 3EI/L^3$$

Equation 3.2

However, the assumption that a bat is a cantilever excludes the significant contribution of the handle and that the handle is gripped at two locations at a set distance (a) apart. Therefore the flexure of portion 'a' should be included during the application of the load (Figure 3.3).

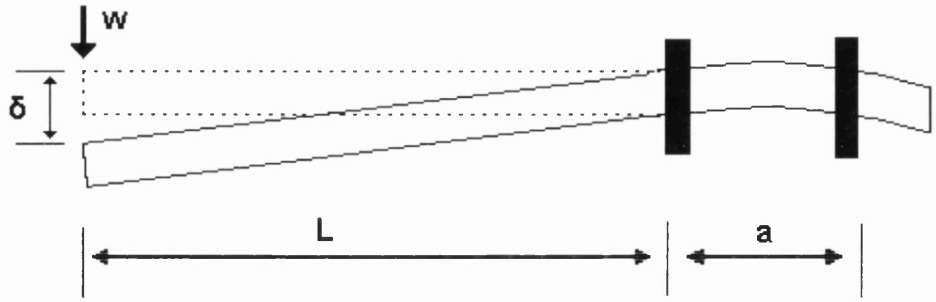

Figure 3.3: Beam with two supports and constant EI.

Therefore, the equation to calculate the deflection of this beam needs to be more complex to take this into account. Thus, the deflection is now a function (f) of portions 'a' and 'L'

$$\delta = -w\, f(a,L)/3EI$$

Equation 3.3

The stiffness of this beam also has to take into account the deflection of both portions (Equation 3.4).

$$K = EI / f(a,L)$$

Equation 3.4

Although Figure 3.3 includes the flexion of the handle between the two supports, it does not include the variation in cross sectional area or Young's modulus that a cricket bat exhibits (Figure 3.4).

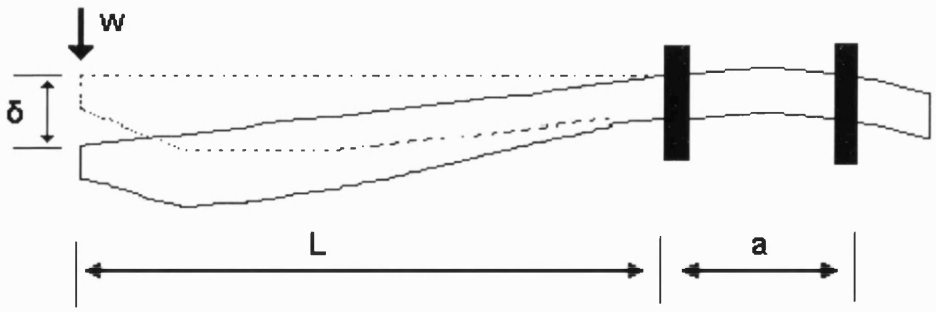

Figure 3.4: Beam with two supports and variable EI.

Therefore, due to the continually changing EI, direct mathematical analysis is not possible and so a finite element approach is needed (Chapter 14).

3.2.3 Summary.

It is recognised that there are many principles, theories and equations relating to the bending and the deflection of beams. However, this chapter aimed to identify some of the main and more basic theories applied to beams under load. It was highlighted that due to the continual changes in cross sectional area and Young's modulus it is not possible to directly establish the exact deflection of a cricket bat, although equations can be applied to simplified shapes (eg. cantilever beams). The magnitude of bat deflection directly influences the post impact ball velocity, vibrational frequencies and loads experienced by a player. Therefore, bat deflection should be measured during the analysis of equipment performance and considered for making design improvements.

3.3 The centre of percussion.

The centre of percussion (COP) is the position where no impulsive forces are experienced following an impact at a correlating conjecture point (Brody, 1981). Although the COP will be further discussed later relating to experimental analysis and player comfort (Chapter 10), it is the aim of this section to investigate methods of establishing it mathematically.

Noble (1985) and Weyrich *et al* (1989) published an equation (Equation 3.5) to calculate the location of the COP on a baseball bat. This method was based upon the measurement of the radius of gyration (Figure 3.5), which is the distance between the axis of rotation and the point of maximum bulk (Kreighbaum & Smith, 1996).

$$q = \frac{k^2}{r}$$

Equation 3.5

where, q is the centre of percussion, k is radius of gyration and r indicates the distance from centre of gravity to the axis of rotation.

This study applied this equation to a cricket bat to calculate the location of the COP. The grip locations employed were the same as during the experimental analysis of the COP (Chapter 10), therefore making it possible to make an accurate comparison of both experimental and mathematical COP locations.

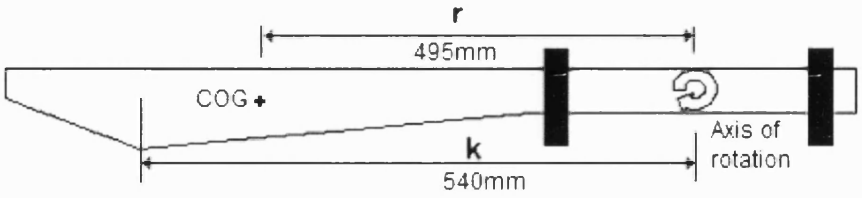

Figure 3.5: Identification of the variables for the calculation of the centre of percussion.

Therefore using Equation 3.5 and the details from the experimentally tested Probe cricket bat,

$$\text{Centre of percussion} = q = \frac{k^2}{r} = \frac{540^2}{495}$$

q = 589mm from the axis of rotation to the COP.

The q value and therefore the cCOP (calculated centre of percussion) is found to be located 111mm from the free end of the bat, which is 49mm below the widest point of the bat (160mm from the free end). This was achieved by subtracting the location of the axis of rotation (700mm from the free end) from the calculated q value. As will be reported in Chapter 10, the eCOP (experimental centre of percussion), was found to be 180mm from the free end of the bat, 20mm above the widest section of the bat. This is illustrated in Figure 3.6,

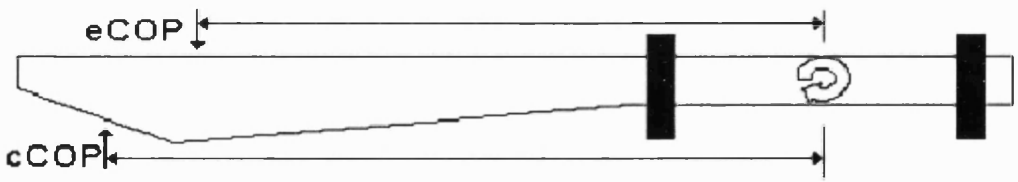

Figure 3.6: Locations of the experimental and calculated centres of percussion.

It was found that there was a 69mm difference between the cCOP and eCOP, highlighting problems in using this equation. Even if the experimental data was not available, it could be assumed that it is unlikely that the COP would be located this low down the bat. From trial and error, players have found that the magnitude of the loads and vibrations are increased when an impact occurs close to the bottom of the bat, thus causing them to avoid this particular impact location.

It could be suggested that although there are differences in the physical properties in wood, a baseball could be considered to be constructed of a homogenous material. However, a cricket bat also includes a cane handle, which has different material properties to the willow blade of the bat. The willow blade was also found to have differing density values due to the effects of knocking-in and pressing during construction (Chapter 7). The lack of consideration for volumetric changes will also have influenced the calculated results. With a baseball bat, the shape can be simplified to represent a cylinder or a cone, however simplification of a cricket bat shape is not possible to the same extent. Therefore, it is necessary to modify this equation to take these variables into account.

Although it has not been previously published, it is considered that the equation reported by Noble (1985) and Weyrich *et al.* (1989) must have included physical parameters and basic material properties to establish the COP. Therefore, this study is assuming that the step before the published equation would have been the following (Equation 3.6),

$$q = \frac{\sum \rho v r^2}{\sum \rho v r}$$

Equation 3.6

where, ρ is the density, v is the volume and r is distance to the centre of mass.

From Equation 3.6 the radius of gyration (k) has been replaced by the density, volume and distance to the centre of mass. This is because the radius of gyration is a component of all of these factors. It was also hypothesised that the material properties and volume components have been excluded from Equation 3.5, as they would have been located on either side of the equation. However, it is believed that due to the distinct alterations in the volume and the density of the materials used to construct a cricket bat, there inclusion is important.

In order to investigate the accuracy of the new equation, a cricket bat shape was drawn and sectioned to enabled the calculation and inclusion of the bat's volume. Although from Figure 3.7 it can be seen that the bat has been simplified, it is a closer representation of an actual cricket bat than considering it to be a rectangular beam. By dividing the bat into portions, it is also possible to include distinct structural changes and the density of each section.

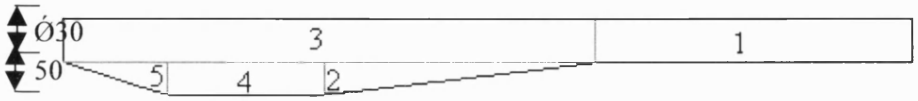

View from the side.

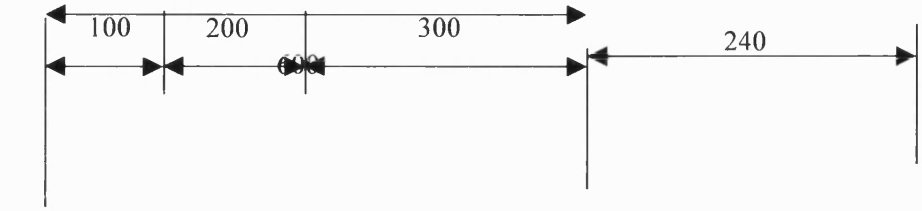

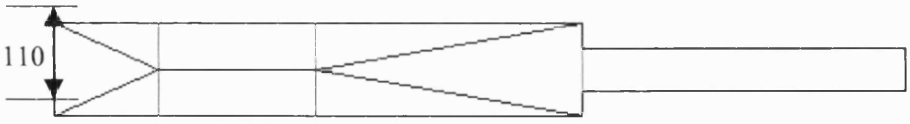

View from above.

Figure 3.7: Simplified cricket bat shape with numbered portions and dimensions.

The five portions are a cylinder (1), two pyramids (2 & 5), a triangular (4) and a rectangular section (3).

Using basic geometry, it was possible to find the centre of mass (x), and the volume (v) for each of the sections. The density (ρ) measurements of the materials used were also included using experimental data (Chapter 7). Table 3.1, displays the data for each portion,

Portion	r (mm)	V (mm^3)	ρ (Kg/m^3)	ρvr (kgm)	ρvr^2 (kgm^2)
1	120	1.70E+05	353.07	7.19E+09	0.862E+12
2	387.5	5.50E+05	343.24	73.2E+09	28.3E+12
3	500	19.8E+05	388.58	495E+09	192E+12
4	600	550E+05	343.24	198E+09	68.0E+12
5	737.5	1.83E+05	343.24	99.7E+09	34.2E+12
Sum (Σ)		34.3E+05		625E+09	324E+12

Table 3.1: Calculated values for each variable of each portion of the cricket bat.

Therefore,

$$q = \frac{\Sigma \rho vr^2}{\Sigma \rho vr} = \frac{324E+12}{0.625E+12}$$

$q = 518.40mm$

Thus, if the axis of rotation is 700mm from the free end of the bat, the location of the newly calculated COP is found to be 181.6mm from the free end (700 - 518.4mm). This cCOP correlates almost identically with the experimental analysis (eCOP), which was found to be 180.0mm from the free end of the bat (Chapter 10). Therefore, it can be assumed that this method of calculating the COP for a cricket bat is considerably more accurate than the simplified equations that have been previously outlined during other studies.

3.3.1 Summary.

Following the use of previously published and newly established equations, it was possible to calculate the position of the COP on a cricket bat. It was found that the calculated results

correlated well with the experimentally defined results produced by this study. Therefore, it can be concluded that these equations offer a simple and effective method of establishing the COP and thus aid in the understanding of cricket bat responses.

3.4 The coefficient of restitution.

Within the analysis of sporting equipment performance and post impact responses, the coefficient of restitution (COR) is often employed. As highlighted during the establishment of the COP, the COR will be analysed mathematically in this section before experimental calculations are carried out in Chapter 11.

Newton's coefficient of restitution (ε), is defined as the ratio between the speed of separation to the speed of approach. During an impact involving two moving bodies (bat and ball), where a mass (M) travelling at a velocity (V), impacts a mass (*m*) with a velocity (*v*), the separation velocity (*v*') of *m* will be relative to the post impact velocity of M (V') (Figure 3.8).

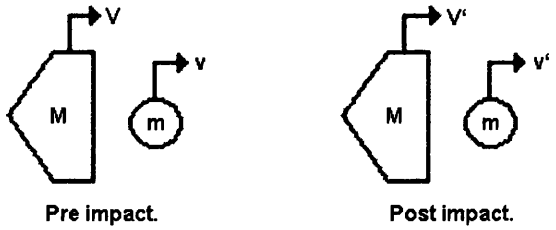

Figure 3.8: Illustration of pre and post impact variables.

During impacts involving sporting equipment, the collision is considered to be semi-elastic due to the deformation (or energy loss through any other manner) of the bat and ball. Consequently the magnitude of this energy loss can be established using the COR (Equation 3.7). Goldsmith (1991) reported the COR is often applied as a ratio to describe the degree of plasticity occurring during the collision.

$$\varepsilon = \frac{v' - V'}{V - v} = \frac{\text{relative difference in post impact velocity}}{\text{relative difference in pre impact velocity}}$$

Equation 3.7

Numerous sports equipment related studies have used this ratio to establish and rank the performance of the implement following impact (Brody, 1987). Newton's coefficient of restitution has also been found to be an appropriate measure of cricket bat performance during static or dynamic tests (Grant, 1998b). However, little has been published regarding the analysis of the COR within cricket bats. Although, Grant (1998b) did suggest that a cricket bat does have a position where the COR is maximised. Within tennis racket analysis, the maximum post impact ball velocity and often the greatest hitting distances are achieved when the COR ratio is at its highest (Brody, 1986). This is because less energy is lost during the impact period, which enables a greater amount to be transferred to the ball and therefore maximise the post impact ball velocity.

From the calculation of the conservation of momentum and the equation for the COR (Equation 3.7), it is possible to establish the following equations for the post impact velocity of the ball (v') (Equation 3.8).

$$v' = \frac{M[(1+\varepsilon)V - \varepsilon v] + mv}{M+m}$$

Equation 3.8

Grant (1998a) had also applied this equation during the analysis of theoretical cricket bat responses. However in this work, the bat was stationary (V=0) as it was clamped under an impacting tube. Therefore, it was necessary to reduce Equation 3.8 to take this variable into account (Equation 3.9).

$$v' = \frac{v(m - M\varepsilon)}{M+m}$$

Equation 3.9

It is considered that Equation 3.9 offers a representative method of calculating the post impact velocity of a ball during an impact onto a static bat.

3.4.1 Discussion.

It is possible to apply Equation 3.9 to the test rig application carried out by this study. If a ball with a mass (m) of 0.16Kg strikes the bat 0.16m from the free end (where ε is 0.43, see chapter

11), which has a total bat mass of 1.13Kg, a post impact ball velocity of $-2.91 ms^{-1}$ is established (Equation 3.10).

$$v' = \frac{9\,((0.16 - 0.7) \cdot 0.43)}{0.7 + 0.16}$$

Equation 3.10

The negative sign indicates the direction of the ball motion as it is opposite to the initial direction. During experimental analysis the post impact ball velocity was $2.6 ms^{-1}$ thus indicating that this equation offers a close representation of the occurrences during actual impacts (Chapter 10). It should be noted that the whole of the bat mass was included, although it can be considered that this should be altered following the inclusion of the clamping rig or mass of the subjects lower body when it is hand held.

During the experimental analysis, the COR will be established using a high-speed camera. Therefore, it will be possible to calculate this variable through the use of positional data (Equation 3.11).

$$\varepsilon = - \frac{d\chi'/dt}{d\chi/dt} = \frac{d\chi'}{d\chi}$$

Equation 3.11

where, d is the integer, χ is the bat motion prior to impact, χ' is ball motion after impact and t is the time period.

As time increments will be kept constant throughout the analysis these can be excluded from the equation.

3.4.2 Summary.

The aim of this section was to report the mathematical methods of establishing the COR during cricket ball and bat impacts. Previously published equations were applied and it was found that there is a distinct correlation between the calculated and measured post impact ball velocities. It is considered that any difference in the calculated and measured post impact velocities were due to the complexity of the three dimensional shape, which the simplified calculations do not take into account. However, it can be concluded that although there are some differences between

the results, this method can be used as an indicator of the post impact velocities following impacts onto static and moving cricket bats.

3.5 Vibration.

3.5.1 Introduction.

With the development of sporting equipment, the analysis of factors that affect the performance and comfort of the user have come under greater scrutiny. One such factor is the nature of the vibrations that are excited within the system following impact. This is because vibrations have a considerable effect on the feeling experienced by the player following impact (Hocknell *et al.* 1996). Therefore, establishing the post impact vibrations are an important factor in analysing and seeking to improve sporting equipment. This section highlights specific areas involving vibrations that influence the performance and comfort of the user following impact. Although more specific equipment related vibration matters are discussed in Chapter 12, this section highlights some of the basic principles prior to future experimental vibration analysis.

3.5.2 Theory.

A vibration is a periodic motion, which repeats itself after a certain period (Den Hartog, 1985). A study of vibrations may be considered as an investigation into the dynamic motions of an implement, as the displacement is relative to the magnitude of the measured vibration. Vibrations of a beam shaped object can occur in an infinite number of shapes, referred to as modes and each of these modes has a discrete frequency. The vibration of a body is classified as either free or forced. Forced vibrations involve the vibration of an object in the response to a system that applies time-varying external forces (Gorman, 1975). The impacted object will then vibrate at a frequency relative to the structure of the impacting object (Fertis, 1973). A condition of resonance will occur when the frequency of the applied force system coincides with one of the natural frequencies of the body (Fertis, 1973). At the resonant condition, the amplitude of the vibration exceeds the estimated values in a shorter time period. If resonance occurs during impacts involving sporting equipment, the subject will experience a distinct

increase in the vibrational shock at the hands and an apparent reduction in the hitting distance achieved, as much of the energy is retained within the system and not returned to the ball.

In free vibrations, the object undergoes oscillatory motion free from external forces (Gorman, 1975). They are caused by forces acting on the body due to changes in inertia and are a result of the redistribution of mass (Fertis, 1973). A freely vibrating body oscillates at one or more of its natural frequencies, the lowest of which can be considered to be the fundamental or natural frequency. The natural frequency of an object for an undamped system (Figure 3.9) is dependant upon the mass and stiffness.

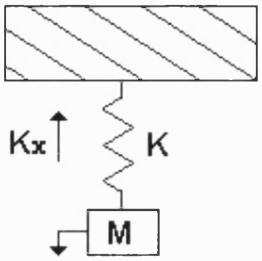

Figure 3.9: Mass and spring system.

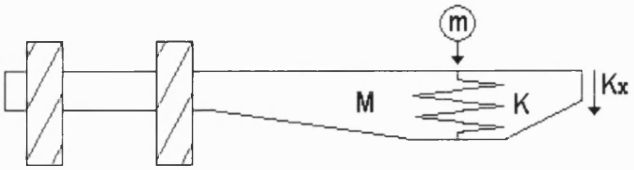

Figure 3.10: Application of a mass and spring system to a clamped cricket bat.

where, K is the stiffness of the spring, M is the mass of the object, m is the mass of the ball and Kx is the displacement of the spring.

The stiffness of a system can be calculated using Equation 3.12,

$$K = F/x$$

Equation 3.12

where, F is the applied force and x is the displacement.

Using the stiffness of a system, it is then possible to establish the natural frequency (ω) of the object (Equation 3.13).

$$\omega = (K/M)^{1/2}$$

Equation 3.13

Harmonic vibrations involve the excitation of the fundamental and subsequent harmonics of the excited system. This is often encountered within an industrial setting as a system is displaced following the application of a force. Without an understanding of the harmonics of a system during use, resonance may be encountered, which has been found to cause a loss of structural integrity (Fertis, 1973). A harmonic motion is symmetric about the equilibrium position (Steidel, 1980). Harmonics are often documented as being a repeated displacement curve, which displays considerable regularity (Figure 3.11), although in principle harmonics can also be irregular. During a harmonic vibration, the maximum displacement of the signal is referred to as the amplitude of the vibration (A). The period (T) is measured in seconds and is the time taken for the displacement to complete a cycle.

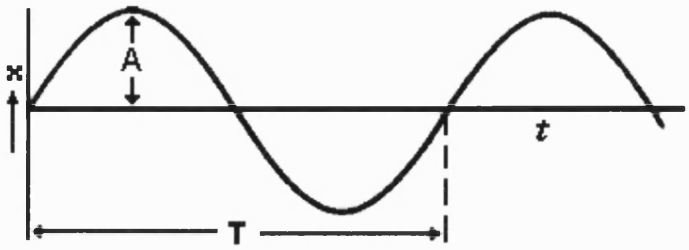

Figure 3.11: Harmonic function illustrating the amplitude (A) and time of an oscillation (T).

The quantity (ω) is normally measured in radians per second and is referred to as the angular frequency, due to the motion repeating itself in 2π radians. Therefore it can be written as Equation 3.14,

$$\omega = 2\pi / t = 2\pi f$$

Equation 3.14

where t is the time period measured in seconds and f is the frequency of the harmonic, which is measured in either cycles per second or Hertz.

As highlighted, the velocities and accelerations of a harmonic motion are also important in understanding the propagation of a vibrational wave. The velocity and acceleration can be derived from Newton's second law of motion (Equation 3.15), which provides an effective method of establishing the motion of a system with a single degree of freedom.

$$F = ma$$

Equation 3.15

Thus,

$$Kx = m\,(d^2x / dt^2)$$

Equation 3.16

Previously, Den Hartog (1985) calculated the velocity and acceleration using the standard definition for harmonic displacement (Equation 3.17), velocity (Equation 3.18) and acceleration (Equation 3.19).

$$x = A\sin\omega t$$

Equation 3.17

$$v = dx/dt = \omega A\cos\omega t$$

Equation 3.18

$$a = d^2x/dt^2 = -\omega^2 A\sin\omega t$$

Equation 3.19

where, x is the displacement, v is velocity, a is acceleration, A is the amplitude and t is the time.

Using these equations, it is possible to establish that each time the mass passes through the position of equilibrium, the velocity is at its maximum and the acceleration is at zero. At maximum displacement, the velocity is zero and the acceleration is at its maximum. Therefore, an acceleration trace is in phase with the displacement and the velocity measurements are completely opposite to the displacement pattern of the vibrational wave.

As previously established, the fundamental frequency is relative to the mass and the stiffness of the system (Equation 3.13), that the amplitude of the wave is derived from Newtons second law of motion (Equation 3.15) and the angular frequency of a harmonic wave is repeated in 2π radians (Equation 3.14). Therefore the frequency of a wave (f) can be established by including all of these components,

$$d^2x/dt^2 = -\,(K/M)\,x$$

Therefore,

$$-\omega^2 A\sin\omega t = -(K/M)A\sin\omega t$$

$$\omega^2 = K/M$$

$$\omega = (K/M)^{1/2} = 2\pi f$$

This gives the following equation, which can be used to establish the frequency of a harmonic wave in Hertz (Equation 3.20).

$$f = (K/M)^{1/2} / (2\pi)$$

Equation 3.20

3.5.3 Damping.

Cricket bats have inherent damping due to the materials they are constructed from (including rubber inserts in the handles), which aim to minimise the vibrations. By damping out unpleasant feeling vibrations, performance can be improved and extended as control is increased and fatigue is often reduced.

Damping can be considered as the resisting forces that dissipate energy during motion. It is a process by which vibrations are steadily diminished in their amplitude (Steidel, 1980). Much of the inherent energy in the system is dissipated as friction, heat or sound until the system is critically damped. The damping force acting on the system is always negative as it is directed against the velocity and amplitude of the vibration. Fertis (1973) noted that damping can be separated into three main forms, namely viscous, coulombic and hysteretic. Each of these damping types influence the subsequent vibrational waves and dampen them using different methods. A system may be influenced by more than one form.

Primarily, it was reported that viscous damping is associated with bodies moving through fluids and its rate is proportional to the velocity of the motion (Fertis, 1973). Steidel (1980) noted that viscous damping is similar to a spring and dashpot system, where loose fitting pistons move through fluid (Figure 3.12).

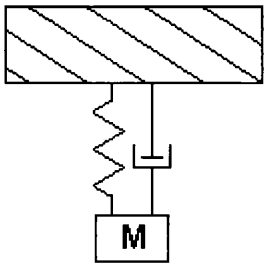

Figure 3.12: Spring and dashpot system.

The viscosity, pressure difference and rate of change in volume influence the velocity at which the vibration is damped. However a vibration absorbing system can only be used when the disturbing frequency is constant as the absorbers are only effective at the natural frequency of the absorbing system itself (Thomson, 1965). Therefore, vibrational frequencies outside the range of the viscous system will be relatively unaffected by this sort of damping system.

Coulomb damping is associated with the sliding of bodies on dry surfaces, which resist motion. This form of damping is dependant upon the contacting surface and the characteristics of the vibrating material and is independent from displacement (Steidel, 1980). Steidel (1980) added that only dry friction damping can stop motion so critical damping is also partly due to coulomb damping.

Finally, it was reported that hysteresis damping is associated with the internal friction of the material (Fertis, 1973). The damping rate is proportional to the amplitude of the deformed bodies displacement and independent from the frequency of the vibration (Steidel, 1980). For example Steidel (1980) added that as a metallic material bends, cooling occurs and therefore heat flows across the structure dissipating energy causing the damping of the system. However at higher frequencies, there is no such heat flow and the damping is decreased. It has been found that the loss of energy is approximately proportional to the square of the amplitude. Hysteresis damping may offer an advantage to a sports equipment manufacturer as following material alterations the damping may be increased. This would either dampen vibrations quicker or diminish their size, thus improving player comfort following impact. This study considers that it is hysteresis damping that is of greatest application due to the solid structure

and apparent deflection of the implement following impact. However due to the effects of airflow, the system may also include viscous damping.

The energy irreversibly dissipated through the damping mechanism of the system is often quantified using the Quality or Q factor. The Q factor is an indicator of the natural damping components inherent in the system. It can be considered to be the ratio between the restoring force of the vibrating system and the maximum damping force exerted by that system. A high Q value is deemed undesirable as large vibrational amplitudes accompany high resonating systems. Simple investigations carried out by this study involving fixed wooden beams has found that the Q factor is high, indicating that there is a sharp resonance and therefore less inherent dampening as found in other materials used for sporting equipment design (eg. carbon fibre). This finding was unexpected due to the structure of wood, which was anticipated to dampen vibrations more effectively than the composite materials.

3.5.4 Vibration of striking implements.

As outlined during this chapter, one factor that influences the performance and 'feel' of sporting equipment is vibration. This subsection seeks to highlight the principal factors affecting the vibration of a bat before discussing the analysis of the nodal sweet spot (Chapter 12). Following ball impact, a racket behaves like a vibrating structure or beam. It is the deflection of the racket that generates a pulse and propagates the vibration following impact (Cross, 1999b). The vibrating implement will then resonate at a fundamental (or natural) frequency and at higher harmonics. Daish (1972) reported that a ball on racket impact excites three modes of vibration. This indicates a fundamental and two harmonics will exist following impact with the ball. Where the vibrational mode has no amplitude a node is located (Figure 3.13). If an impact occurs at one of the nodes, the corresponding modal frequency is minimised or not produced (Brody, 1987). This is also often considered to be the location of a sweet spot. This is because the energy that would have otherwise gone into producing that vibrational frequency is transferred to the ball, thus maximising the post impact ball velocity. Grant (1998b) added that the impact energy will be absorbed by the striking implement if an impact occurs at an anti-node. An anti-node is the location along a modal frequency where the amplitude or displacement is at its greatest (Figure 3.13). An impact at this location leads to the striking distance of the ball being reduced and an increase in the shockwaves transferred to the players hands.

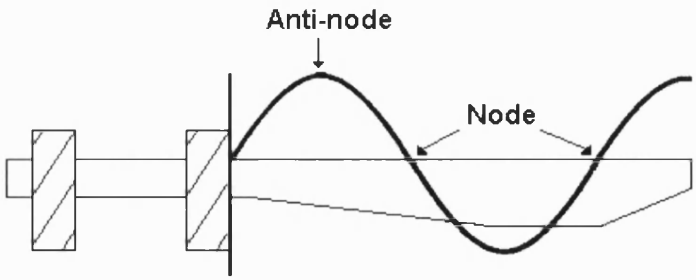

Figure 3.13: Example of a vibrational wave over a cricket bat.

As highlighted, the modal frequencies of a uniform system are dependant upon the Young's modulus and the material density. However, cricket bat willow is not a uniformed material. Therefore, impact force, contact duration, mass, stiffness, mass of the ball and impact location should all be considered (Casolo & Ruggieri, 1991 and Kawazoe, 1993). The amplitude of the vibration is very small when the ball strikes the centre of the racket, but significantly increases when the impact is off centre (Kawazoe, 1993). Once the ball has lost contact with the racket, the vibration continues to travel up and down dissipating the energy in a linear fashion (Cross, 1999b). However if one end is clamped, the vibration suffers a 180° phase reversal at the clamped end, but no reversal at a free end where it is dispersed. Cross (1997) calculated the speed of the transverse vibration to be 100m/s, subsequently a wave travels 0.5m during the $5ms^{-1}$ contact period. This indicates that the vibration should not influence the ball during a cricket bat impact. However, Cross (1997) found that one or two reflections are possible whilst the ball is in contact with a racket. The influence of these pulses at the point of impact depend on the phasing, which could either assist or retard the resultant ball motion.

3.5.5 Summary.

In this section, basic equations and principles regarding the propagation of vibrational waves have been highlighted. It will be seen in the chapters to follow that using these basic techniques establishment of modal frequencies and shapes can be calculated. Although the vibration of sporting equipment has been introduced, it is the intention of this study to establish more specific principles regarding the association between these vibrational factors and the performance of sporting equipment in chapter 12.

4 MATERIALS SELECTION.

4.1 Introduction.

This chapter examines the influence of bat material and bat dimensions on post impact ball velocity and bat vibrations. Although the material properties, bat stiffness and impact efficiency are all interrelated, they will be considered independently to help identify the most important parameters that affect bat performance. This chapter will outline how currently available sporting equipment maximises its performance potential through the selection of optimum materials. It is then highlighted how the principles of material optimisation have not been applied to cricket bat development and how basic theorems can be adopted to maximise the potential of cricket bats. It will then be possible to undertake a material selection process to identify possible material alternatives to those currently used.

4.2 Material selection and sporting equipment.

The emphasis on performance of rackets has led to increased publications identifying improvements through the use of composite materials and oversized dimensions. For example, modifications to tennis racket design and manufacture has led to significant changes in the game. Composite materials (especially CFRP) enable the rackets to be made stronger and stiffer but also lighter with an increased impacting area to maximise post impact ball velocity. This has made wooden rackets increasingly unpopular due to problems with dimensional stability caused by changes in moisture content. Brody (1987) found that following continual impacts, the properties of a wooden racket change causing irregular ball impacts. In most professional sports this would not be tolerated. Due to the rules of cricket, the blade of the bat must be made from wood. However in South Africa, composite cricket bats have been developed by the manufacturer MMS for non-professional and youth leagues (Figure 4.1 and Figure 4.2). This development has been greeted with much animosity by the ICC (International Cricket Council), as it does not follow the traditions of the game. Although scoring has improved as younger players are able to hit the ball further, the potential for fielder injuries has

also increased as found when schools adopted composite baseball bats. In conclusion, the optimisation of equipment performance may not be ideal for everyone.

Figure 4.1: An MMS composite bat rigidly secured.

Figure 4.2: Range of composite crickets bats (South Africa only).

4.3 Material selection and cricket bats.

As mentioned previously, cricket bats have changed very little over the centuries mainly due to the strict rules, geometrical limitations and long traditions. Grant & Nixon (1996b) and Grant (1998b) reported the main aim of cricket bat improvement was to raise the third mode of flexural vibration above the hand excitation spectrum (0-1kHz). By raising the frequencies above this excitation spectrum, players would no longer feel the uncomfortable vibrations (Grant, 1998b). However, it might be argued that the main aim would be to increase the size of the sweet spot.

An investigation of optimum material selection for cricket bats is reported in a chapter of a doctoral thesis by Wegst (1996). However, the procedures adopted in this current chapter are believed to be a more thorough investigation than was previously published. Therefore, this section will identify the equations and boundaries required to identify materials, which might offer an alternative or out-perform the cricket bat willow (*Salix alba*) that is currently used.

There are three primary requirements for a cricket bat material, namely it should be able to withstand high-speed ball impacts without damage, the subsequent vibrations should not cause discomfort to the player and the bat must be as light as possible, while still maintaining enough mass to propel the ball as far as possible. Although, heavier bats have a higher inertia they are swung slower resulting in a lower post impact ball velocity. A lighter bat increases the chances of striking the ball in the middle of the bat due to improved manoeuvrability and it can also be swung faster, thus compensating for the lower inertia. It was also established by Grant (1998b), that the mass of the bat had less of an effect upon the post impact ball speed compared to the bat speed, therefore a lighter bat is preferable to maximise performance.

The need for an alternative wood species was highlighted during 1991 when a series of cricket bats failed during impact. It was reported that the trees from which the bats were constructed had experienced high winds during growth, which caused microscopic damage (Day, 1991). If an alternative species had been identified, this could have been used until an adequate harvest of willow was produced.

In order to investigate the influence of material selection on cricket bat responses, this study will use previously established values (Table 4.1).

Bat properties		**Reference**
Density of willow	$\rho = 349 - 417$ kg/m^3	Chapter 7
Elastic modulus of willow	E = 7.03 ± 0.47 Gpa	Chapter 7
Mass of bat	m = 1 ± 0.1 kg	Commercial values
Cross-sectional area	A = 3.4 · 10^{-3} m^2	Wegst (1996)
Flexural rigidity	EI = 3300Nm^2	Wegst (1996)

Table 4.1: Properties of a cricket bat.

where, the cross-sectional area and flexural rigidity are assumed to be constants.

In order to maximise the equipment performance, it is necessary to establish the optimum material for its construction. Ashby (1999) noted that a structure's design is the contribution of

the functionality, the geometric parameters and material properties. Therefore, the performance can be maximised by correctly selecting a material and optimum geometric dimensions. The process of selecting a material was simplified with the development of material selection charts or merit indices. These provide an objective method of comparing the performance of different materials for a given application (Ashby, 1999). Within an index, a material is displayed in a property region, the size of which indicates the range of the material properties relative to the selected variables. By co-plotting different engineering material properties such as tensile strength, Young's modulus, toughness and density, it is possible to rapidly assess many engineering materials and choose alternatives that would be worth considering further. Figure 4.3 shows an example of an Ashby diagram highlighting the locations of different materials relative to their Young's modulus and density.

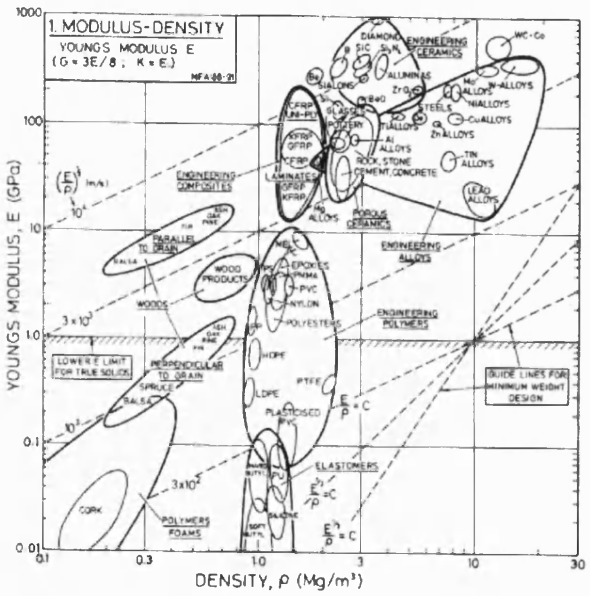

Figure 4.3: Example of an Ashby diagram for material selection.

Young's modulus was plotted against density as these represent important parameters that will maximise the performance, as Young's modulus can be related to changes in post impact ball velocity and density is related to weight and manoeuvrability. Figure 4.3 displays guidelines for material selection, which help identify materials that would perform equally (lie on the line) or those that would perform better (above the line). The line $E^{1/3}/\rho$ (E/ρ^3) has been selected as this represents the selection criteria for flat plates during loading and vibration (Ashby, 1999).

To simplify this process and to enable a comparative study of materials, it is assumed that the cricket bat has a constant flexural stiffness (EI) and is clamped at one end (Figure 4.4).

Although in reality the stiffness does alter significantly along the bat face and it is not rigidly clamped at one end.

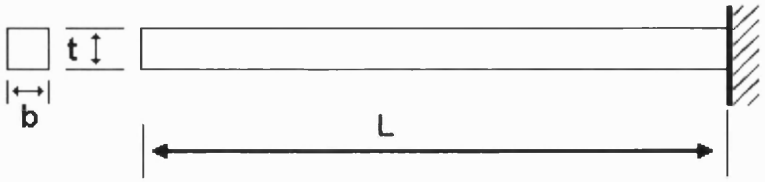

Figure 4.4: Simplified bat.

where, L is the bat length, t indicates the ridge height and b is the width of the bat.

The bat's vibrations during impact also influence the performance of the implement and comfort experienced by the player. The fundamental frequency for a beam with a constant EI can be calculated using Equation 4.1 (Ashby, 1999).

$$f = (cEI / \rho AL^4)^{1/2} = (cI/AL^4)\,(E/\rho)^{1/2}$$

Equation 4.1

where, c is a constant (the constant equals 3 for a cantilever), E is the Young's modulus, I is the second moment of area ($I = bt^3/12$ for a rectangular beam), A ($A=bt$) is the cross sectional area of the beam and ρ is the material's density.

From Equation 4.1, the material property variables (E and ρ) may be separated from the geometric dimensions (I, A and L). Developing the equations by Wegst (1996), Ansell (2004) highlighted how it was possible to rearrange Equation 4.1 to isolate E/ρ^3. Therefore, the guideline associated with flat plates (E/ρ^3) can be used with the merit index of density against Young's modulus, which are important variables for cricket bat analysis. Ansell (2004) expanded the second moment of area (I) and the cross sectional area (A), while including the mass (m) of the beam (Equation 4.2). The mass is included as it is a function of the fundamental frequency of a beam with a single degree of freedom (Chapter 3).

$$m = \rho v = \rho btL$$

Equation 4.2

where, v is the volume.

Therefore,

$$f = (cE / 12\rho L^4 \cdot m^2 / \rho^2 b^2 L^2)^{1/2} = (cm^2 / 12L^6 b^2)^{1/2} \cdot (E / \rho^3)^{1/2}$$

Equation 4.3

This indicates that the highest natural frequency is achievable using a material with the highest (E/ρ^3) ratio.

If the dimensions and mass of a cricket bat are as follows (Table 4.2), it is possible to establish the fundamental frequency for a clamped cricket bat using Equation 4.3.

Component	Variable	Dimension
Bat thickness	T	59mm
Length	L	570mm
Bat width	B	108mm
Mass	M	1246g
Density	P	0. 34Mg/m^3

Table 4.2: Average structural dimensions of a cricket bat.

Using the data from Table 4.2 and Equation 4.3, the fundamental frequency is 15.74Hz, which correlates with the findings of John & Li (2002) (15Hz) and this study (14Hz) for the frequency of a clamped cricket bat.

4.4 The influence of structural dimensions on calculated fundamental frequencies.

Although the equations have been simplified due to the assumptions made regarding dimensions and fixation, it is possible to establish how the fundamental frequency of a cricket bat alters with changes to the dimensions.

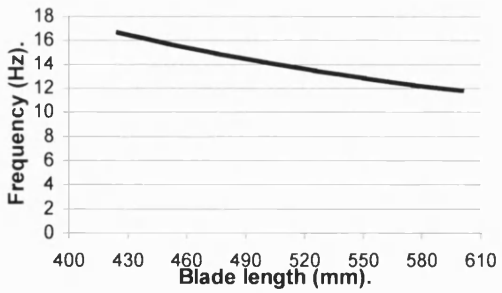

Figure 4.5: Effect of blade length on calculated fundamental frequency.

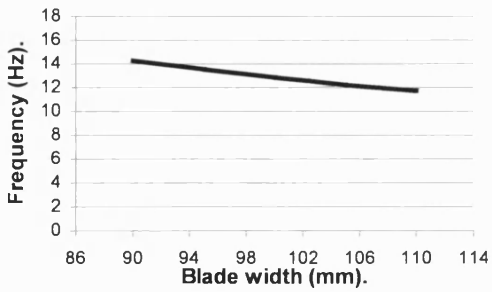

Figure 4.6: Effect of blade width on calculated fundamental frequency.

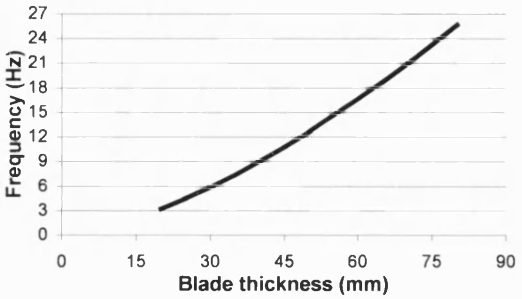

Figure 4.7: Effect of blade thickness on calculated fundamental frequency.

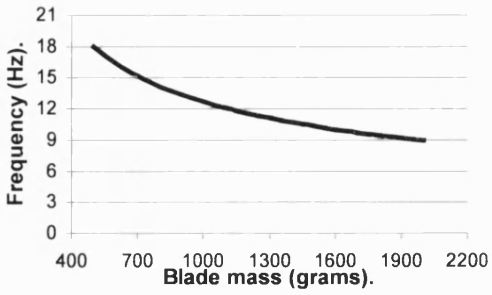

Figure 4.8: Effect of blade mass on calculated fundamental frequency.

Figure 4.5 to Figure 4.8 illustrate the influence of specific changes in geometric dimensions on the calculated fundamental frequency. The parameters refer to the maximum and minimum dimensions that are authorized by the laws of cricket or those that are currently used by bat manufacturers (Table 4.3). From Figure 4.5 & Figure 4.6, reductions in the length and width raise the fundamental frequencies. However, the opposite can be said following alterations in the thickness of the blade (Figure 4.7) where the frequency is increased with an increase in the thickness.

A reduction in length increases the fundamental frequency as the direction of the first mode is longitudinal, thus the time taken for the wave to travel along the implement is reduced. As the length of the blade is reduced, the stiffness is also increased, therefore the bat is unable to deflect to a similar magnitude as before. This also increases the oscillations and the recorded frequency of the bat. An increase in the stiffness and the bat's fundamental frequency has been found to maximise the post impact ball velocity and player comfort (eg. Grant & Paisley, 1997). However, shortening the bat would cause the players to alter their style of batting to accommodate this change, which may lead to a decline in performance. An increase in blade

thickness (Figure 4.7) can also be attributed to an increase in blade stiffness and subsequent rise in the fundamental frequency.

Figure 4.6, demonstrates that as the width is decreased, the frequency increases due to changes in the dimensions of the blade rather than stiffness as outlined earlier. Vibrational frequencies are dependant upon the area of the vibrating structure, so a smaller area enables the wave to travel quicker and more efficiently across the structure, thus recording a higher frequency. A lower natural frequency will also be measured when the width of the blade is increased due to the relative increase in mass, which reduces the oscillation rate and the calculated frequency. Increasing the fundamental frequency with a reduction in the mass has been found to improve player comfort (Brody, 1987).

There are no laws concerning the mass of the bat (Figure 4.8), although, players rarely use bats with a mass over 1451grams (3.2lbs). The natural frequency is found to reduce with an increase in the bat mass as it is unable to deflect at the same velocity and with the same amplitude as when the mass is lower. It can be assumed that an increase in bat mass would be undesirable as a lighter bat can be swung faster with more manoeuvrability, which maximises the post impact ball velocity (Fleisig *et al.*, 2002).

The extremes of the dimensions and the resulting natural frequencies are presented in Table 4.3. The dimensions of the Kookaburra Probe bat are also included to highlight the differences made to the fundamental frequency following changes in the shape of the bat.

Dimensions	Thickness	Length	Width	Weight	Frequency
Min	20mm	432mm	89mm	500g	3.79Hz
Probe bat	59mm (max)	570mm	108mm	1249g	15.74Hz
Max	80mm	600mm	108mm	2000g	21.89Hz

Table 4.3: Influence of extreme dimensions on calculated fundamental frequency.

Table 4.3 illustrates that it would be possible to increase or decrease the fundamental frequency following alterations in the dimensions of the bat. The increase in the fundamental frequency following changes to the bat's dimensions would result in the increase in the other excited

frequencies. If the frequencies are raised sufficiently, players may experience an improvement in comfort as the third or even the second modes are raised above 1kHz and can no longer be perceived.

The Probe dimensions are close to the maximum dimensions possible within the laws of the game, although following a slight increase in the thickness, length and large rise in mass, the fundamental frequency can be raised by approximately 30%. This highlights how alterations within cricket bats are possible and that it is crucial to establish which modifications make a significant improvement in the performance without inhibiting player movement. A more detailed investigation into the effects of structural alterations on post impact responses using finite element computer modelling will be presented and discussed in chapter 14.

4.5 Selection of an optimum material for cricket bats.

Using the Cambridge Engineering Selector programme, it was possible to identify wood alternatives for cricket bats. A guideline with a diagonal slope of E/ρ^3 was plotted as this was reported earlier to be related to the maximisation of bat performance. The location of willow (*Salix alba*) was at the intercept between the x co-ordinate (density) of 0.34Mg/m³ and the Y co-ordinate (Young's modulus) of 7.1GPa. Therefore, the target wood species were those located along this density bearing, but with a greater stiffness. This would lead to an increase in the post impact ball velocity without an increase in the mass of the bat.

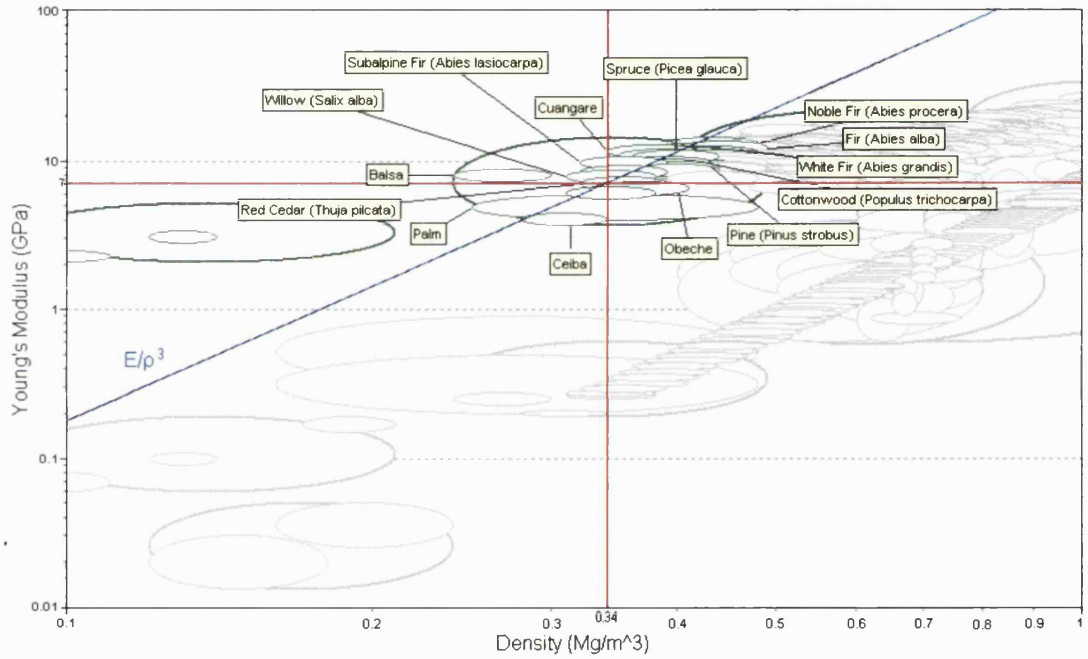

Figure 4.9: Identification of wood species for use as cricket bats.

In Figure 4.9 there are a number of species that intercept or lie above the guideline, although there are few species that have a greater stiffness for a similar density measurement. From this figure, two species of hardwood (willow and cottonwood), softwood (subalpine fir and red cedar) and two tropical species (cunangare and obeche) were selected for further analysis. For clarity, the density and Young's modulus data of these species has been tabulated in Table 4.4.

Species	Density (Mg/m^3)	Young's modulus (GPa)	$(E/\rho^3)^{1/2}$
Willow	0.31 – 0.38	7.1 – 8.7	12.59 - 15.43
Cottonwood	0.35 – 0.43	8.7 – 10.6	11.54 - 14.24
Subalpine Fir	0.32 – 0.39	8.8 – 10.8	13.49 - 16.38
Red Cedar	0.32 – 0.39	7.6 – 9.3	12.52 - 15.22
Cunangare	0.34 – 0.42	10.4 – 12.7	13.09 - 16.26
Obeche	0.33 – 0.41	5.9 – 7.2	10.22 - 12.81

Table 4.4: Data for selected species (Cambridge engineering selector).

This table shows that these species are closely correlated in terms of density but have a higher Young's modulus (excluding Obeche), therefore, justifying their selection for further analysis as they would exhibit a greater stiffness for minimal increase in mass. Thus, a higher post impact ball velocity may be achievable without a reduction in the manoeuvrability that increased mass would have caused. The $(E/\rho^3)^{1/2}$ values have also been included to establish whether there would be any significant alteration in the fundamental frequency as a higher calculated $(E/\rho^3)^{1/2}$, leads to a higher fundamental frequency. The Cunangare and Subalpine Fir have higher $(E/\rho^3)^{1/2}$ showing that these species would have a higher fundamental frequency than willow, although the difference is small (between 4 and 7.5%).

Wegst (1996) established the Janka hardness of each species, which is a measurement of the force required to push a steel ball with a diameter of 11.28mm into the wood sample to the depth of half the ball's diameter. Using the Janka hardness ratings willow (1.7kN) was found to have the lowest rating and that it was the Cuangare (2.07kN) that had the highest rating for hardness (Cambridge Engineering Selector). This led Wegst (1996) to suggest that the tropical wood Cuangare was better than willow for the purposes of cricket bat construction. However during cricket, the bats experience high impact loads rather than extended loading periods. Therefore, the resistance to impact loads has been plotted for each species considered (Figure 4.10). This is a measurement of the hammer drop height required to damage a sample.

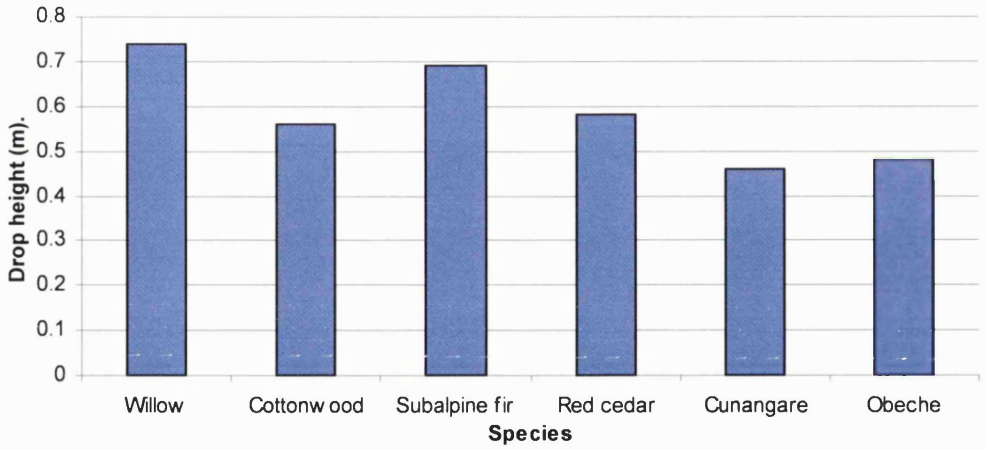

Figure 4.10: Resistance to impact load (Ashby, 1999).

Using an impact test method rather than a continuous load, it is possible to see that willow requires a greater drop height before damage is caused to the sample (Figure 4.10). Therefore, willow is more resistant to impact loads than the other species investigated. Subalpine fir has a slightly lower resistance to impact loads (0.05m), although it was found to have a higher Young's modulus and similar density (mass). Therefore, it may be advantageous to use Subalpine Fir due to the increased stiffness, that would maximise post impact ball velocity and vibrational frequencies. However, the durability would be less than that found during impacts involving willow. The superior load resistance performance of willow is not yet understood although, pressing and knocking-in during manufacture (which is not included in these results) would further increase the resistance to impact loads. This would increase the durability of the face of the bat, improve the resistance to splitting and increase in the density of the top layer (approx 2mm). This would also lead to a rise in the stiffness of the bat, which would increase the vibrational frequencies and the post impact ball velocity. As pressing and knocking-in has not been applied to the alternative species, it is difficult to assess whether such treatment would have a positive or negative effect on the performance of the wood during ball impacts. Therefore, further analysis is required on these species to establish exactly whether they could improve upon or at least match the excellent performance of willow.

4.6 Conclusion.

This chapter established the material selection parameters for cricket bats and five other alternative species of wood to willow using Ashby diagrams. Following further analysis this

study considered that Subalpine fir, would be at least a comparable species for the construction of cricket bats, due to its increased Young's modulus and similarities in density, although durability was found to be less than willow. Subalpine fir may improve the comfort and performance as the fundamental frequency and post impact ball velocity would be maximised due to the increased stiffness. However, willow can still be considered to be the best species for the construction of cricket bats.

5 TESTING EQUIPMENT AND PROCEDURES.

5.1 Introduction.

During this study, various pieces of testing equipment have either been designed and / or purchased to meet the requirements of this investigation. This chapter aims to describe each piece of equipment employed and its particular specifications.

5.2 Application of ball impacts.

To investigate the responses of cricket bats, it was considered important to measure a bat's reactions following a dynamic cricket ball impact. There are various methods of administering ball impacts although it was considered important that the ball impact location could be precisely controlled. It was also considered that the ball should not bounce prior to impact, due to possible variability in impact location, spin and velocity. Direct ball impacts of up to 100mph could be administered using a ball cannon, although this velocity can vary by as much as ±10% according to the manufacturers. It was also considered that accurately impacting a ball onto a stationary bat at 100mph would be difficult, dangerous and might cause irreparable damage to the bat if it was rigidly clamped. Therefore, it was concluded that a simple drop test method would be employed to administer the ball impacts. Using a 5m aluminium tube, the ball would reach a velocity of $9ms^{-1}$ and the bat could be positioned underneath the end of the tube to allow impacts at precise locations. As the speed of the impact was significantly reduced, there were no immediate hazards to people or equipment. Using the aluminium tube also enabled the study to investigate the influence of impact velocity on bat responses by altering the drop height. The ball impact speeds were initially calculated using the equation for particle motion and constant acceleration (Equation 5.1).

$$v = 2as^{½}$$

Equation 5.1

where, v = velocity, a is the acceleration due to gravity and s is the height.

Equation 5.1 is derived from Newton's second law for particle motion, which can be rearranged to enable the calculation of ball drop velocity (Equation 5.2).

$$v^2 = u^2 + 2as$$

Equation 5.2

where, u is the initial velocity of the ball.

This equation was only used as a guide as the ball will also be affected by air resistance and whether it contacted the sides of the tube during the drop. Therefore, it was important to verify the actual impact speeds using the high-speed camera system. Using this method, it was also possible to establish the loss in velocity during the drop, which enabled the study to establish the exact drop heights for the required impact velocities. The chosen equipment set up is shown in Figure 5.1,

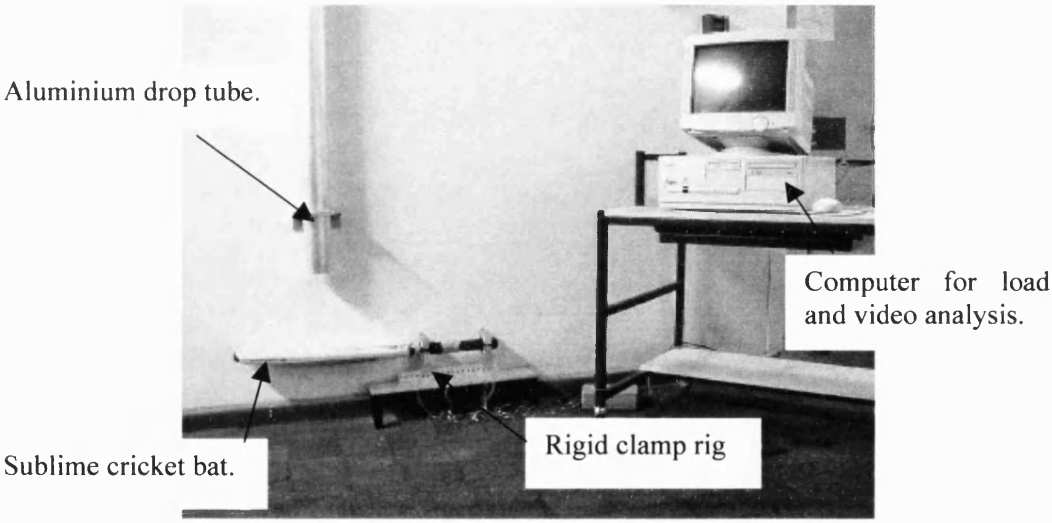

Figure 5.1: Original experimental set up.

5.3 Clamping types.

Various clamping methods including freely suspended (Brody, 1987), rigidly clamped (Cross, 1997) and hand simulator (Hatze, 1998) have been used in previous studies when analysing the response and performance of sporting equipment. The following subsections will identify the different types of clamping methods that this study used to analyse the post impact responses of cricket bats.

5.3.1 Freely suspended.

The simplest method of securing the striking implement for analysis is by suspending it from one end, allowing it to swing freely. Although considered to be rather crude by some investigators, it is the closest condition to being uninhibited by any other outside influence. This method of analysis has been repeatedly used during the analysis of tennis rackets and has been found to be an effective method for implement analysis (eg. Brody, 1987).

5.3.2 Hand held.

Although the aim of many sports equipment studies has been to investigate the occurrences during actual game situations (hand held), using a human subject as a clamping technique may not be ideal due to the inability of humans to replicate exact motions. Although it could be considered that this would also occur during game situations, it does not allow a standard response to be produced unless vast amounts of data are repeatedly collected, which may still not be representative of the whole population. Therefore, human subjects are more of a method of establishing particular occurrences relating to that moment in time. Therefore, this study used a relatively small number of human subjects (5 - 6) as guides to enable this study to establish a realistic clamping method.

5.3.3 Rigidly clamped.

Rigidly clamping a sporting implement does not produce comparable results to actual playing occurrences. However, rigid clamping does provide a method of establishing the actions of the bat following impact under confined and repeatable conditions. By rigidly clamping the bat, it is possible to eliminate certain variables like the motion and damping effects of the human subject, therefore establishing pure bat responses. It was considered to be beneficial to establish post impact responses using a rigid clamping system, thus one had to be designed and constructed. Primarily, the requirements of this system were established and listed,

- The rig must securely hold the handle of a variety of bats.
- The handle clamps of the rig must be moveable along the length of the handle.
- The handle clamps must be secure and not bend or deform when a load is applied.
- The rig must enable the deflection at the end of the bat and the handle to be measured simultaneously.

- The rig must be as lightweight as possible to enable easy portability.
- The rig must not damage the bat in any way.
- The rig must enable vibration analysis and dynamic impact tests to be administered.

The specifically constructed clamping device had two collars, which could be varied to accommodate each of the handles. The two collars could also be fixed at any position along the length of the handles (Figure 5.2 and Figure 5.3).

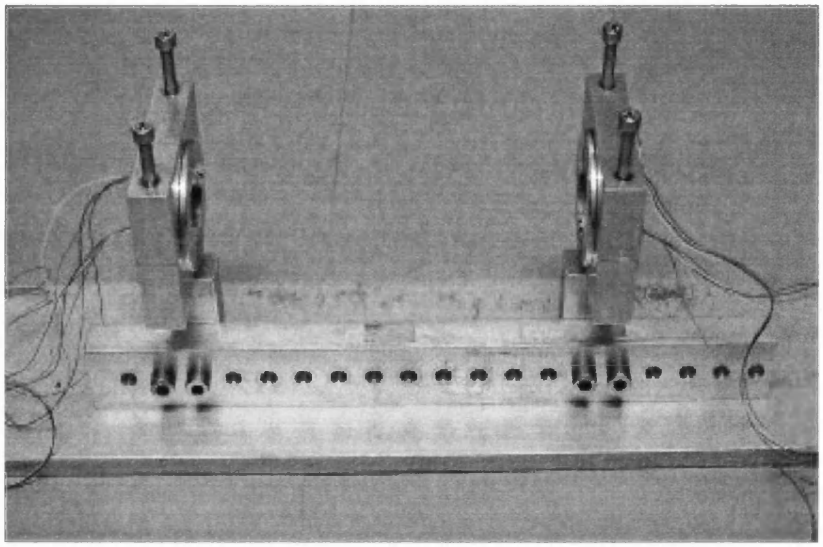

Figure 5.2: Rigid clamping system.

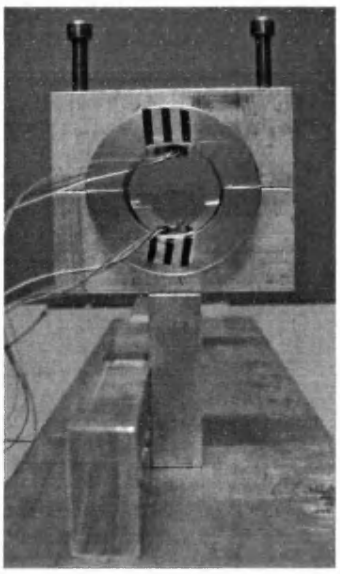

Figure 5.3: Rigid clamp with loads cells in removable collars.

The design also enabled two dial test indicator (D.T.I) gages to be added or removed. This enabled that study to measure the deflection of the bat and the centre of the handle during the application of a static load.

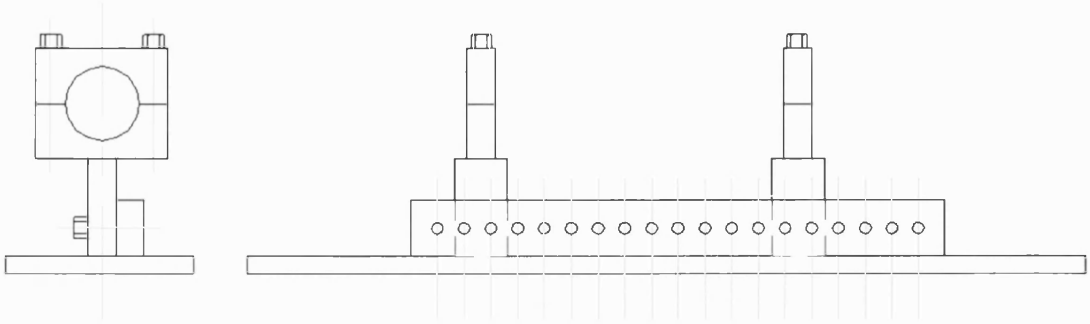

Figure 5.4: Assembly diagram for the rigid clamping system.

Figure 5.4 is the assembly diagram handed to the technicians for the construction of the rig. This diagram shows how the clamping rig was designed to look following construction of the individual parts.

5.3.4 Development of a realistic clamping method.

Studies have previously constructed simulatory systems that represented the responses of a human subject during a ball and bat or racket impact. In particular Hatze (1998) constructed the manu-simulator, which had a controllable arm and clamping system to hold and swing a tennis racket to impact a projected ball. However due to the lack of finances, it was not possible for this investigation to construct such a machine, although, it was possible to construct a more realistic clamping method than rigid clamping. Cross (1998b) suggested that the hand is nothing but a clamping device that pivots about the wrist and is controlled by the damping of the forearm. Therefore, this study constructed a clamping system (the hand simulator) consisting of two adjustable clamps connected by a hinge to a spring and damper unit (Figure 5.5 and Figure 5.6).

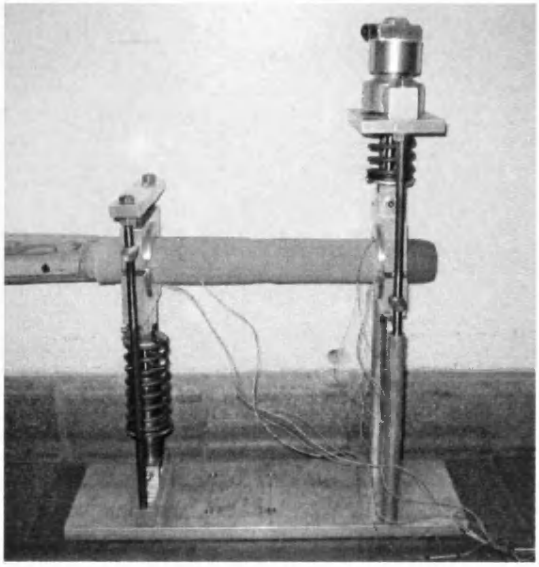

Figure 5.5: Realistic clamping method.

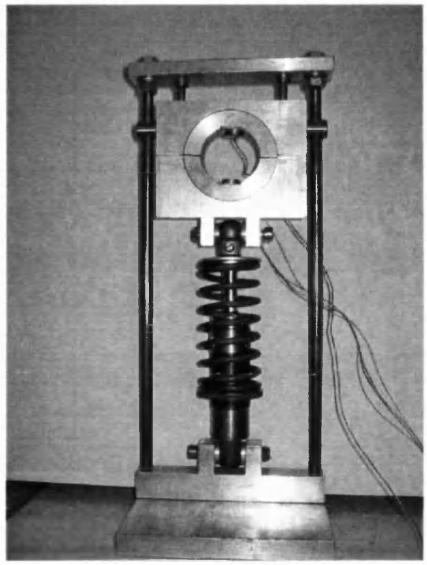

Figure 5.6: Front damper unit.

The rig (Figure 5.5) was constructed using components with the following properties,

Springs: Load required for maximum compression, 361.46N,

Loading rate, 11.33 N/mm

Maximum compression distance, 31.9mm

Free length, 88.9mm

Loaded Length, 57mm

Shock absorbers: Maximum compression distance, 35mm

Damping ratio, 156N/m/s

Oil weight, 1 (thinnest).

During the construction process it was found that information regarding the stiffness and damping ratios of the wrists and forearms were not available. Therefore, this study undertook an extensive period of motion analysis and equipment modification to match the properties of the hand simulator to the average of the human subjects. Primarily, the study chose five subjects to undertake a series of ball and bat impacts. Using the drop ball technique, the subjects held the bat horizontally under the tube and experienced impacts at nine equidistant locations along the length of the bat. Within the subject's hands, four loads cells were positioned to measure the transferred loads. The load cells positions were a combination of the locations outlined by Knudson (1991b) and Cross (1998b) (Chapter 10). After each impact

location had been tracked and analysed, it was possible to establish the responses of a cricket bat. Although it is appreciated the biomechanics of the subjects would be different during game situations, the subjects were instructed to respond in a manner representative of a game. From this human response data, the study could alter the stiffness and damping characteristics of the hand simulator until they matched the average of the human subjects.

It should be highlighted that the clamps were made from aluminium, although the human fingertips are fleshy, soft and deformable that mould to the shape of the held object. This study investigated this area and found that Chang & Cutkosky (1995) had established replica fingertips using a rigid shaft surrounded by soft foam and an elastic skin (Figure 5.7).

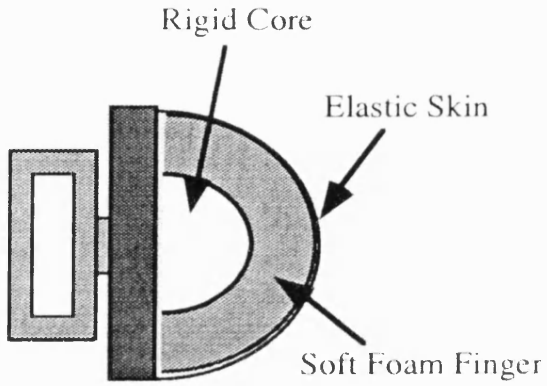

Figure 5.7: Design for replica fingertips (Chang & Cutkosky, 1995).

This method of finger construction was examined by this study although, it was found that it could not be successfully applied to this particular situation as the soft foam moved and the elastic skin repeatedly split during impacts. This caused the actions of the clamps to become unreliable and almost random in nature. Therefore, it was concluded that the addition of a soft replica skin would be omitted from the final design.

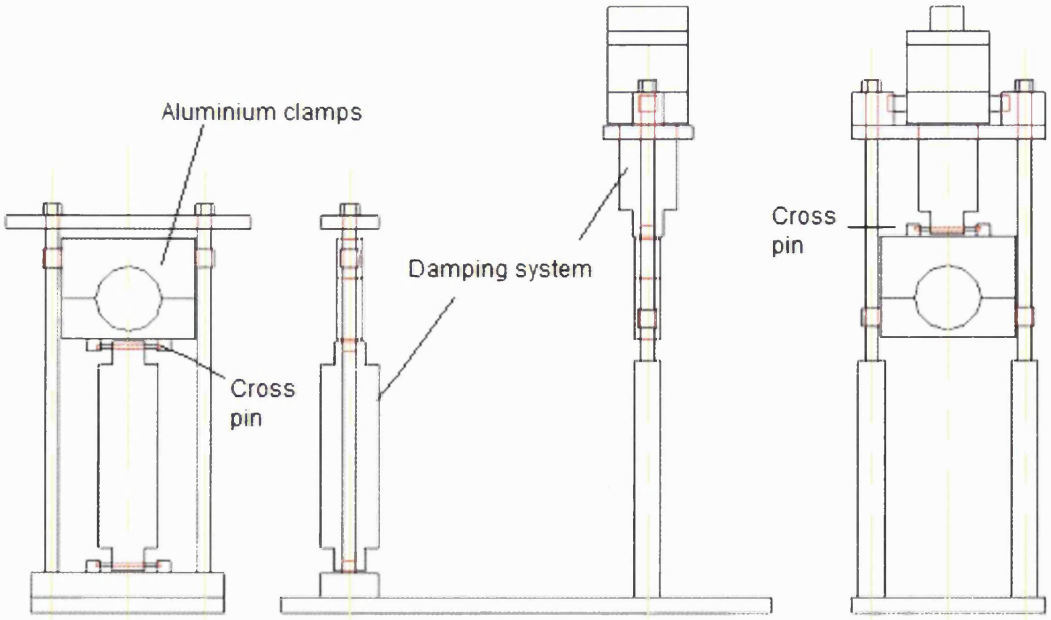

Figure 5.8: Assembly diagram for the realistic clamping system.

Figure 5.8 illustrates the assembly diagram of the hand simulator. From this figure it is clear to see the location of the two damping systems and the cross pins that enabled the clamps to rotate with the motion of the bat.

5.4 Motion analysis.

Large magnitudes of energy are involved during bat and ball impacts, which occur over short time periods. Therefore, not only are the analysis systems required to withstand such impact forces, they are also required to be sensitive enough to take high frequency measurements. Primarily, it was considered important for this study to view the occurrences during the impact period as this would enable the study to measure distinct variables that have a bearing on the post impact bat and ball responses. Prior to the analysis, each bat was separated into 9 impact locations at equal increments of 0.06m. These positions were marked using high contrast dots with crosses printed in the centres, which were stuck along the side of the bat (Figure 5.9). The ball also had high contrast dots, which were grouped in triangular shapes to ensure a dot was always in view (Figure 5.10).

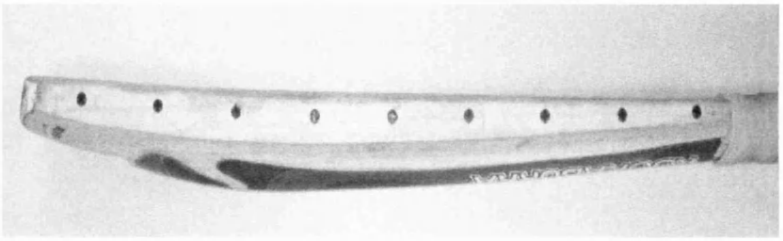

Figure 5.9: High contrast markers on the bat edge.

Figure 5.10: High contrast markers on the ball.

5.4.1 High-speed camera system.

To record the motion of the bat and ball during the impact period, a high-speed camera is required. Due to the short impact period (approx $2ms^{-1}$) a minimum of 1000Hz is required. The camera selected for the analysis of the impacts was a Photron 1280PCI Fastcam–X. The camera was set to capture at 2000Hz with a resolution of 256x1280 pixels, although the shutter speed was 4000Hz to minimise the effects of blurring. Two UNOMAT LX 901 GZ, 1000 Watt halogen spot lamps were also employed to ensure there was sufficient light.

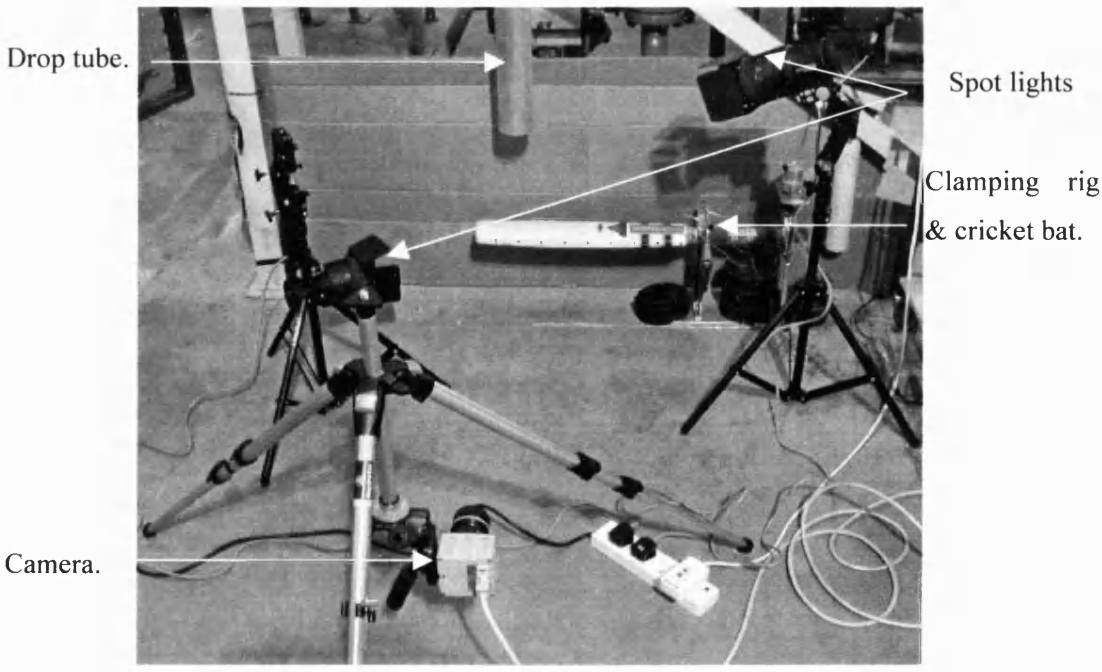

Figure 5.11: Impact area with bat and camera set up.

5.4.2 Data analysis.

After viewing each impact and subsequent bat motion, 1070 frames were saved. To ensure that it was possible to perform frequency analysis, a binary number of frames have to be saved. Thus 1070 frames allow for the first 46 frames to be removed due to possible contamination by the filtering during the analysis, leaving 1024 frames for a power spectrum. Using the Photron motion tools 1.05 automated tracking system, the identified ball and bat locations could be tracked. This records the X and Y co-ordinates of a specified point for each frame of the recorded motion. The calculated co-ordinates were then saved to allow motion analysis.

5.4.3 Load cells.

Another aim of this investigation was to the establish loads that are being transferred to the player following ball impacts. Therefore, four Entran Load cells with a compression measurement range of up to 750N were purchased. These were selected due to their size, load range and sensitivity. As the cells only had a diameter of 13mm, it was possible to fit them inside the clamps or on the subject's hands to record the propagation of the shock load at impact.

5.4.4 LabView.

Once the motion files had been tracked, the exported files were analysed in National Instruments LabView 5.1. This enabled the study to calculate distinct variables from the bat motion, ball motion and load cell data.

From the ball motion data the following variables were established,

- Pre impact ball velocity,
- Post impact ball velocity,

From the bat motion data the following variables were established,

- Bat velocity,
- First and second negative deflection peak,

- First and second positive deflection valley,
- Time to both positive and negative peaks,
- Median power frequency,
- First, second, third and fourth vibrational frequencies,
- Amplitude of the calculated vibrational frequencies,

From the load cell data the following variables were established,

- First and second negative deflection peak,
- First and second positive deflection valley,
- Time to both positive and negative peaks,
- Rate of loading,
- Median power frequency,
- First and second vibrational frequencies,
- Amplitude of the calculated vibrational frequencies,

The data produced by the LabView programme could then be exported into Excel. Graphs could then be produced to establish the average responses of the bat and ball following impacts at each of the specified locations. This was carried out on each of the five bats under each of the clamping conditions.

5.5 Conclusions.

It was the aim of this chapter to outline the processes that have been used to establish an accurate and reliable method of capturing the impact period and post impact responses of a cricket bat and ball. The different clamping methods employed were highlighted along with the construction of a clamping device that simulated human responses. The motion capture systems were also outlined including the methods employed to calculate and correlate the responses of the five first class cricket bats following ball impact.

6 CRICKET BAT HANDLES.

6.1 Construction and flexural stiffness

6.1.1 Introduction.

According to the rules, the handle may be made out of any material as long as it is within the specified dimensions (Chapter 2). Grant (1998b) suggested that the handle offers the most scope for improvements in bat performance. However, improvements to the handle remain relatively unexplored (John & Li, 2002). Therefore, in order to establish the effects of handle construction on bat performance, it was first considered important to establish some simple material properties of different handle types and determine whether structural alterations have a marked effect on flexural stiffness.

6.1.2 Literature review.

Originally bats were made of a single piece of willow but now the handle is a laminated design. The handle typically consists of either 16 pieces of Sarawak cane planed into squares or four rectangular strips of cane. Between the cane sections, rubber or cork is inserted before the handle is glued, sanded and spliced together using twine (Figure 6.1). The handles are often produced separately and are glued and bound onto the bat without regarding their possible influence on the bat's performance.

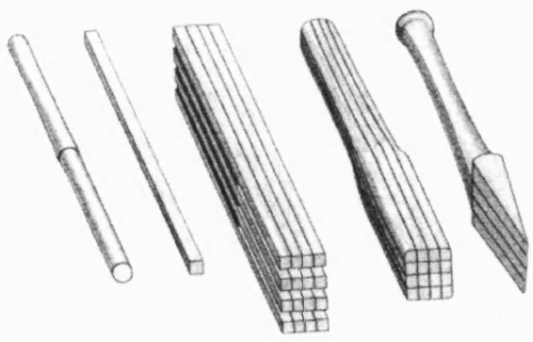

Figure 6.1: Handle construction (Edlin, 1973).

By alternating rubber strips with cane, the handle becomes more compliant and malleable. This reduces the load and vibrations experienced by the player following impact (Grant & Nixon, 1996). Therefore, the greater the number of inserts the greater flexibility and shock absorbent qualities. John & Li (2002) found that the strains during impact were significantly higher in the rubber inserts of the handle. It was concluded that the rubber layers have a major influence on energy absorption during bat deformation. However, a handle with too great a flexibility may improve comfort but will lead to a decrease in the post impact ball velocity. Grant & Nixon (1996) noted that the only measured improvements in a bats performance (which are within the laws of the game), can be made through the removal of the rubber inserts in the handle. It was found that the three excited modal frequencies could be raised by 38.6%, 16.9% and 47.9% respectively. This increase would cause the third modal frequency to be shifted out of the excitation spectrum (0-1kHz) reducing the painful vibrations felt by the players (Grant & Nixon, 1996). The alterations to the vibrational frequencies of the bat following the increase in handle flexural stiffness are shown in Figure 6.2 (Grant, 1998b). Grant (1998b) also considered it beneficial that the flexural stiffness of the bat could be increased without increasing the total mass. This is because an increase in the stiffness has been associated with an increase in the post impact ball velocity without compromising the control of the bat, which is affected by an increase in mass.

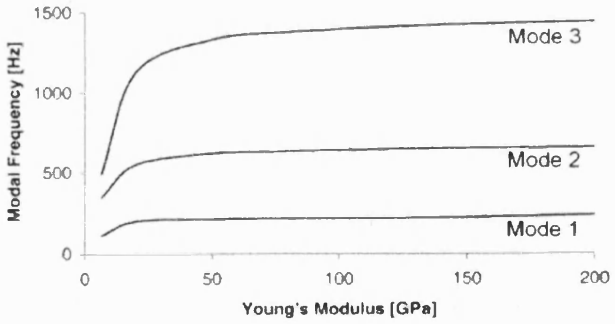

Figure 6.2: Modal frequencies with changes to handle stiffness (Grant, 1998b).

Grant (1998b) found that the modes of vibration increased as the elastic modulus of the handle was increased from 6.6 GPa to 40 GPa (Figure 6.2). Following this point, further increases in stiffness had little effect on the modal frequencies. Alternatively, Knowles *et al.* (1996) found that altering the handle stiffness between 500-3000Nm/rad (original value = 1200Nm/rad) had very little effect on the calculated COR and thus bat performance. Grant & Nixon (1996) had earlier reported that increasing the diameter of the handle as well as removing the rubber inserts would significantly increase the vibrational frequencies. John & Li (2002) also found that it was possible to increase the handle's stiffness and vibrational frequencies by inserting fibre-reinforced rubber layers between the cane sections. It was concluded that using this

configuration, the bat tended to undergo less deformation maximising the energy return to the ball.

In order to establish the mechanical properties of a material, it is often necessary to use a three-point bending method. When using a three-point bending method, the ratio between the outer roller span and rod diameter is an important factor. Harvey *et al.* (2000) reported that during the application of the load, flexural stresses and transverse shear stresses are developed, which have a significant effect upon the measured flexural strength. Harvey *et al.* (2000) added that the effects of the transverse shear stress could be reduced by increasing the span of the outer rollers. It was suggested that a span to diameter ratio of 20 should be applied, although a ratio as low as 10 would still significantly reduce the effects of these stresses.

6.1.3 Experimental set up.

In order to establish the effect of handle construction on stiffness, four handles were produced. Each handle was constructed with Sarawak cane, bonded together using PVA glue and bound using handle twine. Each handle was 430mm in length and approx 35mm in diameter. The inserts were made of 3mm thick natural rubber (IRHD of 65), which had an insertion of polyester fabric. The inserts were cut into strips before being shaped to conform to the dimensions of the handle. These parameters were chosen as they matched many of the commercially available cricket bat handles.

The four handles were,

A bound solid section of Sarawak cane (a),

Sarawak cane cut in half, glued and bound with no inserts (b),

Sarawak cane cut in half, glued and bound with a single rubber insert (c),

Sarawak cane cut into four sections, glued and bound with 3 rubber inserts (d),

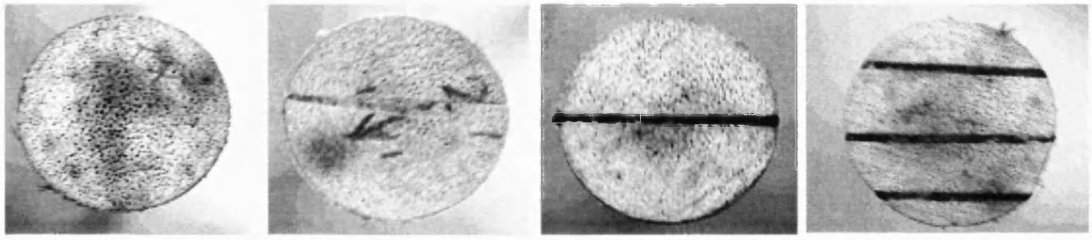

a, b, c, d,

Figure 6.3: Different handle constructions employed.

A three-point bend method was used to establish the flexural stiffness, with the load being applied centrally using an Instron (model 1185). As the length of the handles were standard long handle length, only an outer roller space and handle diameter ratio of 9:1 was possible. The central cross head speed was set at 2mm per minute, with a chart speed of 50 mm per minute to record the deflection and load output. The load was applied until visual deflection could be observed, which corresponded with a compression load of 2kN. The load was not increased any further, due to the possible irreversible damage that may have been caused to the handles. The displacement was recorded in 4 different orientations, when the inserts (or glue line) of the handles were horizontal or vertical (Figure 6.4).

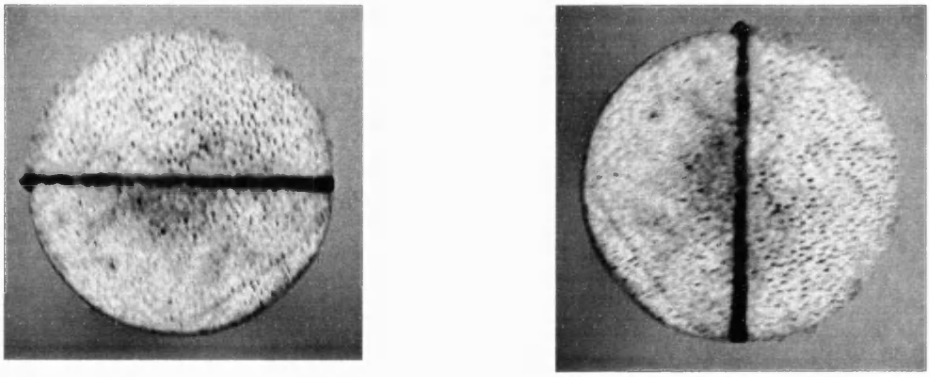

Horizontal. **Vertical.**

Figure 6.4: Orientation of handles during testing.

The handles were tested in the four possible orientations to ensure that the flexural stiffness was not influenced by the construction procedure. This procedure was also carried out on the solid cane section to investigate whether the direction of the cane fibres had an influence on the flexural stiffness. Each orientation was tested five times in an attempt to exclude the influence of compression by the rollers into the Sarawak cane.

6.1.4 Results.

Following the analysis of the deflection traces, it was possible to calculate the flexural stiffness of each of the handles with the inserts either in the vertical or horizontal orientation (Table 6.1).

Handle type	Orientation	Flexural stiffness (GPa)
Solid section	Vertical	13.26
	Horizontal	13.26
No inserts	Vertical	13.35
	Horizontal	12.20
Single insert	Vertical	11.55
	Horizontal	9.32
Three inserts	Vertical	11.00
	Horizontal	6.73

Table 6.1: Flexural stiffness of the different handle constructions

From Table 6.1, it is possible to establish the influence of the inserts and their orientation on the flexural stiffness of the handles. As the number of inserts were increased, the flexural stiffness in the horizontal direction decreased. When the inserts were orientated in the vertical direction, the flexural stiffness was increased relative to the results in the horizontal direction. The flexural stiffness of the handle that was glued was found to have a greater stiffness in the vertical orientation than when the solid section was tested. Finally, it should be noted that no differences were found in the flexural stiffness of the solid cane section regardless of the orientation.

6.1.5 Discussion.

A flexural stiffness analysis of different handle constructions was carried out and analysed. Four different handles were investigated to establish the effects of insert number and orientation on flexural stiffness. Although publications have considered the influence of handle stiffness on

bat performance, little has been reported regarding the actual stiffness of handles currently available in cricket bats.

Inserts are added to the handle of the bat to increase the flexibility, in an attempt to reduce the magnitude of the load and vibrations that the player will experience following impact. However if the handle is too flexible, post impact ball velocity would decrease as energy would be lost during the increased bat deflection. From these results, it is not possible to hypothesize which of these flexural stiffness measurements would have greatest effect on the performance of the bat. However, it would be possible to use these figures in a finite element package to establish their influence on the bat deflection, vibration and associated hand loads, thus establishing the influence of the handle construction type on cricket bat performance.

The greatest degree of flexibility was found when the inserts were oriented horizontally. This was expected as this direction makes the most of the inserted materials flexibility as the horizontal cross sectional area is at its maximum. It was also noted that even the handle with no inserts displayed a reduction in the flexural stiffness when compared to the solid section. This indicates that although the handle was glued together and tightly bound, some slipping between the materials must have occurred. Therefore, the reduction in flexural stiffness of the handle with rubber inserts is not only due to the rubber sections but also the slipping of the material sections over each other.

The flexural stiffness of the handles were found to increase when the inserts were orientated in the vertical direction. This was due to the inserted materials no longer acting along its most efficient plane as the horizontal cross sectional area is reduced. By orientating the inserts in the vertical direction, you have increased the cross sectional area of the stiffer material (the cane), which resists the deflection and therefore increases the stiffness of the handle. Although handles are not currently orientated in this direction, it could be considered that if the aim is to increase the flexural stiffness, then this orientation offers a solution. Rather than increasing the stiffness of the inserted material as suggested by John & Li (2002), which may reduce the damping efficiency, if the rubber inserts are orientated in the vertical direction, the stiffness is still increased without significantly reducing the effect that the rubber has on transient vibrations.

The increase in flexural stiffness with changes in orientation can also be related to some currently manufactured handles. If the handle is constructed using the 16 square sections method, the glue line in the vertical direction may increase the stiffness of the handle as found in this study. However, handles constructed using this square section method may also experience increased slippage during use. Therefore, the flexural stiffness may reduce following extended use of the handle to the possible disadvantage of the player.

Finally, it was found that when the solid section was rotated no differences in the flexural stiffness were calculated. It can be proposed that the orientation of the handle fibres have no influence on the flexural stiffness. Therefore it can be assumed that the fibres are uniformed in diameter, distribution and orientation throughout the handle. As Sarawak cane was originally a living organism, the handles that were tested are only a representation of the responses of all cane handles. However as the handles were all made from the same piece of cane, it was considered that each cane handle had similar properties and therefore it is possible to exclude the effects of different cane sections on the stiffness of the handles.

6.1.6 Conclusion.

The aim of this study was to establish the flexural stiffness of cricket bat handles with different insert numbers. It was found that as the number of inserts increased, the flexural stiffness decreased. This would have a positive influence on reducing the discomfort experienced at the player's hands. The handle stiffness could also be increased by orientating the inserts in the vertical direction, offering scope for future handle design. Although, the findings from this investigation do not enable conclusions to be drawn regarding possible improvements in bat performance, different handle constructions can be used in a finite element modelling package.

6.2 Handle construction and hand loads during controlled cricket ball impacts.

6.2.1 Introduction.

Many of the available cricket bats are now fitted with an oval handle with three inserts rather than the traditional round shape with a single insert. The oval shape has been found to increase the strength and dissipate the shock more efficiently (Laver and Wood, 2001). Titanium and carbon fibre inserts have also been used (Gray Nicolls, Carbo and Titanium series) in an attempt to stiffen the handle and maximise the ball velocity, whilst additionally maintaining the rubber layers to reduce the vibrations and hand loads. As this study is now aware of the influence of handle construction on the flexural stiffness of the different handles, it is the aim of this section to investigate how these alterations in the construction influence the loads that are experienced at the player's hands.

6.2.2 Literature review.

How loads are applied during the impact has a considerable effect on the player's comfort. A player's comfort level can be established using the loading rate of the applied force (Hennig *et al.* 1996 and Milani *et al.* 1997). This is because rate of loading is a reliable method of evaluating a subject's pain perception and thus an estimation of the comfort level during an impact period (Druschky *et al.* 2000). Roberts *et al.* (2001) also noted that it is the length of the impact period that has a direct effect on the perception of comfort. Players evaluate comfort through the perception of the impact load and not necessarily from the magnitude of the impact load itself, due to actions of the nervous system (Kandel *et al.* 2000). It is the use of this perception of the load severity that plays an important role in protecting the body from excessive loads.

Perception is an extremely complex subject and this study does not intend to outline the intricacies of how humans sense and respond to external input signals. However, this study

does intend to explain how player's perceptions to loads are related to comfort following impact. It is important to initially consider that perceptions are not direct records of occurrences as they are subjective analysis of events (Kandel *et al.* 2000). Although, perception is not an absolute measurement and is highly subjective, it does allow tasks to be carried out safely and successfully. The perception threshold of human subjects has been analysed using various methods involving skin indentation depth or applied load (Weber *et al.* 2000). It has been found that the use of skin indentation can vary by up to 25% following the application of the same force on human skin (Greenspan & McGillis, 1990). This is due to the differences in compressibility of the tissue, which is not associated with the mechanical coupling of the skin and the receptors (Greenspan & McGillis, 1990). Therefore, this study considers that it would be more beneficial to measure the force applied at the hands rather than any subsequent indentation of the skin. Following the application of the load, the sensory system quantifies its intensity. Weber *et al.* (2000) reported that it is easier for subjects to perceive a difference between forces of a lower value due to the sensitivity of the sensors and the absolute magnitude of the stimulus. To measure perception of the intensity level, Borg (1970) developed a rating scale of perceived exertion. Although, this scale was originally developed to measure heart patients during walking tasks, it has subsequently been employed during investigations to establish subject perception ratings of load and comfort relative to a reference or standard (eg. Hennig *et al.* 1996 and Milani *et al.* 1997). The comparison of subject perception relative to an applied load has been extensively used during the analysis of shock loads, which could lead to lower limb injuries (eg. Robbins *et al.* 1991 and Kimmeskamp *et al.* 1998). Hennig *et al.* 1996 and Milani *et al.* (1997) also used median power frequency (MPF) and the rate of loading during their analysis of subject perception of impact loads. The MPF of the impact force incorporates the amplitudes of the different frequency components of the force-time signal (Milani *et al.* 1997). Thus a sharper impact force will produce a higher MPF, which the body's sensory system are able to differentiate between rather than the magnitude of independent frequencies.

Previously these studies aimed to investigate whether alterations in material properties and tactile events affect the perceived comfort. Using a similar methodology, it is the intention of this section to investigate how alterations to the material properties of cricket bat handles influence the perceived load and vibratonal shock experienced by human subjects.

6.2.3 Experimental set up.

Six human subjects volunteered to establish the effects of differing handle constructions on perceived and experienced hand loads. Following instructions regarding the nature of the study, the subjects had four Entran load cells (ELFS-B4-500N) fitted at specific locations within their hands (Chapter 10). The signal from the load cells was amplified and then recorded at 1000Hz using a Pico Log data recorder. A load cell was fixed using contact adhesive to the tip of the second finger and the base of the palm of each hand (Figure 6.5). These locations were a combination of those outlined by Knudson (1991b) and Cross (1998b) during the analysis of hand loads in tennis rackets.

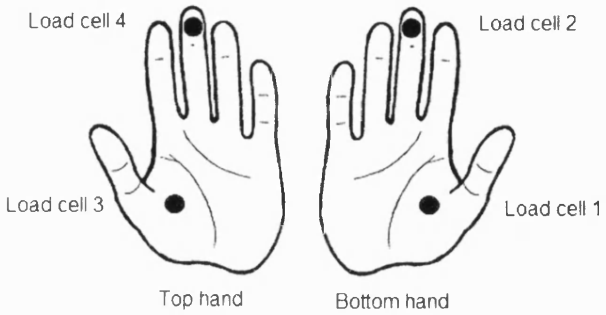

Figure 6.5: Location of load cells on a subject's hand (adapted from Knudson, 1991b).

The four handles described during the previous section were used for this analysis, along with a handle that was covered in a medium-density foam material (Table 6.2). It was considered that this handle construction may dampen the vibrations as well as improve the comfort experienced by the player (Figure 6.6). This handle was presented to the subjects as a standard to act as a comparison for the following impacts as well as being used as a test sample rated relative to itself as the standard, although the subject's were not informed of this.

Handle types and abbreviations.
A solid section of Sarawak cane (solid).
Sarawak cane cut in half and glued with no inserts (split).
Sarawak cane cut in half and glued with a single rubber insert (one).
Sarawak cane cut into four sections and glued with 3 rubber inserts (three).
A solid section of Sarawak cane covered in a medium density foam material (sponge).

Table 6.2: Handle constructions.

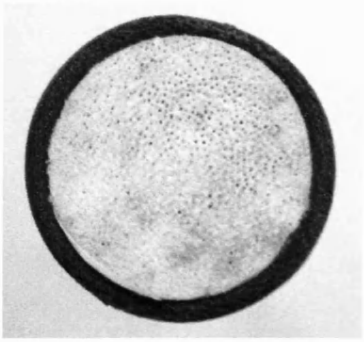

Figure 6.6: Covered handle.

The presentation of the handles was based upon a Latin square calculation. This is a method of establishing a random order, which would make it almost impossible for a subject to estimate. Each of the five handles were presented to the subject 10 times for impact according to the Latin square ordering. Each subject also had a different presentation order calculated in the same manner. Between each test handle, the standard was presented and the subject was informed to use this as a comparison to rate the following impact. To investigate the subject's perception of the impact severity compared to the standard, a Borg scale produced by Hennig *et al.* (1996) was used (Figure 6.7).

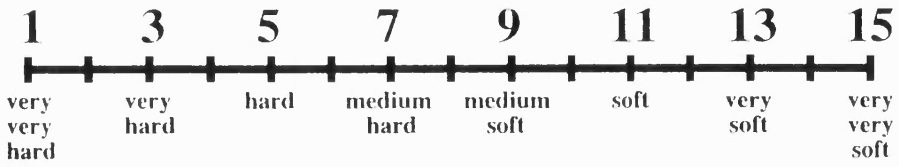

Figure 6.7: Borg Scale for subject perception of impact load (Hennig *et al.* 1996).

Prior to the start of this study, the subjects did not see any of the handles. However, the subject was allowed to experience as many impacts as they required to become accustomed to the sensation of the impact. During this period, the standard handle was used as it was considered that this would aid the subjects in their comparisons during the testing session. Due to the possible discomfort that the subjects may experience during the impacts, an impact load of 15N (pendulum velocity of $3.8ms^{-1}$) was employed. This load had been previously used by Cross (1999b) during the analysis of ball and racket impacts. The impacts were administered using a calibrated pendulum, which had a cricket ball attached to the end (Figure 6.8). The subjects were positioned so the end of the handle was in line with the swinging ball (Figure 6.9). The pendulum also allowed the study to record the load transferred to the handle following each impact to ensure that any subject motion did not affect the experienced loads.

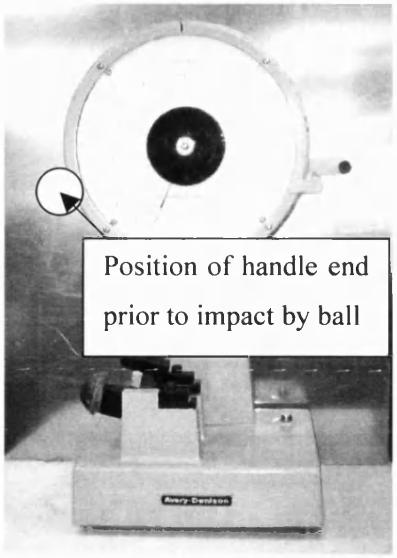

Figure 6.8: Calibrated impact pendulum.

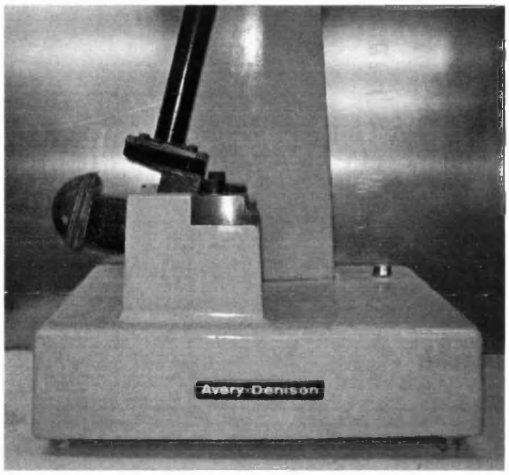

Figure 6.9: Close up of impact location.

Once happy with the testing procedure, a blindfold and earplugs were fitted to the subjects to overcome the problem of adaptive behaviour. Milani *et al.* (1997) had found that following known changes in test samples, subjects made distinct biomechanical adjustments to avoid possible discomfort. Therefore, if the subjects were unaware of the exact changes they would be unable to make any distinct adaptive changes.

Following data collection, the data was analysed using a LabView programme. The programme removed any noise that may have contaminated the signal with a fourth order Butterworth filter. The programme also established the peak force, the time to peak force and calculated the rate of loading. Using a Fast Fourier Transform (FFT) the programme converted the data into a power spectrum, which established the individual modal frequencies and MPF. Each of the ten impacts per handle along with the fifty carried out on the standard handle were analysed before a mean response for each impact condition was established.

6.2.4 Results.

It was found that over 65% of the total impact load was recorded at the first load cell, which was positioned in the palm of the subject's top hand. However, it was found that each of the four load cells recorded similar results. Therefore, the first load cell is displayed in this section

as it was representative of the overall results and the higher loads recorded would have the greatest influence on the subject's perception.

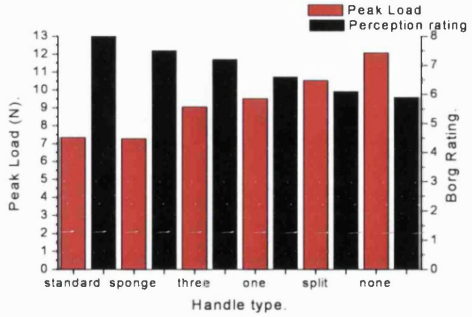

Figure 6.10: Subject perception rating and Peak hand load.

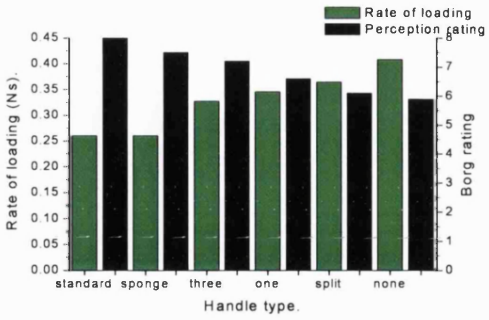

Figure 6.11: Subject perception rating and rate of loading.

From Figure 6.10, there is a distinct pattern that as the peak force increases the subject's perception rating decreases. The subject was able to correctly identify an increase in load and thus an increase in the discomfort experienced. Although the standard and sponge handles were tested independently, they record very similar peak loads. However, the subjects did perceive that the sponge handle was marginally harder when compared to the standard. Figure 6.11 displays a comparison between the perception rating and the rate of loading. As the rate of loading increases the subject's perception rating decreases, highlighting a decrease in comfort following the impact. It is interesting to note that the sponge and standard handles record the lowest rate of loading.

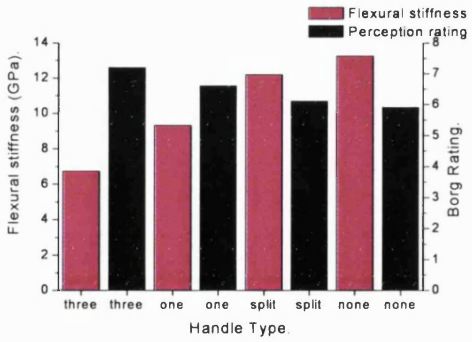

Figure 6.12: Subject perception rating and flexural stiffness.

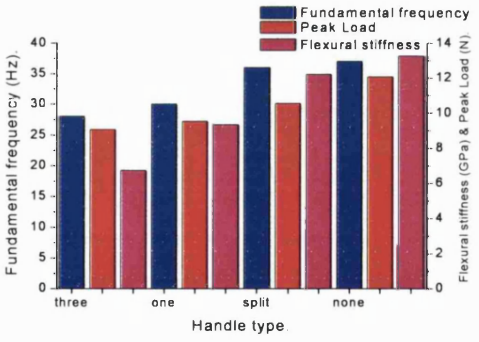

Figure 6.13: Flexural stiffness, Fundamental frequency and Peak hand loads.

Figure 6.12 displays the flexural stiffness (Chapter 6.1) and the subject's perceived rating. As the stiffness increases, the subject's perception rating decreases, indicating a decrease in comfort. Figure 6.13 illustrates the magnitude of the flexural stiffness with the fundamental

frequency and peak loads during the impacts. As the flexural stiffness increases so does the peak load and fundamental frequency.

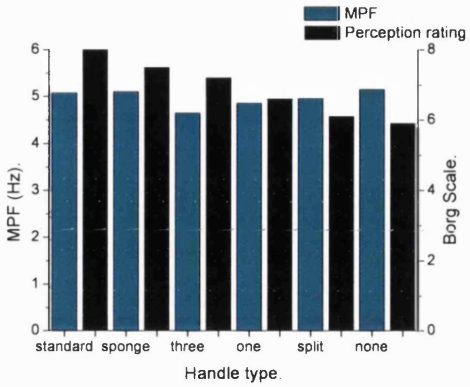

Figure 6.14: Subject perception rating and Median Power Frequency.

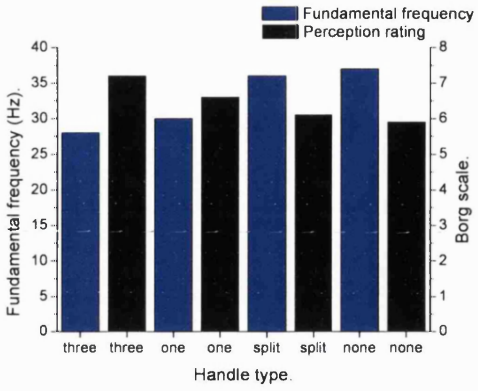

Figure 6.15: Subject perception rating and Fundamental frequency.

Figure 6.14 displays the MPF and the perception ratings for each of the handles. When the standard and sponge handles are excluded, the subject's ratings decrease as the calculated MPF increases. This is not found to occur for the sponge or standard handles. Figure 6.15 compares the subject's perception rating against the fundamental frequency of each handle. As the subject's perception rating decreases (indicating discomfort) the fundamental frequency increases.

6.2.5 Discussion.

The aim of this study was to investigate the influence of handle construction on hand loads and whether differences could be detected using a perception rating system. Five specifically constructed handles were impacted whilst being held by human subjects. During the impacts, hand loads were recorded using load cells and perceived impact severity was measured using a modified Borg scale.

It was found that the solid handle wrapped in foam, which was used as the standard and a test sample repeatedly recorded the lowest rate of loading and peak loads. This was a surprising finding as it was considered that the more flexible handle with the three inserts would not only have record a reduced impact load but also a reduced rate of loading due to an increased

deflection. A reason for this finding would be due to the compression of the foam material, which would have increased the impact period and reduced the rate of loading and applied load recorded at the hands. Goldsmith (2001) reported that shock can be attenuated through the increase in the application time. Therefore by decreasing the rate of loading of the impact force, the perception of comfort is improved. Goldsmith (2001) also noted that the rate of loading is related to the transit times of waves along the specimen. Therefore, by increasing the flexibility and damping properties of the handle, the velocity of the waves will be reduced along with the applied load leading to an improvement in comfort. This concurs with the findings from chapter 6.2, as a reduction in stiffness was associated with an improvement in comfort. Following an increase in the flexural stiffness, the measured load and fundamental frequency increased as they are proportional to the flexural rigidity. A stiffer handle does not deflect as much therefore less energy is lost, increasing the amount transferred to the hands in a short time period. The increase in the measured frequency is also caused by a reduction in the handle deflection.

A subject's perception may differ from the actual recorded measurement data due to how the impact forces are applied. Therefore, subject perception data should be considered with care during the analysis of the striking implements, as simply altering the transference of loads may convince the user that comfort has been improved. The perception results from this study are supported by Stevens & Mack (1959) who also reported a linear relationship between an increase in applied load and a decrease in comfort. Kandel *et al.* (2000) had reported earlier that subjects can often misinterpret the loads of impacts due to other associated factors and therefore report a perceived reduction in the loads when the opposite is occurring. It could be suggested that this did not occur as the subject's accurately perceived an increase in the applied load to the hands. Although, the use of the standard as a test handle did cause some confusion, which may have resulted in some inaccurate perceptions.

The rate of loading is only one of many factors that affect a subject's comfort and variables like peak loads do have a distinct influence on the recorded responses. This study and Hennig *et al.* (1996) found a linear relationship between force loading rate and subject's perception as an increase in rate of loading was associated with an increase in discomfort. This was particularly apparent during the analysis of the handles previously tested for flexural stiffness. However, as the rate of loading increased so did the recorded load transferred to the subject's hands. Therefore, this would have also influenced the subject's response following the impact period.

The distinct differences between the loading rates and peak loads (as reported during lower limb impacts eg. Fisher, 2001) are not identified due to the considerably shorter impact period between the ball and handle, thus any differences are small and not significant.

Reynolds *et al.* (1977) reported that an individual's pain perception was principally influenced by the vibrations experienced. Therefore, the frequency of the vibrations may have the greatest effect on perception ratings following impact. A linear relationship was found between the MPF and subject perception, identifying that as the accumulative vibrational frequencies (MPF) increased, the subjects reported a reduction in comfort. This was supported by Hennig *et al.* (1996), Milani *et al.* (1997) and Roberts *et al.* (2005a) during their analysis of subject perceived comfort and recorded MPF. Roberts *et al.* (2005a) also noted that golf strikes that subjects recorded to have a high pleasantness rating occurred when the amplitude of the vibration was perceived to be low. These findings offer some aid to future development of cricket bats, as it is important to remember that a design should try and make the amplitude and frequency of the vibration as low as possible to minimise possible discomfort following impact.

Roberts *et al.* (2001) noted that the sound of an impact is closely related to player perception and does have an affect upon subject response. Roberts *et al.* (2005b) added that loud, sharp and long sounds were perceived to feel most uncomfortable. It can be considered that as there were limited alterations to the impacting material and the duration of the impact, these factors outlined by Roberts *et al.* (2005b) can be discounted.

Although the subjects correctly identified the differences between the MPF and fundamental frequencies for each of the handles, the differences were limited. This is because more drastic structural alterations must be made to significantly modify the vibrational frequencies. Therefore, even though the subjects were able to report the differences between the handles, the differences in their structure are not significant enough to make considerable effects on the excited frequencies. This supports the suggestion that perception ratings are a culmination of all the post-impact responses and not based specifically on one variable.

The Borg scale has been considered as a subjective analysis method rather than a scientific measurement of comfort and perceived impact severity (Annett, 2002). However, as it is an established method of measuring human perceptions of comfort, the use of it was justified. It is

recognised that any method of perception analysis will be subjective and therefore influenced by the moods of the subject themselves. However, the effectiveness of the Borg scale to produce accurate and reliable results has been outlined by Hennig *et al.* (1996) and Milani *et al.* (1997). This study has found that perception data can be used as a method of identifying distinct factors that influence the responses of the user. Although, it is important to consider that these results are not scientific measurements, they do offer insight into the responses of subjects within established guidelines.

Throughout the testing session, the impact load was measured for both the test and standard impacts. It was found that there was only a 1% difference (SD of ±2%) in the transferred load to the handle following each impact. It was a concern that the reactions of the subjects following each impact may alter the impact force and the perception ratings. Miliani *et al.* (1997) had reported that there was a distinct relationship between biomechanical variables (including alterations in motion) and perception scores. However, it was found that there was little difference in the load transferred to the handles. Hennig *et al.* (1996) had earlier reported that the subjects are able to detect the relatively small deviations in materials properties. This concurs with the findings of this study, as the subjects were able to successfully differentiate between the handle types using the perceived scale although the differences were relatively small.

The impact load used during this study was 15N, which is extremely low compared to the forces that are normally experienced during ball and bat impacts. However, this load had been used during tennis racket investigations (Cross, 1999b) and so can be conveyed to cricket bat impact analysis. In particular, the frequency of the vibration will not be altered following changes in the impact load only the amplitude. The frequency of the vibration is also dependant upon the flexural stiffness of the handle and this would remain unchanged with an increase in the impact load. Regarding the differences in the recorded impact loads, it can also be assumed that the responses are linear as the handle would not enter plastic deformation. Therefore, the small differences reported by this study will become amplified and more apparent to the player's following ball impacts with higher forces.

6.2.6 Conclusion.

It was the aim of this study to investigate the influence of handle construction on the measured and perceived loads transferred to a player's hands following an impact. It was found that as the flexural stiffness of the handles increased so did the measured loads, rate of loading, vibrational frequency and discomfort perceived by the subjects. The main conclusion is that the construction of the handles will have a direct effect on the comfort experienced by the player during a cricket ball impact and a handle that vibrates at a lower frequency offers scope for improved player comfort.

7 MICROSTRUCTURE OF CRICKET BAT WILLOW.

7.1 Introduction.

According to the rules of the game, the blade of the bat must be made from wood. Although the species is not specified, willow has been traditionally used. Cricket bat willow is durable enough to withstand repeated impacts and can absorb some of the shock following the impact that would cause damage to other species of wood (Edlin, 1973). The weight of the wood is considered enough to produce the required momentum for effective ball striking, but not too much to induce fatigue during longer innings. Previous research (eg. TRADA, 1980) has examined the structure and basic material properties of willow, although little has been reported regarding its structure following bat construction. Published reports have also produced contradictory results that seems inconceivable when related to other wood based studies (eg. Grant, 1998b). Therefore, a series of mechanical tests to establish the cellular structure, density and flexural stiffness has been carried out on a grade two willow cricket bat that was acquired from a manufacturer following the completion of the construction process.

7.2 Willow.

There are many species of willow (*Salix*) in Europe but the principal species used for cricket bats is the *Salix Alba* or cricket bat willow. *Salix Alba* is a fast growing hardwood, deciduous with broad leaves and wide annual rings. It is grown in damp areas near water and is often felled well before it reaches its maximum height of 80ft. Willow consists of a whitish sapwood and a pale pink heartwood with an even and straight grain (Findlay, 1975). The quality of the bat is considered to be dependant upon the number of growth rings present in the blade and that between 5 and 8 is recommended (Sayers *et al.* 2000). However, it is the distribution of the cellulose within the structure of the willow that has the greatest effect on the bat's performance rather than the number of annual rings (Grant & Paisley, 1997). This is because the stiffness of the wood is proportional to the volume of cellulose in the cell walls. Therefore, additional cellulose in the walls increases the stiffness of the bat, which may increase the post impact ball velocity.

As highlighted during chapter 2, when a bat is cut (Figure 7.1), it has the long axis running parallel to the tree along the longitudinal axis (Figure 7.2). Therefore the face of the bat shows the radial longitudinal section and the distinctive annual rings that run down the face (Figure 7.3).

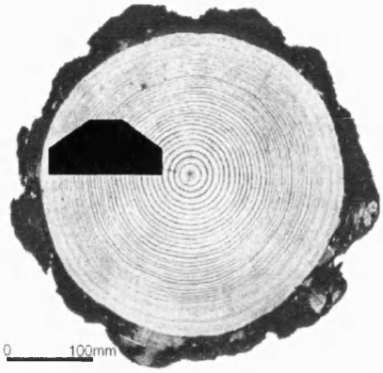

Figure 7.1: Orientation of a bat across the annual rings of a tree (modified Dinwoodie, 2000).

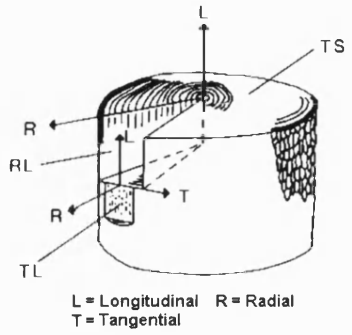

Figure 7.2: Directional orientation of a tree (Ansell, 2004).

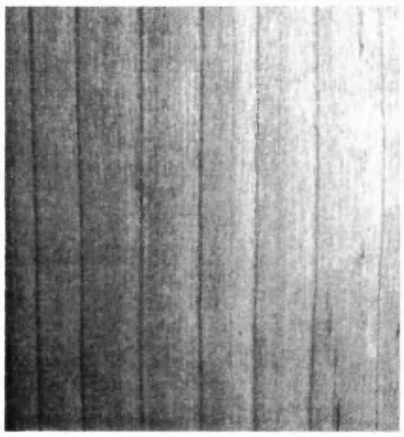

Figure 7.3: Annual rings across the face of a bat.

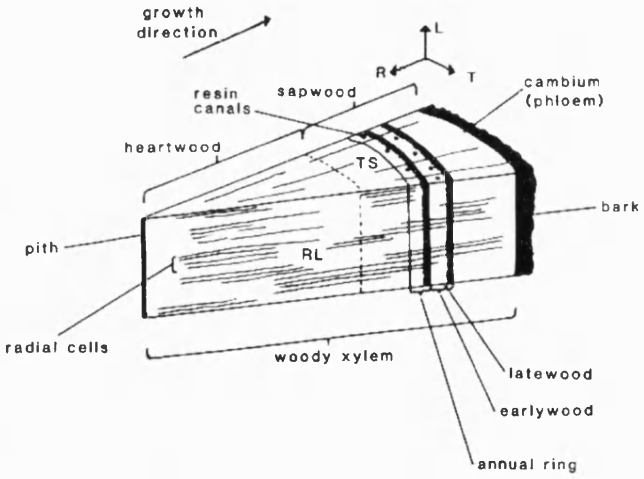

Figure 7.4: Wedge shaped cut away section (Ansell, 2004).

From Figure 7.4, the components that make up a cross section of a tree including the annual rings can be seen. The annual rings are an indicator of the growth period of that tree during the year, which is split into two subsections of late and early wood. The early wood in hardwoods is characterised by large diameter vessels and the latewood consists of smaller diameter vessels (Dinwoodie, 2000). Figure 7.4 also shows the sapwood section, which is used for food storage aiding the growth of the tree, whereas the heartwood section is no longer used for this purpose. The cambium is the live section of a tree, which is positioned under the bark and subdivides radially, thus increasing the width of the tree. Each of these parts throughout the cross section

of the tree have different mechanical characteristics, thus influencing the post impact responses of a cricket bat.

7.3 Cellular structure.

The microstructure of the cricket bat willow has been previously investigated (Grant, 1996 and Grant & Nixon, 1996a). It was found that a section of willow has evenly spaced sap channels (40 per square mm) with a diameter of 100μm and long hollow fibres with a typical diameter of 15-20μm (Figure 7.5) (Grant & Nixon, 1996a). It is this cell structure that contributes to the strength of the wood (Sayers *et al.* 2000).

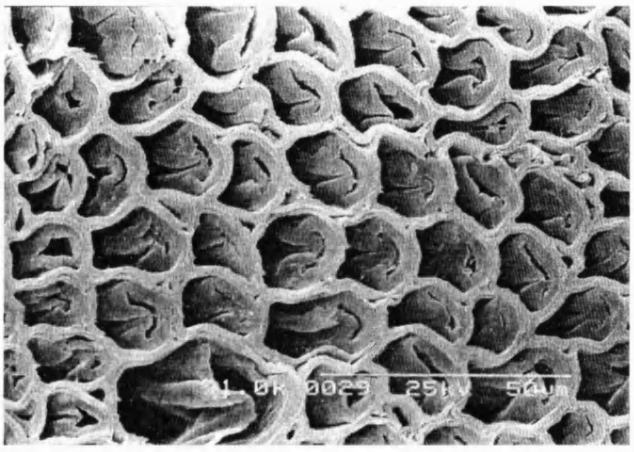

Figure 7.5: Crushed cells of English willow (x1000), (Grant & Nixon, 1996a).

Figure 7.5, displays a section where there is cellular damage caused by lateral compression possibly caused during the pressing or knocking in process.

To investigate the influence of cricket bat construction on the cellular structure, a first class cricket bat was divided into samples for analysis under an electron microscope. The bat was of grade 2 willow, and contained a section of heartwood along one edge. Timber is graded from 1 (best) to 4 (lower quality) prior to purchase. This system is based upon the amount of imperfections (knots and voids) and variations in natural colour. Samples were taken from the face (which had been pressed and knocked-in), the middle (central section, where each sample was surrounded by a minimum of 20mm of willow unaffected by the construction process) and the toe of the bat (Figure 7.6).

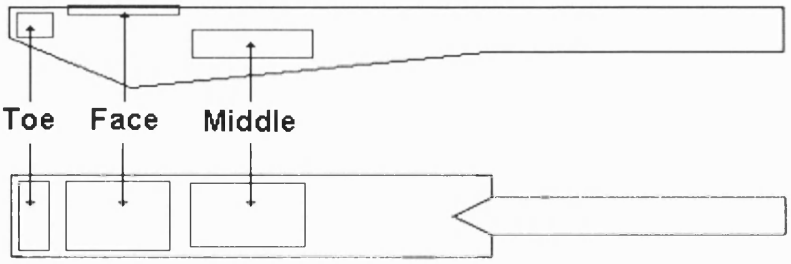

Figure 7.6: Sample locations for electron microscope analysis.

The wood samples were boiled for 1 hour in distilled water before samples of 5mm cubes were cut using a flat razor blade. The samples were organised so the cross section was visible, making it possible to magnify the vessels and surrounding cells of the willow (Figure 7.7). Ten samples were taken from each of the locations from both the sap and heartwood areas. Following preparation and drying, each sample was placed in the electron microscope where the cell structure could be viewed.

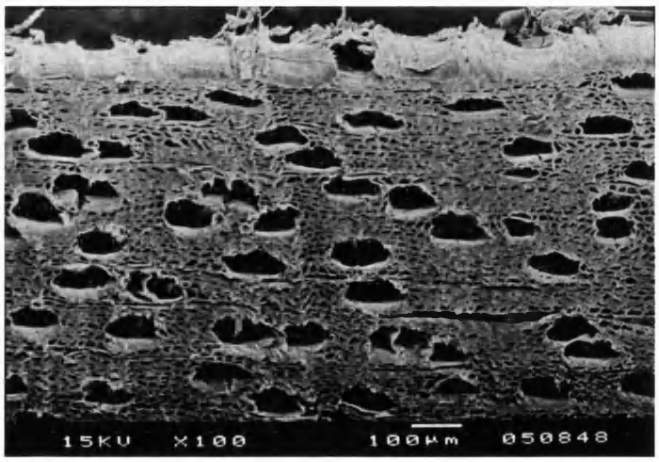

Figure 7.7: Distribution of vessels from a sample of willow taken from the face of the bat.

Figure 7.7, shows the vessels to be roughly evenly distributed and that they decrease in height as they become closer to the face of the bat (top of the picture). The shape and size of the vessels are due to the non-standardised method of knocking-in and pressing. Vessel size and distribution will affect the post impact ball velocity, propagation of vibrations and load distribution following impact as the density and thus the stiffness of the wood will increase.

From Figure 7.8 and Figure 7.9, the difference between the damaged and undamaged vessels can be seen. Much of the damage will have been caused during the construction processes.

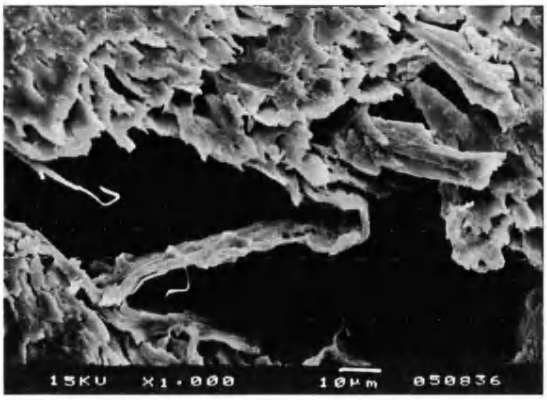

Figure 7.8: Partially crushed cells close to the face of the bat.

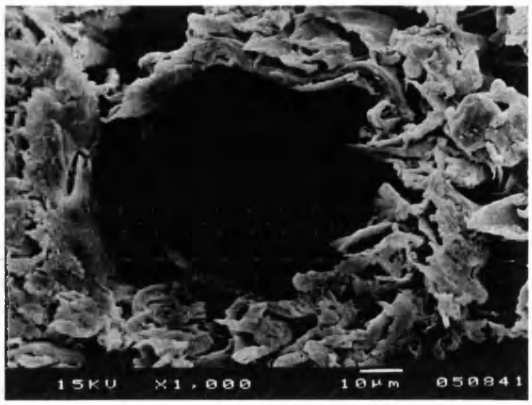

Figure 7.9: Undamaged cell from the middle of the bat.

Using the Optimas imax analysis system, the diameter (perpendicular distance) and breadth (vertical distance) of each cell was measured (Figure 7.10). The Optimas system measures the dimensions of the samples by identifying areas of different contrast, these measurements can then be analysed to produce an average cell size for each sample. The influence of sample location on cell size could also be established.

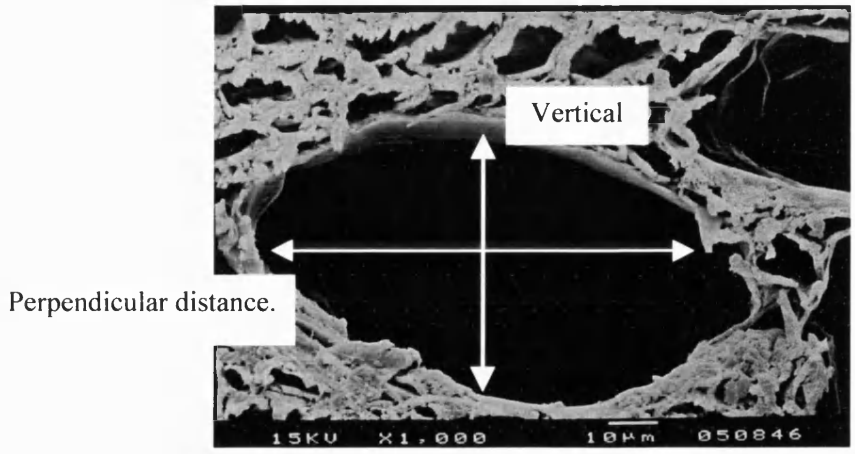

Figure 7.10: Measurement directions of vessels.

Willow type	Location	Perpendicular distance (μm)	Vertical distance (μm)
Heartwood	Middle	169.16	149.91
Sapwood	Middle	159.32	146.00
Heartwood	Bottom	112.22	94.62
Sapwood	Bottom	119.32	95.67
Heartwood	Knocked-in	95.41	37.42
Sapwood	Knocked-in	89.31	26.17

Table 7.1: Effect of wood type and location in the bat on vessel dimensions.

Table 7.1, shows a marked difference between the perpendicular and vertical distances of the willow type with the location in the bat. The vertical distance of the cell decreases by over 100μm when a knocked-in sample is compared to a sample from the middle of the bat. There is no distinct difference between the dimensions of the heartwood or sapwood vessels. Finally, the samples taken from the middle of the bat are over 50μm larger in the vertical direction when compared to the cells taken from the bottom of the bat.

The perpendicular and vertical distances from the knocked-in samples decrease due to the compression of the vessels cell walls. As they are crushed the walls fill the vessel resulting in a reduction of the perpendicular and vertical dimensions. From Figure 7.8, the collapsing vessel wall has reduced the diameter of the vessel on the right. The distances of the sapwood samples concur with the findings of Grant (1996) who reported an average perpendicular distance of approximately 100μm. A section of wood with bigger vessels will be more responsive as it would enable greater degrees of compression and spring towards the ball (thus a higher COR). The reduction in the dimensions of the bottom vessels are mainly caused by the repeated pressing of this area to avoid fracture following impact.

There is little difference in the vessel dimensions in the sapwood and heartwood due to the heartwood originally being sapwood. The Forest Products Society (1999) reported that when sapwood changes to heartwood, no cells are added or lost, nor do the cells change shape. Therefore, it would be expected that the dimensions of the heartwood and sapwood vessels are similar.

7.4 Density.

The density of the wood is dependant upon the species of willow and is determined by the amount of wood substance present per unit volume, although Dinwoodie (1989) noted that this value will be affected by moisture and extractives. Grant & Paisley (1997) noted that the range in weight of the bats that are available are entirely due to the natural variations in the moisture content rather than geometrical dimensions. Although moisture content is often controlled, the density of English willow can vary by ±10% (Grant & Paisley, 1997). Grant & Paisley (1997) observed that differences in cricket bat performance was due to variations in density, stiffness and the distribution of growth rings within the wood. Table 7.2 displays density measurements of willow (moisture content approx. 12%) and samples specifically taken from cricket bats.

Author.	**Density of willow (Kg/m^3).**
Lavers (1969)	417 (cricket bat), 433 (white)
Titmuss (1971)	448-608
Findley (1975)	450
TRADA (1980)	340-420
Farmer (1981)	336-416 (cricket bat)
Knowles *et al.* (1996)	440
Grant & Paisley (1997)	621 (cricket bat)
John & Li (2002)	535 (cricket bat)

Table 7.2: Density measurements from cricket bat willow studies.

In Table 7.2, the density reported by Grant & Paisley (1997) is considerably larger (20% higher than indicated by Lavers, 1983) than any of the other published results. Grant & Paisley (1997) analysed 100 randomly positioned samples of 0.5mm squares, which each contained approximately 10 vessels. It was found that the density varied by about 20% along the length of the blade and ranged from almost $800Kg/m^3$ to approximately $500Kg/m^3$ (Figure 7.11) depending on sample depth (Figure 7.12). This author considers these findings to be curious as none of the previous studies shown in Table 7.2, have reported such great deviations or such high-density figures.

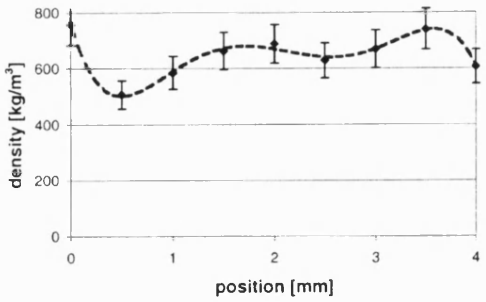

Figure 7.11: Density distribution of the blade (Grant & Paisley, 1997).

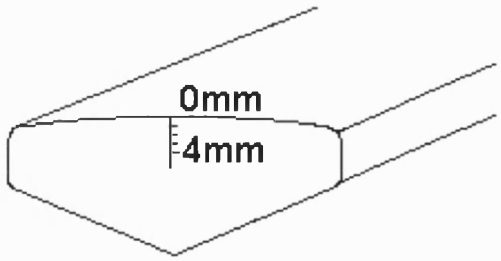

Figure 7.12: Orientation of samples used by Grant & Paisley (1997) relative to a cricket bat.

From previous findings (Table 7.2), the density is almost half the values reported by Grant & Paisley (1997). Even if the reported increases in density were caused by changes in moisture content (±10%) and knocking-in (±20%), this would not lead to such a great increase in density when compared to values of willow reported by Lavers (1969).

Due to the considerable difference in reported results, the density of willow (both heartwood and sapwood) from a grade two cricket bat were measured. The bat had been pressed and knocked-in during manufacture, which enabled the density of knocked-in/pressed and undamaged cricket bat willow to be investigated. Twelve 10mm cubes that included a knocked-in face were tested along with ten 10mm cubes from the undamaged middle of the bat (as explained in section 7.2) and ten 10 x 10 x 2mm samples. These were included to investigate the effects of the knocking-in process. Samples of this number were taken from both the heartwood and sapwood areas of the bat. To determination the density of the selected samples, a British Standard (BS 1902 : Part 1C : 1967, Section 10) was used.

Using this procedure, it was possible to determine the influence of location on the density of cricket bat willow, from a commercially available, hand manufactured bat.

Sample and location	Density (Kg/m³)	Standard deviation.
Heartwood (middle)	348.54	±2.094
Sapwood (middle)	356.69	±4.81
Heartwood (knocked-in cube)	376.34	±15.01
Sapwood (knocked-in cube)	388.58	±12.98
Face of the blade (knocked-in)	416.98	±6.25

Table 7.3: Density and standard deviation of the willow test samples.

Table 7.3 displays the average density values for each section from a first class cricket bat. The sapwood has a lower density than the heartwood at the same location, although these differences are relatively small. The density of the knocked-in sections are greater than wood from the undamaged middle samples. Finally, the greatest density is recorded on the face of the bat. The face samples are 19% denser than the undamaged middle samples. Deviations in the measured results were also greatest from the knocked-in cubes.

7.4.1 Discussion.

The aim of this section was to measure the density of cricket bat willow from a grade two cricket bat using a British Standard (no. 1902) test procedure. The results fell within the boundaries outlined by Farmer (1981) and TRADA (1980). In particular, Lavers (1969) reported that the density of cricket bat willow was 417 Kg/m^3, which almost identically matches the results of this study (416.98 Kg/m^3), although Lavers (1969) did not highlight whether his samples had been knocked-in or pressed as were the particular samples used by this study.

The density of the willow is dependant upon the moisture content, time and force applied during the pressing and knocking-in and the quality of the wood selected for testing. Thus, it can be assumed that the differences in the measured density reported in the literature are due to the natural variations. Therefore, it is unwise to compare literature values too closely. However, Grant & Paisley (1997) recorded a density of between 500 and 800 Kg/m^3 during their analysis of cricket bat willow. The authors do not specify the test method used, so there may be an error in the calculation. The difference between the density of the undamaged middle and the knocked-in samples found by this study and Grant & Paisley (1997) are closely correlated (19 and 20% respectively). Therefore, although the measured densities are lower, the proportional effects of the knocking-in process are very similar.

Although a minimum of 10 samples were taken from each location (total 52), this only makes up 1.5% of the total dimensions of the bat. Therefore a comparatively small area was analysed relative to the size of the cricket bat. However, there is little deviation in the results when samples were taken from the undamaged middle and the face of the bat. Therefore, it can be

assumed that the middle and knocked-in face samples give an accurate estimation of the density of grade two-quality cricket bat willow. A greater deviation was calculated when the knocked-in cubes were analysed. It is suggested that this is due to the non-systematic nature of this process and that knocking-in only affects the top 2mm of the cube, thus the samples would include both knocked-in and undamaged sections.

The density of the heartwood samples from the middle of the bat were greater than the sapwood samples from comparable locations. Dinwoodie (1989) and (2000) noted that heartwood has a decreased permeability when compared to sapwood due to the increase in deposits left inside the cells. Thus preventing the passage of water through the vessels and increasing the measured density. This study considers that the differences in the measured density of the heartwood and sapwood samples is predominately due to cellular deposits as the samples were treated in the same manner and taken from comparable locations. If was also found that the knocked-in sapwood samples had a higher density than the knocked-in heartwood samples. This may be due to the heartwood cells not being crushed to the same extent as the sapwood samples, as heartwood is more durable and resistant to compression (Dinwoodie, 1989). The knocked-in samples possess the highest density as knocking-in crushes the surface cells stopping water from entering the sample and thus, increasing the density.

Density can be used to estimate cricket bat performance as higher density materials should have higher flexural rigidities, which has been associated with an increase in post impact ball velocity. Dinwoodie (1989) noted that an increase in the density of the wood increases the material present in the cell cavities, which has a marked effect on the strength properties. It may be an advantage to a player to select a bat of a known density. The Forest Products Society (1999) reported that a piece of wood (bat) with a high growth rate (many annual rings) and a large percentage of latewood results in a higher density. Therefore, it would be possible to select a higher density bat purely through careful visual analysis.

7.5 Flexural stiffness.

This study also investigated the flexural stiffness of the cricket bat willow. Although this has not been previously measured, Grant (1996) suggested that the surface layer of a bat would be stiffer than the natural wood. Therefore it was the aim of this study to investigate this statement.

Table 7.4, displays the flexural stiffness figures used in previous studies involving the analysis of cricket bats. The reported values are almost identical, although two of the studies (Grant, 1998 and John & Li, 2002) did not report how they measured the flexural stiffness of cricket bat willow and therefore they may have used literature values.

Investigation	Willow flexural stiffness (GPa).
Lavers (1961)	6.6 (cricket bat), 5.8 (white)
Farmer (1981)	6.6 (cricket bat), 5.8 (white)
Grant (1998)	6.6
John & Li (2002)	6.67

Table 7.4: Flexural stiffness of cricket bat willow.

A grade two cricket bat was cut into five samples measuring 15mm x 15mm x 180mm. The samples were taken to include the face of the bat, which had been rolled and knocked-in ready for immediate use in a game (Figure 7.13).

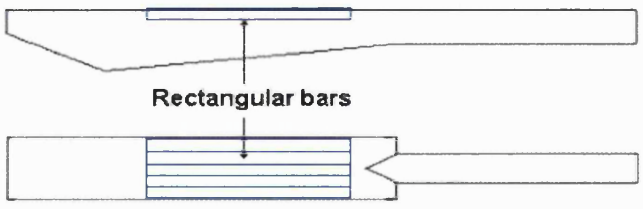

Figure 7.13: Location of rectangular samples taken from a cricket bat.

The mechanical properties of the samples were established using a three-point bending method using an Instron (model 1185). Due to the limitations in the size of the testing equipment, the ideal roller span to diameter ratio of 20 was not possible, although a ratio of 11 was achieved

(Figure 7.14). The central cross head speed was set at 2mm per minute, with a chart speed of 50 mm per minute to record the deflection and load output. The load was applied until visual deflection could be observed, which also corresponded to a compressive load of 500N. This was established as the maximum load for each of the rectangular samples being tested.

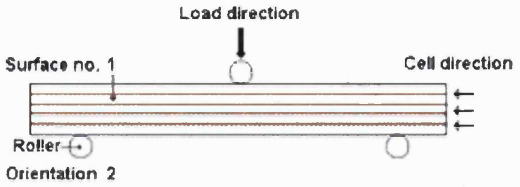

Figure 7.14: Grain direction (horizontal) during sample orientation 2 (side view).

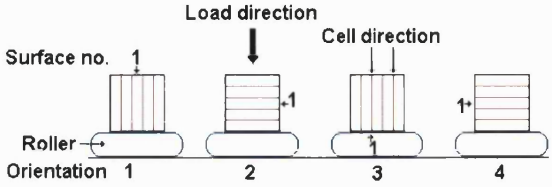

Figure 7.15: Orientation and grain direction of rectangular samples (end on view).

Displacement of the central roller was recorded in 4 different orientations, to also investigate whether the direction of the grain influenced the flexural stiffness of the samples (Figure 7.15). Each orientation was also tested three times in an attempt to exclude the influence of roller compression into the willow samples, which was found to occur during the first trial. The four orientations enabled the study to measure the flexural stiffness when the cells were vertical and horizontal six times for each. Therefore a total of twenty-four deflection tests were possible with twelve in each cell direction. It was not considered necessary to measure the flexural stiffness of the heartwood section as it has been reported that heartwood and sapwood have equal mechanical properties (Forest Products Society, 1999). This previous finding is also supported by the results displayed earlier as little difference was found during density or cellular structure analysis.

Following the measurements of the sample deflection versus the application of the load, it was possible to establish the flexural stiffness in both orientations.

	Orientation of the grain.	
	Vertical (GPa)	**Horizontal (GPa)**
Average	9.39	7.03
Standard Deviation	±1.28	±0.47

Table 7.5: Calculated flexural rigidity of cricket bat samples.

From Table 7.5, the greater flexural stiffness is recorded when the sample was tested with a vertical grain orientation (Sample orientation 1 and 3, Figure 7.15). Dinwoodie (1989) had

earlier noted that the grain orientation will affect the measured elastic modulus, although the flexural stiffness in the vertical orientation is greater than had been previously reported. However, the samples did include a face that had been pressed and knocked-in during manufacture, which compresses the cells and proportionally increases the flexural stiffness. When the cell direction was horizontal, the values are close to the previously published figures for cricket bat willow.

It is believed that the flexural stiffness increases when the grain is vertical due to the effect of the cellular structure. The Forest Products Society (1999) reported that the vertical orientation of growth rings maximised the elastic modulus and resistance to compression. If the grain is orientated perpendicular to the flexion direction (vertically in this study), the more densely packed cells along the edges of the growth rings makes it more difficult to deflect. However when the wood sample was rotated (horizontal set up), the densely packed cells lie in the direction of the flexion, therefore they have a lower cross sectional area and have a reduced effect on the measured stiffness. Thus, the orientation of annual rings perpendicular to the deflection of the bat maximises the stiffness of the bat.

7.6 Chapter conclusions.

All of the sections investigated during this chapter are interlinked, as the crushed cellular structure is associated with an increase in density and the enhancement in the flexural stiffness of the wooden samples. This is advantageous to the player as an increase in flexural stiffness is associated with an increase in post impact ball velocity and thus an improvement in performance. Finally, by crushing the cellular structure, the resistance to indentations and splitting is improved as the density of the sample is increased. Therefore, the face of the bat may last longer before showing signs of mechanical deterioration and a reduction in performance.

8 THE EFFECTS OF BLADE DESIGN ON THE MOMENTS OF INERTIA.

8.1 Introduction.

The moment of inertia is the resistance to rotational acceleration (Beak *et al.*, 2000) and is dependant upon the distance to the axis of rotation from the end of the implement and its total mass (Kreifeldt & Chuang, 1979). Mitchell *et al.* (2000) reported that a heavier racket will have a higher moment of inertia and require greater effort to achieve the same speed as a lighter racket. Although, the larger mass of the racket does enable the ball to be struck faster. The moment of inertia is also a contributor to the feel of an implement during impact (Kreifeldt & Chuang, 1979). This is because feel encompasses feedback from physical (balance and weight) and psychological (sound and vision) inputs during the use of the equipment. The aim of this chapter is to establish the moment of inertia of cricket bats and the effects of structural design on this variable.

8.2 Literature review.

The moment of inertia of a tennis racket is made up of three independent moments (Brody, 1985). These moments are, weight (zero moment), balance (first moment) and dynamic (second moment). The first moment is related to the amount of force required to raise the racket head (Brody, 2000). Within cricket, it could be suggested that player's often establish the first moment during the selection of a new bat, although they refer to this as the pick up. Pick up is an analysis of the feel of the bat in the hands as it is the combination of the force required to execute the back-lift, the balance of the bat and the location of its centre of gravity. If the centre of gravity is closer to the axis of rotation, it is considered easier to lift and feels lighter, although the player may find it harder to achieve the same swing speed as a bat with a lower centre of gravity and larger first moment.

The second moment can be measured along two different axes, either perpendicular to the plane of the frame (x-axis) (swing moment) or along the plane of the racket (z-axis) (polar moment) (Brody, 2000) (Figure 8.1).

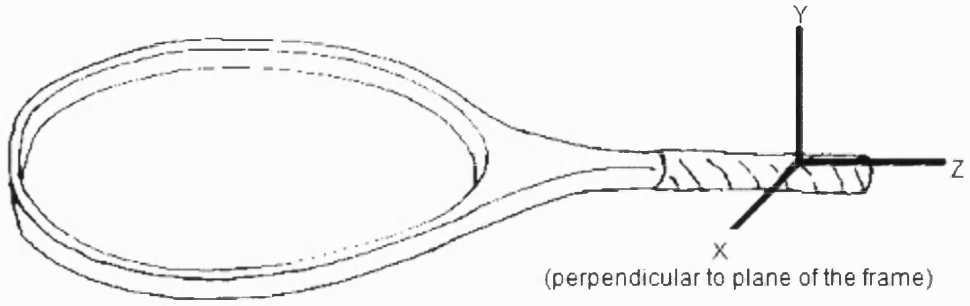

Figure 8.1: Axes of a tennis racket through the location of a tennis player's grip (Brody, 2000).

The swing moment (x-axis) determines the manoeuvrability of the racket about the wrist and how much force is required to swing the racket (Brody, 2000). A racket with a lower swing moment is more manoeuvrable but a larger swing moment produces a greater post impact ball speed (Elliott, 1982 and Brody, 2000). However, if a lighter racket is swung sufficiently fast, the loss in ball speed can be made up. Mitchell *et al.* (2000a) added that there is an important relationship between the rackets moment of inertia, the generation of racket head speed and the final ball velocity.

The second moment of inertia can be increased by enlarging the mass or by spreading the mass further from the axis of rotation (Kreifeldt & Chuang, 1979). This has been found to improve the stability by reducing unwanted racket rotation, improve control and raises the coefficient of restitution (Brody, 1987). By increasing the width of the racket by 10%, the polar moment of inertia will increase by 20% (Brody, 2000). This is due to a reduction in the twisting motion that would have otherwise decreased the energy transferred to the ball. Noble & Eck (1985) earlier suggested that increasing a baseball bats moment of inertia would displace the centre of percussion towards the end of the bat. Therefore, a player could take advantage of the greater swing velocity at the tip and the benefits of impacting the centre of percussion.

To establish either the first moment (balance) or the second moment (swing) a simple torsional pendulum can be employed (Brody, 1987 and Brody, 2000). This can be achieved by

suspending the racket on a wire and measuring the period of torsional oscillations of the implement (Brody, 1985) (Figure 8.2). It is then possible to convert the results into moment of inertia about the centre of mass using Equation 8.1. Brody (1985) described the results as the swing weight of the racket as they represent how heavy the implement feels to the player when it is being swung.

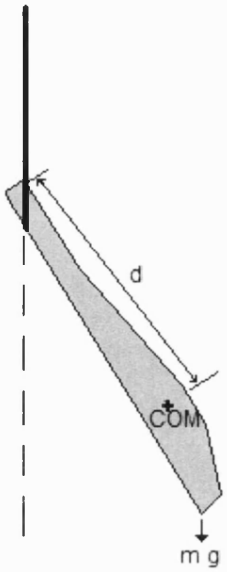

Figure 8.2: Experimental set up of analysis technique.

$$I = T^2 mgd / 4 \pi^2$$

Equation 8.1

where, I is the rotational moment of inertia, T is the average torsional oscillation time, m is the mass of the implement, g is gravity and d is the distance to the centre of mass from pivot point.

8.3 Experimental set up.

Due to the associations between moments of inertia, performance and comfort, it is important to establish the influence that structural design has upon the measured swing moment of inertia. Five first class cricket bats were selected due to their distinct visual differences in structural design. Each bat had approximately the same mass and external dimensions (width and length) (Table 8.1).

Bat	Abbrev -iation	Blade dimensions (Length, width, thickness)			Design feature.	Dimensions (length, width, scoop depth / spine height).		
Fearnley	DF	560	108	59	Traditional	No distinguishing features.		
Gray-Nicolls	GN	560	108	59	4 oval scoops	185	28	14
Slazenger	Slaz	560	108	59	6 small scoops	35	10	10
County	Hunts	560	108	59	2 long scoops	260	22	11
Kookaburra	Probe	560	108	59	Central spine	490	45 (mean)	8

Table 8.1: Bat description and feature dimensions (mm) of the tested bats.

Due to these similarities, the exact effect of structural design on the moment of inertia could be established. Primarily, it was necessary to locate each bat's centre of gravity. This was achieved using a fulcrum to establish the point of balance for each of the bats (Figure 8.3).

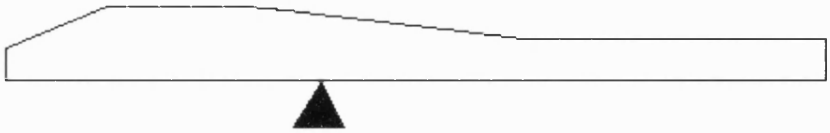

Figure 8.3: Locating the centre of mass for a cricket bat.

Once the COM was established, twine was attached to the ceiling and fixed about the top of the handle as outlined by Brody (1985). This attachment location also ensured that the twine did not interfere with the motion of the bat. The twine measured 0.8m in length and was selected due to its resistance to stretching during the application of a load. The bats were then drawn back 0.3m before being released to swing freely back and forth. When the bat was released a stopwatch was started and five full oscillations were timed to establish an average oscillation time. This process was repeated five times for each of the bats selected. Using data collected from the oscillation tests and Equation 8.1, it was possible to calculate the swing moment of the cricket bats. Brody (1985) reported that this method of measuring an implement's moment of inertia was within 1% accurate.

8.4 Results.

Following calculation, the swing moment of inertia (I) for each of the bats investigated could be compared (Table 8.2).

	Slaz	GN	Hunt	DF	Probe
Weight (Kg).	1.149	1.172	1.131	1.283	1.249
Distance to COM from fixation (m).	1.28	1.26	1.28	1.31	1.35
Average single oscillation (sec).	1.140	1.138	1.142	1.133	1.158
I ($Kg.m^2$)	0.475	0.475	0.470	0.537	0.563

Table 8.2: Components of the swing moment of inertia for each bat tested.

From Table 8.2, it can be seen that all of the calculated components are closely matched for the five bats investigated causing the moments of inertia to be closely correlated. The maximum difference in the moment of inertia is $0.093Kg/m^2$ (15%) between the Probe and Hunt bats.

8.5 Discussion.

The aim of this chapter was to investigate the influence of the structural design on the swing moment of inertia using a torsional pendulum method established by Brody (1985). There are no reports of this method being used during cricket bat analysis, although it would be advantageous to establish each bat's moment of inertia. It was outlined that an implement's moment of inertia is a contributor to the feel (Kreifeldt & Chauang, 1979), balance and manoeuvrability (Brody, 1987). As each of the bats had different structural designs, it was possible to establish whether this influenced their moment of inertia. From the results, it was found that these changes to the bats blade shape do not have any considerable affect. It was considered that this may be due to the bats being roughly the same weight and constructed to the same dimensions. Kreifeldt & Chauang (1979) did report that the moment of inertia is related to the mass of the object, although, Kreifeldt & Chauang (1979) and Brody (1987) suggested that structural changes do significantly alter the swing moment of inertia. It was found that the lowest swing moment of inertia was the bat with sections removed from the blade

(Hunt), while the bat with the largest section along the back of the bat (Probe), recorded the largest swing moment of inertia.

This study found that although the changes were visually apparent, they are not large enough to have a considerable effect on the bat's moment of inertia. Therefore, these structural changes will have little influence on the bat's feel and pick up. Feel also involves psychological feedback, therefore the alterations may be more for aesthetic reasons to convince the user that this bat provides them with an advantage. Although the differences were relatively small, the bats that have prominent central sections (DF and Probe) recorded the highest moments of inertia. By distributing the mass down the centre of the bat, the polar (twisting) moment is decreased, but the swing moment is increased. An increase in the swing moment would increase post impact ball velocity, although with an increase in the swing moment, the manoeuvrability and control are decreased. Thus, this may inhibit a player from hitting the ball further and with as much control.

8.6 Conclusion.

The aim of this chapter was to investigate the influence of structural design on the swing moment of inertia of cricket bats. It was found that the structural differences between the bats had limited effect upon this moment. It was noted that an implement's moment of inertia is related to the feel and manoeuvrability during play. Therefore, it could be assumed that the players would not feel any great differences between the forces required to swing each of the bats. It was established that there were no significant differences in the results due to the diminutive size of the structural changes relative to the dimensions of the bats. It can then be concluded that if a manufacturer wishes to alter the moment of inertia, they should consider more radical designs than those currently employed.

9 FLEXIBILITY OF CRICKET BATS DURING STATIC LOADING.

9.1 Introduction.

Flexibility of tennis rackets has been found to affect post impact ball velocity as well as alterations to the vibrational frequency and the coefficient of restitution of the implement. However, similar investigations have not been performed on cricket bats, although this theory has been studied using simplified computer models (Grant, 1998b). Plagenhoef, (1970) reported that the greater a racket's flexibility, the less force is transmitted to the hands. However, an increase in flexibility will amplify vibrational waves and reduce post impact ball velocity as more energy is retained in the implement rather being transferred to the ball. The method of investigating a racket's flexibility proposed by Plagenhoef, (1970) has been adopted by a number of subsequent investigations (eg. Grabiner, *et al.* 1983). Plagenhoef, (1970) suggested that the handle of the racket should be rigidly clamped and weights hung from the tip. The tip displacement can then be measured following the addition of various loads. Plagenhoef, (1970) recorded the deflection of the racket following the attachment of 5.66kgs to the tip. The 25 rackets tested were categorised into stiff (deflection of between 0.18 – 0.22m), medium (0.23 – 0.27m) and flexible (0.28 – 0.33m). Although this study does not intend to allow the bats to deflect to the same extent as reported, it will be possible to establish the influence of structural design on static bat deflection.

9.2 Experimental set up.

To establish the deflection of the bats with the application of a load, it was primarily necessary to secure each of the bats in position. The rigid clamping system was employed with the two aluminium clamps 210mm apart to secure the bat at either end of the handle. This study added weights in equal increments from 5 to 45 Newtons to monitor the deflection of the bats as a static load was applied. The loads were applied using a specifically designed cradle. The cradle

was positioned 0.16m from the end of the bat to avoid the possibility of the apparatus falling off the end during the addition of the loads and this location also corresponded with the thickest section of the bat. The deflection measurements were taken 0.06m from the free end of the bat using a D.T.I gauge. Readings were taken immediately after the application of the load and after every minute for a total of five minutes (Figure 9.1a). This enabled the study to investigate the immediate and prolonged affects of applying a load to the bats. During the application of the weights, the results were continually monitored to ensure that the bat did not enter plastic deformation as this would have caused permanent damage to the bat. Following the removal of the load (after five minutes), the bat was allowed to rest for a further minute to ensure that it returned to its original state of rest. Using a second D.T.I gage positioned between the supports, it was also possible to measure the magnitude of the handle deflection (Figure 9.1b). Although the handle was rigidly clamped, it was considered that any deflection of the handle would influence the measured bat deflections.

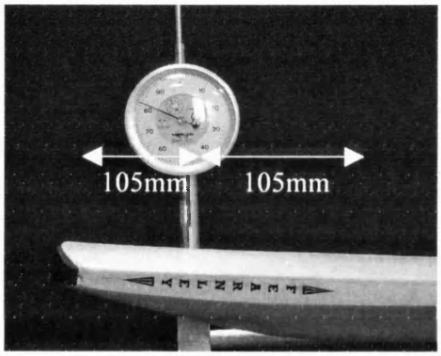

a,

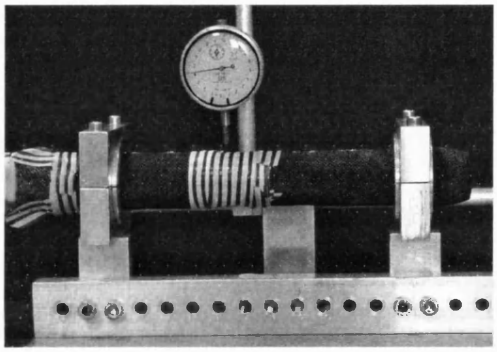

b,

Figure 9.1: D.T.I gages used to measure bat and handle deflection.

This testing procedure and deflection measurements were completed on five first class cricket bats, which were the same grade of wood, the same weight and dimensions (as outlined in the previous chapter). Each of the bats tested did differ in structural design, with visible alterations to the back of the blade and handle shape. To establish an average deflection response for each applied load, each increment was repeated five times for each bat.

9.3 Results.

Using the measurements taken from the D.T.I gages, it was possible to plot the differences in measured bat deflection with increases in applied load and time period.

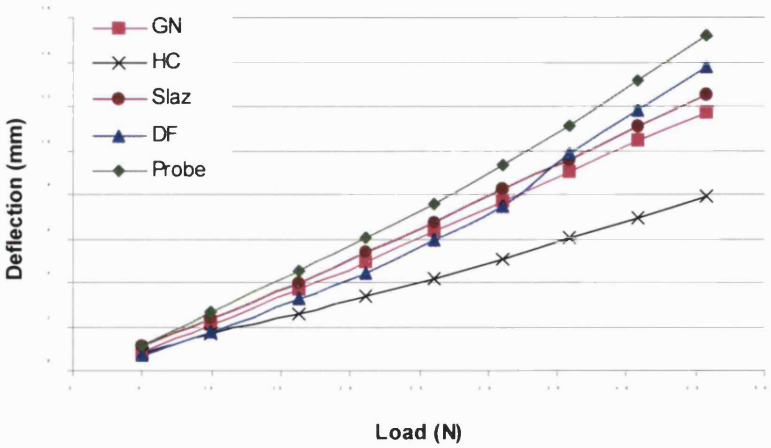

Figure 9.2: Bat deflection (0.06m from free end) following the application of a static load.

Figure 9.2 gives an indication of the flexibility of each of the commercially available cricket bats analysed. It is clear that as the static load was increased, the magnitude of deflection increased and the GN and Slaz bats are essentially linear up to a force of 45N. The Probe, DF and HC bats deviated from linearity demonstrating a small viscoelastic response. It is apparent that the bats did not reach their elastic limit as the deflection trend remained relatively linear throughout the addition of the loads. Figure 9.2 also shows that the deflection magnitudes of four of the bats are similar throughout the testing session. It is only the Hunts County (HC) bat that does not follow the same trend shown by the other bats. The deflection of this bat (HC) following the addition of each load was found to be up to 26% less than the others.

The following figures illustrate the continued deflection following the extended application of the static load. From these figures it is clear to see that the bats continue to deflect with the time that the load is applied. Figure 9.3a shows the deflection of the Gray Nicolls (GN) bat and the Hunts County (HC) bat. Using this information it was possible to establish that the GN bat deflects 5% further over the five minutes of the load being applied. It was found that the HC deflects by a further 7% after the five minutes. Figure 9.3b illustrates the continued deflection of the Slazenger (Slaz) bat and the Kookaburra Probe (Probe) bat. From this figure, it was

established that the Slaz bat deflected by a further 7.6% as opposed to the Probe, which deflected by a further 10.2% after the five minute period. Figure 9.3c displays the continued deflection of the Duncan Fearnly (DF) bat following initial application of the load and following five minutes. It was established that the DF deflected by a further 15.3% after five minutes when compared to its original measured deflection at initial load application. From this figure it is also possible to see the unusual deflection pattern of the DF bat. Unlike the other bats that display an almost linear deflection pattern, this bat has a distinct increase in measured deflection when the load was increased from 35 to 40N.

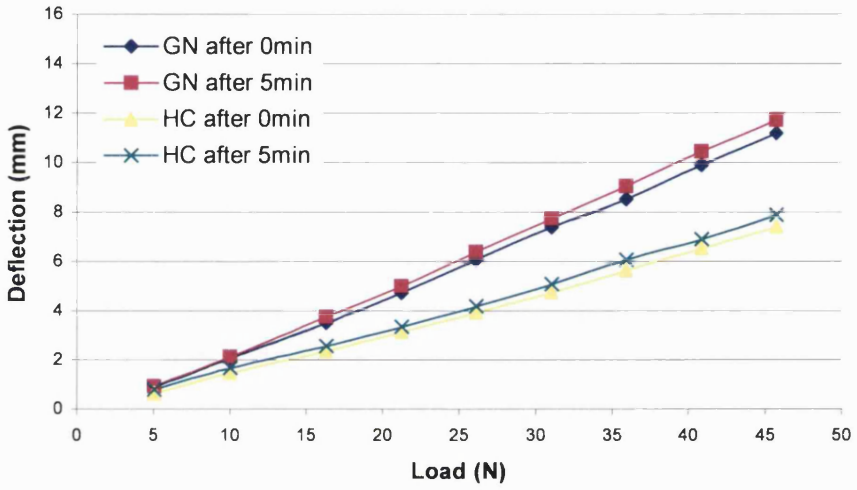

a, GN and HC initial and final bat deflection.

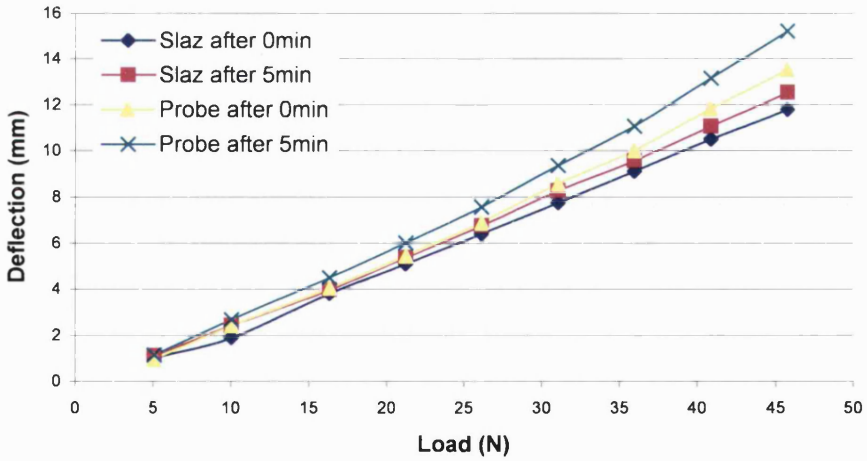

b, Slaz and Probe initial and final bat deflection.

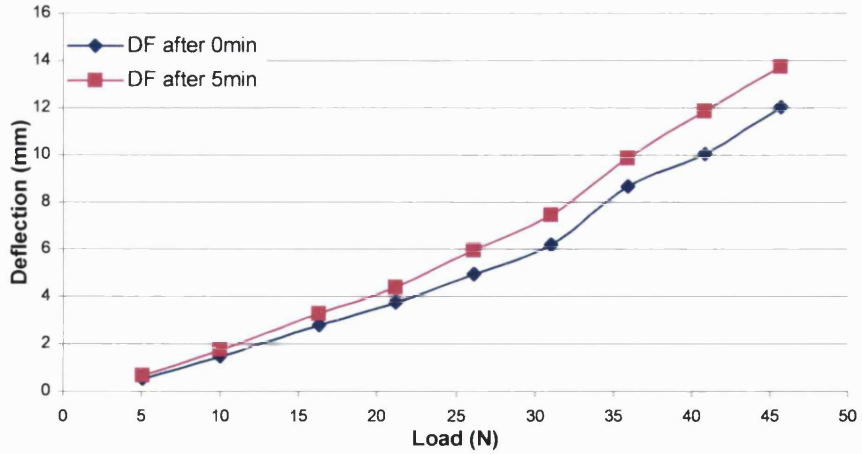

c, DF initial and final bat deflection.

Figure 9.3: Comparison of initial and final bat deflections.

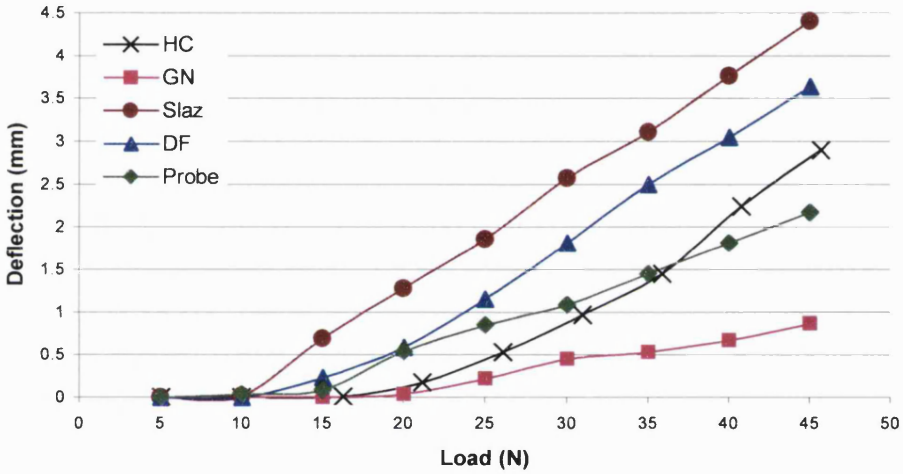

Figure 9.4: Handle deflection during static loading.

Figure 9.4, illustrates the deflection of the handles during the application of the static load to the end of the bat. This figure highlights how the handles do not necessarily deflect as soon as a load is applied to the end of the bat. For the Fearnley (DF) and Slazenger (Slaz) bats, handle deflection did not occur until 10 Newtons had been added. Noticeably, deflection of the Gray Nicolls (GN) handle did not occur until 25 Newtons had been added. It is also apparent that the bats follow a similar linear pattern apart from the Gray Nicolls. The angle of deflection is not as steep for the Gray Nicolls as found for the other bats. It is also possible to see that the deflection of the Gray Nicolls is over four times less than recorded during the Slazenger testing sessions. The Slazenger is found to deflect by 4.5mm following the application of 45 Newtons, while the Gray Nicolls had deflected less than 1mm.

9.4 Discussion.

Flexibility affects the post impact ball velocity and the implement's response following ball impact. The flexibility of the cricket bats were measured in turn by increasing static loads. It was found that all of the measurements followed a linear deflection trend and that the elastic limit was not reached. This linear pattern of deflection with application of static load was also reported by Plagenoef, (1970) during the analysis of tennis racket flexibility. This result would be expected as the bat could be considered to be a cantilever beam, with a single fixation location at one end. The handle was also able to deflect within the clamp because the system is more complex.

One interesting finding was that the Hunts County (HC) bat did not follow the same deflection pattern as the other four bats. Primarily, it was considered that the differences in handle construction may have had an effect upon the magnitude of the deflection of the bat. The Hunts County bat has a large oval handle compared to the standard round handles of the other bats. This increase in width around the base of the handle may have increased the stiffness of the bat therefore influencing the results. The Hunts County bat also has strips of Nomex® honeycomb inserted into the back of the bat (Figure 9.5). Although, it is unlikely that these inserts have a major effect upon the stiffness, it could be considered that inclusions of other materials into the back of the bat may have an effect on the flexural stiffness, vibration and subsequent performance during ball impact. It was noted that there was only a maximum of 3.5mm difference in the measured deflection between the other four bats. This is an interesting finding as it supports the suggestion that the design alterations to the Hunts County bat do influence the measured deflection as none of the other bats contain this additional material.

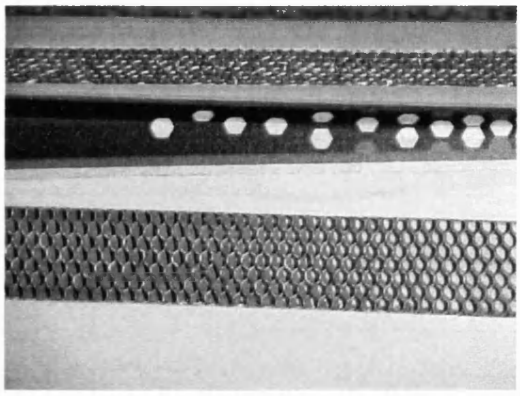

Figure 9.5: Nomex® honeycomb insert in the back of the Hunts County (HC) bat.

It was also shown that with the passage of time, the measured deflection increased by between 5 and 10%. As the initial deflection was measured, it could be considered that this is a form of creep. Creep is defined as the time-dependent and permanent deformation of material when subjected to a constant load (Callister, 1994). Although it is clear that there is no permanent damage to the bat, the deflection of the bat did continue at a continuous rate, which typifies primary creep (Callister, 1994). It could also be suggested that this period of extended deflection is due to the structure of the wooden bat becoming accustomed to the load applied. Due to the natural material that the bat is made from, microscopic damage will occur to the cellular structure during the repeated application of loads. Although, damage to the face of the bat is desirable to maximise the post impact ball velocity, more prevalent structural damage may have negative effects on performance or may even lead to catastrophic failure. Hearn, (1995) noted that materials, which experienced repeated and rapid loads produce minute amounts of plastic strain, which eventually lead to failure. Although creep would never occur during an actual game situation, it is interesting to hypothesise that following repeated impacts and continual deflection, a cricket bat will fatigue. Following extended periods of use, the magnitude of the deflection may well begin to increase as the bat becomes increasingly less resistant to the application of the loads. Therefore, it could be suggested that a bat will decline in performance and eventually fracture following extended periods of use.

From the handle deflection measurements, it was found that the deflection followed a linear trend as reported during the bat deflection analysis. It was noted that limited deflection occurred until at least 20 Newtons were added to the end of the bat. During the bat deflection, the lowest measurement was recorded for the Hunts County. It was suggested that this may have been due to the construction of its handle. However, it was the traditional round handle of the Gray Nicolls (GN) bat that recorded the minimum handle deflection. This study believes that this lack of handle deflection may be due to the construction methods and insert layout used rather than the shape. The Gray Nicolls handle is constructed from a single shaft of cane, split into three pieces with hard rubber inserts rather than the Hunts County handle which is made up of a number of cane pieces with cork inserts. Therefore, it could be considered that in this case the larger bat deflection measured for the Gray Nicolls, is not due to the handle deflection but the deflection of the actual blade of the bat. One reason for this might be the change in structural design of the Gray Nicolls, which has large scallops removed from the back of the bat (Figure 9.6). This will reduce the stiffness of the bat when compared to the other bats, which do not display this structural alteration.

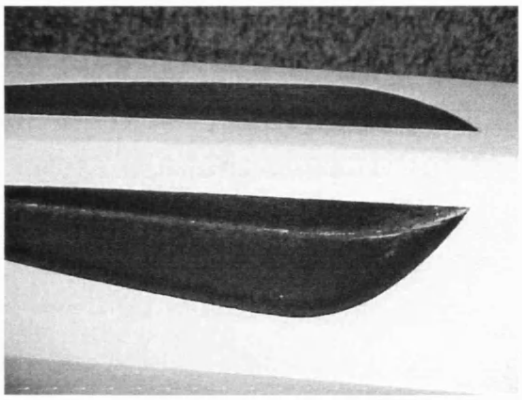

Figure 9.6: Structural alterations to the blade of the Gray Nicolls (GN).

It should be considered that the magnitude of the deflection measured during this investigation is not relative to occurrences during game situations. Although the implement will be gripped by the player's hands, this is not rigid clamping or non-responsive. During impact, subjects will use their whole body to control and maximise the post impact velocity. Therefore, this motion will stop the implement from deflecting in the same manner as reported in this chapter. Although this is a considerable limitation to this study, it is important to establish responsive parameters before improvements or further analysis can be completed.

9.5 Conclusion.

Primarily, this study measured the flexibility of five first class standard cricket bats. It was found that although they differed in structural design, little difference was found in the magnitude and pattern of the measured deflection as they responded in a linear fashion with the increase in applied load. The Hunts County bat was found to deflect less than the others, which may be caused by the inclusion of Nomex® honeycomb into the back of the bat and the width of the handle. Following analysis of the handle deflection, it was found that the handle of the Hunts County bat deflected to a similar extent as many of the other bats and thus it was proposed that the blade of the bat had an increased stiffness relative to the others. It was also discovered that the Gray Nicolls bats deflection was mainly due to the removal of sections from the back of the bat as the handle recorded minimal deflection. From these results, it can be concluded that flexibility can be increased with the inclusion of an alternative material to the blade and different construction techniques employed in the handle.

10 THE CENTRE OF PERCUSSION OF BATS AND RACKETS.

10.1 Introduction.

This chapter concentrates on the centre of percussion and the aim of this particular section is to report on published literature relating to this sweet spot. Due to the lack of cricket related studies, much of the reported work relates to tennis racket and baseball bat impacts. However, some of the techniques outlined can be easily transferred to the analysis of cricket bat responses following ball impact.

10.1.1 Literature review.

Different researchers have defined the centre of percussion (COP) in different ways, although it is best described as the point where shock to the hand is at a minimum as the impulsive force has been minimised (Brody, 1987 and Cross 1998b). Brody (2002) described the COP as a pair of conjecture points such that the translational motion at one of them is cancelled out when the impact of the ball is at the other point. Grant (1998b) suggested that the reduction in load is caused by the rearward recoil of the bat following impact being exactly balanced with the forward recoil at the handle. Therefore, there is essentially no net force on the hands as the racket pivots about this position and does not translate (Brody, 1987) (Figure 10.1). The position of the COP is a critical factor in terms of 'feel' and performance as an impact at this location reduces discomfort at the hands and increases post impact ball velocity (Sykes *et al.*, 1971 and Noble & Eck, 1986).

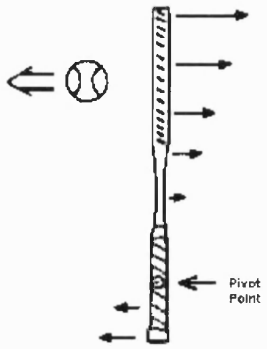

Figure 10.1: Rotation about a pivot point after impact, at which no hand load is felt (Brody, 1987).

Previous investigations have also reported that a unique impact location that improves player comfort and performance cannot be identified. This is because every different grip position has a different COP position making it almost impossible to consciously impact the desired location (Naß, 1998). Cross (1998) suggested that every point on the hands has its own COP depending on the impact location, therefore zero forces may occur at one location whereas large forces could be recorded elsewhere on the same hand. Hatze (1998) claimed that the COP is of limited significance as the forces acting on the hands vary significantly during the impact period. Therefore, the concept of zero hand force following an impact at the COP does not occur during tennis strokes. However, Hatze (1998) found that an impact within 3cm of the COP produced significant reductions in the forces at the hands, indicating that although the COP did not eliminate impulse forces they were reduced. Therefore, the feeling at the hands is more comfortable than if the impact had occurred at a different location.

With cricket and baseball bat impacts where two hands are used to swing the implement, the point that experiences minimum reaction force was found to be at the axis of rotation (Penrose & Hose, 1998 and Cross, 1998a). However, the axis is often positioned between the two hands as they are equally involved in the impact period (Noble, 1985). Noble (1985) and Grant (1998b) also suggested that the physical characteristics, inertial properties, type of shot played, location of the centre of mass and the radius of rotation along with the axis of rotation all affect the location of the COP. Cross (1998) found that the two handed grip used when striking a baseball resulted in a reduction in load to one hand and a significant increase in load at the other. Therefore, the player would feel comfort in one hand but pain in the other. Noble & Eck (1986) found a region 0.05m in length on a baseball bat that had an impulse at the hands close to zero. It was also found that this COP could be moved towards the end of the bat to take advantage of the higher rotational velocity by adding weights to the handle (Noble & Eck, 1986).

10.1.2 Previous experimental analysis of the Centre of Percussion.

The COP location has been found experimentally during controlled impacts on freely suspended rackets (Brody, 1987). A racket was impacted in turn below, above and at the COP using a

tennis ball that was also suspended by a string. Following each impact, high speed photographs were taken to identify the motion of the axis of rotation (Figure 10.2).

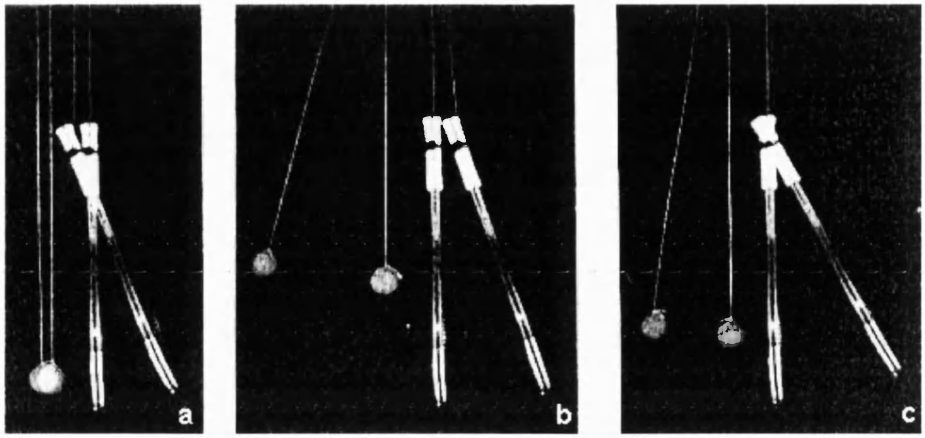

Figure 10.2: Motion of the tennis racket following an impact at the tip (a), throat (b) and COP (c) (Brody, 1987).

From Figure 10.2, it can be seen that an impact near the tip (a) causes the axis of rotation (see black dot on the white handle) to rotate and also translate to the left. This would cause force on the fingers and hands of the player. An impact at the throat region (b) causes rotation and translation to the right. However, an impact at the COP (c) causes no translation only rotation of the racket handle. Following an impact at this point, the player would not experience any translational force on their hands (Brody, 1987).

Knudson (1991b) performed tests in which load cells were attached to the handle of a tennis racket to coincide with the base of the thumb (the thenar eminence) and the lower portion of the palm (the hypothenar eminence) of a player's hand (Figure 10.3). Although the loads measured during this study are not comparable to those occurring during a cricket ball and bat impact, it was interesting to observe that the two load cells recorded different peak load magnitudes as well as the time taken to those peak loads following the initial impact period. Other studies, for example Knudson & White (1989) and Knudson (1991a) have also reported that it was possible to measure hand forces during impacts using force sensing resistors mounted at the same locations as used by Knudson (1991b).

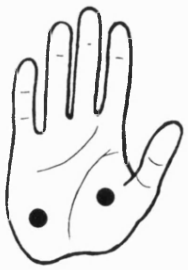

Figure 10.3: Location of load cells during tests carried out by Knudson (1991b).

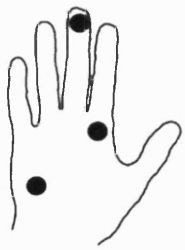

Figure 10.4: Location of piezoelectric cells used during the tests of Cross (1998b).

Cross (1998b) reported how Knudson (1991b) had identified considerable variability in the forces at the hands and how the differences could be minimised if the racket velocity was zero at impact. Cross (1998b) measured hand forces using piezoelectric cells fixed to the handle of a tennis racket. The cells corresponded to the tip of the second finger, the base of the index finger and the base of the palm (Figure 10.4). Subjects were instructed to hold the racket firmly and in a stationary position while a ball was dropped from 0.2m. Cross (1998b) found the force to be constant regardless of impact location, concluding that the COP had no special significance relating to the hand loads.

10.1.3 Conclusion.

This section has reported some previous studies that have investigated the effects of the COP on hand loads during impacts. Contradictory results have been found regarding the exact benefits of the COP and resultant player comfort, although most studies concede that total elimination of hand loads is not possible. Direct measurement of the loads experienced at the hands has been carried out during controlled tennis racket and ball impacts. It is the intention of this investigation to use some of the findings from tennis racket and baseball bat research and apply them to cricket bat and ball impacts to establish the factors that influence player comfort.

10.2 Structural design and the location of the centre of percussion.

10.2.1 Introduction.

It is considered that impacting the COP of a striking implement results in maximising the striking distance yet minimising the reactive loads felt by the batsman. However, very little has been published regarding the post impact responses of cricket bats and their effects on hand loads and player comfort. In contrast as explained in chapter 10.1, tennis racket research (in particular ball impact location) has received considerable attention (eg. Cross, 1998). The aim of this section is to investigate how the impact position and structural design of some first class cricket bats influence hand loads as measured at the clamping locations.

10.2.2 Literature review.

Most sportsmen readily identify the sweet spot of their striking implement in terms of the absence of shock, vibration and force on the hands (Cross, 2001). The sweet spot is also associated with the position that achieves maximum striking distance for a given effort. Each of these features have been related to the same contact point on the bat or racket and the location of this point is affected by the structural design and material properties used. However, the advances in tennis racket design and manufacture has not occurred with cricket bats. Grant (1998) noted that "the perceived quality of a bat's performance is not mechanically tested but determined by the aesthetic appearance of the grain structure". Consequently, a player locates the sweet spot through trial and error, rather than taking a more scientific approach.

As reported in chapter 10.1, it is the location of the axis of rotation that has a major influence on the position of the COP. Therefore, due to the two handed technique used in cricket, a location of minimum handle load may not be found, although a considerable decrease in measured load may occur at certain impact locations. Alternatively, as the bat was found to rotate about the first finger of the lower hand during impact, this was considered to be the COP position (Wood & Dawson, 1977). Although it should be noted that Wood & Dawson (1977) investigated the location of the COP using vibrational analysis, therefore, they may have located vibrational nodes rather than the point of minimum impulsive hand force.

10.2.3 Experimental set up.

Due to the significance of the axis of rotation, it was considered essential to use a clamping device that would enable the bat to move following impact, therefore the hand simulator rig was employed. Four Entran load cells (Figure 10.5) (ELFS-B4-500N) were mounted in the handle clamps to enable the direct measurement of the compressive forces during the impact period. Load cells 1 and 2 were positioned on the bottom and top halves respectively of the first clamp (closest to the blade of the bat). Load cells 3 and 4 were positioned on the bottom and top halves respectively of the second clamp (closest to the top of the handle). The clamps were located 210mm apart and tightened to 8N to replicate the typical positions and force of a player's hands. The signal from the load cells was amplified and then recorded at 1000Hz using a Pico Log data recorder.

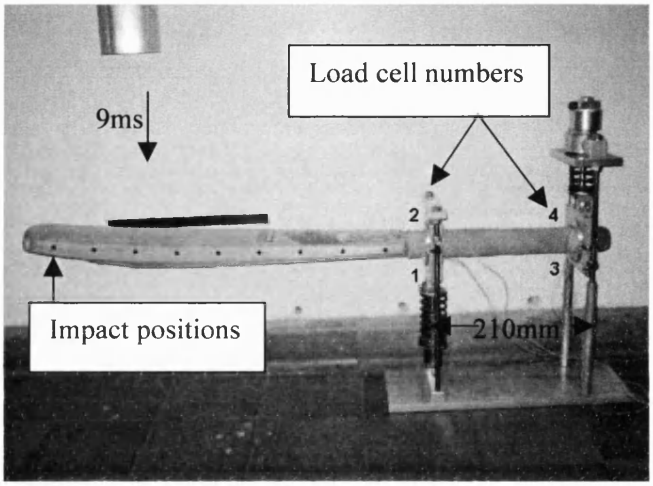

Figure 10.5: Experimental set up and location of the load cells within the hand simulator rig.

The load cell positions were selected as they represented specific locations in the player's hands that experience much of the hand loads during impact. They had also been previously used by Knudson (1991b) and Cross (1998b) during tennis racket impact analysis.

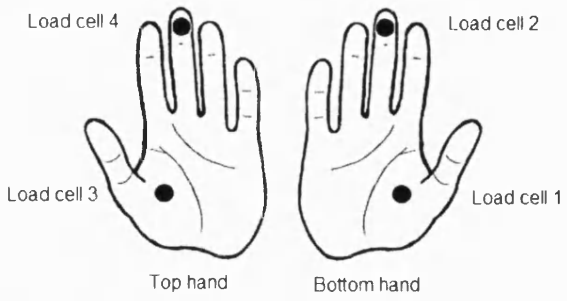

Figure 10.6: Load cell numbers in relation to the position on a players hands (Modified from Knudson, 1991b).

Ball impacts were delivered by dropping a ball down a 5m length of tube, which produced a pre-impact ball velocity of $9ms^{-1}$. The impact velocity was verified using a high speed camera system (Photron 1280 PCI at 2000Hz). The impact position was initially checked using an indicator spray that covered the intended impact position on the blade of the bat. The spray was then removed before data analysis occurred to ensure the ball and bat impact responses were not affected. Impacts were applied at nine positions, 0.06m apart along the length of the bat, with each position experiencing a minimum of six direct impacts. Five first class cricket bats with different structural designs were tested. The bats have virtually the same external dimensions and weight and are defined in Table 10.1 it was only the design feature on the back of the blade that was different between the bats.

Bat	Abbrev -iation	Blade dimensions (Length, width, thickness)			Design feature.	Dimensions (length, width, scoop depth or spine height).		
Fearnley	DF	560	108	59	Traditional	No distinguishing features.		
Gray-Nicolls	GN	560	108	59	4 oval scoops	185	28	14
Slazenger	Slaz	560	108	59	6 small scoops	35	10	10
County	Hunts	560	108	59	2 long scoops	260	22	11
Kookaburra	Probe	560	108	59	Central spine	490	45 (mean)	8

Table 10.1: Bat description and feature dimensions (mm) of the tested bats.

The load cell data was then analysed using the LabView software, which calculated the peak force for each impact. As six impacts were administered at the nine locations along the length of the bat, an average (mean) peak load could then be calculated for each impact location. As the reviewed studies have reported that the loads at the hands are not necessarily completely removed, this study considers that the COP should be more accurately defined. This study will identify the COP at each load cell by highlighting the position of greatest reduction in handle loads when compared to the handle loads recorded following ball strikes at the other impact locations.

10.2.4 Results.

After analysing the results, it was possible to plot the average peak load for each impact location along the length of each bat.

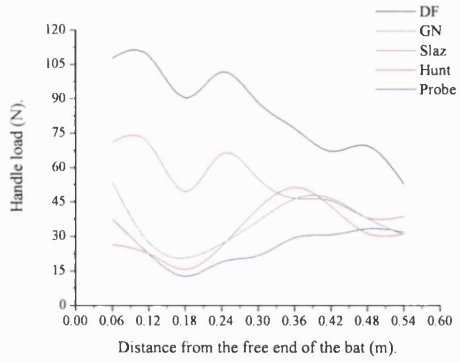

a: Load cell 1.

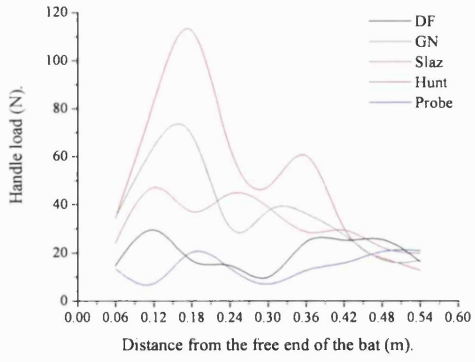

b: Load cell 2.

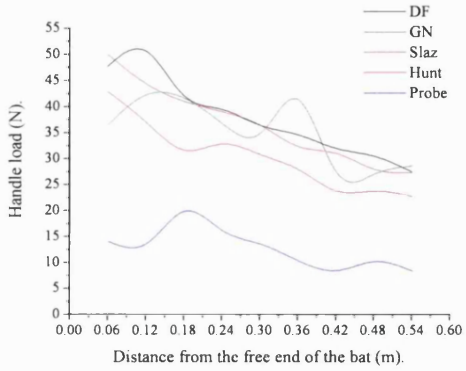

c: Load cell 3.

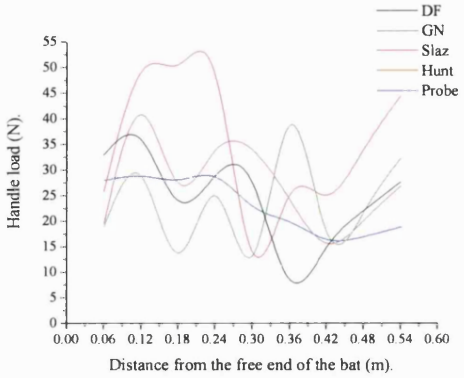

d: Load cell 4.

Figure 10.7: Peak handle loads recorded by each load cell.

Figure 10.7a, presents the average peak handle loads recorded by load cell 1 during impacts along the length of the bat. The Slaz and DF bats display a negative gradient with the recorded load reducing as the impact location is closer to the clamping positions. However, there is a distinct reduction in the loads at 0.18m from the free end of the bat. The Probe, Hunt and GN bats also record a reduction in measured load 0.18m from the free end, although the load distribution pattern is considerably different. As this is a distinct load reduction at 0.18m compared to the handle loads recorded at the other impact locations, it could be hypothesised that this is the COP for this location on the hand (the palm of the bottom hand). Load cells 2 and 4 (figures b and d), display at least two distinct recessions in the measured load that could be considered to represent a COP location. These locations can be seen to differ depending on the bat investigated. From these figures, the Hunt bat records considerably larger loads than any of the other bats tested. The results of the third load cell (c), follow a negative linear trend

with the greatest loads occurring at impacts closest to the free end of the bat (furthest from the hands). However, it can be seen that the Probe, Hunt and GN bats have a depression in the loads 0.42m from the free end. From all the figures, it can be noted that a reduction or a plateau in the force is recorded for most of the bats following an impact 0.18m from the free end.

Due to the possible associations with the magnitude of bat deflection and the influence on transferred loads, it was considered important to plot the peak deflection of each of the bats following a dynamic impact. As repeated impacts were administered at each position, the average of the peak deflections for each impact position is shown (Figure 10.8).

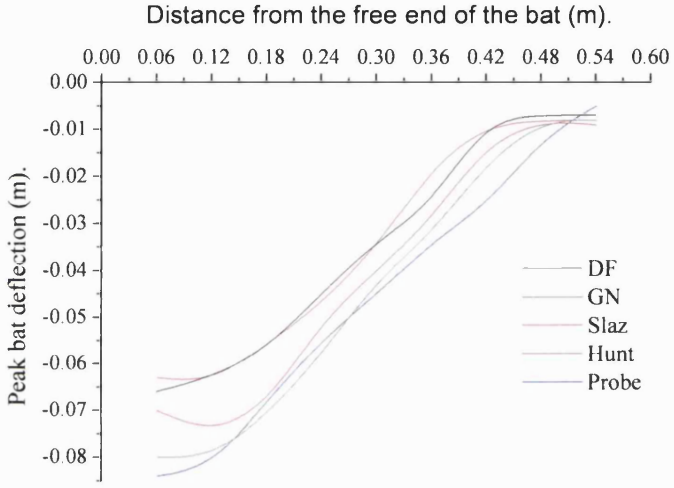

Figure 10.8: Average peak bat deflections during dynamic ball impacts.

Figure 10.8, displays the average peak deflection for each of the five bats investigated. It is possible to note that the Slaz and DF bats recorded that least deflection, while the Probe and GN recorded that most following impacts at each of the locations along the length of the bat.

As a large diversity in the recorded hand loads was established when the bats were in the hand simulator rig, the test was repeated when the bats were rigidly clamped. Although the distance between the clamps (210mm) and the dropping height (5m) were maintained, the clamping load was increased to 300N. This experimental set up would exclude the response of the clamping system and thus isolate the bat's reactions. However, the rigid clamping system does not allow the bats to respond as during hand held conditions (as will be discussed during chapter 10.3).

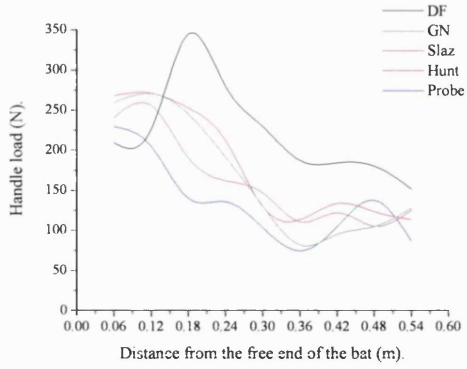

a: Load cell 1.

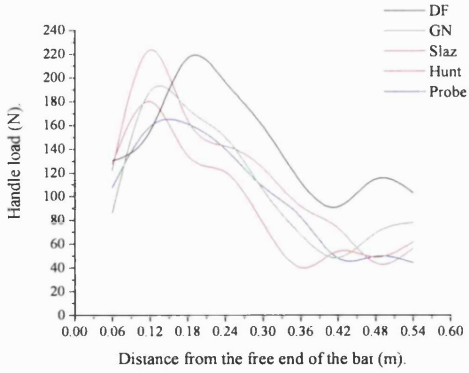

b: Load cell 2.

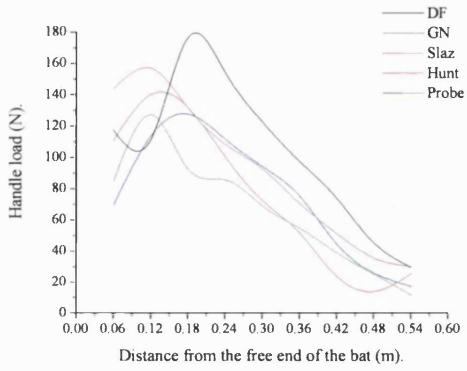

c: Load cell 3.

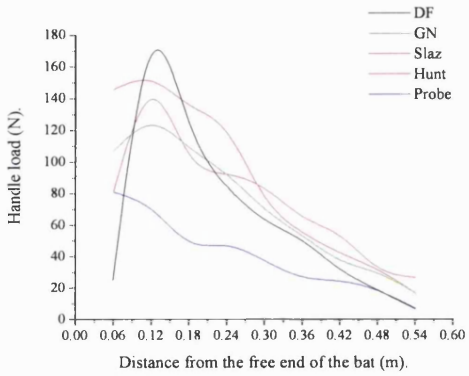

d: Load cell 4.

Figure 10.9: Peak handle loads recorded at each load cell with bats rigidly clamped.

Figure 10.9 illustrates the measured average peak handle loads when the bats were rigidly clamped. Unlike with the hand simulator test results, there are no significant reductions in the measured load (COP), other than towards the top of the bat, typically above 0.36m from the free end. The figures demonstrate a peak magnitude in the loads at approximately 0.12m from the free end, which is close to the thickest portion of the bat (0.16m). There is then virtually a linear reduction in the measured peak handle load as the impact location is moved closer to the handle of the bat. One feature of these results is that the DF bat (black line) has generally a greater peak handle load than the other bats, which all follow similar load patterns. From Figure 10.9a, the measured load during the DF bat condition increases until 0.18m before it also begins to decrease as found during the other four bats. These other four bats (GN, Slaz, Hunt & Probe) have a decreasing load at load cell one (Figure 10.9a) as the impacts are applied closer to the top of the bat. However, load cells 2, 3 and 4 (b, c & d) record a distinct reduction in the handle load for all of the bats as the impact is applied to the end of the bat (0.06m from the free end).

10.2.5 Discussion.

The COP location was determined using controlled cricket ball impacts at specific locations along the length of five stationary cricket bats. Previously, Hatze (1998) reported that the COP could only be found if the hands were stationary at the point of impact. This study used a hand simulator rig to establish the COP location during simulated player responses, whereas the rigid clamping system enabled the behaviour of the bat to be established without the influence of handle motion. Ivanov (1995) suggested that the COP can be located using a fixed axis of rotation, which also implies that human representative clamping systems were not necessary. Loads were measured using load cells fitted inside the clamps of the hand simulator and the rigid clamping system. Locations that exhibited distinct reductions in the measured handle load were considered to be the COP as players would perceive an improvement in comfort relative to the other impact positions.

During the hand simulator impacts, no location displayed a complete reduction in impact load. This result supports that of Brody (1987) who reported that the COP is the position where the load is minimised but not eliminated. Therefore, the point where the impact loads were reduced relative to the rest of the impact locations is the COP. However, load cell three did not have a position that exhibited a drop in the measured load. This finding has not been previously reported and therefore other factors including rotation, translation and vibration of the implement influence the measured hand load.

No distinct reduction in hand load was found as neither of the clamps were located at the axis of rotation. This concurs with the findings of Noble (1985) who reported that the axis occurs between the two clamps. It was however possible to record a reduction in the hand loads following an impact at a specific location, which Cross (1998) also found following impacts on tennis rackets. Wood & Dawson (1977) reported that the axis of rotation occurred at the base of the first finger, which correlates with the results from load cell one. At load cell one, a definite reduction in loads occurred at 0.18m from the free end of the bat. In previously reported tests, the COP was located between 0.14 and 0.20m (Wood & Dawson, 1977) and 0.15m (Daish, 1972) from the free end of the bat regardless of structural design. The results from this study

largely support these previous findings, however whereas others have stated that the COP was independent of structural design, this study has found some differences between the bats.

The Slaz and DF bats recorded a reduction in the impact loads at 0.18m from the free end at the first, second and fourth load cells. Although the reductions were small, a player would feel improvements in comfort at both hands following impact at this location. This opposes the results of Cross (1998) during the analysis two-handed grips on baseball bats. This impact location corresponds with the thickest region of the bat, which absorbs the shock load due to the increase in localised mass and thus leads to a reduction in the measured hand loads. This would not have occurred during baseball bat studies due to the shape of the bat not exhibiting such an increase in mass two thirds of the way down the bat. This location is also close to a nodal sweet spot and the position of maximum COR, which will have had an influence on the shock propagation and transferred load (Chapters 11 and 12).

From the Probe and GN tests, only load cell one records a COP location, 0.18m from the free end. The measured reduction in load was found to be the highest relative to the other bats, thus a player is more likely to notice the changes in hand load and consider that an impact here alleviates the loads they normally experience during impact. However, the GN and Probe bats recorded a peak load at load cell two when impacts occur at this position. As this load cell is on the opposite side (to load cell 1), the player would feel a reduction in the load at the palm but an increase on the fingers. During the Hunt analysis, the load on the fingers, which is recorded by load cell two is considerably larger than the reduction on the palm, which is recorded by load cell one. Thus the discomfort experienced at the players fingers will be greater than the improvements at the palm of the hands. This indicates that it is not possible to have a complete load reduction over the whole hand for these particular clamping locations, with this particular bat. Therefore, a reduction in load is felt at specific locations in the hands rather than the whole of the hand itself. This is supported by the findings of Cross (1998) who noted that low forces may occur at one location where as large forces could be recorded elsewhere on the same hand.

Each of the bats recorded linear reduction in loads, which corresponded with a reduction in the distance between the impact location and the bottom clamp. Although, it should be considered that this linear pattern may occur due to the responses of the handle during the impact phase. If the handle does not deflect, the load will increase at the first and third cells, as the handle rotates and is pressed down on the first cell and pushes up on the third (Figure 10.10a). This is

particularly evident in the results of the DF and Slaz bats. However, if the handle bends at the centre (producing an arc between the clamps) the load will increase on the second and fourth cell (Figure 10.10b). This was found during the analysis of the Hunt bat, which may indicate that the handle is pivoting on the outside edge of the front clamp and not contacting the first load cell correctly, thus leading to an inaccurate load measurement.

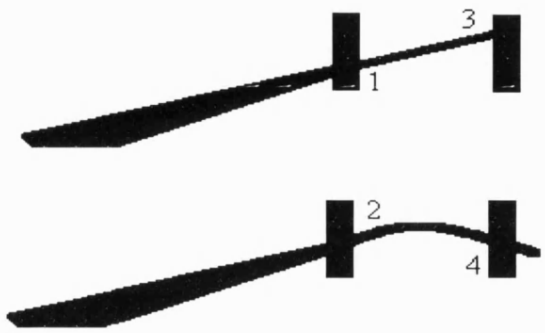

a: Bat rotation.

b: Bat handle bending.

Figure 10.10: Contribution of handle flexion to hand loads.

The Slaz and DF bats recorded the least deflection as well as double the loads at first load cell when compared to the Probe and GN bats. Therefore, the magnitude of the bats deflection has a considerable effect on the loads transferred to the player's hands. With an increase in stiffness, more energy is conveyed to the player's hands as less is lost through deflection of the bat. Although similar results were recorded at the other load cells, it is the first load cell that measures the largest loads. This finding is caused by this cell measuring in the direction of the applied load and subsequent deflection of the bat. Therefore, any reduction in the load at the first load cell will lead to a perception of improved comfort. The third and fourth load cells (at the top of the handle) recorded a decline in the load as the impact positions became closer to their location. This can be attributed to the reduction in the length of the lever between the clamps (pivoting about the bottom clamp) and the impact location. Plagenhoef (1971) suggested that this was the location of the COP, although due to the small differences in maximum and minimum loads, it is unlikely that the player would notice any improvements in comfort.

Although the influence of clamping type will be analysed in the next section, this study was able to investigate the responses of all the bats when they were rigidly clamped. Little difference was found in the distribution of the loads regardless of their changes in structural design. However, the results were considerably different to those experienced during the hand

simulator tests illustrating the effect of rigidly clamping bats. Rigid clamping eliminates most of the handle motion, thus causing the bat flexion to occur at the bottom clamp, 0.6m from the free end. This location is now the axis of rotation, which influences location of the COP.

A reduction in the load at the first load cell occurred following an impact 0.36m from the free end. This location is 0.22m from the first load cell, which is 0.21m from the other clamp (which is 0.002m from the end of the handle), therefore siring load cell 1 at the axis of rotation and thus the COP for that impact location. This highlights how each impact location will have its own COP position on the handle, supporting the findings of Naß (1998). The reduction in the measured loads at cells three and four (top clamp), are due to the location of the impact being closer, therefore reducing the length of the lever (bat) from the axis of rotation (bottom clamp). The first and second load cells also measure an increase in the load as the impact moves closer, indicating that this clamp is no longer at the axis of rotation and is supporting the impact load more. As found during the hand simulator trials, the load is reduced when the impact occurs 0.06m from the end. The deflection was found to be at a maximum here and therefore as the stiffness of the bat is reduced, the amount of energy transferred to the hands is decreased as it is lost through bat deflection.

Although the set up has not directly replicated the occurrences during actual cricket bat impacts, Smith (2001) reported that the COP can be accurately determined using an initially stationary bat or ball. Although the bat was stationary prior to impact it was able to move in the hand simulator rig and respond as during a hand held impact. Some of these results will have been masked by vibrational modes and noise, although the signal was filtered prior to analysis. However, it is considered that this is an accurate method of calculating the COP location.

10.2.6 Conclusion.

This section investigated the location of the COP by impacting specific locations along bats with different structural designs. The first load cell recorded a distinct location of reduced load for each of the bats (0.18m from the free end), which was proposed to be the COP for this clamping location. However, this COP location was only present for two of the bats if all of the load cells were considered, indicating that differences in structural design may have an influence on overall bat responses. A complete reduction in load was not found as the axis of

rotation was considered to occur between the two clamp locations. However, it can be concluded that even with a two-handed grip, distinct improvements in comfort can be achieved following impacts at specific locations.

10.3 Clamping type and the location of the centre of percussion.

10.3.1 Introduction.

In section 10.2, the spring–damper system that simulates the hand held condition (hand simulator rig) was used to standardise the testing procedure and establish bat responses by eliminating the variability of human responses to impacts. However, it was a concern that this rig may not accurately represent a human subject. Therefore, the suppositions regarding the location of the COP and positions of improved comfort highlighted in the previous section would be irrelevant when related to game situations. Therefore, this section considers the effects that different clamping types have on the location of the COP and the loads that are transferred to the clamping locations. Brody (1979) reported that the location of the COP will not be affected by the force applied at the hands at impact. This is probably due to the axis of rotation remaining unchanged during the impact period. However, Smith (2001) found that the type of constraint had a large affect on the loads transmitted at impact, which supports the findings of Hatze (1976) and Elliott (1982) who reported a significant increase in the load at the hands following an increase in the gripping pressure on a tennis racket.

10.3.2 Experimental set up.

Three different clamping methods have been used, rigid clamping, a hand simulator (the spring-and-damper system) and the average responses from five human volunteers. As the aim described in this section has been to investigate the influence of a single variable (clamping type) only one bat (the Probe) was considered. The methodology used was the same as reported in section 10.2 for each impact location and each clamping condition. The load cells were positioned inside the aluminium clamps to measure the forces that were transferred to the handle following the ball impact (Figure 10.11a and b). As during section 10.2, the clamps were positioned 210mm apart and the rigid clamps were tightened to 300N while the hand simulator was tightened to 8N.

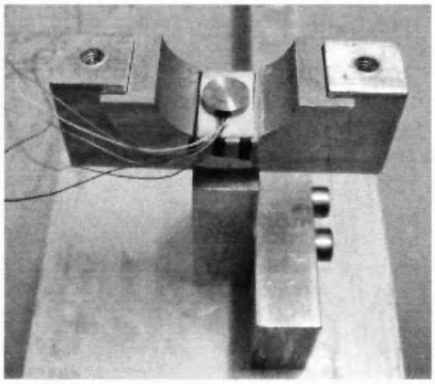

a, The rigid clamping system.

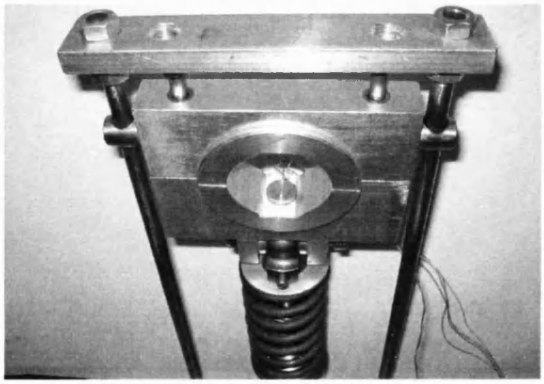

b, The hand simulator.

Figure 10.11: Aluminium clamps for securing the bat handle.

To investigate the loads transferred to the players hands, the load cells were positioned at the same locations on the bat handle as during the clamped conditions. When the subject's gripped the handle, the load cells corresponded with the tip of the second finger and the base of the palm of each hand (Figure 10.12a). These locations were also outlined by Knudson (1991b) and Cross (1998b) during their analysis of hand loads and the COP in tennis rackets. The distance between the hands was also maintained at 210mm as used during the clamped conditions (Figure 10.12b).

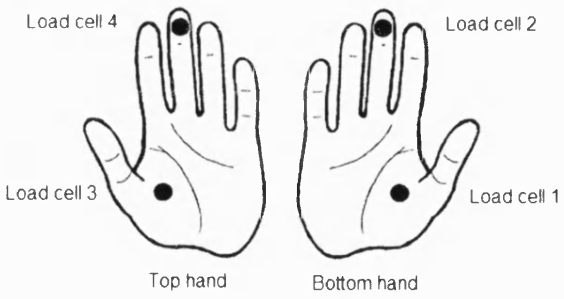

a, Location of load cells on hands.

b, Hand positions on the handle of the bat.

Figure 10.12: Human subject set up.

The subjects were instructed to grip the handle and respond firmly, while holding the bat horizontal during the impact. Each of the impact locations were subjected to repeated strikes until there were six satisfactory for analysis. Impacts were rejected if there had been, movement of the subject prior to or during the impact, double impacts and off centre impacts. Following data collection, the average peak loads for each clamping condition were calculated using the programme in LabView 5.1, (Chapter 5).

10.3.3 Results.

The following figures show the loads at each impact location and for each of the clamping conditions. The four load cells measured handle reaction forces for each impact simultaneously enabling the loads at the clamps or player's hands to be recorded. In this section, only the results that are related to the clamping conditions are reported as many of the trends have been previously discussed during section 10.2.

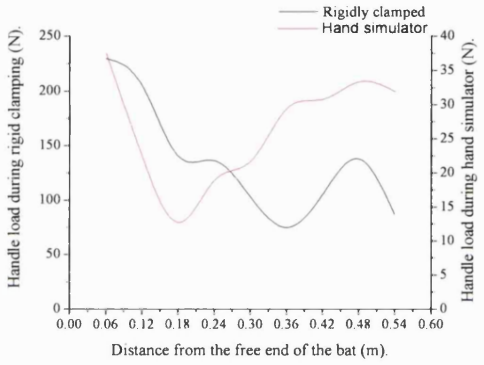

a, Comparison between rigid clamping and hand simulator.

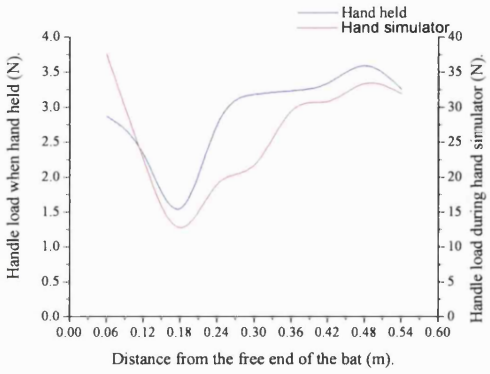

b, Comparison between hand held and hand simulator.

Figure 10.13: Loads recorded at load cell 1.

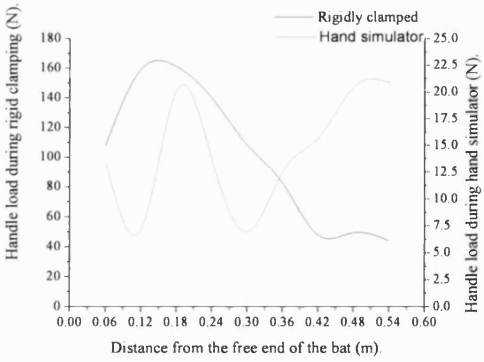

a, Comparison between rigid clamping and hand simulator.

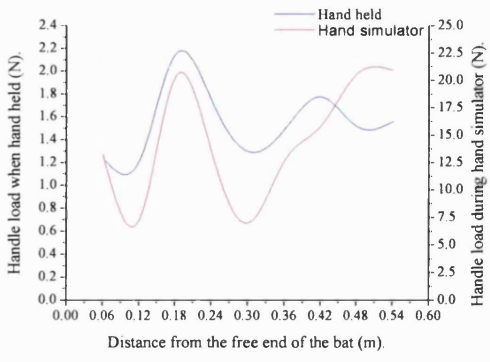

b, Comparison between hand held and hand simulator.

Figure 10.14: Loads recorded at load cell 2.

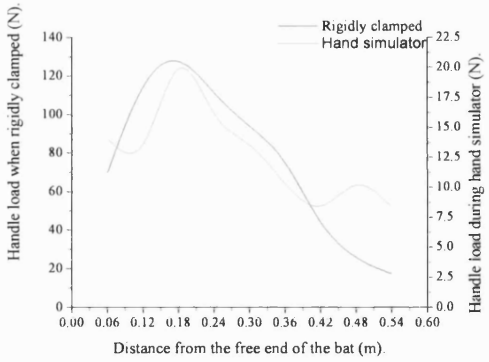

a, Comparison between rigid clamping and hand simulator.

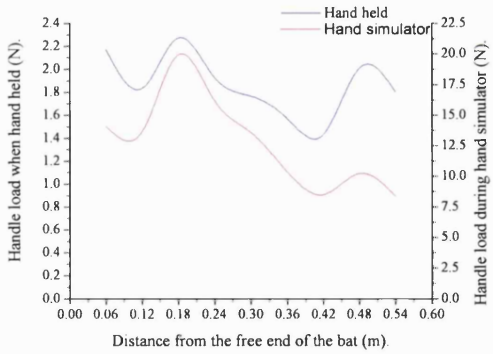

b, Comparison between hand held and hand simulator.

Figure 10.15: Loads measured at load cell 3.

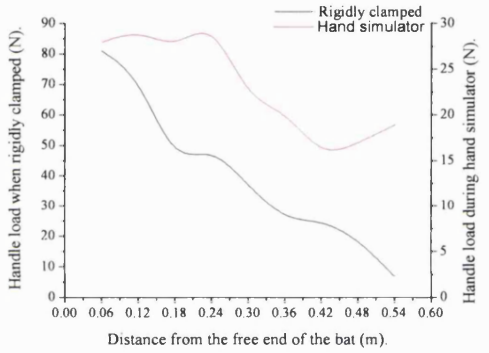

a, Comparison between rigid clamping and hand simulator.

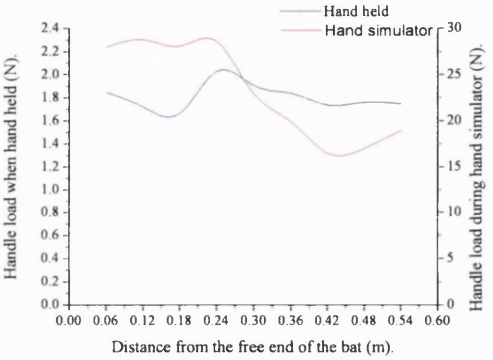

b, Comparison between hand held and hand simulator.

Figure 10.16: Loads measured at load cell 4.

The figures illustrate the recorded loads when the bat was either rigidly clamped, hand held or gripped in a hand simulator. It can be seen that the loads distribution are similar during the hand held and hand simulator tests, however they are completely different during the rigidly clamped impacts. On average the hand held results are a factor of 9.55 less, while the clamped results are a factor of 5.39 more than those recorded during the hand simulator impacts.

10.3.4 Discussion.

This section investigated the magnitude of the handle loads and the COP location following changes to the clamping conditions. The handle loads were measured using load cells positioned within the clamps or player's grip during repeated impacts at nine locations along the length of the bat. It was found that the location of the COP was not affected when the handle was held either by the subject's or the hand simulator. However, the pattern and magnitude of the loads were considerably affected by the rigid clamping system. Brody (1979) reported that the hand load should not effect the location of the COP. This is supported by this study as the load patterns were similar in distribution during the hand held and hand simulator conditions. Brody (1979) based this claim upon subject hand loads rather than any other clamping method, although this does highlight how the hand simulator rig is a comparable method to a human subject. The results from the rigid clamping method are different due to the alteration to the axis of rotation. During the hand held and hand simulated trials, the bat would have been able to rotate following impact. Thus the position of the axis of rotation was between the two clamps or hands as reported by Noble (1985). However during the rigidly clamped impacts, the bat handle is unable to rotate in the same manner, thus the axis of rotation would move towards the bottom clamp, influencing the location of the COP. The practical significance of this finding is that future studies should carefully consider how the sporting implements are constrained before judgements are made concerning the possibilities of improved hand comfort and the location of the COP during impact.

When the bat was rigidly clamped, the measured handle loads at each load cell were found to be 5.39 times higher than the hand simulator, which was found to be 9.55 times higher than when hand held. Hatze (1976) and Elliott (1982) also found that hand loads increased with an increase in the initial gripping pressure. As the gripping force was maintained within the hand simulator at the same load as the pre impact hand held load, the human subject's must have either consciously or unconsciously altered their grip pressure to improve comfort during the impact period, thus causing the differences in measured handle load. Knudson (1991b) noted that hand forces were increased to the point of impact where they were then quickly reduced to lessen the shock before the loads were then increased to control the recoil of a racket. Therefore, the subject's during this study must react in a similar way, lessening the hand loads to improve comfort during the impact period. This finding is inline with the findings of Hatze (1976) who noted that the post impact hand forces can still be small regardless of the impact location due to alterations in the grip tightness made by the player. As the hand simulator grip pressure is constantly maintained, the magnitudes of the recorded loads are different although the load pattern is the same as during the hand held condition. This also indicates that the axis

of rotation is the prominent factor in adjusting the location of the COP and not the pressure applied at the grip locations. The subject's grip alterations during the impact phase will influence the measured results and are unlikely to be consistent throughout the testing session. Therefore, it can be regarded that the hand simulator is a more consistent alternative to the use of human subjects. This suggestion was supported by Kotze *et al.* (2000) who noted that the use of human subjects leads to imprecise results due to a lack of repeatability, the effects of fatigue and the variability in precision and control.

The axis of rotation is maintained during the hand simulator impacts by the actions of the spring and damper system that support the rotating aluminium clamps. Therefore it can be assumed that the spring and dampers of the hand simulator replicated the responses of the subject's forearms and hands, leading to the similar patterns of the handle loads that this study has found. Cross (1998b) found that the muscles and tendons of the forearm act as passive springs and regulate the loads experienced at the hands during racket impacts. However, this study proposes that an increase in the measured loads was found during the hand simulator condition because the spring and dampers require an increased load to overcome the inertial properties in the system.

Although consistent results were produced using load cells, the measuring of single points under the hands or clamps does not provide an indication of the total force transferred from the handle. However, Cross (1998b) did report that it is not practical to sum the forces from many different points under the hand. Therefore, a reasonable assumption can be made using this method of analysis. As the position of the load cells were unchanged for each of the clamping conditions, it was possible to compare the results following each condition and assume they represent the loads that were transferred to the handle following the ball impacts as they are the locations, which would record the greatest loads during impact.

10.3.5 Conclusion.

It was found that the hand simulator recorded a similar load distribution pattern and COP location to the results from the average of five human subjects, although the loads were 9.55 times higher. The rigid clamping condition had a considerable effect on the pattern and magnitude of the handle loads as they were 5.39 times larger than the hand simulator. Therefore, it can be concluded that the hand simulator is a viable and reliable alternative to human hand held impacts during the identification of the COP, although the measured loads need to be considered with caution due to their greater magnitude relative to hand held impacts.

10.4 Impact velocity and the location of the centre of percussion.

10.4.1 Introduction.

At release, bowled cricket balls have been recorded over 100mph (44.7ms^{-1}) with batsmen facing speeds of over 70mph (31.2ms^{-1}) following the bounce of the ball. During these laboratory based studies, it has not been possible to reproduce high velocity impacts using a gravity based device, therefore speed has been reduced to satisfy these criteria. By reducing the impact velocity of the ball, it was possible to investigate whether the location of the COP was affected. Cross (1998b) reported that similar load distribution patterns could be expected regardless of impact speed. Although it is expected that the peak handle loads will be different, it is the distribution of these loads that enable the study to identify the location of the COP.

10.4.2 Experimental set up.

Due to the limitation of the set up, it was only possible to achieve a maximum impact velocity of 9ms^{-1}. The chosen impact velocities were 3, 6 and 9ms^{-1}, in attempt to equalise the differences between the measured loads. An identical set up was used as outlined in section 10.2, which included the use of the hand simulator rig with the clamps positioned 210mm apart and tightened to 8N. This was to enable the results to resemble human handling. As in section 10.3, one bat was selected to exclude the effects of changes in bat construction on the presented results.

10.4.3 Results.

Following the collation of the data, it was possible to establish the influence of reducing the impact velocity on the average peak load and distribution of those loads along the length of the bat. The average peak load was again used to ensure that the results were not produced through chance occurrences.

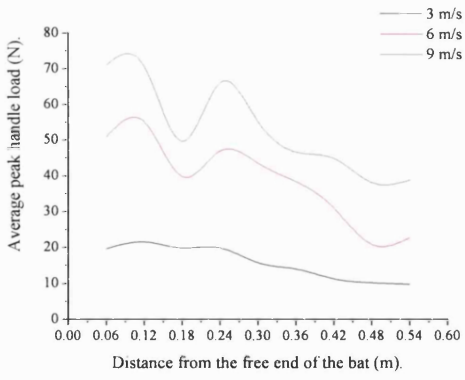

a, Load cell 1.

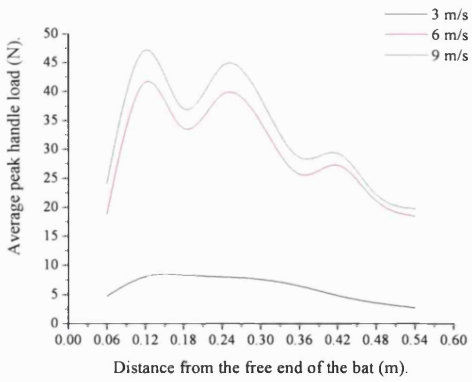

b, Load cell 2.

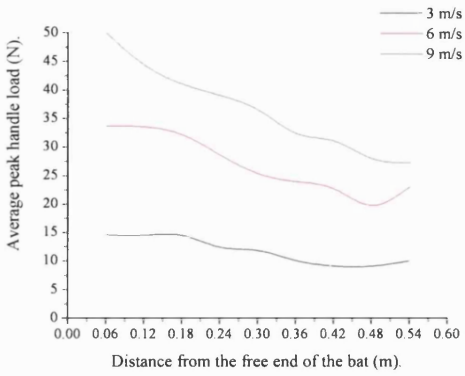

c, Load cell 3.

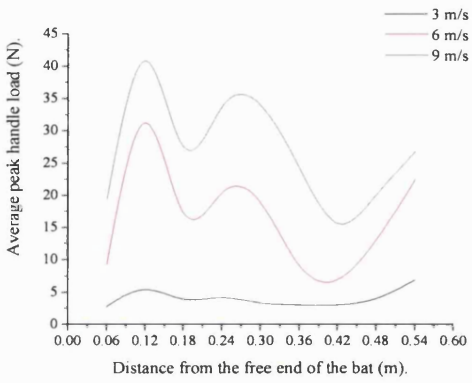

d, Load cell 4.

Figure 10.17: Average peak handle load at different impact velocities.

The figures display the recorded handle loads from each of the load cells (1 to 4) positioned within the clamps of the hand simulator rig (as explained in chapter 10.2). From each of the figures, it is clear that the load distribution patterns during each of the different impact velocities are similar. This is especially apparent when comparing the results from the impacts at 6 and $9ms^{-1}$. However, it is still possible to see that the pattern is still present when the impact velocity was reduced to $3ms^{-1}$, although it is not as pronounced as during the other two velocities. The differences between the measured handle loads are not the same, although the ball velocity was altered in equal increments. The average difference in measured handle load between 3 and $6ms^{-1}$ is 18N for each of the impact locations, while the difference in measured handle load between 6 and $9ms^{-1}$ is 9N for each of the impact locations.

10.4.4 Discussion.

The fluctuations in the measured handle loads, which were correlated with different impact positions along the length of the bat were found to be very similar following ball impacts of differing velocity. This finding was more pronounced between the impact results from 6 and $9ms^{-1}$, rather than during the impacts at $3ms^{-1}$. Although this finding supports Cross (1998b) who reported that impact velocity did not affect the transmission of loads to the hands. Under an impact velocity of $3ms^{-1}$, less energy is transferred into the bat, thus the handle reaction forces are smaller. Therefore, the magnitude of the forces relative to positions along the length of the bat and the location of the COP are less pronounced. This makes it harder to identify a COP position, although a consistent pattern related to the other impact velocities can be recognized. The significance of this finding in relation to actual playing conditions is that a player would not have to change the ball impact location in order to experience a reduction in the handle forces if the pre impact ball speed was modified. Therefore, it can be proposed that the impact speed is not a factor that affects the location of the COP or any highlighted reductions in the handle loads following impacts at specific locations along the length of the bat.

As expected, there is a reduction in the measured handle loads at slower pre impact ball speeds. Daish (1972) and Brody (1979) reported that the contact period between ball and tennis racket is only slightly affected by impact velocity. Therefore, the drop in the measured handle load is due to less energy being transferred to the bat rather than the influence of the contact time between the bat and the ball. It had been expected that an increased ball speed would extend the contact time due to increased bat deflection and ball compression, which would have enabled greater loads to be transferred into the bat and thus the handle. Although greater loads were recorded as the ball impact speed was increased, the higher speeds achieved in a game situation may cause changes in the distribution of the handle loads and thus the COP. Additionally during game impacts, the ball compression and bat deflection will increase, thus further altering the magnitude and possible distribution of the recorded handle loads. These factors must be considered when relating the findings of this study to the occurrences during game situations.

There also seemed to be a relationship between the differences in the recorded handle loads at each impact position as the ball speed was increased. Cross (1998b) reported that the results are almost entirely linear due to the response of the implement being within its elastic limit. It is

possible to calculate the handle loads involving higher impact speeds using this pattern. However, only three points were identified, thus further analysis is required before a relationship can be established as the bat may continue to respond elastically but not necessarily in a linear fashion following an increase in the ball impact speed. The practical significance of this finding is that if a pattern were established, it would no longer be necessary to carry out impacts at high speeds as a scaling factor could be used to calculate the measured handle loads for impacts at different velocities for different locations along the length of the bat.

10.4.5 Conclusion.

This section investigated the affect of ball impact speeds on the measured handle loads. It was found as the velocities were decreased the fluctuations in the measured loads at different impact positions were unaffected, thus it was suggested that the location of the COP would also be unmoved. It was found that as the ball velocity was decreased by 33%, the recorded handle load was decreased by 50%. It was hypothesised that following further analysis with a range of ball impacts velocities, a scaling factor could be established to calculate the handle loads during actual cricket bat impacts.

10.5 Clamping location and the centre of percussion.

10.5.1 Introduction.

Studies have shown how each gripping position affects the COP location due to the movement of the centre of rotation (Brody, 1995 and Cross, 1998). Therefore, this section aims to investigate how the COP and handle loads are altered with changes of grip location in cricket bats. The practical purpose of this is to establish whether a particular grip location could help reduce hand loads during game situations. The experimental studies described in this chapter have used a grip distance of 210mm within the hand simulator rig. However, cricket coaching literature often recommend that the hands should be close together (Ferguson, 1992). If an advantageous hand location could be found, a player may benefit from a reduction in hand discomfort at ball impact and the subsequent fatigue and decline in performance that can be also associated. As the location of the COP depends upon two conjecture points of which one is the axis of rotation, it may be possible to alter the COP position with the movement of the grip location. Noble (1985), reported that baseball players move their hands close together thus shifting the COP further towards the end of the bat to take advantage of the higher velocity. However, this technique of shifting the hands prior to ball impact has not been reported in cricket coaching manuals.

10.5.2 Experimental set up.

Three other gripping locations were used, top grip (TG) middle grip (MG) and bottom grip (BG) (Figure 10.18). This was achieved by positioning the hand simulator clamps 105mm apart rather than 210mm as before. To enable a comparison with the earlier results, the 210mm (wide grip) condition were also included.

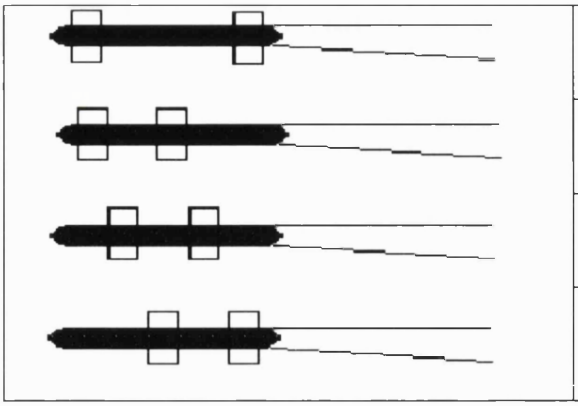

Wide Grip (WG) The clamps are positioned 210mm apart, with bottom clamp 40mm from the top of the bat.
Top Grip (TG) The top clamp is maintained and the bottom clamp is raised to the centre of the handle. The clamps are 105mm apart.
Middle Grip (MG) Both clamps are positioned exactly either side of the centre of the handle. The clamps were maintained at 105mm apart.
Bottom Grip (BG) The top clamp is positioned in the centre of the handle and the bottom clamp is positioned 40mm from the top of the bat. The clamps were 105mm apart.

Figure 10.18: Clamping arrangements.

The clamp loads were measured using four Entran load cells positioned inside the handle clamps of the hand simulator rig, which were tightened to apply 8N prior to impact. Only one bat (DF) was chosen to ensure bat structural design did not influence the results. Six acceptable impacts, free from data collection or experimental errors were applied using the drop tube method. Each of the nine highlighted locations along the face of the bat were impacted at 9ms for each of the clamping set ups. The average peak loads from each load cell for each impact during each set up was then established.

10.5.3 Results.

The following figures show the average peak handle loads and how these loads change following alterations to the clamping and ball impact location.

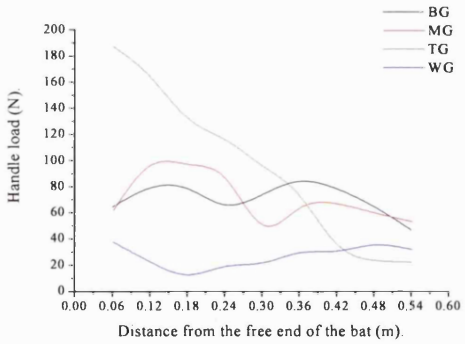

a, Load cell 1.

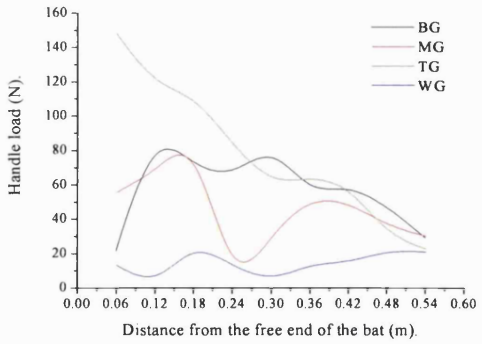

b, Load cell 2.

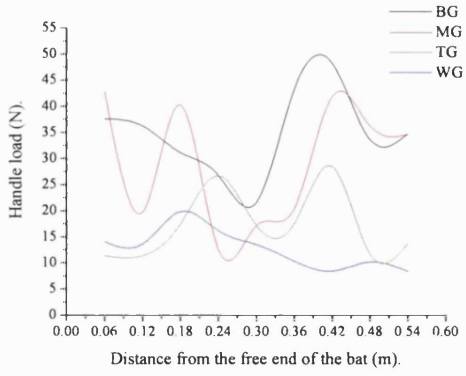

c, Load cell 3.

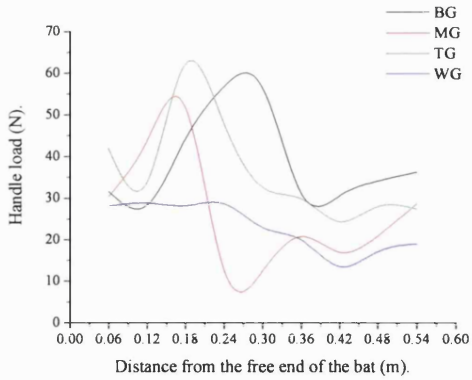

d, Load cell 4.

Figure 10.19: Clamping location and handle load measured during impacts along the length of a cricket bat.

Figure 10.19a to d, show that there is a considerable difference in the location of the lowest peak load (COP position) following changes in clamping location. The wide grip clamping condition consistently displays the lowest handle forces, with two distinct reductions in the load between 0.12 and 0.18m for the bottom clamp (Figure 10.19a and b), and 0.42m for the top clamp (Figure 10.19c and d). These are considered to be the COP positions for this gripping location. The middle grip records the greatest deviation in force along the length of the bat. From Figure 10.19b, c and d, the middle grip condition records a distinct reduction in handle load (COP location) 0.24m from the free end. However, load cell 1 records this drop 0.3m from the free end during the middle grip condition (Figure 10.19a). Figure 10.19a, b and c show that the top grip condition records the highest loads, especially when the impact occurs towards the bottom of the bat. The opposite occurs when the bat is confined in the bottom grip condition, as the handle loads are found to increase as the impact position is moved towards the top of the bat (Figure 10.19c and d). The COP locations for all the load cells during the top grip condition occur between 0.42 and 0.48m from the free end. Finally, the bottom grip condition displays a drop in the measured handle loads (COP) 0.24 from the free end for the bottom clamp and between 0.3 and 0.36m for the top clamp.

Finally, when the handle was clamped using the WG and BG conditions, the distance from each clamp to the COP was the same. For example, even though the load cells from the two clamps measured different COP locations, the COP was found to be 0.4m from the clamp (Figure 10.20). However, a similar trend was not identified for the other conditions.

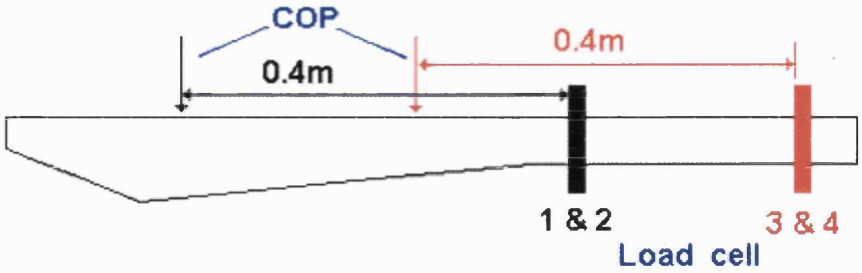

Figure 10.20: Location of COP and associated clamp location during WG condition.

10.5.4 Discussion.

An investigation into the influence of clamping location on the handle loads has been completed using a hand simulator rig. Four gripping locations representing those used by professional cricketers were chosen (Ferguson, 1992). It was found that each gripping position produced different handle load measurements and COP locations. Brody, (1995) and Cross, (1998) both found that the COP moved with hand location. The shifting of the COP is due to the movement of the axis of rotation with each grip position. As the COP is based upon two conjecture points, if one is moved (like the axis of rotation), the other associated point in the bat will also be relocated.

From this data, a player should employ a wide grip, as not only were the loads consistently low, there were also distinct COP locations between 0.12 and 0.18m for the bottom clamp and 0.42m for the top clamp. However if the player was of a high standard, the middle grip condition should be considered. Although following impacts at certain locations (0.18m) the highest handle loads were recorded, impacts between 0.24 and 0.36m recorded either the lowest or second lowest handle load. Therefore, if a player was able to impact between these locations they would feel a considerable reduction in the load at their hands and thus an improvement in comfort. This is the grip location suggested to learners (Ferguson 1992), even though impacts at specific locations would cause amplified discomfort compared to the other grip locations.

The distinct differences in the results support those of Noble (1985) who found that hand proximity did have an effect on experienced hand loads. In this study it was found that by increasing the distance between the hands, a reduction in the loads could be achieved as the load is distributed over a greater area.

The bottom grip condition recorded consistently higher handle loads regardless of the impact location due to the close proximity of the clamps to the impact position. It was also found that the top grip measured larger forces when the impact occurred towards the bottom of the bat, due to the increased distance between the clamp and the impact position. Therefore, if the impact location is over a certain distance from the bottom clamp (eg. 0.4m), the handle load is increased due the effect of a lever action with the bottom clamp acting as a pivot. However, if the impact is close to the bottom clamp (within 0.2m) the handle loads are also increased. This is caused not only by the close proximity of the applied load, but also by the bats inability to deflect and reduce the transferred load. This finding highlights that although each grip location will have a position of reduced handle load (COP) some are more effective than others, resulting in a player experiencing different degrees of improved comfort. Therefore the COP is not only caused by the axis of rotation, it is also associated with the hands proximity to the impact position, the location of the other hand and the position of both hands on the handle relative to the rest of the bat. An example of this collective dependency is that the clamp locations during the WG and BG conditions were both 0.4m from the COP. Although the location of the top clamp is altered and these conditions will have a different axis of rotation, they do have the same bottom clamp location.

10.5.5 Conclusion.

This section investigated the influence of clamp location on the handle loads following impacts along the length of the bat. It was found that a wide grip had distinct COP locations and reductions in handle load that a player would perceived to be improvements in comfort at their hands. The grip around the middle of the handle with the hands close together, which is suggested by coaches recorded some of the highest post impact handle loads. It can be concluded that COP can be altered following the movement of grip locations due to the movement of the axis of rotation and the proximity of the hands to the impact location.

Therefore, a player could tailor their gripping location to maximise the benefits of the COP depending on the impact position of the ball.

10.6 Rate of loading versus peak load for hand force analysis.

10.6.1 Introduction.

Due to the earlier discussed associations regarding the rate of loading and comfort during the impact period (Chapter 6.2), the rate of loading of the handle load may be a more beneficial indicator for the location of the centre of percussion rather then the magnitude of the handle load itself. The rate of loading was also reported to be a more accurate indicator of the possible discomfort that the subject would experience (Chapter 6.2). Therefore, this section aims to investigate whether the distribution of the handle loads and the location of the COP are the same when the rate of loading is considered. This method may identify locations of improved comfort that differ from the measured handle load results (Chapter 10.2). This section will also investigate the influence of the clamping conditions and impact speed on the calculated rate of loading to establish whether the position of minimum rate of loading is affected by these variables.

10.6.2 Literature review.

As discussed, studies have used changes in peak impact loads as an indicator for the location of the COP and player comfort. However, it has been proposed that the loading rate of the measured load can be used as an indicator for the subjects perceived impact load and comfort rating (Fisher & Vogwell, 2002). This is because rate of loading is a reliable method of evaluating a subject's pain perception and thus an estimation of the comfort level during an impact (Druschky *et al*, 2000). Greenspan & McGillis (1990) found that the faster the indentation rate of the skin, the more intense the sensation. Therefore, slower indentation rates required greater indentation depths to produce the same sensation. Thus, a subject may perceive a greater load when the rate at which it is applied (loading rate) is greater than a higher load applied over a longer period. The qualitative differences between our perceptions and the actual physical properties of the stimuli mainly arise from the fact that the nervous system only extracts certain information from the stimuli (Kandel, 2000). Higher loading rates cause discomfort and so attempts are made during the impact period to reduce them (Milini *et al.* 1997

and Fisher *et al.* 2001). Although, published results describing the relationship between force loading rate and the intensity of pain experienced cannot be found, it can be assumed that higher loading rates would be undesirable.

10.6.3 Experimental set up.

Using the results from section 10.2, the rate of loading for each impact position could be established. The rate of loading was calculated by dividing the magnitude of the peak load by the time to that peak (Fisher, 2001). To investigate the influence of ball velocity on the rate of loading, the results from section 10.4 were also included.

10.6.4 Results.

Using the rate of loading (ROL) for each impact position, it was possible to compare the distribution pattern with the average peak handle loads during impacts at 9ms when clamped at 210mm in the hand simulator rig (Figure 10.21a and b).

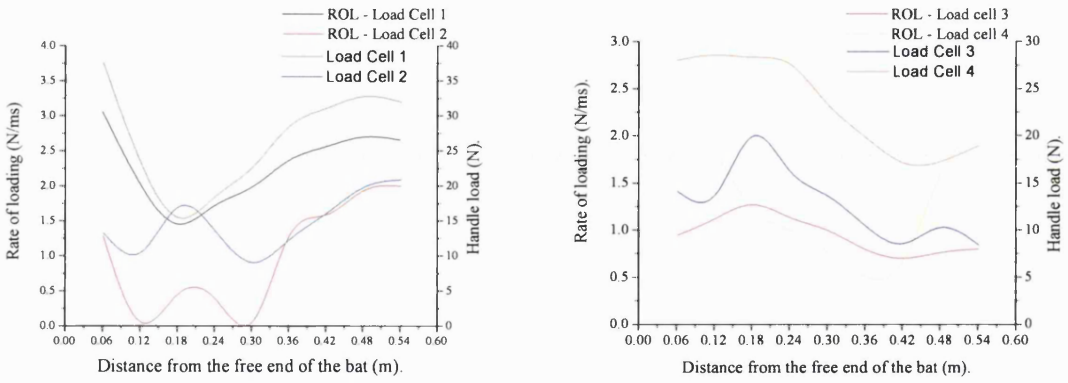

a, Load cells 1 and 2. **b, Load cells 3 and 4.**

Figure 10.21: Rate of loading and peak handle loads during hand simulated conditions.

From Figure 10.21a and b it is clear that the patterns displayed for the calculated rate of loading and peak handle loads are almost identical in their arrangement along the length of the bat. A

noticeable difference between the two results is that the handle loads peaks and valleys are more distinct. For this bat (the Probe) the lowest rate of loading and COP occur at 0.18m from the free end for the first load cell, 0.12 and 0.28m for the second load cell. The position of COP and lowest rate of loading occurs 0.42m for the third and fourth load cells, which are positioned in the second clamp at the top of the handle.

As noted it was also possible to identify the location of the minimum rate of loading using the results from the rigidly clamped bat investigations.

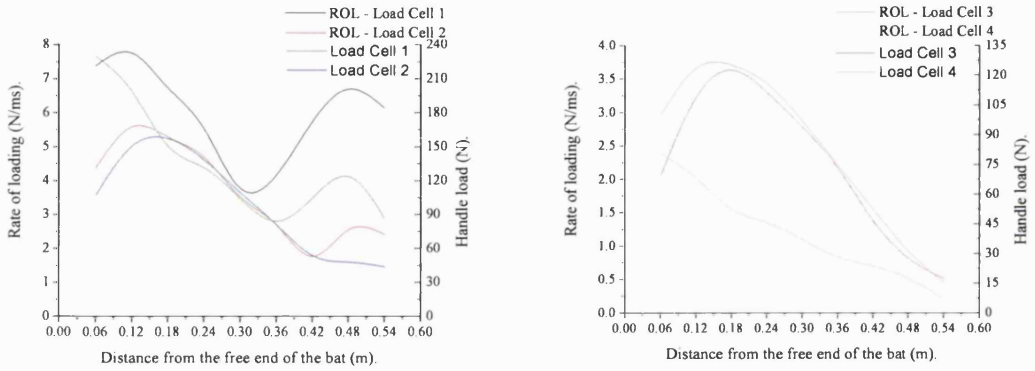

a, Load cells 1 and 2. **B, Load cells 3 and 4.**

Figure 10.22: Rate of loading and peak handle loads during clamped conditions.

As found during the hand simulator conditions, the pattern of the peak handle loads and rate of loading results during the rigid clamping condition are almost identical. Although from the first and second load cell results, the position of minimum rate of loading occurs 0.06m lower down the bat than the COP (Figure 10.22a and b). During this clamped condition, the load cells positioned in the bottom clamp measure a rate of loading twice the value recorded by the clamp at the top of the handle. This pattern was not found during the analysis of the hand held simulator condition rig.

As reported during the experimental set, it was also possible to investigate whether the rate of loading data was affected by alterations in the pre impact ball speed.

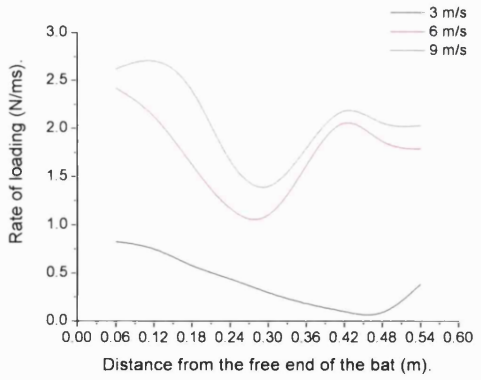

a, Load cell 1.

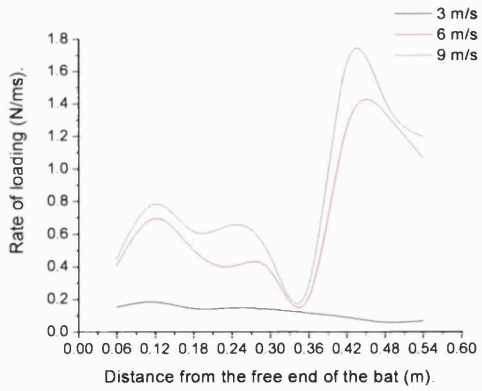

b, Load cell 2.

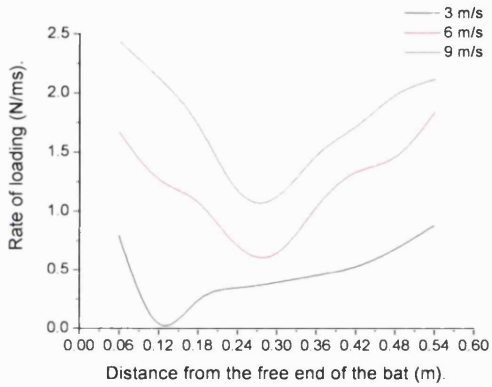

c, Load cell 3.

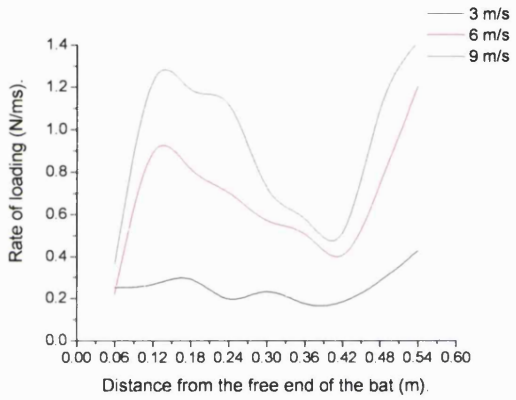

d, Load cell 4.

Figure 10.23: Calculated rate of loading at each load cell with changes in impact speed.

From these figures, it is possible to see that the fluctuations in the rate of loading are unaffected during impact speeds of 6 or 9ms^{-1}. However, it is noticeable that following impacts at 3ms^{-1}, the results are considerably different.

10.6.5 Discussion.

This study compared the peak handle loads and the rate of loading following impacts at specific locations along a cricket bat. Reductions in the rate of loading were related to improvements in

comfort as loads applied at greater velocities have been related to increased subject discomfort (Milani *et al.* 1997). Therefore, calculating the COP using alterations in handle load may not be directly related to 'improvements in feel' as Sykes *et al.* (1971) had suggested. During this discussion the location of the minimum rate of loading will be regarded as the perceived centre of percussion (PCOP).

The shape of the rate of loading trace along the bat was very similar in appearance to the fluctuations of the average peak handle loads with the location of the COP and PCOP coinciding. In chapter 10.2, no distinct COP (zero measured handle force) locations existed, although human subjects had reported improvements in comfort at their hands following impacts at specific locations. Therefore, the improvements in comfort may be due to the reductions in the rate of loading at these positions rather than the reduction in the propulsive forces. This is due to the association between reductions in the ROL and improvements in player hand comfort. As the location of the COP and the PCOP corresponded, it is impossible to establish the dominant factor relating to player comfort, although these two phenomena combine to the benefit of the batsman.

The bottom clamp (load cells 1 & 2), have COP and PCOP positions close (0.02m) to the thickest region, making it more likely that a player would impact these locations during actual play. Therefore, a player would experience a reduction in the load and the associated improvements in comfort at the bottom hand. Additionally, due to the close proximity to the thickest region they may also be able to take advantage of higher COR values (Chapter 11).

During the rigidly clamped condition, the bottom clamp (load cells 1 & 2) recorded a rate of loading twice that of the top clamp (load cells 3 & 4). This did not occur during the hand simulator condition, highlighting how differences in the clamping type influence the distribution, magnitude and the application of the load experienced at the gripping location. The restricted motion of the rigidly clamped handle led to the concentration of the load and increased rate of loading, which would lead to greater discomfort at the players bottom hand as it is closest to the ball impact position. However during the impacts involving the hand simulator, the rig deflects and thus distributes the load more evenly and over a longer period (as shown in the results). However, the concentration of loads at one location may be advantageous if the associated COP or PCOP was impacted as the relative effects would be greatly magnified.

The COP and PCOP occur at similar locations due to the short contact period between the bat and ball, thus having little influence on the calculations of the rate of loading. During other sports related impacts like heel strike during running, the impact period is much longer, thus extensive changes in the length of this period are possible. Therefore, changes have been found to have a considerable influence on the transference of load to the person and perceived comfort of the impact. Due to the possible reductions in post impact ball velocity, it would be disadvantageous to increase the contact period in an attempt to improve player comfort. However, with an increase in the pre impact ball speed (as during game situations), the contact period may be extended sufficiently through ball compression and bat deflection to take advantage of a changing ROL.

The rate of loading and the location of the PCOP were unaffected by the reduction in ball speed from 9 to 6ms^{-1}. However, the rate of loading during impacts involving a ball speed of 3ms^{-1} were noticeably different. These differences are due to the low impact velocity having little effect on the propagation of shock loads. From section 10.4, handle load peaks and COP location during the 3ms^{-1} impacts seemed to be undeveloped and thus the differences in these rate of loading results are a direct consequence of this.

The results displayed are only an indicator of the COP and PCOP locations due to the limitations of the testing procedure, which include the use of a stationary bat prior to impact, specific clamping positions and low impact speeds. Therefore, it is unlikely that these conditions will occur during an actual game situation. However, this experimental set up produces reliable and accurate bat responses that would otherwise be difficult to establish during an actual cricket match. It is proposed that these results can be used to develop the understanding of cricket bat responses during dynamic ball impacts

10.6.6 Conclusion.

This section investigated the rate of loading of the peak handle loads as it can be related to perceptions of hand forces and player comfort. As the locations of the COP and the PCOP

occurred in the same position, it was hypothesised that both of these factors contribute to improve player comfort during impact. When the bottom clamp was analysed, the COP and PCOP occurred close to the thickest section of the bat, indicating that a player may well impact this position on a regular basis during actual play. The rate of loading was also unaffected by differing the impact speed as long as it remained above 6 ms^{-1}. Therefore, it can be concluded that the rate of loading could be used as an effective method of establishing player comfort at their hands during actual game impacts.

10.7 Chapter summary.

Previous literature has reported contradictory results regarding the exact benefits of the COP, although direct measurements of hand loads have not been made during cricket. A distinct reduction in the handle load was recorded at 0.18m from the free end, however this predominantly occurred at the first load cell that represented loads at the subjects palm of their bottom hand. It was deemed that a considerable reduction in all the hand loads was not measured due to the clamping locations not being at the axis of rotation. It was found that the ball impact speed did not affect the location of the COP and that the hand simulator rig provided a reliable alternative to using human subjects. It was discovered that by moving the grip locations, the position and magnitude of the COP could be altered. It was observed that a wide grip would reduce the hand loads the furthest and thus provided the player with greater comfort. The rate of loading was also investigated due to its association with a player's perception of comfort (Milani *et al.* 1997). It was found that the position of lowest loading rate occurred at the same position as the COP and the PCOP was unaffected by impact speed. In conclusion a COP does occur in cricket bats, although it is only possible to reduce the large hand forces and not completely eliminate them.

11 THE POWER REGION.

11.1 Introduction.

The power region is the position on a bat or racket in which at impact the maximum energy is transferred to the ball thus producing the greatest struck ball speed. To establish the power region the coefficient of restitution (COR) is used, as it is an effective method of calculating the post impact performance of sporting equipment as described in chapter 3. This chapter looks at how the bat design influences the COR and thus the power region. Past research is reviewed and the results of tests carried out on five bats are presented.

11.2 Literature review.

Most prior analysis of the COR and the location of the power region has been carried out on tennis rackets and due to a racket's construction, changes in the COR ratio along the length of a racket face are extreme. Brody (1986) noted that if the stiffness of a tennis racket is too high, the ball will deform more during the impact and energy dissipation will increase. However if the implement is too flexible, energy will be lost due to increased deflection. Changes in the COR along the length of a cricket bat were attributed to the continual variation in the flexural stiffness and surface hardness (Grant, 1998b). Differences in the structural design and variations in the properties of the wood will also influence the COR.

Some studies claim that any location on the face of the racket that displays a COR ratio of above 0.5 is a sweet spot (Brody, 1987). However, most rackets (tennis, squash & badminton) have a maximum COR of about 0.85 (McCutchen, 2002), which compares with 1 for a perfectly elastic collision. The position of maximum COR on a tennis racket is located near the throat due to the increased rigidity of the racket at this point (Brody, 1986 and Kawazoe, 1993). However during the swing, the velocity of the tip is greater than that of the throat as it is further from the axis of rotation. Therefore, the highest post impact ball velocity is achieved by striking the position of greatest rotational velocity, not the region of maximum COR (Brody, 1986). Hatze (1994) noted that impacts would not occur at the position of maximum COR as it

is too near the throat of the racket, therefore a player should utilise an effective power region, centred around nodal positions (Figure 11.1). Due to the close proximity of each sweet spot, it has been suggested that the sweet spots do not exist independently but as a larger zone (eg. Naruo & Sato, 1998).

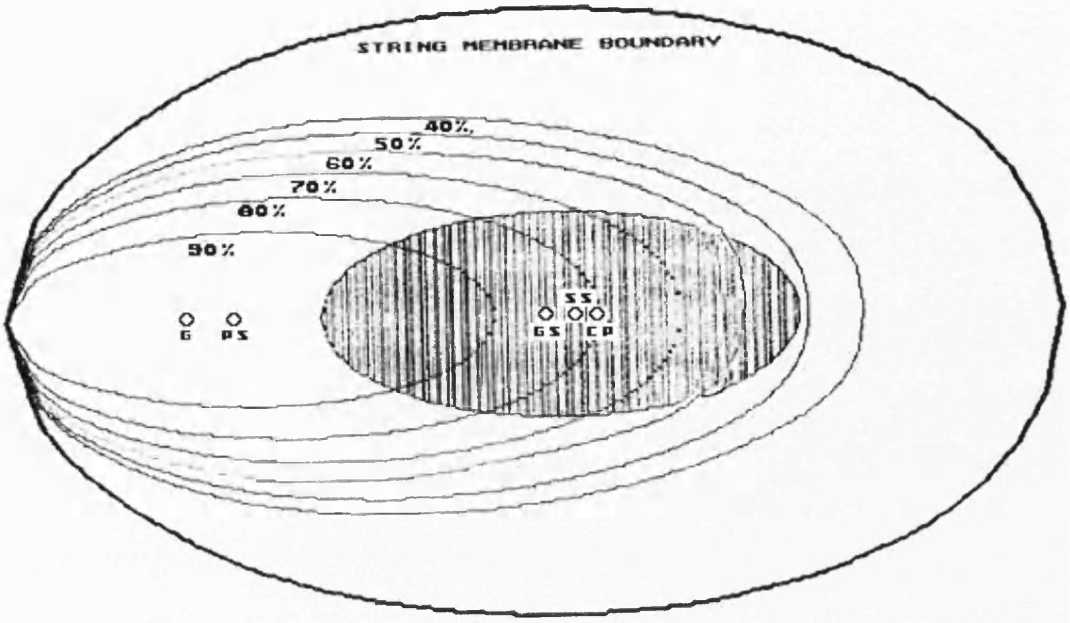

Figure 11.1: Contour map of a tennis racket strings, indicating the effective power region (shaded area) and COR calculations (as a %) (Hatze, 1994).

where, G is the Centre of mass, PS is the Power spot, GS is the Centre of strings, SS is the Nodal sweet spot and CP indicates the Centre of percussion.

The aim of this study is to identify the position that produces the maximum post impact ball velocity with a disregard for the shock or load experienced at the player's hands. It is currently unknown whether it is possible to correlate diminished hand loads with the position of maximum COR, however, if loads are found to increase, players must decide whether they prefer improved performance or personal comfort.

11.2.1 Previous experimental analysis of the power region.

If the ball impact location can be controlled and maintained, the calculation of the COR may be used for assessing bat performance analysis. As Grant (1998b) suggested, "the COR can be used as a reliable indicator for bat performance". Brody (1987) reported that the COR can be established by dropping a ball from 0.3m onto a clamped racket (Figure 11.2). The rebound

height is then measured and the location that records the maximum rebound height is the point of maximum COR.

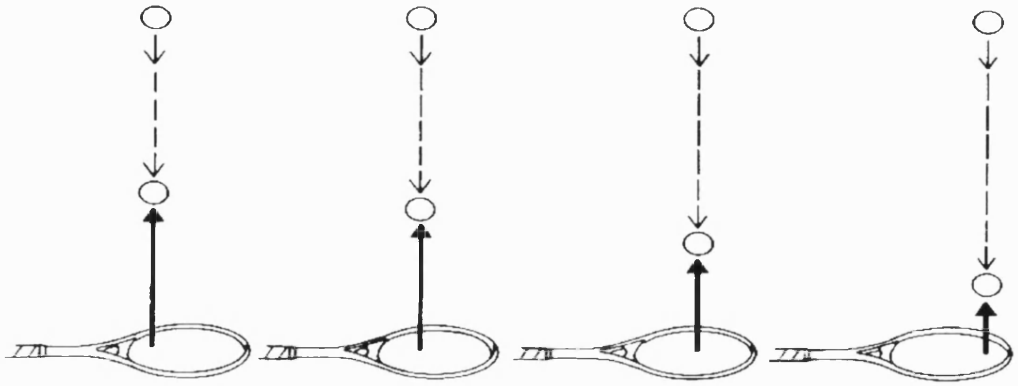

Figure 11.2: Variations in the coefficient of restitution for a stationary clamped racket (Brody, 1987).

where, the black arrows indicate the rebound height following impact at the location.

As discussed earlier and illustrated in Figure 11.2, the position of maximum rebound height was found to be at the throat of the racket along the longitudinal axis. Brody (1987) also noted that under these conditions, the tip of the racket can be the position of maximum rebound height due to the flexion of the racket, which may cause the ball to be struck twice. Firstly when the ball initially impacts and again as the racket returns to its original position, thus transferring more energy to the ball causing the rebound height to increase. Kawazoe (1993) and Cross (1997) found the COR was at its lowest at the tip due to increased flexion of the racket away from the ball.

When static objects are impacted, Hatze (1993) reported that calculations only produce the apparent coefficient of restitution as the actual COR is relative to the racket velocity (Chapter 3). When the object is rigidly clamped, the COR is also reduced as a result of the energy loss caused by the static implement (Hatze, 1992b). The following table illustrates the differences in calculated COR from previous studies, although the clamping conditions are reported to be identical.

Study.	Clamping condition.	Calculated COR values.
Hatze (1992b)	Simulated strokes	0.758 - 0.855
Elliott (1982)	Simulated strokes	0.57 – 0.66
Hatze (1992b)	Rigidly clamped handle	0.608 - 0.699
Hatze (1993)	Rigidly clamped handle	0.38 – 0.447

Table 11.1: Calculated COR values for tennis rackets under different conditions.

In Table 11.1, the lack of correlation between the reported COR by previous studies can be seen. Although an investigator repeated an earlier study (Hatze, 1992b and Hatze, 1993) they produced markedly different results under the same conditions. This identifies how the COR can be significantly changed by not only the clamping conditions but also the racket type and testing conditions. An earlier study by King Liu (1983) demonstrated that the rebound velocity of the ball is unmodified by the clamping condition during impact. However from Table 11.1, it could be considered that this is not necessarily accurate.

11.2.2 Conclusions.

The aim of this chapter section (11.2) was to summarise important findings of previously published investigations carried out on the COR of sporting equipment. It was found that due to differences in testing procedures and implements tested, conflicting results are produced. Therefore, it is not always possible to directly compare previously published COR figures. Attention was drawn to the fact that there have been a limited number of cricket bat studies that have specifically established the COR, although the experimental set up used for other bats and rackets can be applied to cricket bat analysis.

11.3 The effect of structural design on the coefficient of restitution.

11.3.1 Introduction.

Most commercially available cricket bats vary structurally and there are often extravagant claims that the differences significantly improve performance. To investigate such claims, this study establishes the position and magnitude of the COR of five first class cricket bats of differing structural design. Whereas some previous studies have calculated the COR using mathematical equations or finite element computer packages, experimental tests have been used during this chapter to determine the responses of cricket bats under dynamic ball impacts.

11.3.2 Specific literature review.

The COR defines the size and position of the sweet spot on a striking implement (Grant, 1998b). Knowles *et al.* (1996) found that a typical modern cricket bat has a maximum COR of between 0.45 and 0.49 along the length of the bat. Penrose & Hose (1998) used Matlab to construct a one-dimensional beam to simulate a cricket bat. They accurately modelled the weight (1.002kg) and locations of centre of mass (502mm from the tip) so that they could analyse the influence of the construction materials on the COR. The ball impacted a single node approaching perpendicular to the bat (beam), the impact time was confined to 0.7msec with a pre impact velocity of $30ms^{-1}$, the results are shown in Figure 11.3.

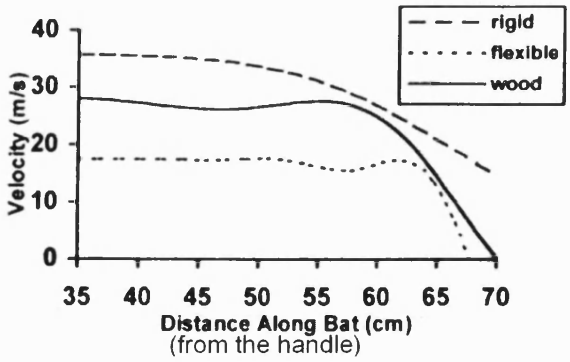

Figure 11.3: Variation of post-impact ball velocity for bats of varying stiffness (Penrose & Hose, 1998).

From these results (Figure 11.3), Penrose & Hose (1998) found that the peak post-impact ball velocity occurred close to the 1st flexure node (55.1cm from the handle tip) and the rigid bat produced the higher post-impact ball velocity. Penrose & Hose (1998) found that the flexible and wooden bats produced a similar pattern, although no explanation was offered for this finding.

Penrose & Hose (1998) also tested two basic designed cricket bats, one with and one without a single large scallop in the back. Grant (1998b) and later Cross (2001a) reported that the redistribution of weight around the edges of the striking implement can improve control and performance. Penrose & Hose (1998) allowed the bats to either translate ($9ms^{-1}$) or rotate ($15ms^{-1}$ at the toe end) prior to impact. It was found that the traditional designed bat out performed the scalloped design (Figure 11.4).

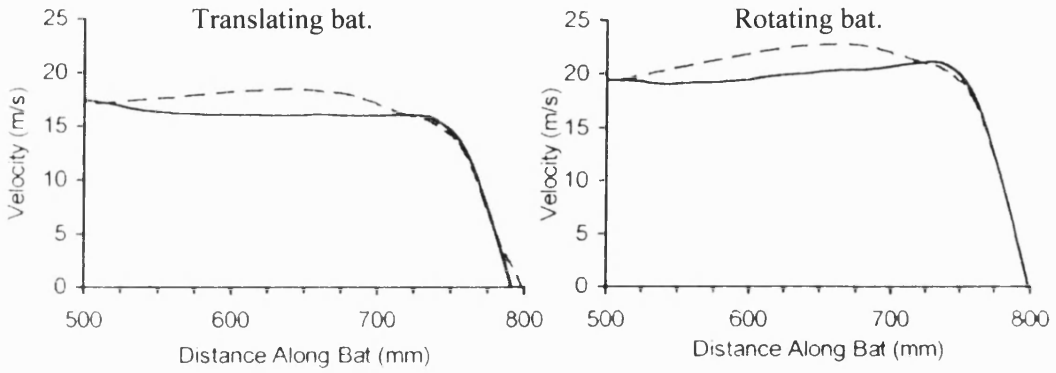

Figure 11.4: Variation in post-impact ball velocity with changes in impact position from the handle tip (Penrose & Hose, 1998).

where, The dashed line represents the traditional designed bat, and the solid line is the scalloped bat design.

It was found that the maximum post-impact velocity occurred close to the position of the node of the 1st flexural mode (608mm) for the traditional design, but this did not occur for the scalloped design. The magnitude of the post-impact velocities related to a peak COR of 0.7.

When a ball impacts a sweet spot, the coefficient of restitution is at a maximum and the resultant vibrations and hand forces are minimised (Cross, 1997). However, following an impact at the tip of a racket, the rebound height is minimised and the vibrations are maximised (Cross, 1997). Cross (1997) referred to this position as the dead spot and suggested that it was caused by the deflection of the racket away from the ball and the transference of energy directly into the racket as it was stationary.

11.3.3 Experimental set up.

Five first class cricket bats differing in structural design were tested during dynamic ball impacts. The bats were secured in the hand simulator rig, with the clamps set 210mm apart and tightened to 8N to replicate the hand locations and pre-impact gripping pressure of the hand held trials. Nine impact locations set at 0.06m intervals were marked on the side of the bat using high contrast markers. The ball was also marked with high contrast dots to enable the motion to be accurately captured. The bats were positioned under the 5m tube and a dropping ball would produce an impact velocity of $9ms^{-1}$. Each impact location in turn experienced six direct impacts that did not involved double impacts or any further contact with the ball following impact. The flexible clamping system was checked after each impact and alterations to the clamps were made whenever necessary. The impacts were recorded in two-dimensions using a Photron 1280 PCI Fastcam-X, with a frame rate of 2000Hz and a shutter speed of 4000Hz to decrease blurring. An example of the captured ball motion can be seen in the following sequence of figures (11.5). For ease of understanding and clarity, frames have been excluded due to the high capture rate and the high contrast markers have been removed.

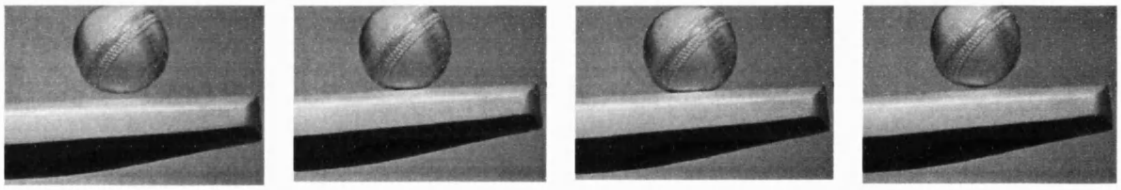

Pre impact | Ball contact | Max ball deformation | Post impact

Figure 11.5: Ball impact motion sequence.

Following capture, the motion of the ball prior to and following impact was automatically tracked using the Photron motion tools software. The pre-impact ball motion was tracked until 2 frames (1 millisecond) before impact and the post impact ball motion was tracked from 2 frames after impact both for a minimum of 35 frames. This was to ensure that the contact between the bat and the ball did not influence the calculated speeds. The pre and post impact speeds were calculated incrementally by dividing the ball movement by the time interval.

11.3.4 Results.

The COR of the five bats displayed in Figure 11.6, was established as the ratio of the post impact velocity relative to the pre impact velocity.

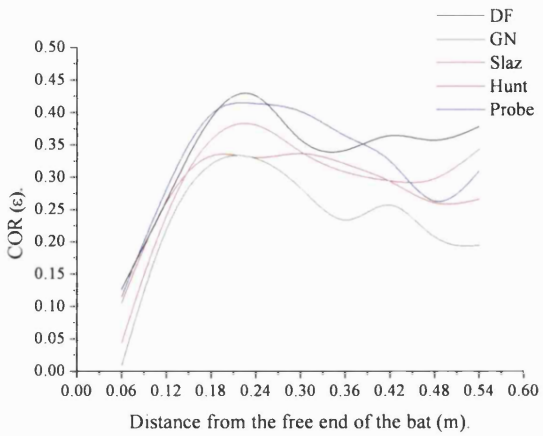

Figure 11.6: The COR along the length of five leading cricket bats for hand simulator.

As it can be seen from Figure 11.6, the position of maximum COR lies between 0.17 and 0.23m from the free end of the bat and ranges between 0.32 and 0.43. The ratio then tends to decrease until approximately 0.48m from the free end of the bat. The subsequent impacts that occur further than 0.48m from the free end, display an increase in the COR. It is also interesting to note that the position closest to the free end (0.06m) has a very low COR of between 0.03 and 0.13. The bat that records the greatest COR (0.43) is the DF bat, while the lowest COR (0.32) is the GN bat. This can be related to a difference in performance (COR) of 25%. Finally, the Probe bat maintains a high COR along much of its length following a peak COR 0.19m from the free end, which is 0.03m above the thickest section.

As it is believed that the COR relates to bat deflection, the peak deflection value of each impact location following an impact at that location has been established (Figure 11.7).

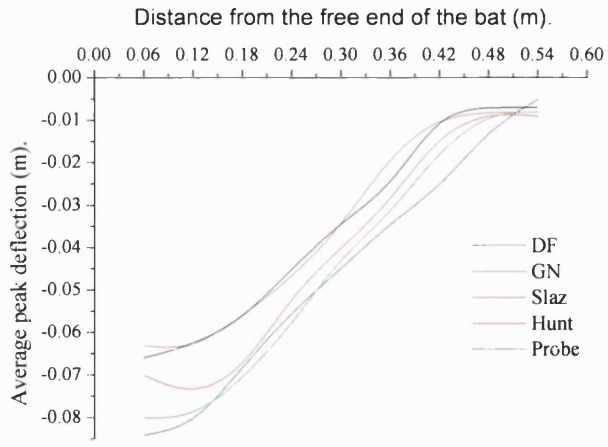

Figure 11.7: Average peak bat deflection of each impact location.

It can be seen in Figure 11.7, that the shape and magnitude of the deflection for each of the bats is similar. The bat's deflection (excluding the Probe) level off between 0.06 and 0.12m, and between 0.48 and 0.54m from the free end.

As the motion of the hand simulator will have influenced the responses of the bats, the COR (Figure 11.8) and the deflection (Figure 11.9) for each impact location when the bats were rigidly clamped has been included.

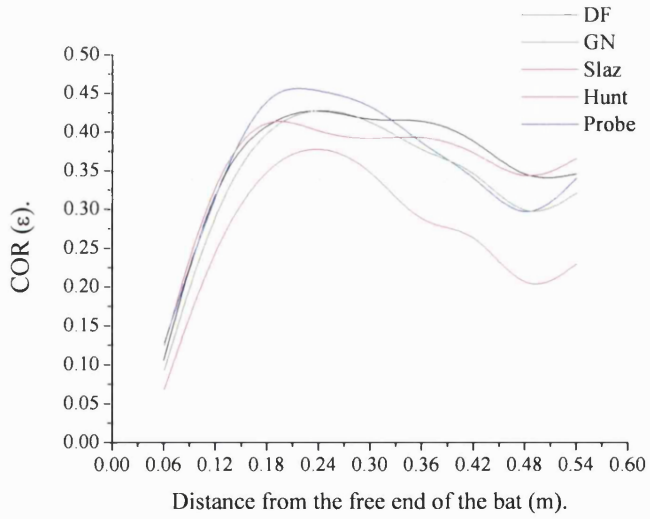

Figure 11.8: Variation of COR when the bat is rigidly clamped at a grip spacing of 210mm.

From Figure 11.8, it is observed that the Probe bat has the highest COR value with a peak COR of 0.45 and the Slaz bat has the lowest COR (0.37). This correlates to a COR reduction of 18%

between the Probe and Slaz bats. Although the COR calculated during this experimental set up are larger than those reported when the bats were in the hand simulator, it is interesting to note that the distribution of the COR along the length of the bat is very similar. It should also be noted that although there is a reduction and then increase in the COR as the impact positions move closer to the clamping location (0.6m from the free end), this is not as prominent as during the hand simulator trials (Figure 11.6).

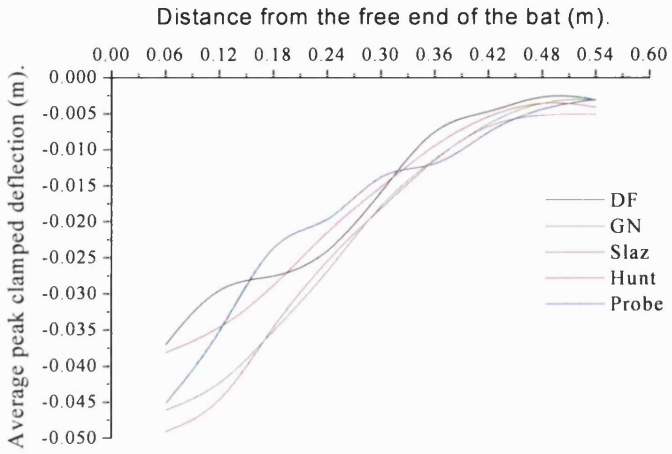

Figure 11.9: Impact position deflection during a dynamic impact when the bat is rigidly clamped.

From Figure 11.9, it is clear that the magnitude of the measured deflection when the bats are rigidly clamped is less (up to 0.03m) than the measured deflection when the bat was in the hand simulator. This highlights the extent of the hand simulator's motion on the measured bat deflection. The deflection is not as linear through the middle section (0.12 to 0.42m) or as smooth as shown in Figure 11.7. Although, there is a similar 'S' shape to the measured deflections as found during the hand simulator results.

It was hypothesised that the deflection of the bats during the impact phase may have a greater influence on the post impact ball velocity (as found during tennis) rather than the peak bat deflections, which occur well after the ball has lost contact with the bat.

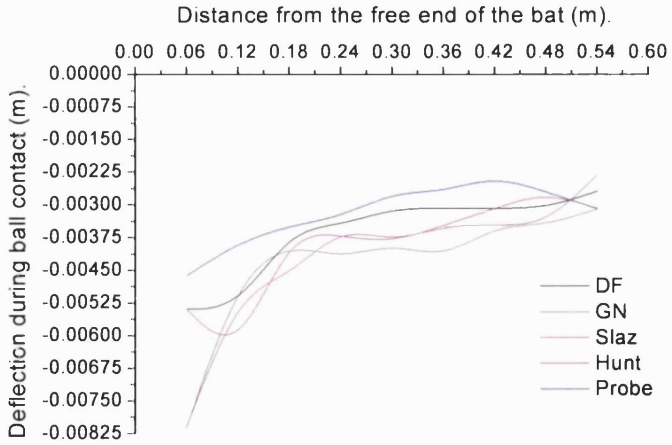

Figure 11.10: Average bat deflection during ball contact.

From Figure 11.10, it is possible to see that the Probe bat displays the minimum deflection along the length of the bat during the ball contact period. The deflection patterns of the Hunt and DF bats display distinct curvature following impacts at 0.12 and 0.18m. The Slaz and GN bats have the greatest degree of deflection following an impact at the end of the bat. Finally, it should be highlighted that an impact 0.54m from the free end occurs at the join between the handle and bat.

Using the measured deflection and known impact force of the ball (calculated from static deflection measurements), it was possible to establish and plot the stiffness of the bats when they are in the hand simulator or rigidly clamped.

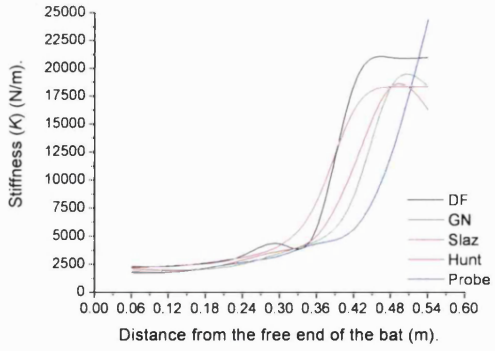

Figure 11.11: Stiffness when the bats are in the hand simulator.

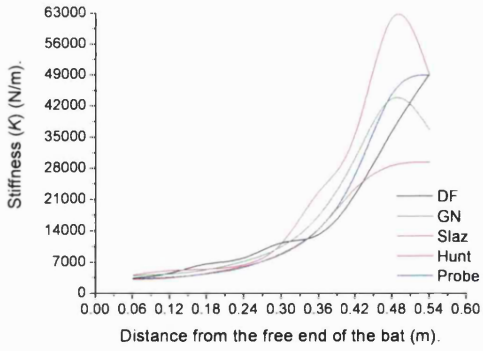

Figure 11.12: Stiffness when the bats are rigidly clamped.

Figure 11.11 and 11.12 show the calculated stiffness of the bats analysed. There is a linear increase in the stiffness as the position is further from the free end of the bats (towards the clamps). However above 0.36m from the free end, there is a considerable increase in the calculated stiffness. This finding occurs during the hand simulator and rigidly clamped trials. It is also noticeable that there is a plateau or reduction in stiffness when the impacts were administered 0.54m from the free end.

As it is difficult to establish whether there are any changes in stiffness around the position of maximum COR, Figure 11.13 is a magnification of the impact positions up to 0.3m from the free end. The results displayed in Figure 11.13 were taken from when the bats were rigidly clamped as it was considered that the motion of the hand simulator may cause errors and disparity in the results.

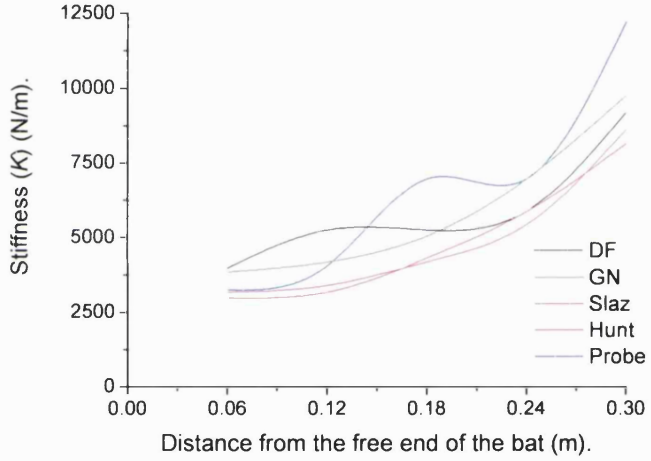

Figure 11.13: Magnification of the position of maximum COR.

Figure 11.13 shows the deviations in the stiffness for each of the analysed bats. It is clear that the DF bat has a peak in the stiffness at 0.12m and the Probe bat has a stiffness peak at 0.18m from the free end.

To highlight any differences in performance, the stiffness was also analysed relative to the COR (Figure 11.14). The bats displayed, recorded the highest and lowest COR (DF and GN respectively) to highlight the greatest differences between the analysed bats.

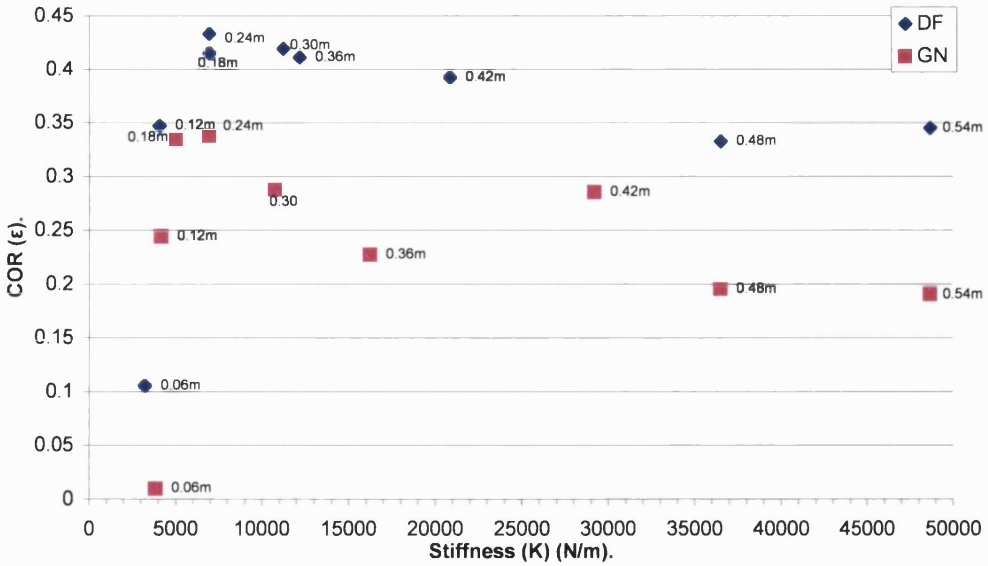

Figure 11.14: The COR and stiffness of the DF and GN bats when in the hand simulator.

Figure 11.14 illustrates the calculated COR and stiffness relative to the impact location along the length of the bat, which is indicated next to each data point. Both bats display a distinct similarity in the pattern of stiffness relative to the calculated COR. The pattern displayed by the bats show a peak COR at a stiffness of 6850 N/m with either extremity displaying a reduced COR value. When the calculated stiffness values of the DF bat are between 5000 to 12000 N/m, the highest COR values are recorded.

11.3.5 Discussion.

Bat performance has been determined through the calculation of the COR for five first class cricket bats of differing structural design. Limited literature had been found regarding experimental results of cricket bat COR, although studies had reported COR values using different modelling techniques. The location of maximum COR was found to occur between 0.18 and 0.23m from the free end of the bat and the differences in structural design have limited effect on its magnitude.

The bat with the largest COR (0.43) during the hand simulator trials was the DF. This finding shows that over 50% of the ball speed is lost following the impact period. The transference of energy from the ball into the bat is lost through bat deflection, shock load, vibration

propagation, ball compression, sound and heat. As the bat is stationary at impact relative to the ball, a greater magnitude of energy will also be transferred into the bat thus lowering the COR. Cross (1997) considered impacts onto stationary implements to be one of the causes of dead spots. As it is unlikely that this situation would occur during a game, the reported COR values of 0.7 (Grant & Thethi, 1994 and Penrose & Hose, 1998) may be possible. This is because the COR is associated with the rotational velocity of the bat during the impact period (Hatze, 1993). However, the COR values from this study do correlate with the models of Knowles *et al.* (1996) during their analysis of cricket bats.

During a rigid body analysis, the position of maximum COR on a cricket bat was found to occur close to the free end due to the absence of inertia (Grant, 1998b). However it was noted that if inertia was included, the position of maximum COR would rise towards the COM of the bat as found during this study. As the hand simulator rig enables bat motion, inertial properties of the bat will have influenced the results. However, Grant (1998b) did not report a drop in the COR at the end of the blade, which was found in this study. An impact at this location (0.06m from the free end) causes most of the energy to remain in the bat, which results in a considerable reduction in post impact ball velocity and thus the calculated COR. A reason for this finding is that the bat deflects at the same rate as the expansion of the ball causing the ball to have nothing to expand against and thus a reduction in the post impact velocity is recorded. Cross (1997) had found this occurrence in tennis rackets at 0.08m from the end, while Penrose & Hose (1998) referred to this position due to the low post impact ball velocity following cricket bat and ball impacts (Figure 11.3).

Even though Penrose & Hose (1998) used a one-dimensional beam, Figure 11.3 displays a similar pattern to Figure 11.6, which was produced by this study. In particular, both figures show a dip in the COR at approximately 0.47m from the top of the handle (Penrose & Hose, 1998) or approx 0.42m from the free end (in this study), a peak in the COR towards the bottom of the bat, before a significant drop to almost 0 at the end of the bat. Penrose & Hose (1998) found the peak COR to occur approximately 0.14m from the end of the bat as opposed to between 0.17 and 0.23m from the end of the bat during this study. Although there is up to 0.09m difference in the positions of maximum COR, the similarities in COR distribution along the length of the bat substantiate the results of this study. It would be expected that Penrose & Hose, (1998) would find some differences in the reported results due to the theoretical analysis techniques employed rather than experimental methods of this study.

The DF bat, which is a more traditional style with much of its mass evenly distributed, recorded the highest calculated COR. It was also noted that the Probe maintains a high COR along much of the bat (between 0.20 and 0.36m from the free end). Crisco *et al.* (2000) noted that the mechanical limitations of a baseball bat can cause a plateau following extensive deflection or amplified vibrational waves. It is unlikely that the results for the Probe are caused by the limitations of the bat due to the low pre-impact ball velocity, which wouldn't have created the disadvantageous events found by Crisco *et al.* (2000). The maintenance of a high COR matches the findings of Brody (1985), who reported that due to the wooden construction and limited deflection, there is no definitive position of maximum COR in baseball bats. The Probe has a large central spine along the length of the blade, which stiffens the bat during the impact period and maintains the COR. The other bats do not have this feature, which can be associated with the reduction in COR that they record. Consequently (from Figure 11.10), if the deflection during the impact period is reduced, more of the energy is transferred to the ball and thus the COR is maximised along the bat. The profile of the Probe bat also has a considerable reduction in mass towards the handle, which leads to the decrease in the COR between 0.42 and 0.48m from the free end of the bat. It was also noted (although it is more prominent in the results of the Probe), that the COR increases at the intersection of the bat and the handle (0.54m from the free end). This is caused by the changes in the material properties of the impacting area as the ball impacts the bottom of the cane handle. The COR will also increase as this impact location is closer to the bottom clamp, which increases the stiffness at this location (Figure 11.14). Although the DF displayed the highest COR value, it is the Probe that could be considered to perform better overall as the design of the bat ensured a high post impact ball velocity almost regardless of the impact location.

The shape of the Probe's deflection is almost linear, suggesting the bat deflects as a solid section rather than flexing towards the end as particularly prominent during the Hunt analysis. This flexion of the Hunt indicates a reduction in the stiffness, which is caused by the removal of large sections from the back of the bat. This would also increase the speed and amplitude of vibrational waves and the deflection, while reducing the damping of the bat's motion following the impact. Therefore, less energy is transferred to the ball leading to a decrease in the COR.

As the impact only lasts approximately 2 milliseconds, the ball has lost contact with the bat before the peak deflection occurs at approximately 32milliseconds. Therefore, the ball will not

be affected by the motion of the bat at this time. Penrose & Hose (1998) noted that bat responses following impact only have a small influence on the outcome of the ball. Consequently, the deflection of the bat during the contact period was reported during this chapter. It was found that the Probe had the lowest contact deflection and maintained a high COR along the bat, while the GN recorded the most contact deflection and the lowest COR. It is considered that if the bat deflects less during the contact period, the ball will be able to expand against it, thus maximising the post impact ball velocity and COR. As the DF bat had the lowest peak deflection, a low contact deflection, the largest peak COR and an extended high COR, the COR must be a combination of these two deflection measurements.

During the analysis of the peak bat deflection, the results from the Hunt bat were found to curve following impacts at the bottom of the bat. This was also found during the contact deflection analysis, illustrating that ball contact may influence the peak bat deflection. It is proposed that this distinct deflection shape is caused by one of the vibrational modes. If this impact position corresponded with the anti-node of a mode, the amplitude will be magnified, thus influencing the COR and the post impact response of the bat.

Following impacts at 0.54m from the free end, the COR and deflection patterns were completely altered. The differences in the results are a product of the material interactions of the willow bat, cane handle and the impacting ball. This is because this impact position is at the join between the handle and the bat. Grant, (1996b) also found a node of the first mode close to this position. Therefore, the first mode would not be excited causing much of the energy (that would have otherwise have been lost in wave propagation) to be transferred to the ball, thus increasing the COR. The correspondences between the nodal positions and the COR will be discussed later in chapter 13.

This study also investigated bat deflection and COR when the bat was rigidly clamped, although the clamp locations were maintained. Primarily, the COR was found to be very similar to those recorded during the hand simulator trials, suggesting that the measured COR is almost independent of the clamping method employed. Thus supporting the results of King Liu (1983) during their studies. It could also be suggested that the COR is independent from the actions of the handle, as the handles motion is significantly impeded when it is rigidly clamped as opposed to being largely uninhibited when it is in the hand simulator. The peak bat deflection is also

greater during the hand simulator tests mainly due to the compression of the spring and damper system. Therefore due to the similar recorded values, the COR may also be unrelated with peak bat deflection. This supports the earlier suggestion that deflection during the contact period is of greatest significance.

The stiffness of the bats were plotted during both clamping conditions, although it was considered to be more comparable if the results from the rigidly clamped impacts were analysed to exclude the motion of the hand simulator rig. The DF and Probe had a peak in the calculated stiffness, 0.12 and 0.18m from the free end respectively, although the stiffness considerably increased towards the handle region. Theses locations corresponded with a reduction in the measured deflection when the bats were rigidly clamped. As the stiffness is calculated from the peak deflection measurements this was expected. However, these peak locations were not repeated in the COR results, highlighting the independence of the COR from the peak bat deflection.

When the stiffness of two selected bats (GN & DF) were plotted, it was possible to see that a bat stiffness of 6850N/m led to a peak COR. The DF bat had more impact locations close to this stiffness value and thus a larger and more constant COR was recorded when compared to the GN bat. This opposes the findings of Knowles *et al.* (1996) who reported the COR increased in a linear fashion with an increase in stiffness. This difference to the previous study may be due to the greater range in bat stiffness analysed by this study. There is a peak rather than a linear trend as a very flexible bat (a low stiffness) will deflect too much reducing the energy transferred to the ball. However, a high stiffness will also reduce the COR due to increased compression of the ball, although there is considerably less deflection at this point. The optimum stiffness value of 6850N/m is a third larger than the average stiffness figure reported by Knowles *et al.* (1996) of 4000N/m and double the figure reported by Lavers (1969). This disparity is due to Lavers (1969) calculating the EI from a green rectangular beam section rather than the pressed irregular shape of the cricket bat. The minor structural changes made by manufacturers have been found to have little effect on the measured stiffness. However if a manufacturer was aiming to maximise performance, they should aim to make a bat with a constant stiffness of between 4000 and 12000N/m, with a stiffness of 6850N/m at the position of preferred impact. It is important to consider that following alterations to the stiffness, the amplitude of the vibraitonal modes and shock loads transferred to the hands will be changed, which may or may not be a positive affect.

Finally, it has to be considered there is no single factor that has greatest affect on the COR of the bat. Although this study has only investigated the structural design of the bat, it has found that it alone only has a limited effect on the bats performance. However, there are many other variables that will affect the post impact ball velocity as they change the transference of energy to the ball. These include, the relationship between impact location and modal vibration, centre of percussion and, grip type and location. The ball will also influence the calculated COR, as it is also constructed from a non-homogeneous material, which will alter in compliance throughout the testing session, directly effecting the COR. All of these factors must be considered before suggestions can be made in an attempt to improve bat performance through the increase in the COR.

11.3.6 Conclusion.

A study was carried out to investigate the influence of a bat's structural design on the location of the maximum COR. It was suggested that although this position was in a similar location for all the bats, the magnitudes were found to be marginally different. This finding indicated that the structural design had a small influence on the performance of the bats during dynamic impacts. It was also considered that bat deflection during the contact period had a large effect on the COR due to the close correlation between the results. The bat with the highest COR was made in a more traditional design with the mass evenly distributed, although a bat with a large spine was found to maintain a high COR along much of its length. It was calculated that a stiffness of 6850N/m leads to a peak in the COR and it was proposed that manufacturers should attempt to construct bats with a stiffness close to this value. Finally, it was acknowledged that there are many other factors that influence the performance of the bat and the post impact ball velocity, although the structural design is one of them.

11.4 The effect of clamping type on the coefficient of restitution.

11.4.1 Introduction.

The effect of clamping type and grip tightness upon post impact ball velocity has been extensively studied for tennis racket and baseball bats. Although, it was primarily the aim of this study to investigate whether the hand simulator is a representative comparison to hand held impacts, it is also possible to investigate the effects of grip firmness and clamping conditions on the COR of a cricket bat. It is unclear whether any literature has been published regarding the use of a flexible clamping system that simulates the responses of a hand held impact. Therefore, this section will also establish how impact position, grip type and grip tightness influence the measured COR.

11.4.2 Literature review.

The firmness of the player's grip is a major contributing factor to the magnitude of the post impact ball velocity as it affects the deflection of the racket during impact (Baker & Putnam, 1979). A firm grip also increases the striking mass of the implement, further increasing the post impact ball speed (Plagenhoef, 1970). The impulse transferred from the racket to the ball can also be increased by 15% with an increase in grip tightness (Hatze, 1976). Previous studies often use rigid clamping devices during racket analysis, although due to the significant differences in post impact behaviour, the results are of academic interest (Casolo & Ruggieri, 1991 and Cross, 1997). Adair (1998) reported that the grip type influences the ball during impact as the propagated impulse has time to return to the ball whilst it is still in contact with the racket. Daish (1972), Watanabe *et al.* (1979) and Liu (1983) reported that the intensity of the grip did not affect the post impact ball velocity or implement responses. However, Baker & Putnam (1979) and Weyrich *et al.* (1989) reported that clamping condition or grip firmness did affect racket responses after the ball had lost contact with the racket. Cross (1997) concluded that regardless of whether the handles are clamped or hand held, the response of the racket varies significantly due to differences in construction techniques and geometrical design.

11.4.3 Experimental set up.

A single first class cricket bat was used, as the responses of a single bat could be easily transferred to other cricket bats as earlier COR results had been very similar. By using a single bat, any bat related variables that may influence the results are also eliminated. The bat used was the DF (Duncan & Fearnley Gold), which had demonstrated the largest COR, although the clamping conditions may have influenced the reported values. Four clamping conditions were employed, rigid clamping, freely suspended, hand held and a flexible clamping system (the hand simulator rig).

The experimental set up used during this study was the same methodology reported earlier for each of the clamping conditions. Primarily the bat was secured in the rigid clamping system, which had the clamps set 210mm apart with a clamping load of 300N. The average of five human subjects were defined as the second clamping condition. They were instructed to grip the handle of the bat at the same locations as used during the rigid clamping system, while positioning the bat under the five metre drop tube. Although, it is accepted that the body position of the subjects would be different to the actual gaming situation, the subjects were instructed to respond firmly in a manner as close to occurrences during a game. Two loads cells were stuck to the tip of the second finger and the base of the palm of each hand (Knudson, 1991b and Cross, 1998). The subjects were then allowed to become accustomed with the testing procedure. Prior to impact, they were correctly positioned and then informed of the ball release to ensure they were ready for the impact. Freely suspended tennis rackets have been used to investigate the COR (eg. Cross, 1997), thus the cricket bat was suspended from the ceiling using twine, which was stretch resistant. The twine measured 0.8m in length and was attached around the top of the handle. Finally, the results previously displayed in chapter 11.2 were used for the hand simulator condition.

The nine impact locations along the length of the bat were each impacted six times using the dropping ball method. During the freely suspended condition, the ball was also suspended using twine so it was in contact with the blade at rest to ensure perpendicular impacts (Brody, 1987 and Wilson & Davis, 1995). Using a protractor attached to the ceiling, the ball was drawn back 50 degrees before being released to swing freely towards the bat (Wilson & Davis, 1995). Cross (1998a) reported that the COR is not dependant upon pre impact ball velocity, therefore

this method was sufficient to establish the COR. However, it should be considered that as the impact velocity increases, the ball deformation and bat deflection will increase and thus the COR may decrease. Only impacts along the central axis of the bat were accepted to eliminate the effects of off centre impacts.

As during chapter 11.2, the pre and post impact ball motion was tracked until 2 frames (1 millisecond) before and after the impact, to ensure the results were not influenced by bat contact. The tracked marker motion enabled the study to establish the pre and post impact ball speeds and calculate the COR.

11.4.4 Results.

The average COR was calculated for each of the impact locations along the length of the bat during each of the clamping conditions. The results are displayed in Figure 11.15.

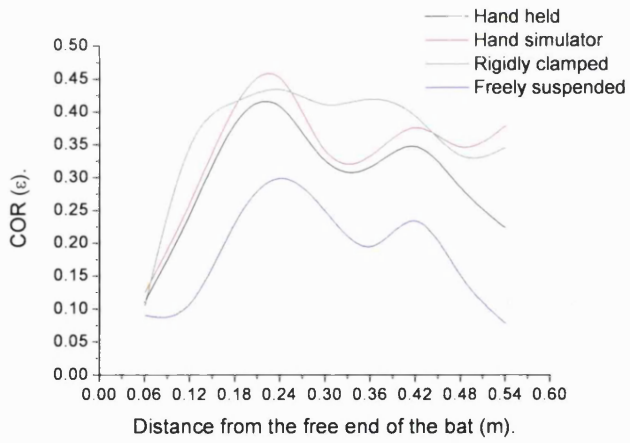

Figure 11.15: COR of the DF bat for different clamping conditions.

From Figure 11.15, it can be seen that the results from the freely suspended, hand held and the hand simulator conditions follow a similar pattern. The hand simulator records the highest COR (0.45) and the COR during the freely suspended condition is much lower (0.28). The rigidly clamped condition does not follow the same pattern as the other clamping conditions. However, all of the clamping conditions display a minimum COR of below 0.13 at 0.06m from the free end. Following impacts at 0.54m from the free end, the COR increases for both the

hand simulator and rigidly clamped conditions. However, the COR drops sharply during the hand held and freely suspended trials at this location. Finally, during the freely suspended, hand held and hand simulator conditions, there is a second peak in the COR at approximately 0.42m from the free end.

11.4.5 Discussion.

This chapter section established the effects of different clamping methods and grip tightness on the COR of a first class cricket bat. Four different clamping methods were employed, freely suspended, hand held, rigidly clamped and a hand simulator. Using these results, it was also possible to ensure that the results produced using the hand simulator including the location and magnitude of the COR correlated with those of an average human subject. Finally, it was possible to establish the influence of clamping type on the magnitude of the COR along the length of a cricket bat.

It was found that the hand simulator and hand held trials followed very similar patterns of calculated COR along the length of the bat. However, it should be noted that the hand simulator rig recorded marginally higher COR values, although these differences were not found to be significant. It is considered that the hand held and hand simulator followed similar trends due to the actions of the spring and damper systems reproducing the motions of the subjects during the impact phase. However, it is the aluminium clamps that would have predominantly caused the differences in the results, as they do not contain the same compliant material as the soft tissue of the hands. Although as the initial gripping force was set to represent the subjects standard gripping force, this factor was minimised. The variation between the two conditions may have also been caused by differences in inertial properties. If the hand simulator has a higher moment of inertia, the bat will not deflect away from the ball as quickly, thus reducing the energy loss as the ball has something to rebound against. Changes in inertia were considered to be the major contributor to the occurrences of a dead spot in tennis rackets (Cross, 1997). Although the hand simulator is found to respond in a similar fashion to the human subjects, humans will continually alter their responses including grip force to fit the situation and maximise comfort. Consequently, slight changes will cause the apparent differences between these two clamping conditions. This also highlights why it is beneficial to use a hand

simulator rather than human subjects, as the hand simulator responds in an identical manner for each impact.

Following an impact at 0.06m from the free end, all of the conditions record a similarly low COR. This substantiates the claims reported in section 11.2 that this impact region may be a dead spot. This low COR is caused by the increased deflection at this location, which reduces the energy transferred to the ball. This is a consequence of the increased distance between the clamps or hands and this impact location. As this finding occurred during each clamping condition it can be suggested that at specific impact locations, the COR is unaffected by the clamping condition supporting studies like Watanabe *et al.* (1979).

Following an increase in gripping tightness (hand held to rigid clamping), the COR was found to increase by an average of 16%. This correlates with the findings of Plagnehoef (1970) and Hatze (1976) who noted an increase of between 10 and 15% following a similar increase in the grip tightness. Although there is a close correlation between this and previous studies, these results do not include the hand simulator results, as this condition recorded higher COR ratios at specific positions than even the rigidly clamped condition.

The freely suspended, hand held and hand simulator conditions all displayed a second smaller COR peak 0.42m from the free end. This may be caused by the close proximity of this impact location to a nodal position. If this impact occurs on a node, no energy will be used in propagating this mode therefore, maximising the energy transferred to the ball. Vibrational modes and the location of nodes will be discussed and analysed in chapters 12 and 13. This finding can also be related to the clamps employed during the rigidly clamped and hand simulator conditions. Although the hand simulator responds in a similar manner to that of the human subjects, the bat is still secured using aluminium clamps. The clamps are close to this location and they stop the bat from deflecting to the same degree as during the hand held and freely suspended impacts. This reduces the energy loss through bat deflection and thus artificially increases the COR. The close proximity of the clamps may cause the vibrational wave to be rebounded, leading to the ball being struck twice by the bat and thus maximising the COR as established during tennis racket impacts (Brody, 1981). However, it would be expected that this response and result would be maintained as the impacts moved towards the clamps rather than just recording a single peak. Although as the impacts occur closer to the clamping

locations, the compression of the ball may increase which would lead to a reduction in the measured COR. This finding highlights a weakness in the hand simulator rig as the results are no longer consistent with the hand held trials following an impact at this location.

The rigidly clamped condition does not give a close representation of the bat responses found during the hand held impacts. However, the rigid clamping system does allow this study to explain some of the differences between the hand simulator and the hand held impacts. The results also highlight how important it is to use a representative method of clamping before comparisons can be drawn with hand held occurrences or even actual playing situations. This concurs with Cross (1997) who following the analysis of tennis racket responses, reported that rigid clamping results were non-transferable to game situations.

Cross (1998) suggested that the results during freely suspended impacts were only 1% away from hand held impacts. From these results, a reduction of between 17 and 65% in the COR was discovered when compared with the hand held condition. This identifies that set up conditions have a considerable influence on the post impact responses of the ball, which has not been previously reported during tennis ball and racket impacts. The main reason for this finding is the firm response of the subject during the impact period unlike the freely suspended condition that has no fixation device to inhibit post impact motion. Therefore, the primary use of the freely suspended results is to establish how the bat would have responded when it is free from external influences. It has been found that the COR pattern during the freely suspended condition was similar (although smaller) to the hand held condition. Therefore, the differences between these two conditions are purely due to the actions and subsequent effects that the hands have on the motion of the bat.

As the motion of the freely suspended bat is not inhibited, much of the energy from the ball is transferred directly into the bat. Daish (1972) noted that this occurs during billiards or snooker, when the white ball is seen to stop immediately after impacting the object ball. This phenomenon normally occurs during central impacts, rather than during eccentric impacts as during this study. However, a similar although not identical outcome will occur as the momentum from the ball is transferred into the stationary bat initiating its motion. As the impact is not a central impact, some energy is returned to the ball enabling the measurement of the post impact speed, although much of it is transferred to the bat.

A limitation of this study is the orientation of the bats during the impact period. Although this will have little influence on the post impact responses, it is important to identify. During the freely suspended impacts the bat was hung vertically using twine. Therefore, the direction of the bats mass is in a different orientation than when the bat was positioned horizontally under the drop tube. This will have altered the inertial properties of the bat and thus the transference of momentum during the impact period. It is also important to recall that the ball during the freely suspended impacts was also hung by twine and therefore this will also have influenced the post impact responses and may have reduced the post impact ball speed as the ball is unable to react in a completely natural manner.

During the drop ball tests, the impact can be considered to be eccentric due to the centre of gravity of the two colliding bodies not being in line. However, when the bat and ball are suspended, the impact could be considered to be a rotational impact, as this involves a change in angular velocity of the striking body (Goldsmith, 1991). Although, the use of implement suspension for equipment analysis has been previously used and verified, the transference of energy occurs in a different manner, thus influencing the COR. Therefore, studies involving the use of pendulums (like this study) for the calculation of energy transfer (including COR) should be considered with some reservation. An alterative consideration is that during a game, the cricket ball follows a curved path originating from the bowler and thus towards the bat like a pendulum. Therefore, the impact conditions involving the freely suspended condition although not ideal, may be more representative than during the direct ball impacts of the drop test. The methods employed were selected as they produce repeatable and reliable results although they are not completely representative of actual game occurrences.

Another reason for this difference between the tennis literature and this study will be due to the impacting surface and the transference of energy. During the impact period, the strings of a tennis racket deform and then return to their original position helping to transfer much of the energy to the highly elastic ball. This will occur in tennis rackets almost regardless of clamping conditions as highlighted by Watanabe *et al.* (1979). However, the solid surface of the bat is unable to transfer as much of the energy following impact thus reducing the post impact ball speed and calculated COR.

11.4.6 Conclusion.

The aim of this chapter section was to illustrate that the simulated hand clamping rig produced realistic and representative COR values when compared to an average hand held condition. It was found that the hand simulator rig produced a similar pattern along the length of the bat although the COR was found to be slightly higher, which was associated with the increased inertia and the use of aluminium clamps. The freely suspended results were found to have a similar shaped COR, although the magnitude was considerably less. Concerns were also raised regarding the reliability of this testing method. Finally, the rigidly clamped condition was found to produce completely different results when compared to the hand held impacts. Therefore, it can be concluded that the hand simulator rig provides a realistic and reliable method of capturing human representative responses during bat and ball impacts.

11.5 The effect of impact speed on the coefficient of restitution.

11.5.1 Introduction.

Throughout a game of cricket the delivered ball velocity will alter depending on the type, standard and fitness of the bowler. Ball impact speed during a game can be up to $40ms^{-1}$, although this study has only used impact speeds of $9ms^{-1}$. Therefore, it is important to establish whether changes in the pre impact ball speed would have an effect on the COR. The ball impact speed has been reported to be independent of the physics of a collision, therefore speed does not affect the results (Cross, 1998a). However, this study aims to verify this statement and the influence of altering the impact speed on the measured COR of a cricket bat.

11.5.2 Literature review.

There is little published experimental analysis of cricket bat COR following alterations in impact speed, although Grant & Thethi (1994) did investigated different pre impact ball velocities (20, 30 and $40ms^{-1}$) using a simple rigid body computer model. The bat was rotated about the centre of the handle at 40rad/s for each impact velocity. However, Grant & Thethi (1994) did not report the dimensions of the bat, the material properties, the clamping system employed and if the handle construction was considered.

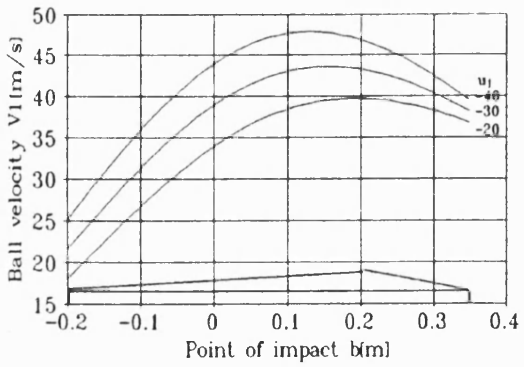

Figure 11.16: Post impact ball velocity with varying approach velocity (Grant & Thethi, 1994).

From Figure 11.16, the position of the maximum COR for each impact speed is visible. This position was found to shift towards the centre of mass (COM) with increasing impact velocity. The COR was measured relative to the COM and therefore, as each bat type will have a different centre of mass (caused by changes in its structural design), the calculated position of the maximum COR from Grant & Thethi (1994) could be applied to this current study. Grant & Thethi (1994) reported that the typical COR was 0.7, although the maximum COR was found to be above 1 following pre impact velocities of 30 and 40ms^{-1} and almost 2 following a pre impact velocity of 20ms^{-1}. It should be noted that these findings are impossible as a perfect elastic collision only has a COR of 1.

11.5.3 Experimental set up.

Using the experimental set up outlined during chapter 11.2, the impacts were administered at nine locations along the length of one of the bats. A single bat (Probe) was chosen to reduce the influence of structural design on the measurement of the COR variable. The handle of the bat was secured in the hand simulator with the clamps set 210mm apart as used previously. As the test procedures were standardised, it was possible to alter the variable of pre impact ball speed. Three different impact velocities, 3, 6 and 9ms^{-1} were chosen due to the limitations of the testing procedure. Each impact location experienced six direct impacts, which were recorded using the high-speed camera system. It was then possible to track the motion of the ball to establish the pre and post impact speeds and calculate the COR for each impact position.

11.5.4 Results.

Figure 11.17, illustrates the alterations in the calculated COR for each of the impacted locations along the length of the bat for each impact speed.

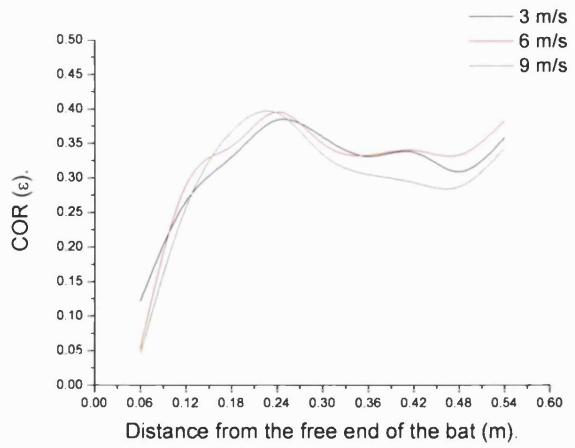

Figure 11.17: COR following impacts of differing speed.

From Figure 11.17, a similar pattern in COR regardless of ball impact speed can be seen. Although, the COR increases by 0.012 as the impact velocity increases from 3 to $9ms^{-1}$. Figure 11.17 also highlights that as the pre impact velocity increases, the position of the maximum COR moves towards the end of the bat and away from the COM. Finally, it was found that during impacts above 0.3m, the pre impact velocity of $9ms^{-1}$ records the lowest COR.

11.5.5 Discussion.

The coefficient of restitution was calculated following impacts with three different pre impact ball speeds. During a similar tennis study, Brody (1979) reported that the COR only varies slightly with changes in the pre impact ball speed. This study supports this previous finding as only a small difference in the calculated COR was found with changes in pre impact speed.

The apparent similarities in the COR patterns along the length of the bat are explained by Newton's third law of motion, which outlines that every 'action and reaction are equal and opposite'. Thus, a forward force from the ball onto the bat during the impact will have an equal backward force from the bat onto the ball. Therefore, as the COR is a ratio relative to the pre and post impact conditions, there will be limited differences in the COR value regardless of the initial ball speed. Any differences that are noted will be due to variations in the response of the bat and ball during impact, which would be caused by their non-homogeneous nature.

When the ball speed is increased, the differences in the responses of the bat and ball will also be magnified thus causing the noticeable differences in the COR. In particular the actions of the ball will change with the impact speed due to variations in the surface compression. It was found that as the pre impact speed increased, the COR was reduced, which can be partially attributed to an increase in energy loss following greater ball compression (mainly the leather covering). An increase in the surface compression will cause a reduction in the COR as the energy lost during compression is not recovered. This concurs with Daish (1972) who found that increasing the impact velocity decreased the COR during golf and tennis due to extensive ball compression. However, as a cricket ball has a hard inner core, significant ball compression will not occur during game situations much beyond the compression reported during this study. Therefore, it is proposed that the energy loss through ball compression highlighted by this study is almost the maximum encountered.

Another variation in the impact responses will be changes in bat surface deformation, which are caused by differences in the surface rigidity along the bat's length. Sayers *et al.* (2000) investigated bat surface hardness and reported that it varied significantly depending on the density, moisture content and amount of knocking-in at each location. Therefore, an increase in the pre impact speeds would exploit these differences in surface hardness, causing alterations in the calculated COR. Although it is possible that each impact will experience different surface conditions, as repeated impacts were administered at each location for each impact speed, these can be excluded from the results.

This study noted that the position of maximum COR moved 1mm away from the COM (towards the end of the bat) as the speed increased. This finding opposes the results of Grant & Thethi (1994) who found the position of maximum COR moved towards the COM following an increase in impact velocity. This disparity in results is mainly due to the difference in techniques employed (rigid computer model rather than an experimental analysis). As highlighted, Grant & Thethi (1994) did not report their construction techniques and found COR values over 1. Therefore, this particular model may not be sufficiently accurate to establish specific alterations in COR distribution with changes in velocity. However, Grant & Thethi (1994) did use higher ball speeds and a rotating bat. The movement of the maximum COR found by this study may be due to the static nature of the bat and that the peak COR was found

to move closer to the thickest section as the higher impact speeds maximise the effect of the increased mass (inertia) at this location.

Finally, it can be considered that a batsman may be able to maximise the COR value by correlating their swing velocity with the incoming velocity of the ball. Therefore, minimising the energy loss through excessive ball compression and bat deflection, while maximising the energy transferred to the ball. Daish (1972) reported that during golf, there is an optimum swing velocity that maximises the post impact ball velocity and if swing speed is further increased, little or no improvements are made.

11.5.6 Conclusion.

The aim of this section was to investigation the effect of pre impact ball speed on the measured COR of a cricket bat. It was found that the ball speed did not have a significant influence on the measured COR. This observation is explained by Newton's third law of motion regarding actions and reactions. It was also noted that certain factors including the magnitude of ball and bat deformation during impacts may have an influence on the calculated COR. Although, it was hypothesised that their effects will not be obviously noticed by a batsman.

11.6 Gripping location and the coefficient of restitution.

11.6.1 Introduction.

During the course of a game, a player will change the location of their hands on the bat handle to overcome unexpected bounces of the ball or deliveries from the bowler. Often players have different grip configurations for each individual shot, although it is normally the aim of a batsman to try and hit the ball further or avoid a fielder. Therefore, this section aims to establish whether the changes in gripping locations affect the calculated COR of a first class cricket bat. This study has been unable to find any previous literature regarding the effects of grip location on post impact ball velocity, although coaching manuals often suggest particular hand locations without justification.

11.6.2 Experimental set up.

Four different clamping positions were chosen to establish the effects of grip location on COR. As outlined in chapter 10, the grip locations were set 105mm apart around the top, middle and bottom of the handle along with a wide grip variable, which involved the clamps being positioned 210mm apart at either end of the handle. The clamps were part of the hand simulator rig and tightened to 8N to represent the pre impact load of an average human subject. A single bat (DF) was impacted using the drop ball test method with pre impact ball speeds of $9ms^{-1}$ at the nine locations along the length of its blade. Using the high-speed camera system (2000Hz), the pre and post impact speeds were calculated to establish the COR during each impact at each bat location for each grip location.

11.6.3 Results.

From Figure 11.18, it is possible to establish how the calculated COR changes following impacts at the different locations with each of the grip locations.

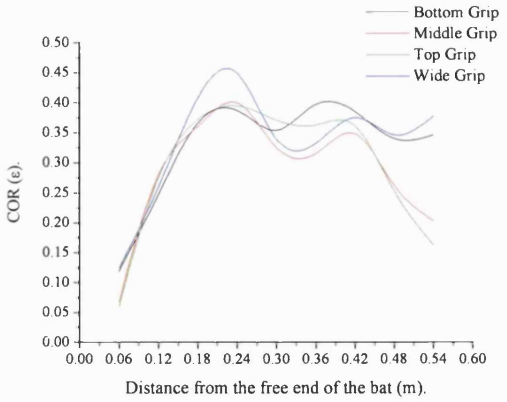

Figure 11.18: Calculated COR with alterations in grip location.

Using Figure 11.18, the calculated COR's along the length of the bat follow similar patterns for each of the grip locations, with the position of maximum COR originating at approximately 0.22m from the free end. It can also be seen that the widest grip produces the highest COR and has a COR distribution pattern almost identical to the middle grip condition with the first and second peaks in the COR occurring at the same position. The second peak during the bottom grip condition can also be seen to be of similar magnitude to the maximum COR recorded during this condition. Finally, the top grip seems to maintain its maximum COR along much of the bat (0.18 to 0.42m). However, during this condition the lowest COR peak was calculated.

To help explain why the COR was affected by the grip locations, the deflection of the bat during each location has been plotted (Figure 11.19). As reported earlier in this chapter, it is the deflection of the bat during the contact period that may have most influence on the COR.

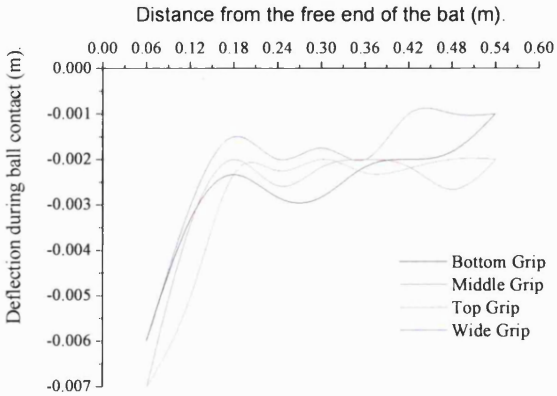

Figure 11.19: Bat deflection during ball contact for each grip location.

Figure 11.19, shows each of the grip locations recorded a similar degree of deflection during ball contact. The least deflection occurs when the bat was held using the wide grip and it is the bottom grip, which exhibits the greatest degree of deflection during ball contact.

Due to the lack of difference between the deflection measurements when the ball was in contact with the bat, the peak deflection has also been plotted (Figure 11.20). It was considered that this may explain the cause of the differences between the measured COR for each of the grip locations.

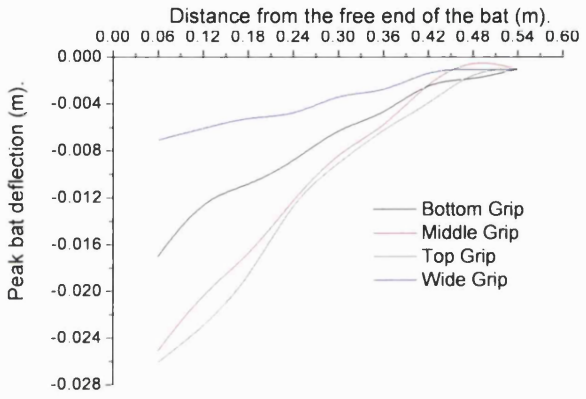

Figure 11.20: Peak bat deflection following alterations in grip location.

Figure 11.20, shows that the top grip location has the greatest deflection following impact and the wide grip has the least. Unlike the two previous figures, there is a clear distinction between the responses of the bat with each of the grip locations.

11.6.4 Discussion.

The aim of this section was to investigate whether a player could alter their grip location in order to maximise or move the position of maximum COR. This study is unaware of any other investigations that have considered the possible benefits of grip location on cricket bat performance. It was found that the point of maximum COR was at the same position for each of the gripping locations (0.22m from the free end for this bat type). As the bat type was maintained, the differences are purely related to the changes in the grip location, indicating they have little influence on the position of the maximum COR. It is considered that this occurs primarily due to the COR being related to the responses of the bat rather than the clamping

conditions (as outlined earlier in chapter 11.4). This is advantageous for cricketers as it indicates that as long as they impact the position of maximum COR, the location of their hands will have little effect on its magnitude.

The small differences in COR found with each grip locations may be due to the location of the axis of rotation. The two grip locations with the highest COR were the widest and middle grip conditions, which due to the location of the clamps have the axis of rotation at the centre of the handle. Both of these conditions also followed a similar distribution pattern of the COR along the length of the bat highlighting this possible association.

Although the COR was at a maximum at a similar location for each grip location, the magnitude of the COR was affected. Primarily, it was considered that this was due to energy loss through bat deflection during the ball contact period. However, very little differences between the magnitudes of deflection during the impact period were established. Although, it was noted that there was correlation between the peak measured deflections (during contact and peak) and the COR. For example, the contact deflection during top grip condition was maintained along the length of the blade as found during the COR results. From this finding, a player should choose this gripping location as a constantly high COR would ensure a high post impact ball speed regardless of impact position.

From Figure 11.20, the average peak bat deflection at each impact location was established. The deflection measurements show that when the clamps were 105mm apart, the deflection decreased with a reduction in the distance between the impact location and the bottom clamp. This is due to changes in the length of the lever that the bat creates between the applied load (the ball) and point of fixation (the clamps). This supports the results during chapter 10.5, as the top grip displayed the highest hand loads due to the distance between the clamps and the impact location. Therefore, the deflection and hand loads are increased with the lever length, while the COR is reduced. The combination of these factors and the locations of the sweet spots will be discussed later in chapter 13. The wide grip recorded the least deflection due to the spreading of the clamp locations to both ends of the handle. During this instance, the handle creates an almost central pivot position (about the bottom clamp), which reduces the deflection and energy loss following impact and thus maximises the COR.

11.6.5 Conclusion.

It was the aim of this section to investigate whether it would be possible for a player to maximise the COR by altering their grip location. Four grip locations were chosen and it was found that the COR could be maximised by having the hands 210mm apart. It was suggested that this was associated with a reduction in bat deflection. It can be proposed that a player should try and move their hands as far apart as is comfortable to maximise the COR and thus the performance of the bat.

11.7 Chapter summary.

The COR was investigated during this chapter and it was found that there were distinct differences in the recorded values due to different interpretations of the definition and the analysis equipment used by previous studies. Using high-speed camera images, it was found that the differences in the bat's structural design did not affect the position of maximum COR but they did influence the magnitude of the calculated values. It was reported that a bat stiffness of 6850N/m would lead to a peak COR and a design that incorporated a large central spine would maintain a high COR further along the bat. The distribution of the COR was found to be comparable when the hand held and hand simulator trials were analysed, although the results were completely different when the bats were rigidly clamped. The pre impact ball speed was found to have little effect on the COR, although it was possible to maximise the COR value by moving the clamps further part. In conclusion a high-speed camera can be used to accurately establish pre and post impact ball speeds for the calculation of the COR. This can then be used to determine the performance potential of cricket bats and investigate how the COR can be altered during different impact conditions.

12 NODAL SWEET SPOTS.

12.1 Introduction.

Nodes of vibration have received considerable interest especially during the analysis of sweet spots and hitting performance of hand held sporting equipment. This may be due to suggestions like that of Hatze (1998) who reported that the COP was of limited use due to its constant movement during tennis strokes. Brody (1986) and Cross (1998) have also reported that wooden baseball bats do not have a power region and therefore the nodal sweet spot was of greater importance. In golf, Hocknell *et al.* (1996) noted that the perception of 'feel' is related to the vibrational frequencies following impact. Therefore, the nodal frequencies of striking implements are of greatest interest when aiming to analyse and improve the performance of a club, bat or racket. This chapter will initially highlight previous literature regarding the locations of vibrational nodes and the possible improvements in performance and comfort experienced following impacts at these locations. This study will then look at how bats of differing structural design influence the location of the nodal sweet spots and whether their locations can be altered following modifications to the experimental set up.

12.1.1 Literature review.

Following ball impact, the striking implement behaves like a vibrating structure (Casolo & Ruggieri, 1991). The player will sense a fundamental frequency and one or two other harmonic vibrations as these are below 1kHz and within the excitation spectrum of the hands (Grant 1998b). Where the vibrational mode has no displacement or amplitude a node is located (Gough *et al.* 1983). If an impact occurs at a node, the corresponding modal frequency is minimised or not produced (Brody, 1987). This is the location of the sweet spot as the shock although not eliminated, is minimised to an acceptable level (Cross 1998a). Therefore, the sweet spot is not a distinct location as its size is dependant upon the magnitude of the vibration the player is willing to withstand (Brody 1987). Grant (1998b) noted that following impact, the energy will be transferred to the ball if the impact occurs at a node, but absorbed by the striking implement if an impact occurs at an anti-node. An anti-node is the location along a mode where the amplitude or displacement is at its greatest. The frequencies, mode shape and node locations of the implement are dependant upon the Young's modulus and density of a

geometrically uniform material (Grant & Paisley, 1997). As cricket bat willow is not a uniform material, the impact force, contact duration, the implement's mass and stiffness, mass of the ball and impact location should also be considered (Kawazoe, 1993). It can be considered that the stiffer the implement, the higher the frequency of oscillation and greater the post impact ball velocity (Brody 1987). However, it has been found that higher frequency oscillations reduce control and comfort while increasing fatigue (Brody, 1981, Hocknell *et al.* 1986 and Brody, 1987). Therefore, impacts at the nodes of the second or third mode could improve comfort as the higher frequency vibrations will have been minimised. However, the large energy contained within the fundamental frequency, which has been associated with a decrease in the post impact ball velocity will not be reduced.

During the experimental analysis of cricket bats, Grant (1996), Grant & Nixon (1996b) and Grant (1998b) found three modes of vibration were excited below 1kHz. Grant & Nixon (1996b) and Grant (1998b) reported frequencies from a freely suspended cricket bat. The first and fundamental mode had a frequency of between 91.1 and 133.5Hz, the second between 328 and 437.8Hz and the third between 558.4 and 698.5Hz. Grant & Nixon (1996b) (Figure 12.1) and Grant (1998b) (Figure 12.2) did not publish the exact positions of the nodes, although from the diagrams it is possible to estimate the location of the nodes along the length of the bats.

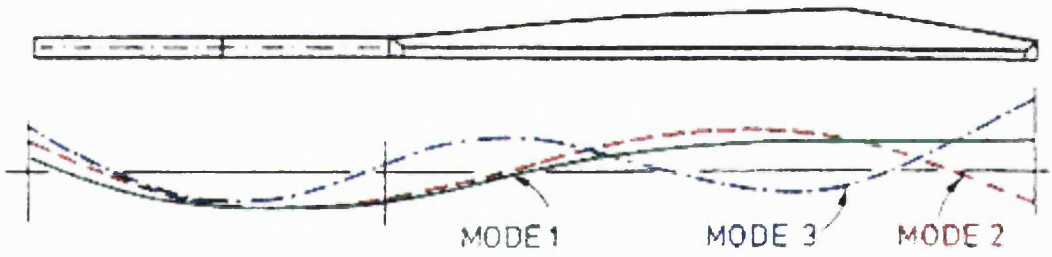

Figure 12.1: Modes and node location of a cricket bat (Grant & Nixon, 1996b).

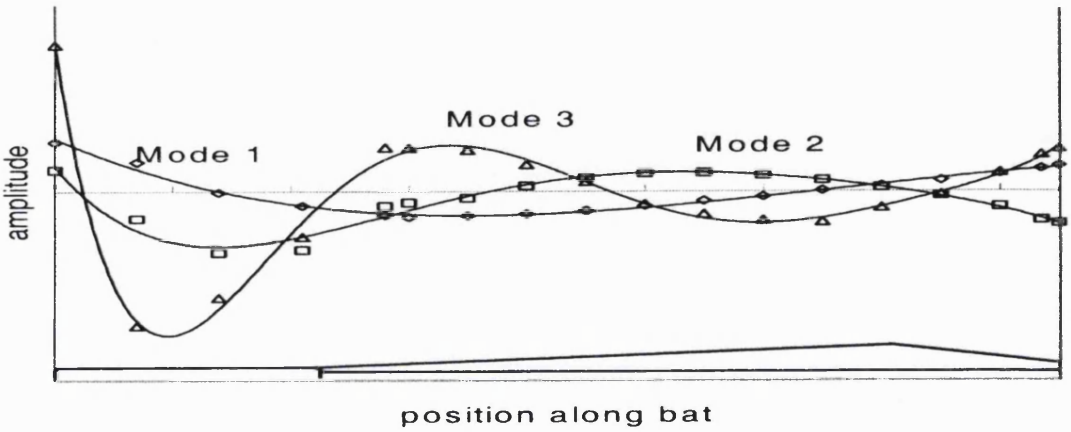

Figure 12.2: Mode shapes and location of flexural vibrations of a cricket bat (Grant, 1998b).

Grant (1998b) did outline the location of the nodes that coincided with the thickest section, finding them 209mm, 124mm and 94mm from the free end respectively for each of the excited modes. An anti-node was also found at the end of the blade, which was attributed to the string suspension method employed. Grant (1996) had found that the lower node of the first mode coincided with the anti-node of mode 3, although Grant (1998b) did not report this.

Knowles *et al.* (1996) performed a vibrational analysis on a traditional wooden bat and a bat constructed of thermoplastic. The bats were rigidly clamped, while the vibrations were excited using hammer impacts at twenty-three points along the length of the blade of the bat. The vibrational frequencies were captured using an accelerometer positioned on the reverse of the bat. Knowles *et al.* (1996) also measured vibrations following ball impacts on the traditional and composite bats. Nine impact locations along the length of the bats received ball strikes while the bat remained rigidly clamped (Table 12.1).

	Traditional wooden bat		**Composite bat**	
Impact type	**Hammer**	**Ball**	**Hammer**	**Ball**
Mode 1	24.1	19.6	15.47	16.5
Mode 2	239.8	247	311	326
Mode 3	376.2	*Not excited*	713	*Not excited*

Table 12.1: Vibrational frequencies (Hz) of two types of cricket bat (Knowles *et al.* 1996).

Using Table 12.1, the composite bat displays a lower first modal frequency but a much higher second and third modal frequency when compared to the traditional bat, although the third mode is not excited during the ball impacts. Knowles *et al.* (1996) reported that the composite structure of the bat maximises the hitting distance and reduces impact forces. It was concluded that further analysis was required due to the unrealistic clamping conditions and lack of knowledge regarding the fatigue performance of the thermoplastic.

Using Matlab, Penrose & Hose (1998) constructed a one-dimensional beam to calculate the modal responses for a rigid, wooden and flexible bat. It was found that much of the energy was absorbed by the 1st and 2nd modes and that it would be beneficial to design a bat where the COP

and the node of the 1st mode coincided. Penrose & Hose (1998) suggested this would lead to improved comfort as the vibrations and hand forces would both be attenuated simultaneously.

The effects of structural design on the vibrational frequencies were also investigated by comparing a traditionally shaped wooden bat against one with a large scallop removed from the back of the bat (Table 12.2).

	1st Mode		2nd Mode		3rd Mode		4th Mode	
	Freq.	DNP	Freq.	DNP	Freq.	DNP	Freq.	DNP
Traditional bat	93.9	608	383.9	665	602.2	694	1022	724
Scalloped bat	94.05	605	375.3	675	570.8	706	1022	721

Table 12.2: Frequencies and positions of the furthest node (DNP) from the handle tip (mm) (Penrose & Hose, 1998).

No significant differences were found in the vibrational frequencies of either bat, although, the traditional bat had its position of maximum COR closer to the node of the first mode. This would be beneficial as the undesirable vibrations would be reduced whilst still maximising post impact ball velocity.

12.1.2 Conclusion.

There are considerable differences in the modal frequencies that have been published and outlined in this chapter. These will be caused by the procedure, either experimental or modelling and the clamping method, either suspended or clamped. Differences in the experimental results are caused by the non-homogenous nature of the bat and the application of the impact. The computer models were also over simplified using rectangular cantilever beams rather than the complex geometry that makes up the actual bats. Although, it is the purpose of this chapter to investigate the modal responses of cricket bats during controlled impacts, it is important to remember that these results are unique to the bats that are used. Although literature produces an insight into the reaction of cricket bats during actual play, they do not represent all cricket bats that are available.

12.2 Clamping type and nodal sweet spot location.

12.2.1 Introduction.

Batsmen clearly recognise and appreciate the relative comfort following an impact at a sweet spot. The removal of painful vibrations and jarring on the hands whilst propelling the ball further than usual has increased the interest (mainly in tennis) to improve and enlarge the sweet spots. However, cricket bat manufacturers simply regard the position of the sweet spot as the point where the bat is thickest (Laver & Wood, 2001). Although it is well documented in tennis research, there are few publications that have examined the influence of clamping conditions on vibrational frequencies. Therefore, this section examines the location of the vibrational nodes and established how there location can be altered with changes in clamping type.

12.2.2 Experimental set up.

In order to investigate the influence of clamping condition on vibrational frequency and nodal location, four methods of gripping a first class cricket bat were used: rigid clamping (using two locations), free suspension (from the handle end), manually held and a hand simulator (spring-and-damper system). The rigid clamping rig was secured to a structure to enable the bat to hang vertically downwards (Figure 12.3). The clamps were positioned 210mm apart and tightened to 300N, which was verified using the four Entran load cells positioned inside the clamps (Figure 12.4). Load cells 1 and 2 were positioned on the bottom and top halves respectively of the first clamp (closest to the blade of the bat), while load cells 3 and 4 were positioned on the bottom and top halves respectively of the second clamp (closest to the top of the handle). The signal from the load cells were amplified and then recorded at 1000Hz using a Pico Log data recorder.

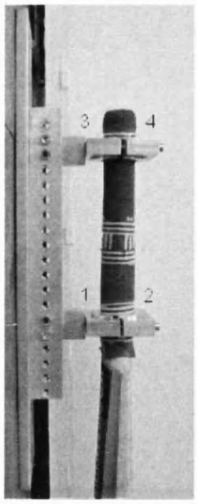

Figure 12.3: Clamped bat and load cell positions.

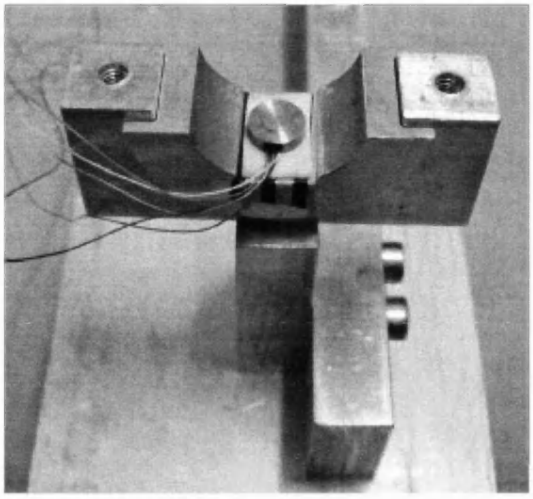

Figure 12.4: Position of load cells inside a rigid clamp.

The bat's response was also measured when it was freely suspended to the ceiling using a piece of twine 0.8m in length and fixed around the top of the handle (Figure 12.5).

Figure 12.5: Freely suspended bat about the handle end.

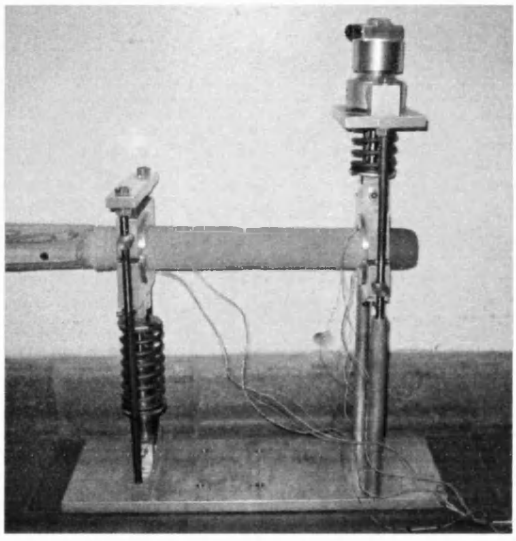

Figure 12.6: Hand simulator rig.

Figure 12.6 depicts the bat in the hand simulator, which was included to establish whether it closely replicated hand held responses. The clamps were positioned at the same locations as during the rigid clamping condition (210mm apart), although a constant load of 8N was maintained to replicated the average human gripping load (Fisher & Vogwell, 2003). Finally, five human subjects held the bat during the controlled impacts. The subjects were instructed to

assume a stance and respond in a manner (firmly) as they would during a game, although the should not actively move the bat towards the ball. The handle was gripped at the same locations as used during the clamping conditions and the gripping load was recorded by attaching the Entran load cells to the tip of the second finger and at the base of the palm of each hand (Chapter 10).

An Isotron tri-axial accelerometer (Modal 61A-100) was attached at 0.03m increments, totalling 28 positions along the length of the bat. Using a Pulse vibration system with multi-analyser (Type 3560 C), a vibrational scan of 0 to 1.6kHz was completed immediately after each impact. The impacts were applied at the bat's thickest region (0.16m from the free end) using an Endevco modal hammer (model 2302), which enabled the study to remove the input frequencies of the hammer impacts. The experimental set up is shown in Figure 12.7.

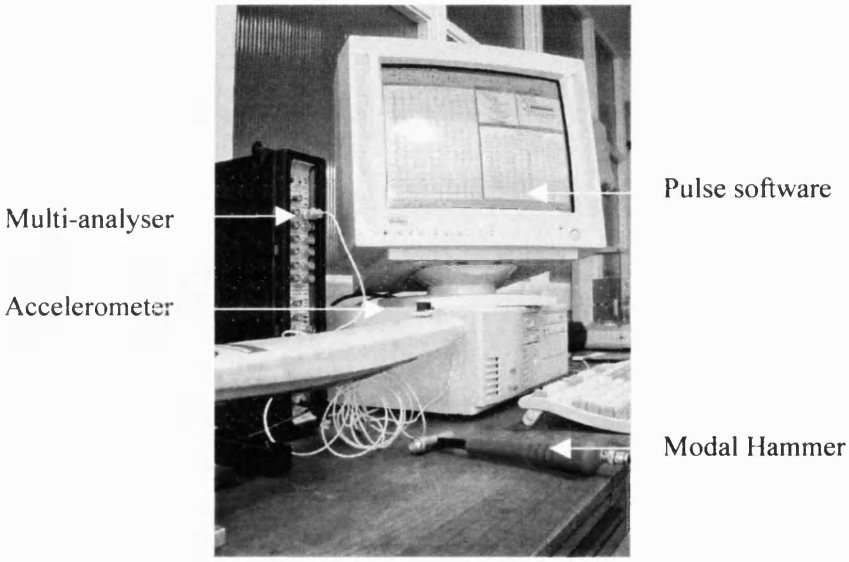

Figure 12.7: Experimental set up.

Ten impacts were applied at each of the 28 accelerometer positions before an average was calculated. A detailed frequency analysis was then completed along the whole length of the first class cricket bat (including the handle) for each of the clamping conditions.

12.2.3 Results.

Using the Pulse vibration system, the first three excited modes following impacts along the length of the bat were established (Table 12.3).

Frequency (Hz) / Bat condition	Mode 1	Mode 2	Mode 3
Clamped	14	312	800
Suspended	112	328	536
Hand simulator	40	272	556
Hand Held	40	292	508

Table 12.3: Comparison of measured vibrational frequencies (Hz).

From Table 12.3, there is a considerable difference in the frequency of the first mode when the bat is hand held, freely suspended and clamped. However, the frequencies of the first mode during the hand simulator and hand held conditions are the same. Similarities (within 56Hz) in the frequencies between all of the clamping conditions can also been seen for the second and third modes. Although, the frequency of the third mode during the clamped condition deviates considerably from this close correlation displayed by the other conditions.

The location of the nodes for each of the excited modes were also established and are presented in Table 12.4. Due to the reported differences in frequencies of the first and third modes, the locations of the nodes are also different. Although, the similarities in the frequency of the second mode (as reported during the analysis of Table 12.3) are highlighted by the close proximity of the nodes during each condition. An example of this is that the second node of the second mode was found in the same location regardless of the clamping condition. It can also be noted that there is only a 0.03m difference in the location of the first node of the second mode. Interestingly, the third mode during the rigidly clamped condition had four nodal locations rather than the three found during the other conditions. The correlation between the frequencies of the hand simulator and hand held conditions are also shown in the propinquity of the node locations.

Node location / Bat condition	Mode 1	Mode 2	Mode 3
Clamped	0.60	0.18, 0.60	0.15, 0.33, 0.60, 0.72
Suspended	0.24, 0.68	0.18, 0.60	0.15, 0.42, 0.66
Hand simulator	0.30	0.18, 0.60	0.12, 0.30, 0.48
Hand Held	0.30	0.15, 0.60	0.12, 0.33, 0.51

Table 12.4: Comparison of node location (from free end in metres) for the excited modes.

To help in the understanding of the modal patterns (including node and anti-node positions) during each of the clamping conditions, the shape of each mode has been plotted in the following the figures (Figure 12.8 & 12.9). It is important to note that the clamps or hands are located at 0.6m and 0.81m from the free end of the bat, which also corresponds to 0.03m from either end of the handle.

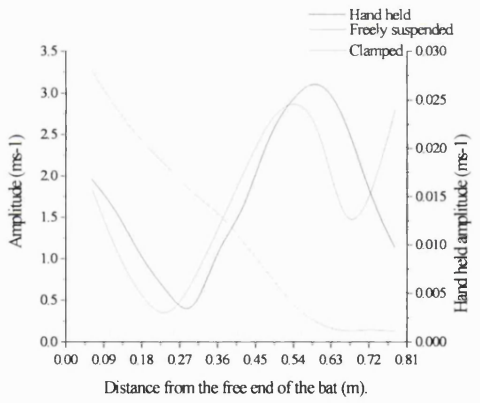

Figure 12.8: First mode during each clamping condition.

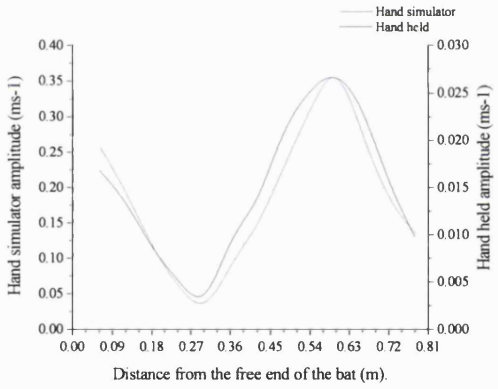

Figure 12.9: Comparison of hand held and hand simulator.

Primarily, the hand simulator condition has been separated from the other conditions due to the reduction in the amplitudes relative to the other conditions and to ease the comparison between the hand simulator and the hand held conditions. The influence of the clamping arrangement is clearly visible for each of the clamped conditions. The magnitude of the first vibrational mode for the rigidly clamped condition is almost completely reduced at the location of the first clamp (0.6m from the free end), although this location is an anti-node during the hand held, hand simulator and freely suspended conditions. Anti-nodes are recorded at the end of the bat for all

of the conditions and at the end of the handle during the freely suspended condition. From Figure 12.9, the similarities between the hand simulator and hand held conditions are visible. It is clear that the nodes (0.3m) and anti-nodes (0.03 and 0.6m) are located in the same positions.

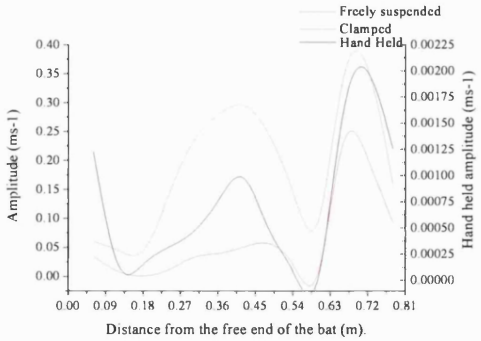

Figure 12.10: Second mode during each clamping condition.

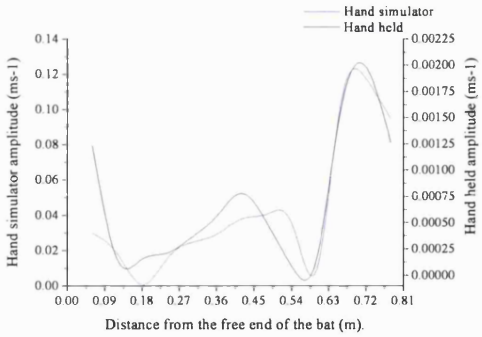

Figure 12.11: Comparison of hand held and hand simulator.

Figure 12.10 and 12.11 depict the second vibrational mode for each of the clamping conditions. From the figures and the results reported in Table 12.4, it is clear that the nodes of the second mode during each of the clamping conditions occur close to the position where the bat is at its thickest (0.16m from the free end). Nodes also occur at both clamping/gripping locations (0.6m and 0.81m from the free end), thus amplitudes at these positions are low. It can be seen that the amplitude of the second vibrational mode is almost 10 times less than during the first mode and that the vibrations are greatly reduced when the bat is hand held. There is also a distinct correlation between the hand held condition and the hand simulator, although the amplitude is 100x's greater during the hand simulator impacts, thus illustrating the damping qualities of the player's hands.

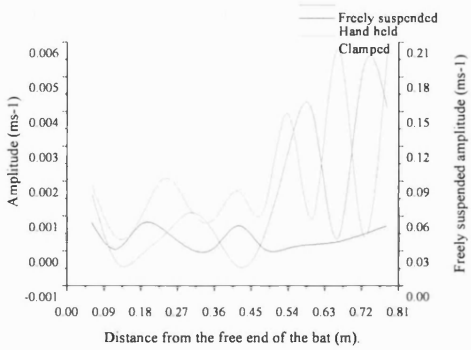

Figure 12.12: Third mode during each clamping condition.

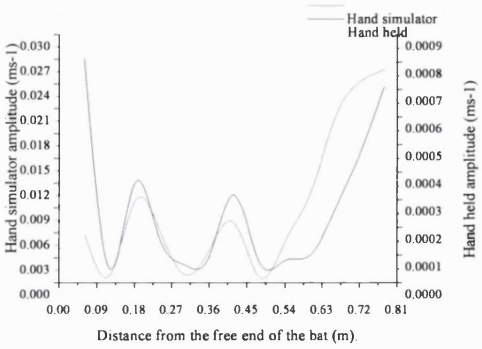

Figure 12.13: Comparison of hand held and hand simulator.

Figure 12.12 & 12.13 display the shape of the third and final mode excited below 1kHz. It is clear that the amplitude of this mode is significantly less than the previous two modes, other

than during the freely suspended condition as a similar magnitude to the second mode is recorded. From Figure 12.13, the differences in the measured frequency of the hand held and hand simulator conditions are visible as the location of the nodes can be seen to occur in slightly different positions.

12.2.4 Discussion.

The vibrational frequency and node locations were recorded during the application of controlled impacts when a bat was rigidly clamped, freely suspended, gripped in a hand simulator and hand held. It was discovered that there were considerable differences in the frequency of the fundamental and third modes during the rigidly clamped condition when compared to the other gripping conditions. However, the results during the hand simulator were closely correlated to the hand held condition. As the impact frequencies of the instrumented hammer were removed using the capture software and the bat type was maintained, the differences in post impact responses are directly related to the clamping system employed.

The frequency of the modes during the freely suspended condition are close to or within the boundaries set out earlier by Grant & Thethi (1994) and Grant (1998) during their analysis of freely suspended cricket bats. The first vibrational mode was reported to be between 91.1 and 133.5Hz (112Hz during this study), between 328 and 437.8Hz for the second mode (328Hz during this study) and between 558.4 and 698.5Hz (536Hz during this study). The vibrational frequencies reported by Knowles *et al.* (1996) during clamped conditions were also found to be close to the results recorded during the first and second modes, although the third modal frequency was found to be considerably different. Knowles *et al.* (1996) recorded frequencies of 14.7, 339 and 1087Hz for the first three modes as opposed to 14, 312 and 800Hz found during this study. These correlations with previous studies validate the methods employed by this study and display that they are representative of cricket bat responses.

The results during the freely suspended condition are the bat's natural frequencies as it is not influenced by any external source. This analysis method can be used not only as a form of comparison to previous studies but also as a simple way of exciting the natural frequencies of

the bat. This method has been used during other studies during both tennis racket analysis (Brody, 1987) and cricket bat research (Grant & Thethi, 1994 and Grant, 1998). However, these findings are of limited significance as this method is prone to errors due to the influence of the cord type, its attachment location and the constant motion of the bat during the impact period. During studies involving freely suspended bats, Grant & Thethi (1994) and Grant (1998) located the two nodes of the first mode, in the handle and towards the middle of the bat. These nodes were also found during this study although the location of the node within the blade of the bat was higher than previously reported. Due to the higher location, it is unlikely that a player would impact it during actual play, although due to its more accessible position, a player may impact the node of the second mode.

The shape of the freely suspended and hand held modes are different over the handle of the bat. However, there is little difference in the shape of this mode when the bat is hand held or gripped in the hand simulator. It can be suggested that the propagation of the wave during the freely suspended condition, seems to be interrupted by a higher frequency mode as it passes over the handle. This finding may be caused by the twine attachment at the handle and therefore this will be investigated in chapter 12.4. Although the twine does allow the bat to vibrate in a more natural manner when compared to the other conditions, the results will still be influenced by the attachment and thus the results should be considered with some caution.

Using vibrational fundamentals described by Den Hartog (1985), this study may have recorded a non-harmonic periodic motion. Therefore, two sine waves of different frequencies are recorded, the fundamental and first harmonic during the excitation of the bat. However, this would have been apparent during the analysis of the vibrational frequencies at these locations. The modes were measured at the same frequency and therefore can be considered to be the same wave. However, due to changes in the density, elastic modulus and cross sectional area, the wavelength is altered as the velocity of the wave through the different sections change. Thus, the vibrational wave is able to travel at a greater velocity through the handle than the larger denser wooden blade of the bat, leading to the elongation of the wave when passing through the blade. During the hand held condition, the influence of the mass and damping of the hands suppresses this wave shape, leading to a smoother modal distribution along the whole of the structure. This is because the hands slow (dampen) the vibrational wave to a similar velocity over the handle to the velocity over the blade. Thus, it can be proposed that the

vibrational results during the freely suspended results are unrealistic when compared to the occurrences during hand held impacts or those during actual use.

Cross (1998) found the location of the nodes moved and the magnitude of the vibrational frequency decreased when a racket was hand held compared to freely suspended. This study did note a shifting of the node location and a reduction in the magnitude and frequency of the vibrations. However, this study found a reduction of 72 and 36Hz for the first and second modes respectively compared to the 7Hz reported by Cross (1998). The hand held results will be affected by the way the player is holding the handle, including grip pressure and hand location. Although, these factors were maintained throughout this study using loads cells attached to the subjects hands, variations between this study and Cross (1998) are evident. A reduction of this magnitude suggests that the subjects during this study actively responded during the impact period. Their increased motion and gripping load causes the hands and lower arms to become a part of the bat, thus increasing the mass, damping properties and deflection of the bat during the impact period.

This study has identified the location of the vibrational nodes and anti-nodes for each condition. Grant & Tethi (1994) and Grant (1998) also recorded the location of the anti-nodes during their analysis, although they did not report their exact locations on the cricket bat. Grant (1998) reported that following an impact at an anti-node, the energy absorbed by the bat is increased. No anti-nodes occurred within the preferred impacting region (the thickest section) for the first two modes when the bat was hand held or freely suspended. However, an anti-node does occur at the thickest point when the bat was rigidly clamped. Therefore, much of the energy from an impact at this location would be retained within the bat. This would lead to a reduction in the post impact ball velocity and player comfort when compared to impacts at other positions.

The magnitude of the first mode is much larger than the other excited modes. Therefore, this mode would have the greatest influence on player comfort and post impact ball responses. During the hand held and hand simulator conditions, a node occurred 0.3m from the free end of the bat. If an impact occurred at this position, the player would feel a considerable reduction in the vibrations experienced at the hands, making this position the nodal sweet spot for a hand held cricket bat. However due to the raised location of this node, it is unlikely that the player would impact this position during actual play. It should also be considered that any increase in

the post impact ball velocity following impact at the nodal position would be reduced due to the reduction in rotational velocity at this raised location.

From the shapes of the first mode, it is possible to see that the clamped vibrational mode is considerably different to the other conditions. It is considered that this is due to the rigid clamping system not allowing the handle to vibrate above the first clamp (0.6m from the free end). Therefore, the bat purely vibrates from this location to the free end, creating the shape of the first mode. This finding highlights why it is unrealistic to consider rigidly clamped bats respond in a similar manner as those during actual playing conditions.

The frequencies of the second modes were similar for each clamping condition, suggesting that this mode is independent to the clamping condition. The main reason for this finding is that the node locations are at the same location as the clamps (0.6 and 0.81m from the free end). As the amplitude at this location is low, the vibrational wave is not affected by restricted motion caused by the clamps. Therefore, the bat is allowed to respond as during the freely suspended condition. It could be suggested that this is a gripping sweet spot as the energy transferred into the clamp or hand at this point would be reduced. The lack of supporting literature regarding this suggestion may be due to previous studies clamping their equipment away from a vibrational node and therefore this result would not be recorded.

Another aim of this section was to establish if the hand simulator produced results representing those during the hand held condition. It was clear that there was a distinct correlation between these two conditions, although the difference was increased as each mode was investigated. It was found that there was a difference of 4Hz between the first modes, 20Hz between the second and 48Hz between the third. The similarities are due to the hand simulator acting in the same manner as during the hand held condition. Cross (1998b) reported that it is the actions of the forearms that have the greatest influence on the post impact responses of a baseball bat. Therefore, as the spring-and-damper units were correlated with the actions of a human subject, subsequent similarities to the hand held results support the suggestion of the importance of the forearm during the impact period. It can also be proposed that aluminium clamps can be successfully used as an effective clamping method as long as the load is maintained at a similar magnitude to those during the hand held trials. It is also important to allow the clamps to rotate to enable a more flexible motion of the bat during impact. However it should be noted, that the

amplitude of the vibration was significantly higher during the hand simulator impacts when compared to the hand held condition. This is due to the damping of the soft tissue of the hands as any other differences in the motion of the bats would have been displayed with changes in the vibrational frequencies. Although there is a considerable difference between these amplitudes it is almost of academic importance as the location of the nodes and anti-nodes are of greater interest when assessing sweet spot locations. The amplitudes are important however when the post impact ball velocities and player comfort are being assessed.

12.2.5 Conclusion.

In this study the vibrational modes and node locations of a first class cricket bat have been measured when the bat was rigidly clamped, freely suspended, in a hand simulator and hand held. It was found that three modes were excited below 1kHz during the controlled impacts, which correlated with previous studies. The hand held and freely suspended modes followed a pattern with some degree of similarity for each of the modes, although it is during the first and second modes that they produce the closest node (ie. Sweet spot) locations. During the rigidly clamped condition, the bat did not produce a nodal location within the blade of the bat. The hand simulator was found to correlate very closely with the hand held condition, highlighting it as an appropriate method of producing results that could be applied to game situations. It was also found that the second mode was independent of the clamping condition due the position of the nodes at the clamp locations. During the analysis of the second mode, nodes were found to be located towards the thickest region of the bat making it likely that players would impact this location. This would lead to a reduction of that mode, improved player comfort and an increase in the post impact ball velocity.

12.3 Structural design and nodal sweet spots.

12.3.1 Introduction.

Most commercially available bats have structural alterations that are advertised to enhance performance and comfort, although these claims are unsubstantiated by external researchers. Therefore due to the association between vibration and player comfort, it is important to establish whether these structural designs alter node locations or the amplitude of the excited modes. Due to its high amplitude, the first vibrational mode would have the greatest effect upon the comfort experienced by the player following impact. Therefore, it would be of greatest benefit if the structural alterations moved the node of this mode to the position of preferred impact (thickest location). As reported, the clamping condition has a considerable influence on the vibrational responses of cricket bats, therefore the hand simulator should be used throughout the analysis of each bat. This condition would give a close comparison to cricket bat responses during hand held game situations, while ensuring repeatable responses that are not always possible during subject hand held conditions.

12.3.2 Experimental set up.

The influence of structural design on the vibrational responses resulting from controlled impacts were investigated by comparing the behaviour of five first class cricket bats. The model and manufacturer of each bat was chosen as it represented the best that is currently available and also had distinct structural alterations. The bats had the same external dimensions and weight, and were not knocked-in, thus avoiding the influence that these factors may have upon the performance of the bats. The same experimental methodology outlined in the previous section of this chapter (12.2) was employed for each of the selected bats. This involved the accelerometer being attached at 0.03m intervals along the length of the blade while an instrumented hammer impacted the thickest region (0.16m from the free end). The gripping loads were maintained at 8 Newtons using the load cells positioned inside the clamps of the hand simulator rig. The signal was captured using the Pulse vibration system to establish the excited frequencies below 1kHz as these frequencies can be perceived by players.

12.3.3 Results.

Following the exclusion of the instrumented hammer from the recorded vibrations, the frequencies of the excited modes below 1kHz for each of the five bats was established.

Bat	DF	GN	Hunt	Slaz	Probe
Fundamental frequency	32	44	40	48	40
Second mode	298	284	292	294	272
Third mode	568	564	588	560	556

Table 12.5: Bat type and excited frequencies (Hz).

Table 12.5 displays the frequencies of the three excited modes of vibration, which were below 1kHz. It is clear that there is a close correlation between each of the modes, although as the mode number increases the difference between the measured frequency also increases. The maximum difference between the fundamental frequencies is 16Hz, while there is 26Hz between the second modal frequencies and 32Hz between the third excited modes.

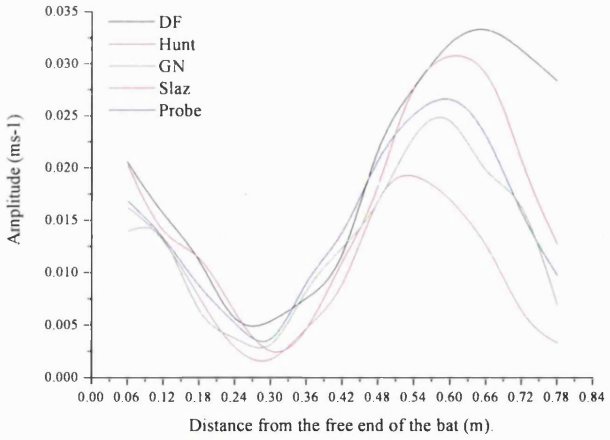

Figure 12.14: Magnitude of the first mode for each bat type during the hand held condition.

Figure 12.14 shows the amplitude and shape of the first mode for each of the five bats during the hand simulator condition. The shape and node locations (between 0.28 and 0.32m from the free end) are very similar for each of the bats, although they each exhibited different structural designs. The amplitude and location of the anti-node is slightly different for each of the bats, ranging between 0.51 and 0.63m from the free end. These differences in modal shape are

supported by the recorded frequencies (Table 12.5). For example, the bat with highest frequency (Slaz) displays the smallest distance between the node and anti-node locations, while the bat with the lowest frequency (DF), displays the greatest distance between the node and anti-node locations.

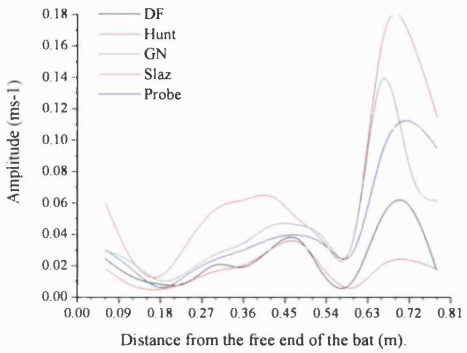

Figure 12.15: Second mode when hand held.

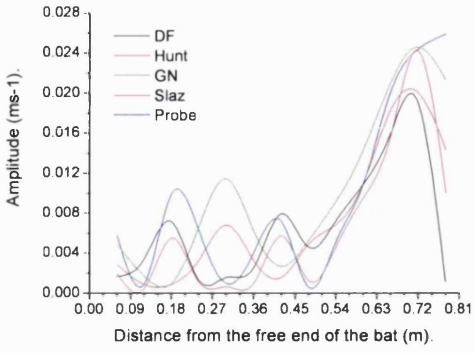

Figure 12.16: Third mode when hand held.

Figure 12.15 illustrates the similarities in shape, node and anti-node locations of the second mode for each of the investigated cricket bats. The nodes are located between 0.15 and 0.18m, and between 0.57 and 0.6m from the free end, while the anti-nodes occur between 0.42 and 0.45m, and between 0.66 and 0.69m from the free end. The free end of the bat can also be considered to be an anti-node, although there is no distinct peak as with the other identified locations. Although there is a similarity in the shape of this mode, there are differences (average 32%) in the amplitude of the vibrational signal with the Slaz and Hunt bat's recording the highest and lowest respectively. Figure 12.16 displays the shape of the third excited mode. This figure illustrates the variability in excited frequency and nodal location as the bats do not follow the same pattern of vibration along the length of the blade. Although it is noticeable that the GN and Hunt bat record the same node and anti-node locations, which is 0.12m further up the blade than those recorded by the DF, Slaz and Probe bats. For example, these three bats display an anti-node at 0.18m from the free end, while the GN and Hunt bats have an anti-node 0.3m from the free end. This pattern continues along the length of the bat, although all bats record an anti-node in the centre of the handle (0.69m from the free end).

12.3.4 Discussion.

The excited vibrational modes below 1kHz were analysed when impacts were administered using an instrumented hammer. The first mode was found to record the largest amplitude and was only marginally affected by the structural alterations made to each of the bats. It was found that the first mode had a single node located around 0.3m (±0.2m) from the free end. It is unlikely that a player would impact this location as it is 0.14m above the thickest point, the position of preferred impact. It was also noted that an anti-node originated at approximately 0.6m from the free end, the location of the bottom clamp (hand). At this point the amplitude of the vibration is at its greatest, thus having a grip location here would lead to an increase in the discomfort experienced as much of the vibrational energy would be transferred to the hand.

The shape of the first mode is a complete harmonic wave over the length of the bat. Therefore, the frequency of the first mode (between 32 and 48Hz) is the number of times the wave travels the length of the bat in a second. The Probe bat is 0.84m long and recorded a frequency of 40Hz, thus the wave is travelling at 33.6 metres per second. If an impact occurred 0.16m from the free end and the hand is positioned at 0.6m, it would take the wave 13.09millisconds to travel the 0.44m to the bottom hand. From this calculation, it can be assumed that the rebound of the excited wave would not influence the actions of the ball during the contact period as it only lasts 2 milliseconds. It is considered by this study and supported by previous investigations (eg. Cross, 1998a) that due to the diminutive amplitudes, the higher frequency modes would not have an effect upon the actions of the ball even if they did return to the position of ball contact.

Changes to the location of the nodes were found when the third mode was analysed, as the GN and Hunt bats had nodes and anti-nodes 0.12m further up the bat than the other three bats tested. These locations are thought to be shifted due to the large portions removed from the back of the GN and Hunt bats. The node locations of these bats are 0.18m from the free end, only 0.02m above the thickest section. Therefore, a player is more likely to impact this location and minimise this mode. However, as the amplitude of the third mode is small, it is unlikely that the player would notice any significant improvement in comfort. The movement of the third mode is possible as the amplitude of this mode is so small, however significant structural alterations need to be made to shift the node locations of lower modes (first or second) and markedly improve player comfort. Therefore, the superficial alterations to the bats are not substantial

enough relative to mass of the bat to make any significant difference to the vibrational frequencies. If a manufacturer was attempting to make alterations to the vibrations and shift the sweet spot, significant structural changes or alternate materials should be considered. The effects of alternate materials were discussed earlier in this chapter, as deviations in the modal shape were found as the wave passes over the handle rather than the bat.

None of the bats recorded a modal frequency that was considerably different from the other bats. Therefore, demonstrating that the structural alterations do not cause a considerable shift away from a standard frequency. The DF represents the most traditionally shaped bat and although this has a lower fundamental frequency, the difference is not considerable enough to make an impression on the shape of the mode. Grant (1996) reported that a higher fundamental frequency (maximised E/ρ^3) is associated with improved comfort. Therefore, the designs of the modern bats (eg. Probe) although small, do offer a marginal improvement in the post impact responses of the bat. In chapter 9, the effects of design alterations to the bats were also found to have little influence on the static flexibility. The flexibility of the bat will influence the magnitude, frequency and propagation of vibrational waves. Therefore, these results not only support the similarities in static flexibility but also highlight that the superficial design changes are not adequate enough to cause changes to the vibrational frequencies.

The slight differences between the analysed bats may be due to the differences in the micro-structure of the wood. Although the bats would have been pressed during construction, they had not been "knocked-in" and were therefore not match ready. Grant & Nixon (1996b) reported that vibrational frequencies can be increased by 30% in beam samples and 10% in bats following the compression of the surface layer, therefore causing a comparable increase in vibrational frequencies recorded by the bats. The collective effects of drastic structural changes and knocking-in, may offer the manufacturer a means of raising the frequencies (especially the fundamental) and improving player comfort.

12.3.5 Conclusion.

It was the aim of this study to establish the modal frequencies and shapes of the three excited modes below 1kHz following controlled impacts. It can be concluded that the design alterations made to the bats have little influence on the first or second modes following impact. It was noted that the location of the nodes of the third mode were shifted to the position of preferred impact due to structural alterations. However, due to the amplitude of this mode it is unlikely that any significant benefits in comfort will be experienced if the third mode was reduced.

12.4 The influence of orientation on excited vibrational modes.

12.4.1 Introduction.

Previously the cricket bats were suspended from their handles using twine in an attempt to excite the natural frequencies as the bat was not in contact with any other object. During the analysis it was proposed that the twine may influence the shape or frequency of the excited modes (especially the fundamental) as the shape was considerably altered as it passed over the handle region. Although it was hypothesised that this was due to the changes in cross-sectional area and material characteristics, it was not possible to eliminate the effects of the twine on the handle's vibrations. Therefore, one of the bats was hung from the bottom of the blade to establish whether there were any changes in the measured frequency or shape of the fundamental mode.

12.4.2 Experimental set up.

The same experimental set up was used during this investigation as outlined earlier in this chapter, although only one bat was investigated (Probe). The bat was suspended from the bottom of the blade from a piece of twine 0.8m in length. The tri-axial accelerometer was attached at 28 positions at equal increments of 0.03m along the length of the bat, while ten impacts were administered using the modal hammer 0.16m from the free end. Following each of the impacts, the excited vibrations below 1.6kHz were recorded using a Pulse multi analyser, which allowed the analysis of the recorded vibrations.

12.4.3 Results.

Following the analysis of the controlled vibrations, it was possible to investigate the effects of suspending the bat from the handle (HBH) (chapter 12.2) or hung from the bottom of the blade

(USD). From Table 12.6, it is clear that the three excited modes are the same frequency regardless of the bat's orientation.

Frequency (Hz)			
Bat	**Mode 1**	**Mode 2**	**Mode 3**
HBH Probe	112	328	536
USD Probe	112	328	536

Table 12.6: Modal frequencies of the bat hung by the handle (HBH) and upside down (USD).

Using the data from the multi-analyser, it was possible to plot the shape of the vibrational modes (Figure 12.17 & 12.15).

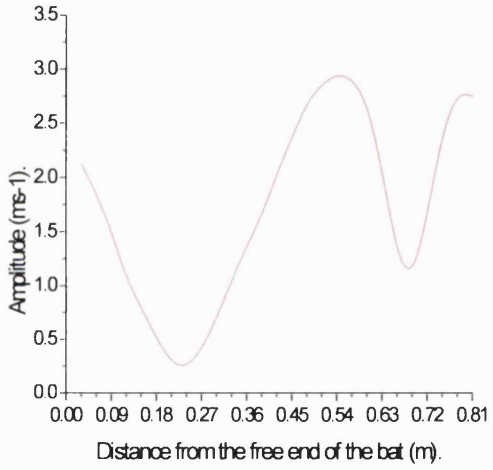

Figure 12.17: Fundamental mode HBH.

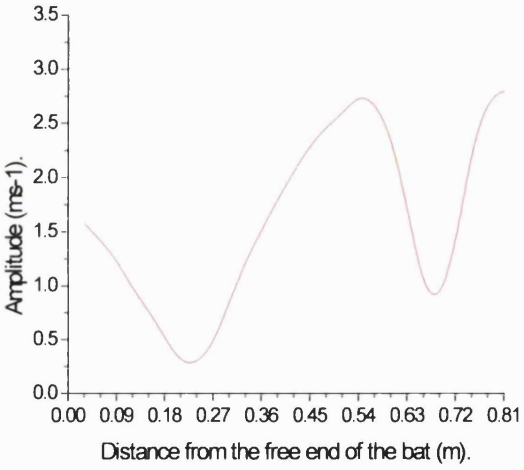

Figure 12.18: Fundamental mode USD Probe.

Figure 12.17 & 12.15 show that the shapes of the fundamental frequencies are almost identical for each test, including node location and the magnitude of the signal. The two figures show a steeper curve around the handle region of the bat (0.6 to 0.81m) when compared to the curve over the blade of the bat.

12.4.4 Discussion.

The aim of this study was to investigate the influence of the twine attachment during the excitation of vibrations when a bat was freely suspended. It was a concern that the twine attached to the handle influenced the vibration and could be a contributor to the different shape of the vibration curve over the handle. Therefore, the vibrations of one of the bats was recorded when it was suspended from the bottom of the bat rather than the handle. It has not been previously published if the direction or location of the twine had significant effects on the vibration of sporting equipment, therefore it was necessary to carry out this particular study.

It was established that the modal frequencies and node locations were unaffected by the attachment location of the twine and the orientation of the bat. Therefore, it can be assumed that the twine has little influence on the vibration of the system. It can be suggested that freely suspending sporting equipment provides an ideal experimental set up to investigate the responses when the implement is not in contact with any other object. As the frequencies and magnitudes of the excited vibrations were almost identical, it can also be assumed that this testing method is repeatable, which removes the doubts concerning the possibility that the published results are inimitable.

12.4.5 Conclusion.

It was found that the twine had no influence on the measured vibrational frequencies or shape of the wave over the bat when the hanging direction was rotated. Thus it was noted that the distinct wave shape over the handle was not caused by the twine attachment but by the differences in material properties, density and dimensions. Therefore, the vibration is unable to travel at the same velocity throughout the whole of the structure as earlier suggested in chapter 12.2.

12.5 Post impact bat motion and oscillation decay rate.

12.5.1 Introduction.

The contact period between a baseball bat and ball has been found to last 1ms (Crisco *et al.* 2000) and during this study, the cricket bat and ball impact period was approximately 2ms. However once the ball is no longer in contact, the bat continues to respond to the impact through oscillations. The time period of the oscillations have not been reported for cricket bats, although it has been noted that a tennis racket returns to its original position after 15ms (Brody, 1987). Although, the total racket recoil has been found to last for 200ms regardless of the clamping condition of the racket (Cross, 1998). It has been found that a racket displaces downwards following the impact before returning to its original position after a small overshoot (Cross, 1997). The downward displacement and following overshooting produces the fundamental vibrational wave, which contains large magnitudes of energy. Therefore, this study will investigate the total oscillation time as it is an indicator of the energy present in the system, which can be associated with player comfort and post impact ball velocity. One of the main components of feel is the sensation in the hands (Hocknell *et al.* 1996). Therefore, the extent and magnitude of the post impact oscillations have a major influence on the perceived comfort of the player. Thus, even though the ball has lost contact with a tennis racket, the impact period does not end until the bat has returned to its original resting position up to half a second after ball contact (Cross, 1997). The aim of this study is to establish the total period of bat oscillations and the rate of decay following impact and how the construction of the bats influence these responses.

12.5.2 Experimental set up.

It was the intention of this study to establish the time elapsed for the whole of the impact period and not just the ball and bat contact time. Therefore, ball impacts 0.06m from the free end were analysed for the whole of the oscillation period as this location demonstrated the greatest degree of deflection. As during chapters 10 and 11, the ball impact was administered using a drop ball technique with a ball impact speed of $9ms^{-1}$. The motion of each of the five bats were recorded

and analysed using the high-speed camera system. At 2000Hz it was possible to accurately track the motion of the bat until the oscillations deceased. The bats were tracked when they were rigidly clamped and in the hand simulator to investigate the affects of clamping type on the oscillations and decay rate. The motion of the bat was plotted following the impact to establish the time period and decay rate of the oscillations. The decay rate was calculated by dividing the magnitude of the initial downward motion of the bats end (negative peak) by the time taken to return to a state of rest (Fisher, 2001).

12.5.3 Results.

Using the tracked motion of the first impact location (0.06m from the free end), it was possible to measure the initial deflection and subsequent oscillations of the bat following ball impact at this location.

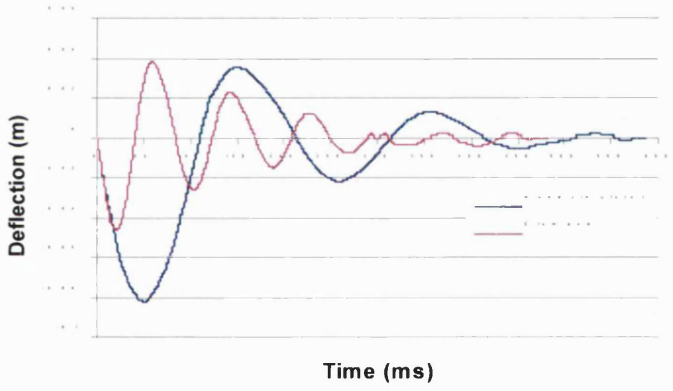

Figure 12.19: Probe bat oscillations following ball impacts using different clamping methods.

Figure 12.19, illustrates the difference in the measured deflections between a bat in the hand simulator and rigidly clamped. The rigidly clamped bat displays a 43% smaller initial downward peak than during the hand simulator impacts. However, the motion during the rigid clamps and hand simulator conditions are almost identical for the first 18ms. The positive peak of the bats motion during the clamped condition is greater in magnitude than for the hand simulator although the clamped peak occurred 88ms earlier. The deflection of the rigidly clamped bat decays before the hand simulator as it concludes after 480ms rather than 585ms after initial ball impact.

The subsequent results are illustrations of the bat deflection following ball impacts when the bat is rigidly clamped. Although this method does not completely represent hand held impacts, it eliminates the motion and damping properties of the hand simulator (Figure 12.19). This analysis also enables the study to establish the influence of the structural design on post impact bat responses, which were found to be affected by the hand simulator rig.

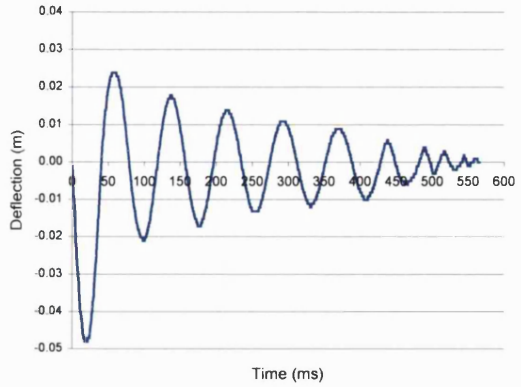

Figure 12.20: Slaz bat oscillations.

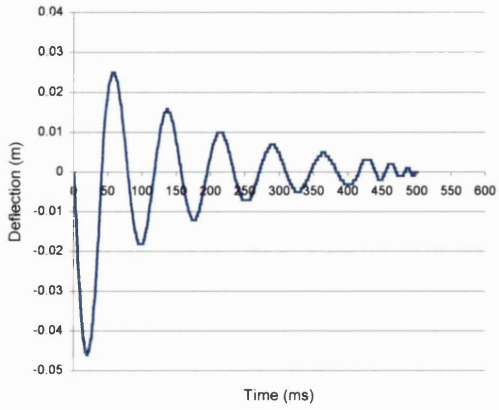

Figure 12.21: GN bat oscillations.

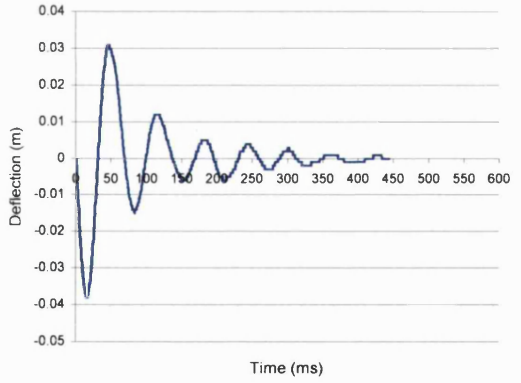

Figure 12.22: Hunt bat oscillations.

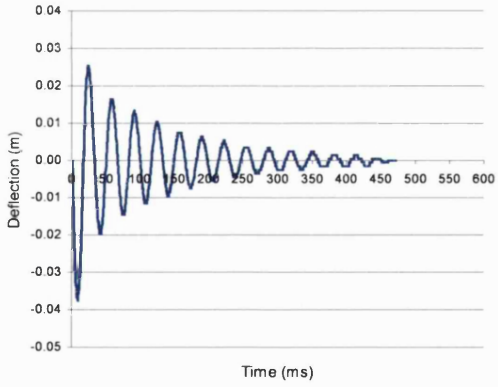

Figure 12.23: DF bat oscillations.

All of the bats follow a similar pattern of deflection, although the oscillations of the DF bat (Figure 12.23) are steeper and fluctuate more times than any of the other bats. However, the DF records the smallest initial deflection (38mm) and shortest oscillation period (432.5ms). It is the Slaz bat (Figure 12.20) that records the greatest initial deflection (48mm) and continues to

oscillate for the longest period (563ms). Finally, it is the clamped Probe bat (Figure 12.19), which displays the greatest positive peak (39mm).

Using the time taken for the bats to return to their resting positions and the magnitude of the first negative peak, it was possible to calculate the decay rate of each of the bats. The results from these calculations are displayed in Table 12.7.

	Slaz	Hunt	DF	GN	Probe
Max negative peak (mm).	48	38	38	46	45
Time to rest (ms).	563	432.5	459.5	496.5	463.5
Decay rate (ms^{-1}).	0.0853	0.0879	0.0827	0.0926	0.0971

Table 12.7: Calculated decay rate for each of the analysed bats.

Table 12.7 shows that the bat with the greatest negative peak (Slaz) does not have the lowest decay rate as it is the DF bats motion that decayed fastest. From Table 12.7, it is the oscillations of the Probe bat that decay the slowest, which can be associated with it recording the second highest negative peak and highest positive peak.

The visible differences in the oscillations of the analysed bats are also supported by the variations in the measured fundamental frequencies (Table 12.8).

Bat / Method	Slaz	Hunt	DF	GN	Probe
Motion data	14.24	16.60	20.35	14.37	15.84
Modal Hammer	14	17	19	15	15

Table 12.8: Comparison of vibrational frequencies when the bats are rigidly clamped.

From this table, it can be seen that the DF bat recorded the highest fundamental frequency, which correlates well with Figure 12.20d, as the gradient of these oscillations were steeper than any other bat. The calculated frequencies also correlate with the magnitude of the initial bat motion, as the large negative and positive deflection peaks displayed earlier (Figure 12.20a) correlate with the low frequency of the Slaz bat (Table 12.8). From Table 12.8, a clear

correlation can be seen between the calculated modal frequencies of the motion data and the measured frequencies using the modal hammer, substantiating the use of the modal hammer.

The deflection and corresponding oscillations will have an influence on the calculated COR when the bats are rigidly clamped. Therefore, the calculated COR (chapter 11.3) are shown in Figure 12.24,

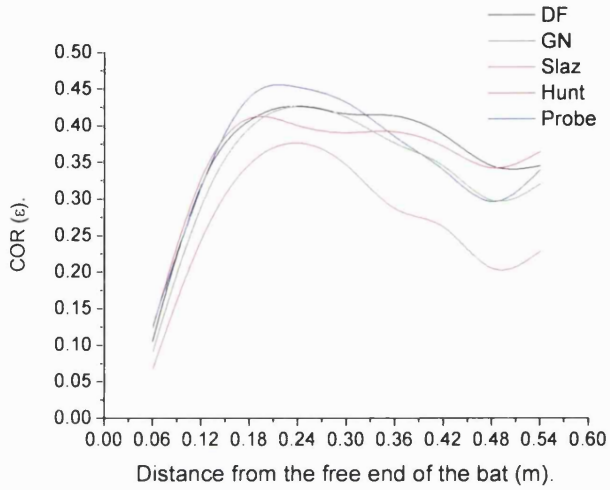

Figure 12.24: COR of each cricket bat when they are rigidly clamped.

From Figure 12.24, it is clear that the Slaz bat has the lowest recorded COR, while the Probe bat has the largest. It is noticeable that the other three bats are closely correlated between these two bats. It is also clear that the DF seems to maintain a constant level of COR along much of the length of the bat (0.18 to 0.40m). These results regarding the affects of structural design on COR were further analysed in chapter 11.

12.5.4 Discussion.

The aim of this investigation was to establish the time taken for each bat to return to a state of rest following ball impact at 0.06m from the free end. It was also possible to establish the rate of decay, which is influenced by the construction of the bat. It was discovered that the initial measured deflection was not necessarily an accurate indicator of the decay rate and that this rate will have an influence on the measured COR. The fundamental mode was analysed as the bat

deflection replicates the motion of this mode. This mode also contains the most energy, therefore having the greatest influence on player comfort and ball velocity following impact. From the figures, the bat that displayed the greatest number of oscillations was also found during the experimental trials to record the highest frequency. Therefore, this shows how the graphical illustrations of the post impact motion (as displayed in this section) substantiate the experimentally calculated vibrational results displayed in chapter 12.3.

It was found that the shape and time period of the bat oscillations were considerably affected when the bat was in the hand simulator or rigidly clamped. This result opposes Cross (1997), who found the clamping type had little influence on the post impact responses including oscillations. The continuation of the downward motion (by 43%) and the extension of the oscillation (by 105ms) were due to the compression of the damper units and not due to the deflection of the bat. However, it was noted that the initial 18ms was the deflection of the bat as the recorded downward motion was almost identical regardless of clamping method. Even though the hand simulator condition is a closer representation to a hand held condition, it is difficult to establish the influence of the structural alterations of each bat on the post impact responses. Using the hand simulator rig, the structural alterations were found to have little influence on the responses of hand held bats. However by isolating the blade of the bats using a rigid clamping method, the slight differences in post impact response could be identified. Using the modal hammer results from this chapter (12.2), it was also possible to verify the modal frequencies calculated using the high-speed camera. The vibrations were found to be very similar regardless of impacting technique (modal hammer v's direct ball impacts) and therefore it can also be proposed that the input frequencies of the ball has little influence on the vibrations of a cricket bat. Thus, it is the clamping method that has the greatest influence on the bat vibrational frequencies.

When the bats were rigidly clamped, they displayed a larger positive peak than when they are held in the hand simulator. This would have partially been caused by the flexion of the handle, which wouldn't have occurred during the hand simulator trials as the rotating clamps would have controlled the handle's motion. The differences were predominantly caused by the motion of the dampers in the hand simulator, which controlled the motion of the bat. The dampers absorb much of the energy following impact by providing resistance to the bat's motion, which decreases the number of oscillations. This lower frequency response is beneficial, as it is the higher frequencies that cause the greater discomfort to a player (Hocknell *et al.* 1996).

As reported earlier in this chapter, it was the rigidly clamped results that had the lowest fundamental frequency, although from Figure 12.19, it is the hand simulator that has a lower frequency of oscillation. Although this seems contradictory, these visual differences are due to the motion of the hand simulator and not representative of the bat's oscillations. Thus, for motion data (as shown during this study) the disparity between the modal hammer technique and direct measurement of bat oscillations are clear. This finding confirms why this study chose to use modal hammer vibration analysis rather than calculations from motion data especially during hand held and hand simulator results.

Cross (1997) reported that a tennis racket deflects down then up past its original position before returning to a state of rest. The deflection of the bat during clamped conditions oscillates between 7 and 14 positive peaks as it passes the original resting position lasting for up to 563ms, 363ms longer than found during tennis racket analysis (eg. Cross, 1997). The differences in the oscillation time are related to the flexural stiffness of the two implements. Willow has a flexural stiffness of 9.39GPa as opposed to the carbon fibre used for tennis rackets, which can be up to 200GPa. As tennis rackets are found to oscillate for a shorter period and with a reduction in amplitude, less energy is lost in the system therefore more can be transferred to maximise the post impact ball velocity. This is displayed in the significant differences between the maximum COR values of tennis rackets (0.85) and cricket bats (0.45).

It was the Slaz bat that displayed the greatest magnitude of deflection and longest period of oscillation, although it was the DF that recorded the lowest decay rate. This is due to the decay rate being a ratio of the first negative peak and the time taken for the bat to reach its original state of rest. For better understanding this has been displayed in Figure 12.25,

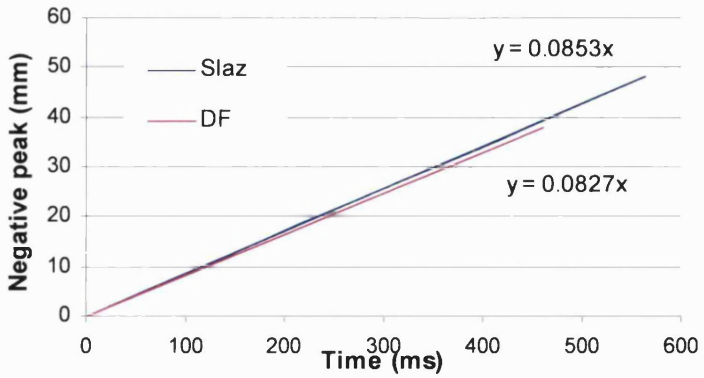

Figure 12.25: Comparison of the decay rate for the Slaz and DF bats.

Using Figure 12.25, the Slaz bat is seen to oscillate for longer at the larger magnitude, but the oscillations decay faster than during the impact involving the DF bat. This suggests that the Slaz bat with its larger oscillations is able to dissipate energy faster than having a bat with smaller and multiple oscillations. As the higher frequency of the first mode has been related to player discomfort, bats with extended deflection and longer oscillation periods (lower frequencies) are favourable. However, increased deflection at impact would decrease the post impact ball velocity due to increased energy transfer to the bat and movement of the bat away from the ball, which reduces the rebound efficiency. Therefore, a player faces a choice between comfort or performance. The Probe bat had the greatest decay rate following impact due to continual large oscillations. Although the Probe did not possess the largest negative deflection, it did record the largest positive peak and therefore was able to dissipate the energy contained within the system quicker than any other bat.

There are small differences in the response characteristics of each bat following ball impact. However, these differences in the oscillations and decay rate will influence post impact ball velocity and player comfort respectively. The oscillations of the bats can be related to the COR as they are an indicator of the energy remaining in the bat rather than being transferred back to the ball. For example, the Slaz bat had the greatest deflection and oscillated for the longest period and subsequently recorded the lowest COR. The Probe bat had the largest clamped COR and also recorded the fastest decay rate, suggesting that less energy was stored in the bat and a greater amount was returned to the ball, thus increasing the COR. The bat with the least initial deflection and the shortest oscillation period was the DF bat. It was noted that this bat had the second highest and constant COR along the length of the bat.

12.5.5 Conclusion.

It was the aim of this section to investigate the decay of the bat's motion following ball impact. It was found that the magnitude of the deflection had a negative effect on the time required for the bat to return to its original state of rest. The higher frequency response of the DF bat also caused the decay rate to be extended. Finally, it was found that the Probe bat, which had the fastest decay rate led to a higher COR, as much of the energy was returned to the ball rather than expended during the oscillations of the bat. Thus supporting the earlier hypothesis that there is an optimum stiffness to maximise the COR and decrease unpleasant oscillations. This degree of stiffness (as displayed by the Probe bat) enables a specific degree of deflection that avoids high frequency oscillations and extended deflection, which were both found to be detrimental to the COR and player comfort. Therefore, much of the energy is transferred to the ball maximising the post impact ball velocity and associated COR.

12.6 Chapter summary.

The modal frequencies and node locations of the first three excited modes were investigated. It had been reported previously that only vibrations below 1kHz were experienced by players and thus these were of greatest interest. During hand held and hand simulator trials, the lowest nodes of the first three excited modes were located 0.3m, 0.18m and 0.12m from the free end respectively, although these were considerably different during the other clamping conditions. The structural design and the orientation of the bats were found to have limited influence on the location of the nodes, although the excited modes were considerably affected by the handle of the bat. It was proposed that the decay rate of the vibrations had an influence on the COR and thus a faster decay rate would enhance performance. In conclusion the modal responses of cricket bats have been established thus highlighting the location of the sweet spot. If a ball impacts this location, improvements in player comfort and enhancement of struck ball distance will be achieved.

13 COMPARISON OF SWEET SPOT LOCATIONS.

13.1 Introduction.

In tennis racket studies, it is found that the peak COR, COP and nodal sweet spots coincide (eg. Brody, 1986). This study investigates whether such coincidences also occur with cricket bats. It is proposed that each of the sweet spot location is not independent but are within close proximity to each other. In previous chapters the influence that each sweet spot has on the post impact bat responses has been independently reviewed. This outlined how changes to the set up either through clamping methods, impact velocity or structural design had an effect on the sweet spot locations.

13.2 Experimental set up.

Having established that for the bats tested, the structural design and pre impact ball speed have not altered the location of the sweet spots, it may be that there is a relationship between the sweet spot locations and the post impact bat and ball responses. Therefore, this chapter aims to establish if the three sweet spots (peak COR, COP and Nodal) coincide and how they each affect the post impact performance, either through changes in player hand comfort or post impact ball velocity. As the location of the sweet spots can move by changing variables such as the gripping of the handle, the results presented are based on specific conditions. In these tests a ball impact speed of $9ms^{-1}$ is used when the bat is held in the hand simulator rig with the clamps located 210mm apart and tightened to 8N. It was found in during chapters 10, 11 and 12 that this produced the results that most closely replicated actual use.

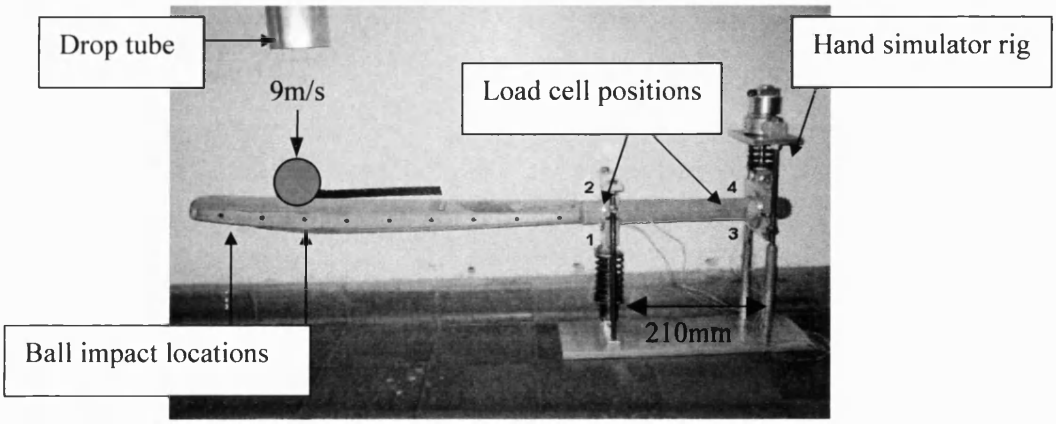

Figure 13.1: Experimental ball striking set up for the COP and COR analysis.

To help understand the results, Figure 13.1 displays the location of the load cells and shows the ball impact positions. Load cell 1 is located at the palm of the player's bottom hand, while load cell 2 corresponds with the fingers of the same hand. Load cell 3 is positioned at the palm of the top hand and load cell 4 is at the fingers of that hand (Figure 13.2).

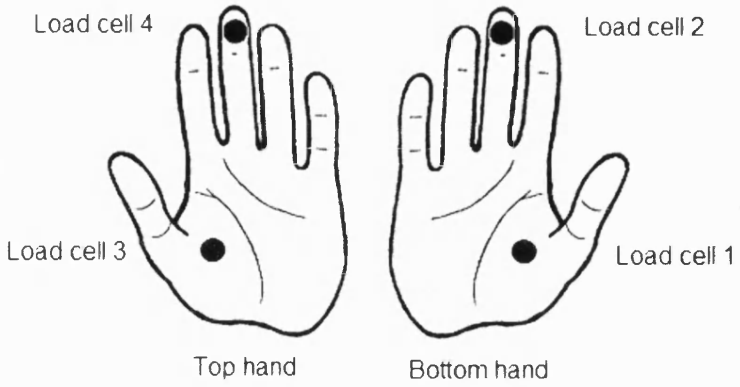

Figure 13.2: Load cell numbers in relation to the position on a players hands.

As in chapter 10, the average of the recorded peak loads are presented in this chapter for each of the load cells. These loads are the mean of the peak forces recorded at each impact location, for six impacts. The COP was also investigated and defined in chapter 10. It was found that there were no distinct impact locations that led to zero hand force. Therefore, it is proposed that the impact position that corresponded with the greatest reduction in hand load would be considered by the player to be the COP.

This chapter will also compare the proposed COP and COR with the nodal sweet spot and modes of vibration. The set up for the vibration test was similar as for the drop ball tests, but a calibrated hammer was used instead to administer the impacts 0.16m from the free end. The excited vibrations were recorded using an accelerometer mounted (using contact adhesive) at 0.03m increments along the length of the bat.

13.3 The influence of the COP on the measured COR.

13.3.1 Introduction and literature review.

Impacts at the COP led to a reduction in the hand loads, thus the energy following impact must be distributed elsewhere. Many research papers have compared the COP with the COR during tennis racket and baseball bat impacts. Noble & Eck (1985) and Weyrich *et al.* (1989) found that impacts at the COP produced a significantly greater post impact ball speed following baseball bat and ball impacts. Therefore, its was concluded that the location of the maximum COR must correlate with the position of the COP (Sykes *et al.* 1971). Bryant *et al.* (1977) and Noble (1985) measured the post impact ball velocity and subject's interpretation of whether the COP was impacted on a baseball bat. Bryant *et al.* (1977) and Noble (1985) found that the greater the deviation from the COP, the greater the reduction in the post impact ball velocity. Noble (1985) noted a significant variability between the results of each subject and this was considered to be due to the lack of direct measurement of the COP. However, using the high-speed camera system and the synchronized force data from the load cells, it was possible for this study to establish the exact occurrences of these variables during each impact. It is proposed that a direct correlation between the COP position and maximum COR will be found, due to the transference of energy from the bat to the ball rather than to the players hands.

13.3.2 Experimental set up.

In chapter 10, the location of the COP was investigated, while in chapter 11, the position of the maximum COR was identified. The results from these sections have been combined to establish whether there are correlations in their locations.

13.3.3 Results.

Only the results for one of the five first class cricket bats, the Probe bat is displayed as this identifies the location of each peak adequately.

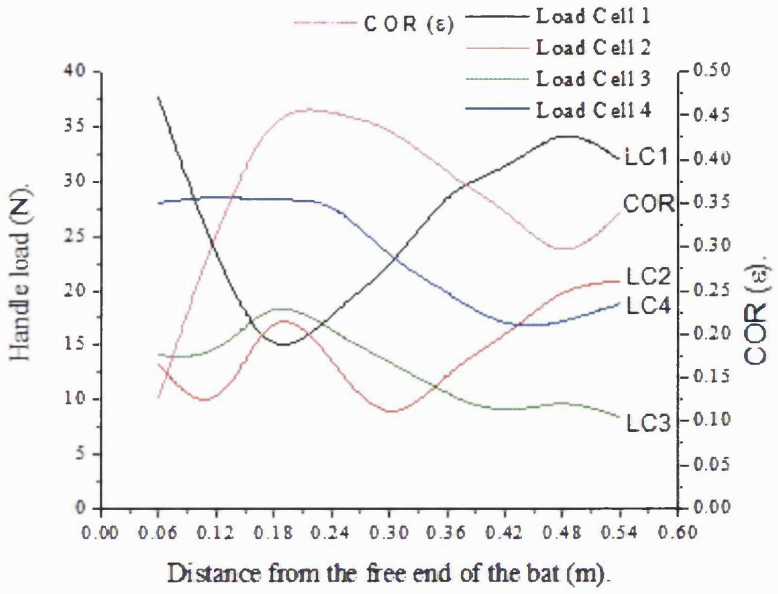

Figure 13.3: Comparison between the COR and the handle loads.

Figure 13.3 displays the variation of COR along with the average peak loads recorded by each load cell. The COR distribution is almost opposite in shape to the handle load distribution measured by load cell 1 (palm of bottom hand, see Figure 13.2). Changes at the first load cell were considered to have greatest effect on player comfort due to its location and magnitude (chapter 10). The large peak in the COR correlates with a distinct reduction in the measured load, which was considered to represent the position of the COP in chapter 10. The loads at the second load cell follow a pattern that for much of the length of the bat seem to be unrelated to the COR results. However at 0.48m from the free end, the measured hand loads increase as the COR decreases. It is also noted that the highest load has occurred at the position of maximum COR (0.18m from free end). The loads at handle positions three and four follow a similar pattern to the calculated COR, although load cell 3 mimics the shape of the COR more closely as the contours of load cell 4 occur one impact position before those of the COR. It is important to note that at the position where the handle load at load cell 1 is at a minimum (0.18m from the free end), the other load cells record their highest handle loads. However as the position of the COP is defined by this study as the location where the greatest reduction in hand load occurs compared to the normal load along the length of the bat, it is deduced that load cell 1 measures the position of COP. It was also hypothesised that the grip location that displayed the greatest

reduction relative to the other grip positions was also the COP. Therefore, 0.18m can be considered to be the COP.

13.3.4 Discussion.

The location of the minimum hand load (COP) of the first load cell (base of the palm) coincided with the position of maximum COR (power spot) at 0.18m from the free end of the bat. It is suggested that it is the first load cell that has the most influence on the perceived comfort experienced by the player due to its location within the hand and the relative load reduction when compared to the normal loads experienced at this location. Knudson (1991b) and Ferguson (1992) reported that the base of the palm of the bottom hand (position of load cell 1) produced resistance to the impact forces and that it was this hand that controlled the shot. Therefore, it can be proposed that reductions in load at this location would lead to a significant improvement in player comfort as the expected hand forces at that location would no longer be experienced.

The COP occurs at the bottom handle clamp (0.6m from the free end of the bat) as this is the axis of rotation for a ball impact 0.18m from the free end. Therefore, the handle load at this location, which was recorded by load cell 1 is reduced. Following an impact at this location the energy created during the impact is redistributed, either to amplify vibrational modes or transferred to the ball. This leads to an improvement in the comfort at the hands experienced by the player and an increase in the striking distance of the ball. It was also found that as the measured load at load cell 1 increased the COR decreased, highlighting a possible correlation between these variables. It can be hypothesises that it is the changes in the measured hand force that affect the calculated COR. As discussed during chapter 10, the forces are redistributed either to other locations in the hands or transferred to the ball to maximise post impact ball velocity. Although it was noted that there was an increase in handle load at the other load cell locations, this was not comparable to the reduction in the handle load at load cell 1. Therefore, much of the remaining energy must have been transferred to the ball causing the recorded increase in COR.

From the analysis of the measured handle loads relative to the COR, it was noted that there did not seem to be any correlation between the COR and loads at the second or fourth load cell

positions. These load cells are located at the fingers and it has been previously reported that forces at the fingers did not influence the post impact ball velocity (Knudson, 1991). This is due to the recorded loads on the fingers indicating the load required to stop the handle from being pulled out of the hands and to generally stabilise the cricket bat. This is because it is the palms of the hands that resist the loads applied during the impact rather than the fingers due to the direction of the impacting force.

13.4 The effect of nodal sweet spots on the COR of cricket bats.

13.4.1 Introduction and literature review.

If impact occurs at a node of a vibrational mode, that mode is not excited, thus transferring the energy that would have been used to propagate this excitation to the ball. Therefore establishing the magnitude of the first mode of vibration and the location of its node is important as it may correlate with the position of maximum COR or influence its size. It will also be possible to estimate the exact influence that each of the vibrational modes have on the post impact ball velocity depending upon the changes (if any) in the calculated COR. The mathematical model of Penrose & Hose (1998) investigated the influence of each vibrational modes on the responses of the ball following impact. It was noted that the first mode had the largest influence on post impact ball velocity as it had the greatest amplitude.

13.4.2 Results.

Using the results from chapters 11 and 12 with the set up as described earlier in this chapter, it was possible to plot the modes of vibration against the COR at each impact location. Firstly, this study concentrates on the first mode of vibration, due to the large amplitude of this mode, before investigating the second and third modes.

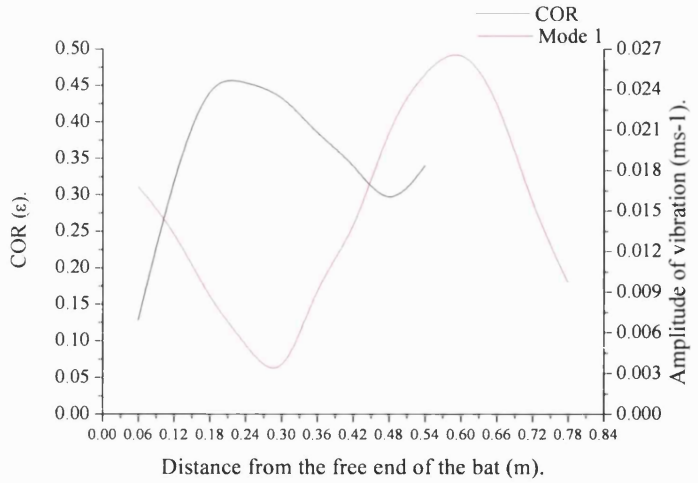

a: The first mode of vibration.

From Figure 13.4a, the position of maximum COR is located 0.12m lower down the bat (0.18m from the free end) than the node of the first mode (0.3m from the free end). Even though the location of the nodal sweet spot does not correspond with the position of maximum COR, the high COR value is maintained until after this nodal position. As the COR value begins to decrease (0.3m from the free end), the amplitude of the first mode increases. This patterns is also repeated below 0.18m from the free end, where the COR decreases as the amplitude of the first mode increases.

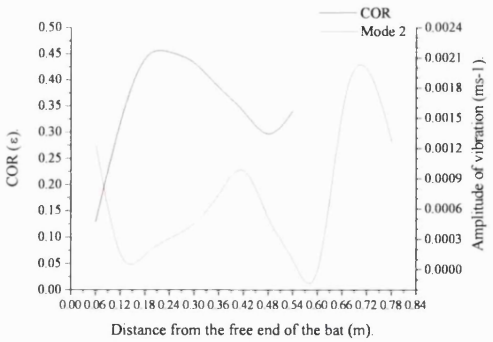

b: The second mode of vibration.

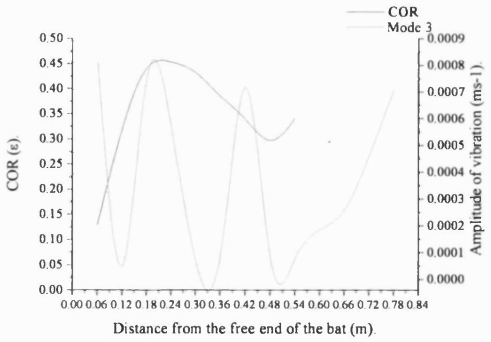

c: The third mode of vibration.

Figure 13.4: Comparison of modal frequencies with the COR.

Figure 13.4b and c illustrate the relationship between the second and third modes and the COR following impacts along the length of the bat. In comparison to the magnitude of the first mode, the second and third modes are considerably smaller (10 and 100 times respectively). However, it is still important to investigate whether they had any influence on the COR. From Figure

13.4b, the node location of the second mode (0.15m from the free end) occurs 0.03m from the position of maximum COR. It was earlier noted that at 0.18m from the free end, the COR decreases as the amplitude of mode 1 increases. The same could be considered to occur in Figure 13.4b, suggesting that the combination of the increasing first and second modes cause the COR to reduce. The remaining fluctuations of the second and third mode Figure 13.4c, seem to be unconnected to the shape of the COR along the length of the bat. Therefore, due to relatively small amplitudes and seemingly unconnected pattern, the second and third modes can be considered to have little influence on the shape of the COR unless they are connected to the larger first mode.

13.4.3 Discussion.

The node location of the first mode was found to be close (0.12m) to the position of maximum COR. It was also noted that as the impacts were administered closer to the bottom of the bat where the amplitude of the vibration increased, the calculated COR was reduced. This is inline with the findings of Penrose & Hose (1998), who reported that there was a connection between the location of the node of the first mode and an increase in the COR. The increase in the calculated COR occurs as the energy that would have otherwise been transferred into propagating the vibrational mode has been imparted into the ball, thus maximising the post impact ball speed and calculated COR. Therefore following an impact 0.3m from the free end of the bat, this study perceives that the player would consider they have impacted a sweet spot, as there is a reduction in the vibrations at the hands and an amplification of the post impact ball velocity. The COR was also noted to be extended to the node location (0.3m), thus indicating that although the position of maximum COR occurs further down the bat, the reduction in the mode enables the high COR to be extended.

Along with the findings from the previous section (13.3), it could be suggested that the reduction of the handle loads has the greatest affect on the COR, but a high COR can be maintained by a reduction in the first mode of vibration. This is proposed as the peak COR was

directly opposite the COP position, although a high COR is still apparent at the node of the first mode. By having a node location away from the COP, the COR is extended further along the bat than would have otherwise been possible. This concept that has not been previously suggested, that by shifting the node and COP positions further apart, it may be possible to have a high COR (above 0.4) along much of the bat's length.

It could also be hypothesised that the lowest node location of the second mode may influence the COR due to the close proximity of the node to the maximum COR. Although the amplitude of the second mode is small, the reduction of a vibrational mode will still aid in the amplification of the post impact ball velocity and calculated COR. As the node of the first mode is also close to this position, any effects that the reduction in the second mode may have on the ball will be amplified.

13.5 Comparison of the COP and nodal sweet spots in cricket bats.

13.5.1 Introduction and literature review.

The advantages of impacting the node of an excited mode have been outlined. However, Hatze (1998) suggested that locating the COP is of limited benefit as it does not occur during game situations as found during static racket tests due to the constantly shifting axis of rotation. Penrose & Hose (1998) also considered the COP to be irrelevant as the location of this sweet spot is based upon the assumption that a cricket bat is rigid. Therefore, any reduction in the handle load is caused by ball impacts at the nodes of vibration. Cross (1998) reported that location of the COP corresponded with a node of the fundamental mode, which led to a reduction in the load at the lower hand during baseball. From the findings of Cross (1998), it can be hypothesised that there is a vibrational COP rather than a purely load related COP (as earlier defined). Following an impact at this identified location, an improvement in hand comfort would be perceived due to a combined reduction in the possibly painful vibrations and hand loads. For this to occur in cricket bats, the location of the nodal sweet spot must correspond to the proposed COP. This would not only then lead to improvements in the comfort, but also an increase in the striking distance as increased energy is transferred to the ball during the impact period.

13.5.2 Results.

Using the results from the COP and vibration analysis (chapters 10 and 12) which employed the set up described earlier in this chapter, it was possible to plot the load and vibration measurements along the length of the Probe bat to establish any correlation.

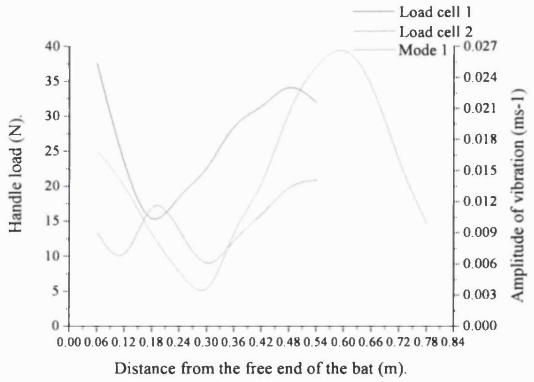

Figure 13.5: Comparison between the bottom clamp handle loads and the first mode of vibration.

Figure 13.5 displays the fundamental mode and the handle loads measured by the first and second load cells. These load cell positions represent the palm (Load cell 1) and fingers (Load cell 2) of the bottom hand (clamp). The COP for the first load cell was proposed to occur 0.18m from the free end of the bat, while the node of the first mode occurs 0.3m from the free end, 0.12m further up the blade of the bat towards the clamps. However, a node in the first mode does occur at the same position as a reduction in the handle load recorded by the second load cell. Thus, this measured reduction in hand load may be caused by the diminution in the amplitude of the first mode at this location.

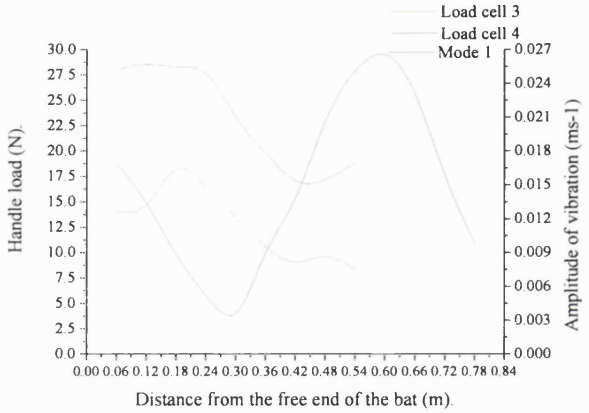

Figure 13.6: Comparison between top clamp handle loads and the first vibrational mode.

From Figure 13.6, the location of the node of the first mode seems to have no correlation with the reductions in the handle loads measured by the third and fourth load cells. These load cells represent palm (Load cell 3) and fingers (Load cell 4) of the top hand on the handle. From these results, it is suggested that the first mode of vibration has no influence on the handle loads that would be transferred to the top hand of the player.

Due to the close proximity between the node of the second mode and the position of maximum COR, it was considered important to investigate any connections between the hand loads including the suggested COP position and the nodes of the second vibrational mode.

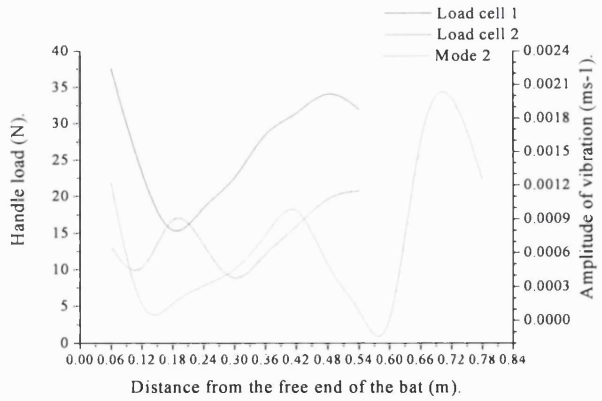

Figure 13.7: Comparison between the bottom clamp load (cells 1 & 2) and the second mode.

Figure 13.7 illustrates that the nodal locations of the second mode do not show a relationship with the hand loads recorded by the first and second load cells. However, the location of the first node of the second mode (0.15m) is close to the positions were the measured force is seen to decrease (0.18 and 0.12m for first and second load cells respectively). However, these locations of nodal sweet spot and load reduction are considered to be independent of each other.

It was also possible to establish whether there was a correlation between the handle loads recorded by the third and fourth cells (top clamp) and the shape of the second mode of vibration (Figure 13.8).

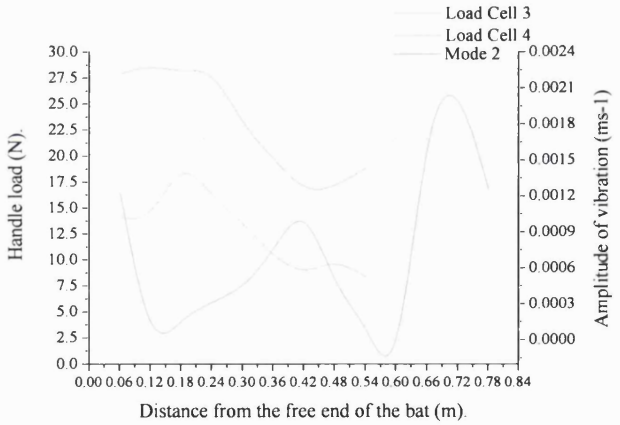

Figure 13.8: Comparison of top clamp handle load (cells 3 & 4) and the second mode.

From this figure it can be seen that the location of the first node (0.12) of the second vibrational mode is close to a peak in the handle loads recorded by the third and fourth load cells (0.18 and 0.2m respectively). It is considered that these two factors are unrelated, as it would be expected

that the handle load would decrease rather than increase following an impact at a vibrational node. Although, as the load cells measure impulsive load and not vibration and the magnitudes of these waves are too small to cause dramatic oscillation of the bat, it is unlikely that there propagation would be recorded by the load cells.

Due to the small amplitudes of the vibrational modes and the obvious disparity in the results between the COR and the nodal locations, the third mode has not been displayed.

13.5.3 Discussion.

The proposed position of the COP (the palm of the bottom hand / Load cell 1) does not correspond with the location of the node of the first mode, contradicting the findings of Cross (1998) during tennis racket analysis and Penrose & Hose (1998) during mathematical modelling studies of cricket bats. Due to the difference in bat construction and experimental set up, disparity between Cross (1998) and this study was expected, however similarity between the results of this study and those of Penrose & Hose (1998) were anticipated. The differences in the results between Penrose & Hose (1998) and this study may be due to this study having been experimental rather than a finite element analysis. Penrose & Hose (1998) also used simplified shapes and rigid rotating clamps rather than the hand simulator rig, which simulated human responses. As found in this study, rigidly clamping the cricket bat considerably influences the amplitudes and frequencies of the excited vibrations due to the restricted motion and the relative shortening of the implement. This causes the vibrational modes to undergo a phase reversal at the rigid clamps, that would not have otherwise occurred had the bat been hand held or, in the case of this study, in the hand simulator rig.

The COP and nodal locations are two distinctly different variables, as they are associated with the impulsive forces and modal vibrations experienced at the hands. Although it would be beneficial to player hand comfort if these two locations correlated, it should not be considered that they necessarily would be. The shape of the vibrational mode is influenced by the dimensions of the bat, its material properties and the clamping methods applied to the bat, while the COP is related to the location of the axis of rotation at the point of impact. Therefore, it can

be hypothesised that although the COP and nodal positions did not correlate during this situation they may correlate under different testing conditions, with a different bat type or as the player swings the bat and moves the axis of rotation.

The node of the first vibrational mode did correlate with the COP of the second load cell, which would lead to an improvement in comfort at the fingers of the player's bottom hand. Penrose & Hose (1998) noted that it would be advantageous if a cricket bat could be designed where the COP and a node of a vibrational mode coincided due to the post impact benefits. The benefits that the player would experience would be the reduction in the vibration and impulsive loads at the hands, while noticing an increase in the struck ball distance. It is suggested that with this clamp (grip) location, the player is able to correlate the COP associated with the fingers of the bottom hand (Load cell 2) with the node location of the first mode. This would lead to a marked improvement in hand comfort as it is this mode that contains the greatest amount of energy relative to the other excited modes of vibration. However, it is unlikely that the player would experience improved comfort at both hands as no prominent trends appeared between the third and fourth loads cells (top hand) and the first mode.

It is important to remember that each player's response to vibrations and hand loads will be different due to their perception of comfort and their particular tolerance to the associated stinging and jarring at their hands. Therefore, it is difficult to establish the exact level of player sensitivity to particular amplitudes and which specific vibrational frequencies are preferable. This study has not aimed to establish which frequencies are most innocuous to the user but has used the amplitude of the excited frequencies as an indicator to establish the possible level of comfort/discomfort experienced at the hands.

13.6 Chapter summary.

This chapter investigated whether any of the sweet spot locations (max COR, COP and nodal) coincided along the length of a cricket bat. It was found that the proposed COP and maximum COR were located at the same position (0.18m), although the location of the node of the first mode was found to be located further up the bat (0.3m from the free end). However, even this location might still enhance the COR. It was proposed that by having two distinctly different locations for the COP and nodal sweet spot, the magnitude of the COR was maintained over a greater distance along the blade of the bat. The maximisation of the COR at these locations is due to the energy from the impact being transferred to the ball rather than being distributed elsewhere, either through impulsive forces or modes of vibration. Thus unlike during tennis racket analysis, it is advantageous to locate the sweet spots slightly apart to maximise and maintain the COR for longer than may have otherwise been possible. This chapter also discovered that the nodal sweet spot (node of 1st mode) did not correlate with the COP. Therefore, a player may experience a reduction in the vibrations that may cause the painful stinging sensation associated with striking a node of a vibrational mode but still encounter an increase in the hand loads. From these results a player would have to decide which particular improvement in feel they had experienced when striking balls at nodal sweet spot.

14 FINITE ELEMENT MODELLING AND ANALYSIS OF CRICKET BATS.

14.1 Introduction.

Finite element (FE) modelling and analysis has increased following the development of user-friendly computer packages. These programmes remove the need to solve the complex mathematical equations that FE modelling is based upon. FE analysis divides complex structures into smaller elements, which are individually evaluated before being summated to create a collective response. FE models can be constructed as a solid, liquid or gas in one, two or three dimensions. They are then analysed using mechanical, electrical or thermal loads, which are applied statically or dynamically. Geometric shapes are defined using x, y, and z co-ordinates and elements are used to create the shape of the item under investigation. The material properties and specific constraints (clamps etc.) are then included at this pre-processing stage. Once the loads are applied, the model is solved to establish the responses of the constructed body. The post-processing stage of the programme enables the mechanical responses, such as deflection, vibration and strain or changes in electrical field, voltage etc. to be established. In this chapter, published work is discussed in which FE modelling has been used to analyse cricket bat performance and the effect that alterations to material properties or geometric dimensions make. Finally, a model that has been constructed to simulate the experimental results is presented to assist model validation. Alterations are then made to various parameters to assess their impact on bat performance.

14.2 Literature review.

To investigate the influence of the various dimensions and weight on the stiffness and the first three modes of vibration, Grant & Nixon (1996) and Grant & Paisley (1997) developed a basic FE cricket bat model. A limitation in these studies is that they assumed the blade to be a homogenous isotropic material, however, English willow is neither of these. Such assumptions therefore result in errors in the calculated data.

To match the overall mass of the bat and establish comparable results to experimental work Grant & Nixon (1996a) had to increase the willow density by 50%. Grant & Paisley (1997) also found the modal frequencies were 20% lower than their experimental findings. Grant & Nixon (1996a) and Grant & Paisley (1997) reported that none of the current design features had a significant effect on flexural frequencies or bat performance. Although, an increase in ridge height and handle radius did have a significant effect on the bat's vibration frequencies. The removal of the handle rubber inserts was also found to raise the frequency of the third mode by 50% (Grant & Nixon, 1996a).

Penrose & Hose (1998) produced two basic cricket bat models with identical mass (1.002Kg) and centre of mass locations, although one included a large scallop in the blade of the bat. The Young's modulus of the handle was taken to be 500MPa, with a Poisson's ratio of 0.2 and a density of 400Kg/m^3. Penrose & Hose (1998) modelled the bat as an orthotropic elastic material by estimating the values of willow. Alternatively, John & Li (2002) developed a traditionally shaped bat, which was rigidly clamped at two locations around the handle to simulate experimental tests for verification purposes (Table 14.1). The bat model was also analysed when the handle was fixed at the end.

	Experimental	**Finite Element Model**	
	Clamped at two locations		**Fixed at end**
Mode 1	15	16.52	13.44
Mode 2	222.85	208.10	125.67
Mode 3	672.22	605.81	474.26
Mode 4	1688.33	1338.42	842.45

Table 14.1: Experimental and FE calculated frequencies of a cricket bat (Hz) (John & Li, 2002).

The FE model produced similar results, although the error between the results increased with the measured frequencies. John & Li (2002) concluded that FE is a feasible method of calculating the behaviour of cricket bats, even if simplified models are used.

A concern with the accuracy of the results published by Grant & Nixon (1996a), Penrose & Hose (1998) and John & Li (2002) was that the material properties used to define the bat were either from an unspecified origin (John & Li, 2002), estimated (Penrose & Hose, 1998), or

altered (Grant & Nixon, 1996a). Therefore, the material properties were modified until the FE results correlated with the experimental results. Due to the nature of wood, the material properties will not be uniform throughout the bat, but for the purposes of comparison it is necessary to base the properties on typical data such as published results or from properties obtained directly from tests performed on cricket bats.

14.3 Model construction.

To analyse the influence of structural design on cricket bat responses, an FE bat model was constructed. The modelling computer package Ansys was used to create a model that could be verified using the experimental results previously outlined in this thesis. The Gray Nichols (GN) bat was selected for the purpose of modelling as it has a radical design, with large scallops removed from the back of the bat (Figure 14.1 a & b). Therefore once an accurate and reliable model bat is constructed, the dimensions of the bat can be greatly altered to investigate their influence.

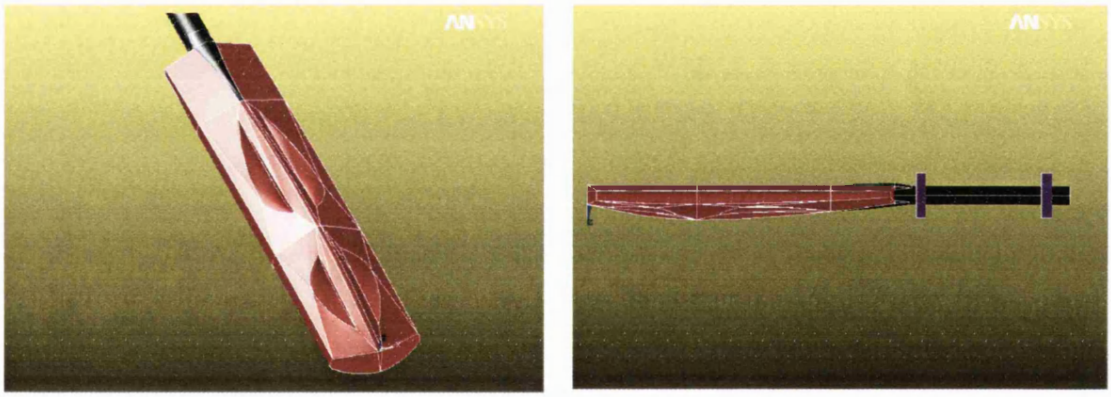

a, Contours of the back of the bat. **b, Horizontal profile of the bat.**

Figure 14.1: Images of the modelled GN bat.

A mesh was constructed using a key point method, where each contour of the bat is given a number of three-dimensional co-ordinates (x, y & z). Numerous key points were entered along the path of curves to ensure the spline curve option followed the required radius of curvature. The key points were combined to create areas, before being grouped into two distinct volumes, the handle and the blade, which are glued together. Glue lines secure two volumes together using contact elements while maintaining the material differences, although they respond to

each other at the connected intersections. The rigid clamps were constructed as replica aluminium blocks with holes to allow the handle of the bat to go through.

14.3.1 Element type and mesh construction.

To perform an analysis, it is necessary to model the bat using a mesh of elements. There are many element types that might be used and it is often difficult to establish which element is most appropriate for a particular investigation. Each element type has its own attributes, although it is possible to make fine alterations to each element to ensure they fit accurately and are concentrated around specific areas of interest. Elements are either one, two or three-dimensional, two-dimensional elements are triangles or quadrilaterals (Figure 14.2), where as three-dimensional elements are normally cubes, tetrahedrals, pyramids or prisms (Figure 14.3).

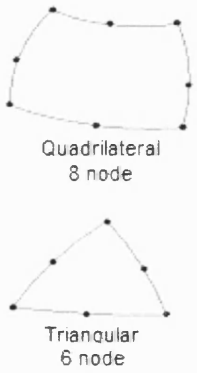

Figure 14.2: Two dimensional element shapes (Ansys, 1997).

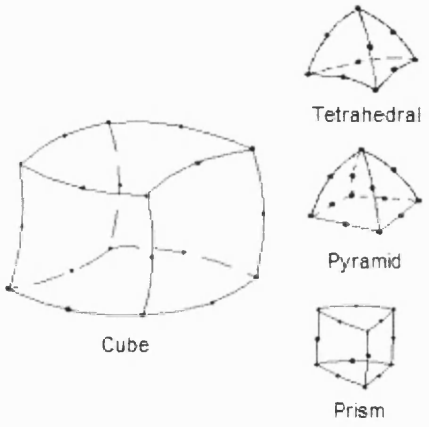

Figure 14.3: Three dimensional element shapes (Ansys, 1997).

The selected element type was the Tetrahedral, a three dimensional solid element consisting of 10 nodes (Figure 14.4). It is designed specifically for a structurally solid mass and is best suited to irregular shapes (as found in the back of the bat) and having point loads applied.

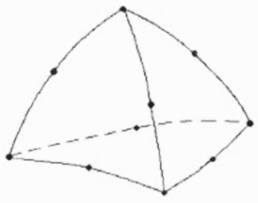

Figure 14.4: Element type employed (Ansys, 1997).

When each element is linked, it is referred to as meshed and the configuration of the elements that create the mesh can either be mapped or free. A free mesh has no restrictions in terms of element size and has no specific pattern of application (Ansys, 1997). Alternatively a mapped mesh has a regular pattern and is generally only applied to simple shapes.

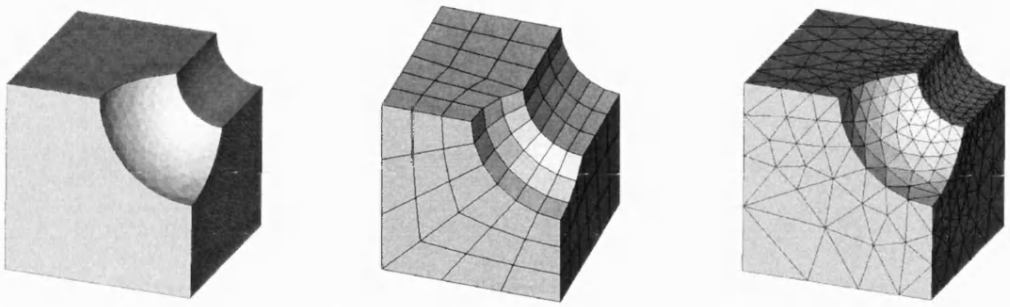

a) Not meshed. **b) Mapped meshing.** **c) Free meshing.**

Figure 14.5: An example of alternate mesh arrangements over a solid block (Ansys, 1997).

From Figure 14.5, there is a clear difference in the arrangement of the elements that create the mesh (b & c) over the unmeshed block (a). There is a linearity in the application of the elements using the mapped method unlike the free meshing where individually sized elements are selected to best cover the shape. In particular, the size of the elements are considerably smaller when they cover the finer details of the curved surfaces. As the bat is not a regular volume, a mapped mesh cannot be fitted accurately to the fine intricacies and deviations of the modelled bat.

Once this mesh type was chosen, the maximum element size was selected to fit the contours of the model, although free meshing allows the mesh size to be reduced. The element size may be selected between coarse (10) or fine (1) within the Ansys package depending on the requirements of the model (Figure 14.6). The coarser the mesh the less accurate the shape is modelled and the lower the accuracy. However, a fine mesh increases the accuracy, but with an increase in the calculation time, CPU power and memory space required. Once a general size was selected, element SmartSizing was employed, which is a free meshing process that calculates the optimum element size to fit the contours of the volume. This is achieved by repeatedly redefining the curvature and proximity of the element relative to the features of the designated structure (Ansys, 1997).

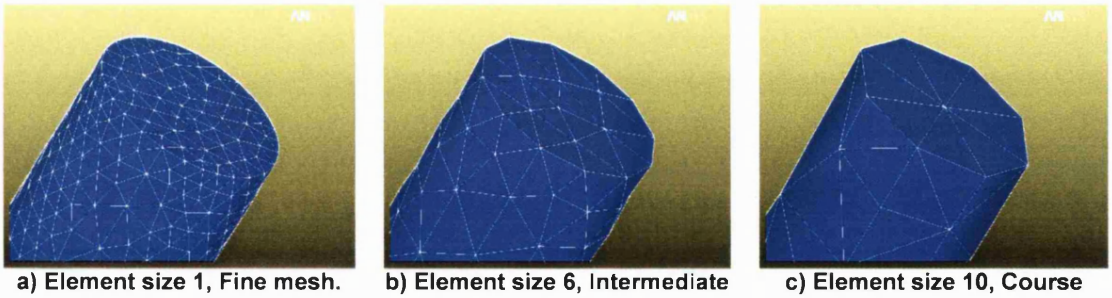

a) Element size 1, Fine mesh. b) Element size 6, Intermediate mesh. c) Element size 10, Course mesh.

Figure 14.6: The effect of different element sizes on shape definition.

Figure 14.6, demonstrates the influence that the element size has upon on the definition of the geometric shape. When element size 1 is applied to the end of the handle the cylindrical nature of the handle is maintained, however as the distance between the elements is increased the handle shape is distorted (element size 10). Using element size 10, the top of the handle is separated into 7 sections that cause the shape to have straight edges rather than a smooth curve. The handle meshed using element size six is also included to show that although the cylinder of the handle is not completely round, it does closely represent the desired shape. Due to the compatibility of this element size to the model shape and that the reductions in the computing time and memory space, this element size was considered to be most appropriate.

To establish the optimum element size, the GN cricket bat model was meshed using the ten different sizes. The handle was fixed at the end and the deflection was measured at the end of the bat following the application of a 2000Newtons static load, 0.16m from the free end.

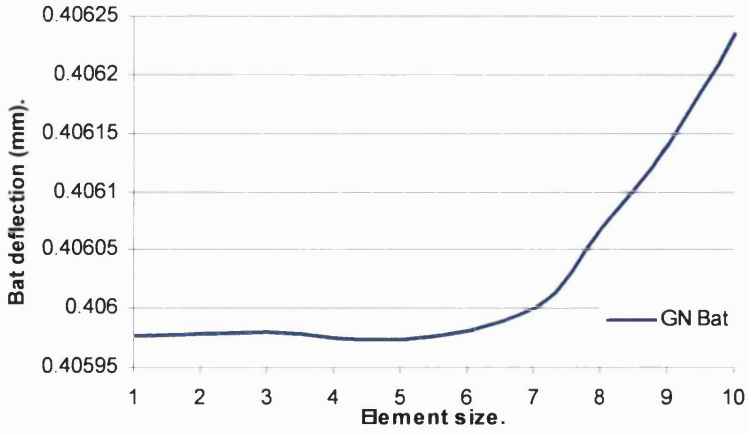

Figure 14.7: Effect of element size on bat calculated deflection.

From Figure 14.7 it can be seen that the measured deflection under the application of the load converges to a steady level when element size six or lower is used. Although there are slight changes in the measured deflection when the element size is further reduced, the difference between the size one and six is negligible when compared to the higher element sizes. Once the element size rises above size six the measured deflection is larger, due to the inability of the larger element sizes to accurately map the contours of the GN model.

Therefore, it was decided that element size six was most appropriate as this created an even distribution of larger elements over the main bat, while SmartSizing a tight mesh around the more complex shapes or the contact point between the handle and the blade. Using this element shape and size, only 11 of the total 28069 (0.04%) elements used violated the shape warnings. This indicated that these particular elements did not display equal angles around the whole of the shape. As the same mesh was applied to all models, the load could be applied at exactly the same location thus ensuring that there were no discrepancies in the testing procedure.

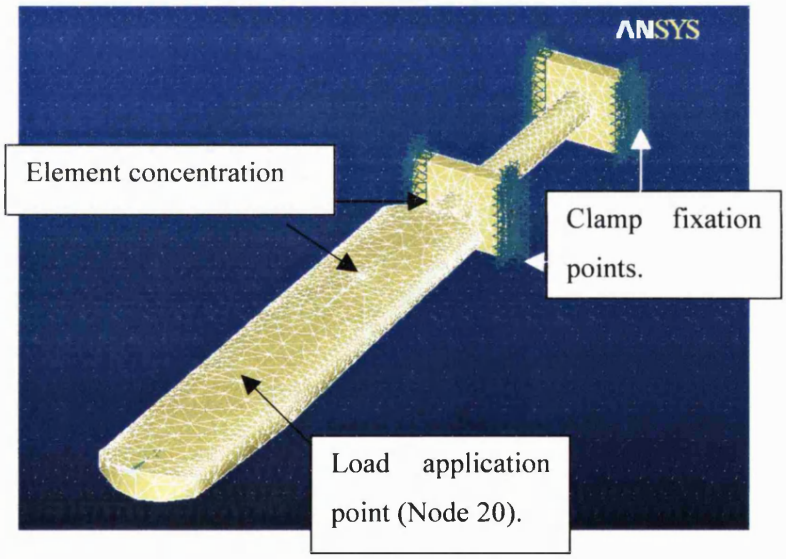

Figure 14.8: Meshed GN cricket bat.

Figure 14.8, illustrates the meshing and the fixation of the clamps (blue arrows). This figure shows the evenly distributed mesh over the bat face and the concentration of elements at the point where the handle and blade of the bat meet. This was important as this location experiences the greatest stress loads and is often the location of failure during use.

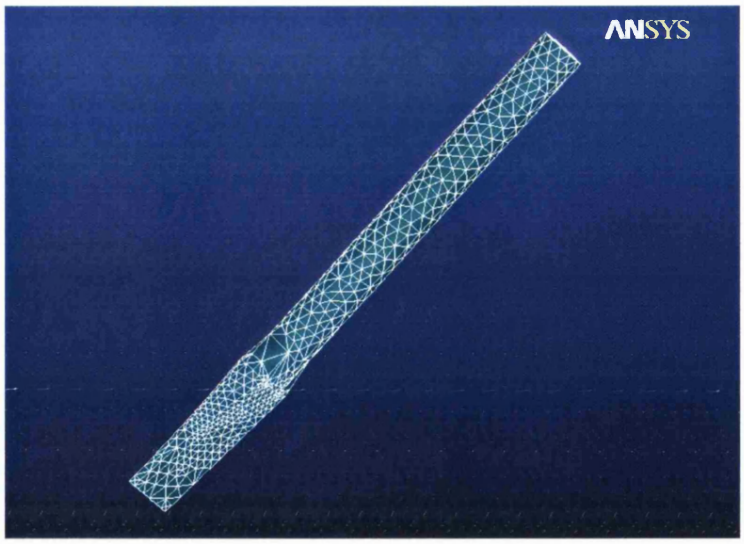

Figure 14.9: Fine mesh around the handle of the GN bat.

Figure 14.9 shows the fine mesh applied to the handle. As the handle was rigidly clamped, any movement between the clamps would be small, therefore a finer mesh would ensure any motion was accurately recorded.

14.3.2 Application of loads.

Although it was not possible to use dynamic loads due to the limitation of the Ansys FE package used, it was possible to apply a static point load. In chapter 9, a load/deflection relationship was established. Using these results and the measured deflections under dynamic impacts, it was possible to establish the magnitude of the equivalent static load required to achieve the same deflection (Figure 14.10).

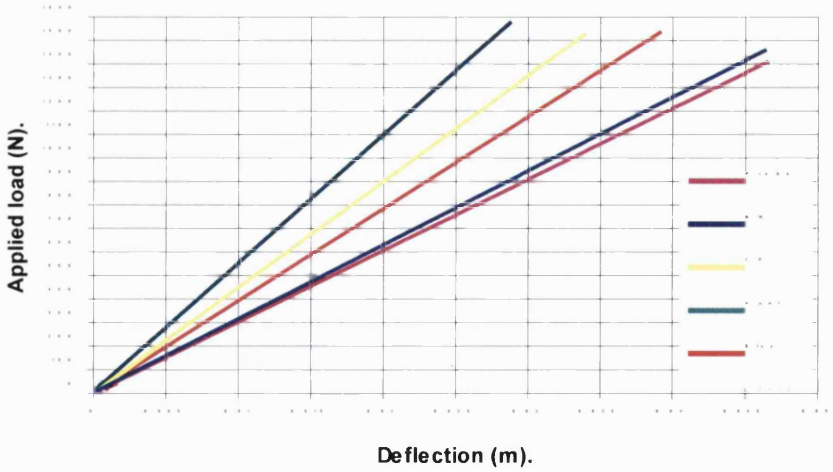

Figure 14.10: Factored load and deflection of five first class cricket bats.

14.3.3 Material properties.

Each material applied to the model was considered to behave linearly, elastically and isotropically with the properties given (Table 14.2). Although this is considered to be a limitation of this study, this process enabled average parameters to be entered.

Property	Willow	Cane handle	Aluminium clamp
Elastic modulus (GPa)	9.39	6.735	71.7
Poisson's ratio	0.37	0.17	0.33
Density (Kg/m³)	388.58	358.7	2700

Table 14.2: Assumed material properties for cricket bat components.

This data was obtained for the cricket bat analysis described in chapter 7, therefore they are representative material properties of cricket bats. The Poisson's ratio displayed in Table 14.2, were taken from an online materials research website (Doren, 2003). This study did not calculate this material property, as there is little deviation in the available data, unlike the published data regarding the material properties of cane and willow. The data for the aluminium clamps was also taken from the same materials research website (Doren, 2003). From Table 14.2, the elastic modulus of the willow is one third greater than the handle data that represents the construction type that includes three rubber inserts, which most cricket bats use. The calculated density between the willow and the cane are similar, although the density for the aluminium is considerable higher. The similarity between the cane and willow is due to the cellular structure of the two natural materials, which were found to have a similar porosity.

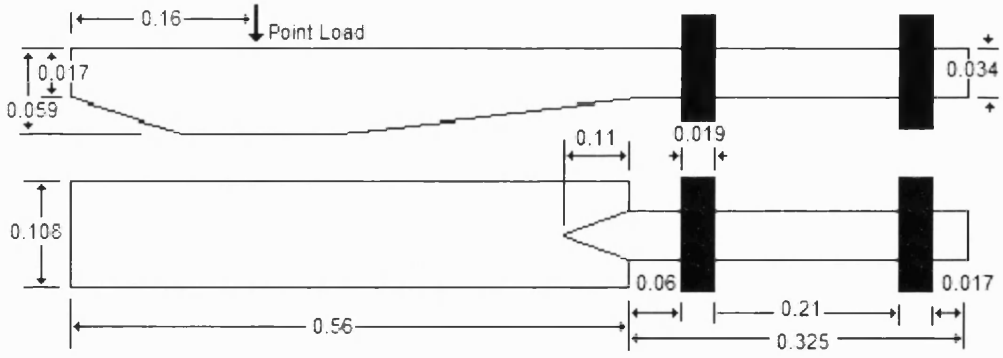

Figure 14.11: GN model bat dimensions and location of clamps and loading point.

The aim of this section was to investigate the influence of bat dimensions and it was reported in chapter 12, that the hand simulator created difficulties in establishing structural changes. Therefore, it was thought to be more beneficial to rigidly clamp the bats during the application of the load. The FE results could then be correlated directly with the experimental data to ensure an accurate model was produced before design alterations were made.

14.3.4 Model analysis.

Primarily, this study aimed to validate the models using deflection measurements to ensure it responded as found during the experimental analysis. Once the mesh was satisfactory and the clamps were fixed in position, a point load was applied. For the GN bat to deflect as during the dynamic study, a point load of 1440N was applied (part 14.3.2). As during the static deflection tests, the load was applied at the thickest section (0.16m from the free end) (Figure 14.12), as this location was considered the position of preferred impact.

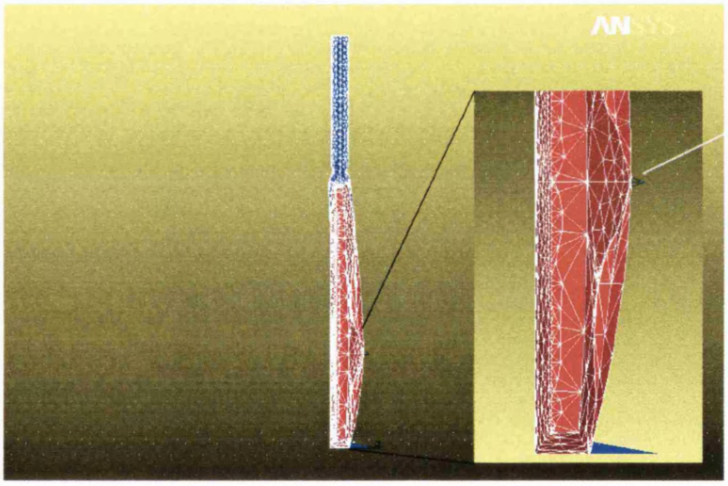

Figure 14.12: Location of applied load.

Once the load had been applied, it was possible to measure the resulting deflection of the bat.

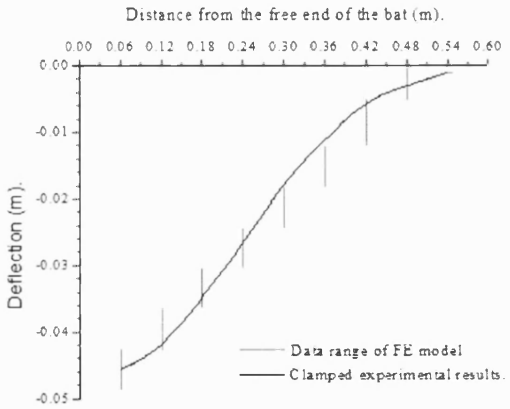

Figure 14.13: Deflection measurements of experimental and modelled GN bat.

Using Figure 14.13, it is clear that there is a distinct correlation between the FE model and the experimentally measured deflection calculations. Therefore, this method of model construction, meshing and application of loads can be considered to represent deflection during ball impacts.

To verify this model, the clamping locations were also altered (Figure 14.14) to ensure that the reported results (Figure 14.13) were not dependant upon this particular set up.

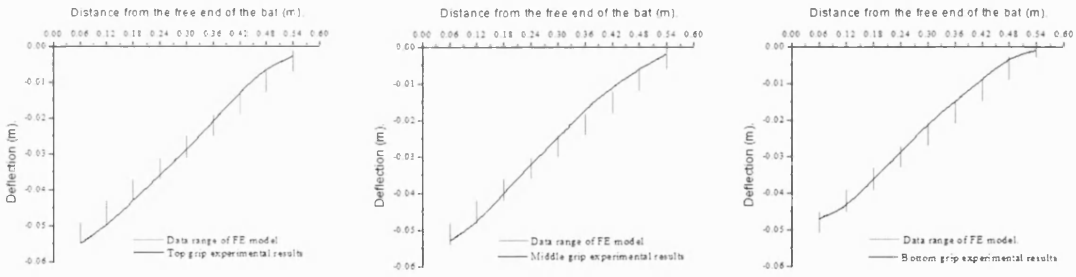

a) Top grip condition. b) Middle grip. c) Bottom grip.

Figure 14.14: Comparison of experimental and FE deflection with different clamping locations.

From these figures, it can be seen that there is distinct similarity in the deflection measurements for each of the locations (within 5%), thus verifying that the FE model matches the experimental results. Although, the differences in the top and middle grips suggest that the handle is slightly stiffer than it is during the experimental impacts. The over estimation of deflections by the FE model of the bottom grip condition is caused by the increased stiffness of the face of the bat that was not included in the FE model.

A modal analysis of the model was also performed using the same set up techniques while investigating the excited modes below 1kHz. Although a static load was applied it is possible to establish the modes of vibrations using a Block Lanczos method within the software. This method uses Lanczos algorithms, which calculate the fundamental and resulting harmonics. The frequencies are established using the dimensions and the material properties (density and stiffness), similar to the equations outlined in chapter 3. The FE results could then be compared with the experimental vibrational analysis under the same test conditions.

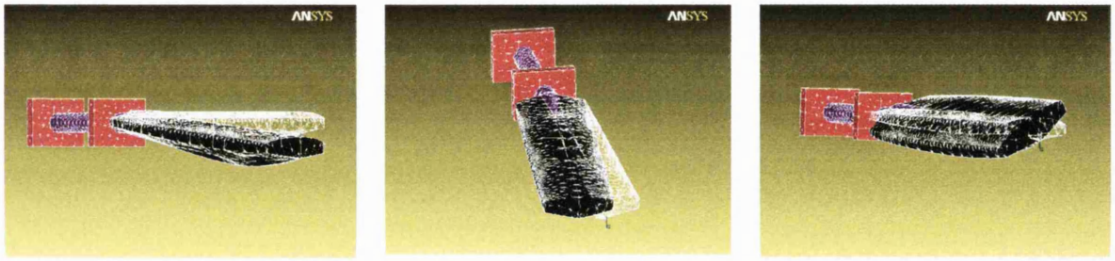

a) Mode 1 **b) Mode 2** **c) Mode 3**

Figure 14.15: Direction of excited modes.

Figure 14.15 illustrates the three excited modes below 1kHz, including the resting positions (hollow white elements) and the maximum deflection in the direction of that mode. The colours in the figures also represent the different materials present in the model. From Figure 14.15c, it can be seen that the third mode is a transverse wave rather than a longitudinal as for the first mode (Figure 14.15a) and a shear wave in the second mode (Figure 14.15b). Due to this transverse direction, the player would be unable to control this wave to the same extent as the other modes. Therefore the third mode is almost free to vibrate and would have a significant effect on off-centre impacts.

	Mode 1 (Hz)	**Mode 2 (Hz)**	**Mode 3 (Hz)**
Experimental	16	312	888
FE	15.51	346.82	881.61

Table 14.3: Comparison of modal frequencies from experimental and model investigations.

From Table 14.3, all three modal frequencies closely correlate to those from the experimental analysis (Chapter 12.2). Although it is interesting to note that the greatest deviation is found in the second mode and not the third mode as published by John & Li (2002).

Although it is noted that the direction of waves are different when investigated in three-dimensions, it is possible to establish the location of the nodes in the longitudinal direction as presented in Figure 14.16.

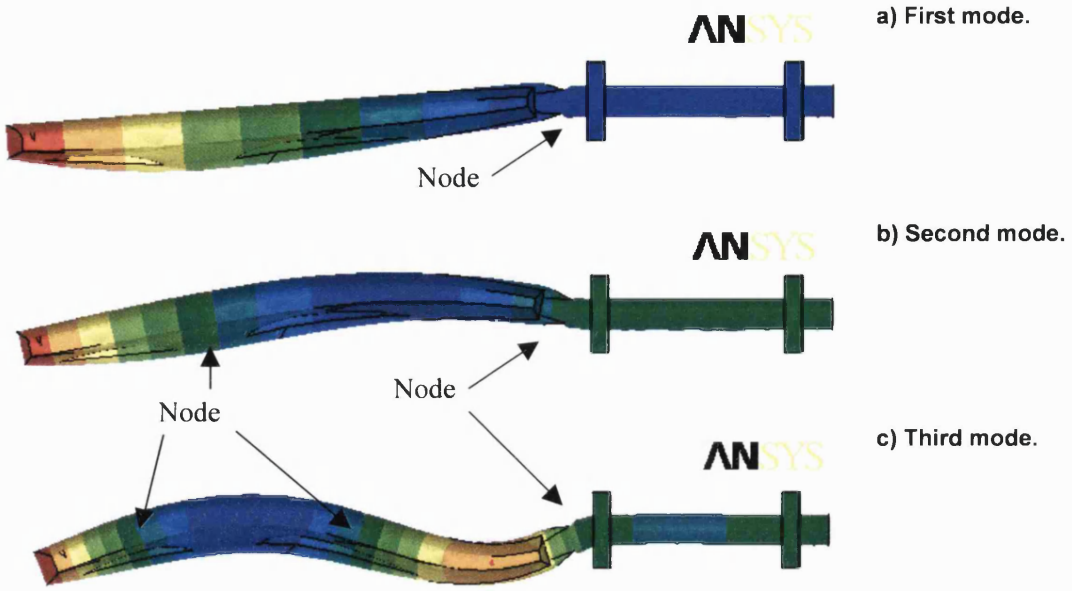

Figure 14.16: Location of nodes in the longitudinal direction.

The nodes have been indicated for each excited mode, although a node is at the location where the colour of the bat matches the rigid clamp as this is a position of zero displacement. From the chapter that investigated the effects of clamping on node location (Chapter 12.2), there is visually a close correlation with positions illustrated in Figure 14.16.

The location of the nodes can also be calculated by locating the position of zero displacement from the free end of the bat for each vibrational mode (Table 14.4).

	Mode 1	**Mode 2**	**Mode 3**
Experimental	0.6	0.18, 0.6	0.15, 0.33, 0.6
FE model	0.57	0.195, 0.59	0.13, 0.31, 0.6

Table 14.4: Location of nodes for experimental and FE model bat (in metres from free end).

From Table 14.4, there is a close relationship (within 0.03m) between the experimental and FE established node locations. The location of the nodes are important in sport equipment analysis, thus any improvements in the bat must include the ideal placement of the nodes along the length of the bat.

To establish how repeatable this FE model is, another of the experimentally tested bats was considered. The Probe bat was selected as it had a distinct spine along the length of the back of the blade and it continually performed well during the experimental testing.

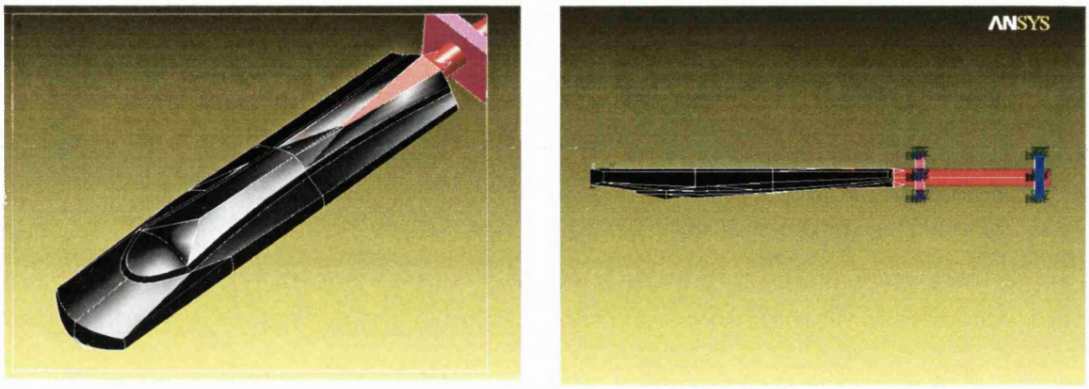

a, Contours of the back of the Probe bat. **b, Horizontal profile of the Probe bat.**

Figure 14.17: Images of the modelled Probe bat.

The contours and profile of the Probe bat are shown in Figure 14.17 a & b. Different colours are used to distinguish between the blade, handle and clamps.

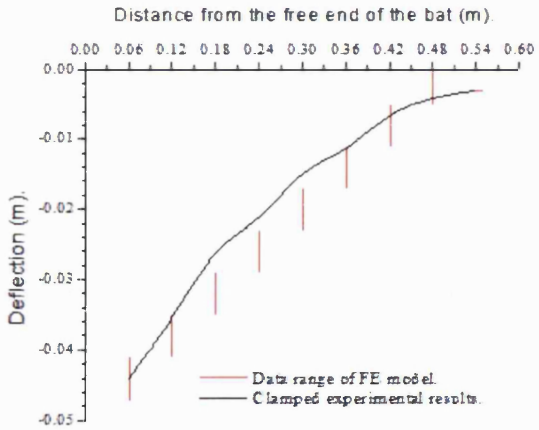

Figure 14.18: Comparison of the experimental and FE Probe bat.

	Mode 1 (Hz)	Mode 2 (Hz)	Mode 3 (Hz)
Experimental	14	312	800
FE (Probe bat)	11.633	313.11	874.76

Table 14.5: Comparison of experimental and FE vibrational responses of the Probe bat.

As can be seen from comparing the results in Figure 14.18 and Table 14.5, there is a close correlation between the experimental and FE results. The experimental deflections fall close to

the FE model ranges, although the modal frequencies are not as close as with the GN model. However, they closely represent the actual behaviour during vibration analysis. It can be noticed that the larger deflection of the FE model displayed in Figure 14.18 is reflected in the lower fundamental frequency shown in Table 14.5 as this mode occurs in this direction.

14.3.5 Potential for structural alterations.

Since there was a close comparison of results between the FE model and the experimental results for the GN bat, this was used to establish the consequence of making dimension changes. The GN bat also has advantages as its design includes scoops and their effectiveness could be established. Using the GN model, modifications were made to the following variables, Blade Length (BL), Blade Width (BW), Blade Thickness (BT), Ridge Height (RH) and Scoop length, width and depth (SD).

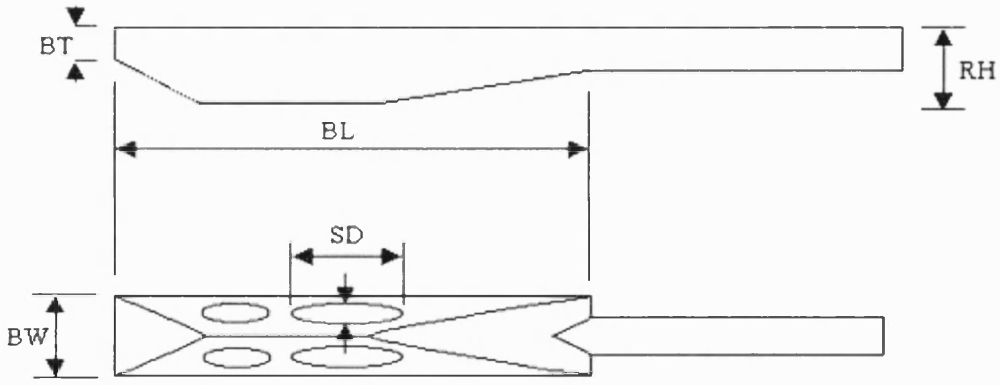

Figure 14.19: Investigated structural variables.

The limits for the dimensions used were either dictated by the laws of the game (ECB 2000) or published in current commercial catalogues (Slazenger, Gray-Nicolls, Fearnly & Kookaburra) or from Grant & Nixon (1996) and are shown in Table 14.6. The minimum and maximum scoop length are not specified, thus percentage alterations in the size of the scoops were applied. For example, the width and depth of the scoops were increased in proportion to the percentage increase in the length. However, the maximum size of the top scoop could only increased by 30% before it infringed on the lower scoop. Any further alterations would therefore have radically changed the design, thus possibly introducing errors. As the load was applied at the thickest section (ie. between the two scoops) changes were only made to the larger top scoops as they would influence the deflection.

Variable	Minimum dimension.	Current.	Maximum.
BL	0.443 (-21%)	0.563	0.603 (+7%)
BW	0.088 (-18%)	0.108	0.108
BT	0.004 bottom, 0.010 middle, 0.004 top (-78%)	0.018, 0.024, 0.018	0.032, 0.038, 0.032 (+78%)
BH	0.006 bottom, 0.016 middle, 0.012 top (-83%)	0.036, 0.064, 0.049	0.072, 0.124, 0.098 (+50%)
SD	0 long, 0 wide, 0 deep (-100%)	0.0185, 0.026, 0.010	0.0295, 0.0416, 0.016 (+40%)

Table 14.6: Minimum, current and maximum dimensions (m) of structural changes.

As the construction of the model ensured that the bat's ridge was separate from the scoop shapes, it was possible to alter these dimensions independently. In other research, the ridge height was found to have the greatest effect on the post impact responses of the bat (Grant, 1996). When the depth of the ridges was reduced to a minimum thickness (6mm), the scoops became the sections that protruded from the back of the bat (Figure 14.20).

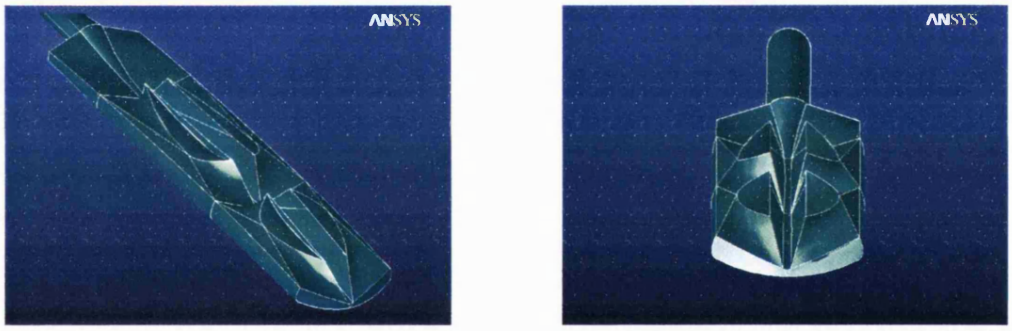

Figure 14.20: Protruding scoops from the back of the bat as the ridge was dramatically reduced.

Since this investigation has sought to establish the effects of various factors these sections were maintained. However, the scoops cause the mass of the bat to be maintained despite the central spine of the bat being almost removed.

Following the dimension changes, it was possible to determine the changes to the mass and location of the centre of mass. The centre of mass can be used as a measure of the balance and comfort experienced when lifting the bat in readiness for an impact. The peak deflection and modal frequencies were also recorded as they are related to the post impact ball velocity and player comfort.

14.3.6 Results.

Each of the following figures highlights how the vibrational frequencies, deflection, mass and positions of the centre of mass of the GN bat can be altered with changes to the dimensions (as a percentage) within the boundaries set out in Table 14.6.

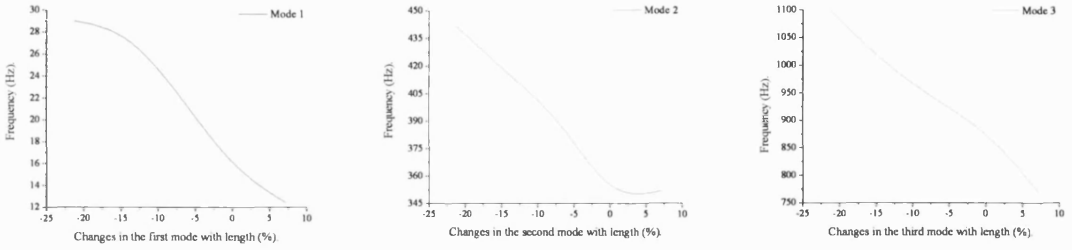

a) First mode **b) Second mode** **c) Third mode**

Figure 14.21: Variation in measured bat vibration with changes to the length of the blade.

In Figure 14.21, it is clear that as the length of the bat is decreased the measured vibrational frequency increases. When the length of the blade of the bat is reduced by 15% (from 563 to 483mm), the third mode is raised above 1kHz. The first and second modes do not rise at an equal rate as the third mode of vibration. It was found that the first and second modes reached peaks of 29 and 442Hz from their original positions of 15.5 and 346Hz respectively. When the length of the bat was decreased, it was found that the frequency of the first mode continued to decline to 12.4Hz, while the second mode maintained a frequency around 350Hz. The third mode continues to decline as the length of the bat is decreased.

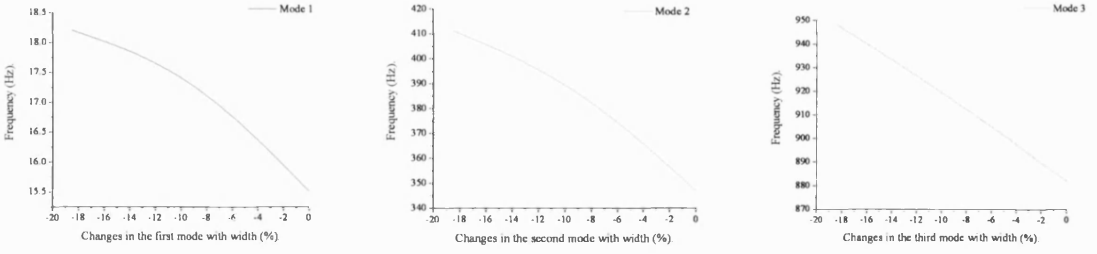

a) First mode **b) Second mode** **c) Third mode**

Figure 14.22: Variation in measured bat vibrations with changes to the width of the bat.

Figure 14.22 illustrates how the vibrational frequency alters following changes to the width of the bat. A reduction in width has limited influence on the measured vibration, as there is only a slight increase in the measured frequency. The first mode displays the least variation in frequency following dimensional alterations, decreasing by just 2.7Hz. However, if the bat's width were decreased further the vibrational frequency of the third mode would be raised above 1kHz.

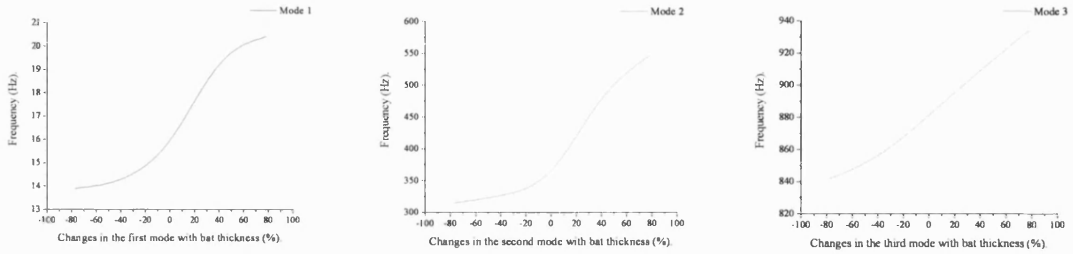

a) First mode **b) Second mode** **c) Third mode**

Figure 14.23: Variation in measured bat vibrations with changes to the thickness of the blade.

From this figure, it can be seen that each mode follows a similar pattern after changes are made to the thickness of the bat. The frequencies tend to plateau at either extreme of the altered dimensions and the greatest rate of change occurs around the current dimensions (0%) of the commercially available cricket bat. It was found that if the thickness of the blade was increased by 40%, the 1st mode was be increased by 4Hz, the 2nd by 145Hz and the 3rd mode by 27 Hz. The third mode could rise above 1kHz if the blade thickness was further expanded. However, in reality a player would not be able to use it effectively and therefore there would be no advantage in attempting this modification and reaching this frequency.

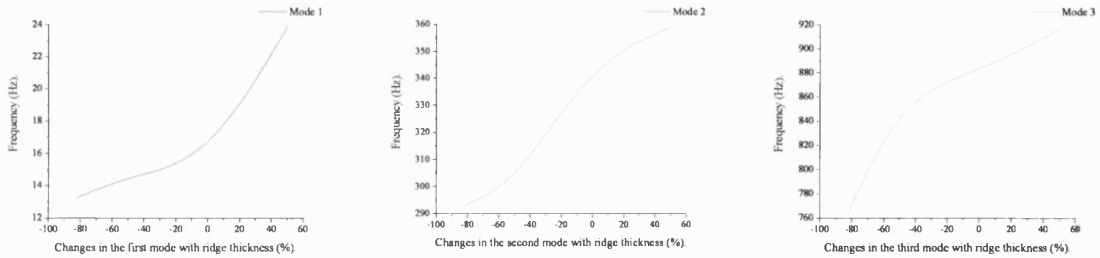

a) First mode **b) Second mode** **c) Third mode**

Figure 14.24: Effect on bat frequencies following changes to the bat ridge thickness.

Figure 14.24 displays how the frequencies of the first three modes change as the size of the ridge along the back of the bat is altered. The calculated modes show the similar changes in the measured frequency around the original position of the bat as shown in Figure 14.23. This shape is more apparent in the results of the first (a) and third modes (c). The difference in frequency at the extremes of the changes for the first mode was less than 10.6Hz, 65.8Hz for the second mode and 154Hz for the third mode.

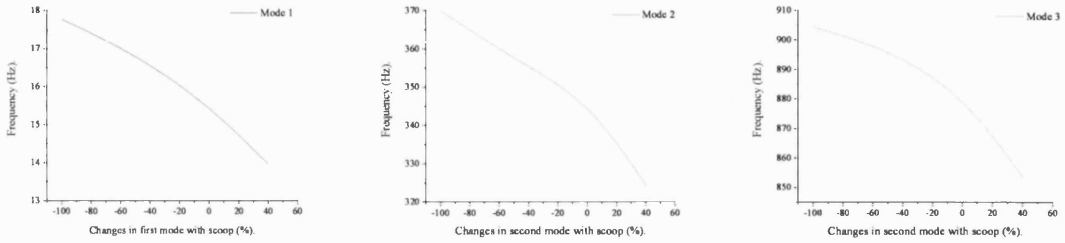

a) First mode **b) Second mode** **c) Third mode**

Figure 14.25: Variation in measured bat vibrations with changes to the size of the scoops.

There is very little change in the frequency of the excited modes following the dimensional changes made to the size of the scoops (Figure 14.25). However, the slight changes that are visible indicate that the frequencies are increased when the scoops are reduced, and lowered when they are increased in size. It can be considered that when the scoops are completely removed (-100%), the bat now represents a more traditional design.

It was also possible to calculate the alterations to the mass of the bat following the changes in dimensions. The following figures examined these changes and therefore it can be established whether they would be advantageous to a player as the mass affects the control of the bat.

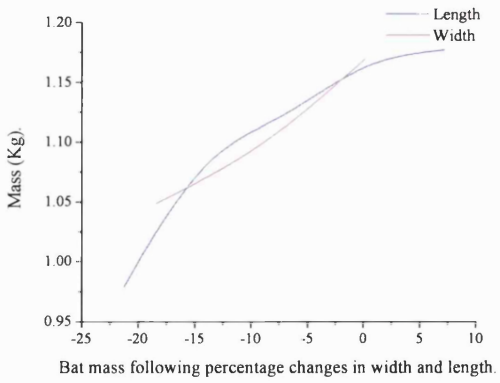

Figure 14.26: Influence of size on the calculated mass of the bat.

It can be seen from Figure 14.26 that as expected, the mass of the bat decreases as the width and length of the bat are reduced. It was found that when the width and length of the bat are reduced by 15%, the mass is reduced by 10% and 13% respectively.

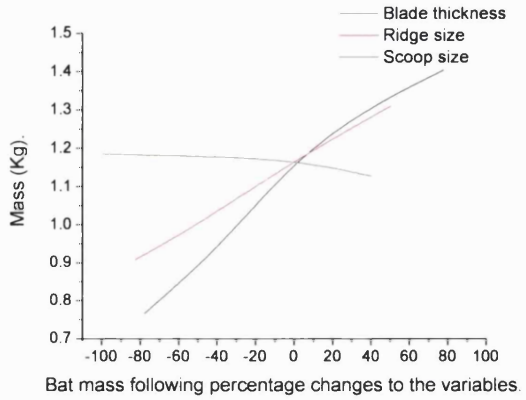

Figure 14.27: Influence of structural changes on the calculated mass of the bat.

From Figure 14.27, the scoop size has a negative relationship, while the ridge size and blade thickness have a positive relationship with changes in the mass. Once the scoops had been reduced by more than 40%, they have little influence on the mass, although they only decrease the mass by 0.04Kg when they are increased by 40%. The mass is most affected by changes to the blade thickness rather than the other two variables displayed. For example, a reduction in ridge size by 80% reduces the mass by 0.251Kg, however when the blade thickness is decreased by 80% the mass is diminished by 0.414Kg.

As discussed earlier, an important factor in the analysis of bat performance is the deflection following ball impact, thus the peak deflection for each of the bat conditions was calculated following the application of the static load.

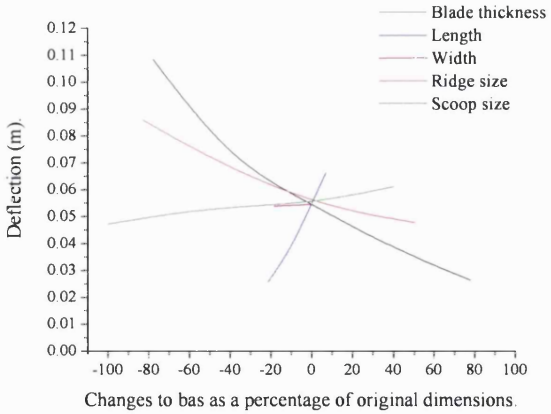

Figure 14.28: Effect of changes in bat dimensions on measured deflection.

Alterations to the width of the bat had little effect on the deflection of the bat, while the size of the scoops only influenced the deflection measurements when they had been increased or decreased by 40%. The thickness of the blade has the biggest effect on the deflection as a reduction of 80% increases the deflection by 50% and a thickness increase by 80% reduces the deflection by 49%. This also shown an almost linear relationship present between these two variables. The changes to the ridge size do not effect the deflection as much as following alterations to the thickness. As a ridge reduction of 50% was found to increase the deflection by 24%, although a ridge increase of 50% decreases the deflection by 12.5%. Finally, when the length of the blade was shortened, the deflection was reduced in a linear pattern. The magnitude of this result was found to be the greatest when compared to the other variables displayed.

The position of the centre of mass (COM) was also identified following changes to the dimensions of the bat. Each COM has been allocated a letter and number, which indicates the type and dimensions set for each alteration as a percentage of the original GN bat. For example T=+78, denotes the COM position when the blade thickness was increased by 78%. The current dimensions of the GN bat are also included. It was only necessary to plot these diagrams in two dimensions due to the symmetrical nature of the bat.

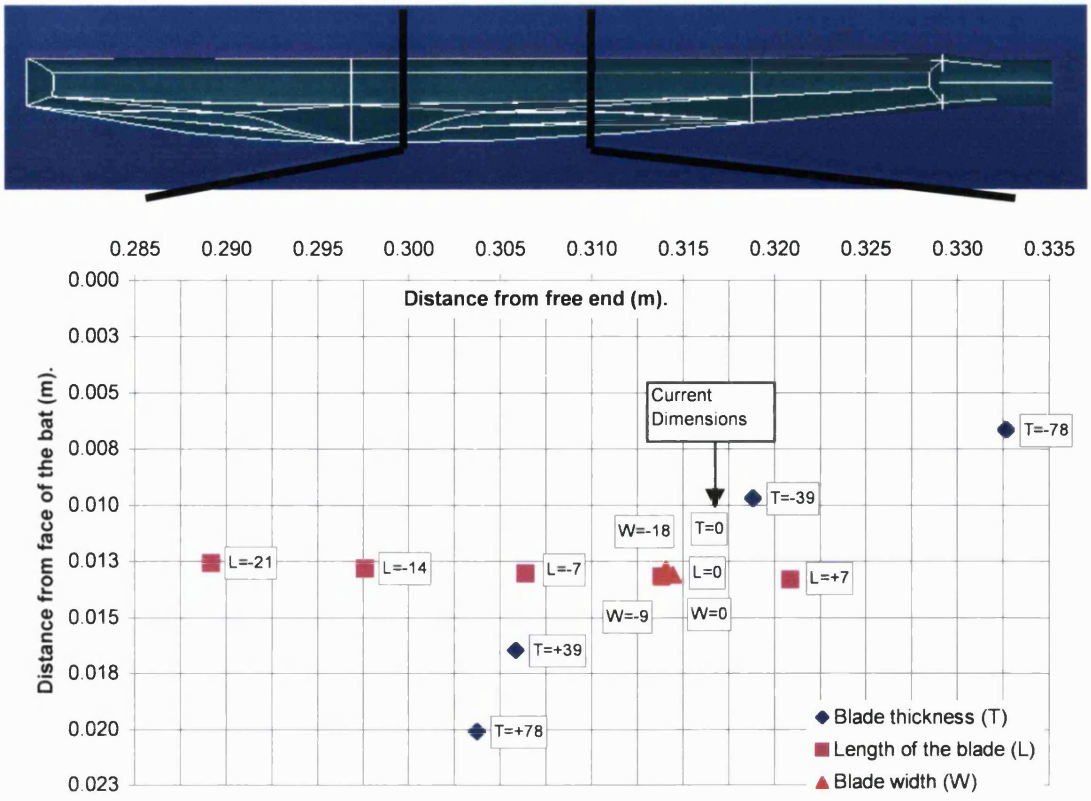

Figure 14.29: Location of the centre of mass with alterations in bat dimensions.

Structural alterations made in this study (which are at the extremes stated in the laws of cricket) have little effect on the location of the COM, as the COM remains within a 0.05m section (between 0.285 to 0.335m from the free end). It is the alterations to the length and the thickness of the blade that move the COM to the extremes of this area. As the thickness of the blade is increased, the COM moves further away from the face of the bat and closer to the free end. Finally, changes to the width of the bat had little influence on the movement of the COM.

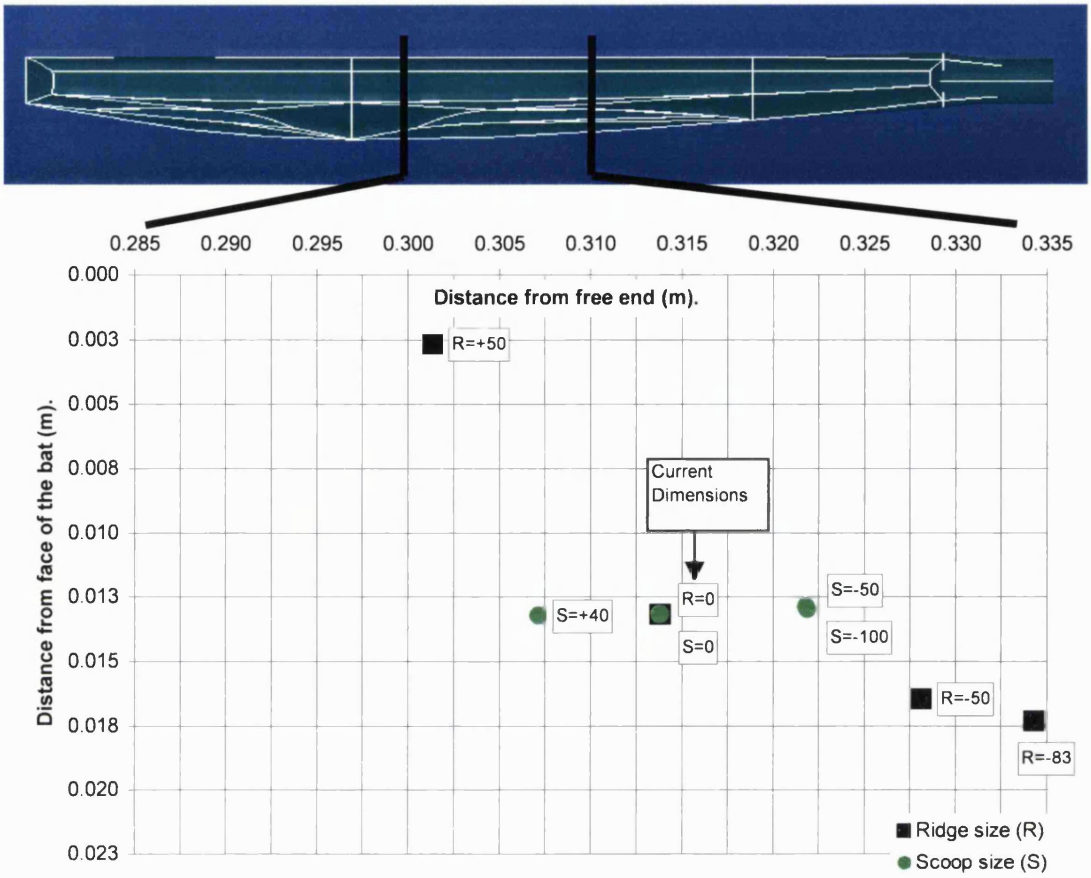

Figure 14.30: Location of the centre of mass with alterations in ridge and scoop size.

Figure 14.30 shows the movement of the COM following alterations to the ridge and scoop size. When the ridge at the back of the bat is increased, the COM moves closer to the face. However, the sizes of the scoops have little influence on the location of the COM.

14.3.7 Discussion.

FE modelling establishes the effects of geometric alterations on structural responses. This chapter established whether structural dimensions influenced the post load responses of a cricket bat. A model of the GN bat was used due its comparability to the experimental results. The GN bat has scoops along the back of the blade, thus requiring more key points than the other bats to ensure that each surface was closely matched to the actual dimensions of the

original bat. This created a more complex model and thus increased the comparability between the model and the experimental results. The scoops also offered the greatest scope for structural alterations, as relatively small alterations could be made without significantly affecting the original dimensions of the bat.

Primarily, this study investigated the influence of the structural changes on the frequency of the three vibrational modes excited below 1kHz. Recording three excited modes below 1kHz correlated with the experimental work and previous studies that investigated cricket bat responses. The length of the blade was modified as this would have a major influence on the measured frequency of the longitudinal vibrations, although no previous publication had investigated this adaptation. As the length was decreased, the frequency of the vibration was increased for each of the three modes. When the blade was shortened by 80mm (from 563-483mm) the third mode was raised above 1kHz. An improvement in comfort would be perceived as a vibration above 1kHz cannot be felt (Grant & Nixon, 1996). Grant & Paisley (1997) reported that by increasing the blade stiffness, the third mode could be raised above 1kHz, although this was achieved through changes to the material properties rather than the structural design as in this study. The frequency of vibration of a beam is dependant upon its length from the clamp and the magnitude of the deflection (chapter 3). Following a reduction in length, the frequency is raised as the length of the wave is reduced and the vibration can oscillate along the length of the structure in a time shorter period. With a reduction in the length of the implement, the deflection is also reduced, which also raises the vibrational frequencies.

The changes to the length had the greatest influence on the deflection when compared to the other variables as a relatively small alteration is associated with a large change in the calculated bat deflection. A stiffer bat will also dampen out the subsequent vibrations quicker and thus exhibit a greater Q value. Reducing the deflection would maximise the potential to propel the ball further as less energy is lost in subsequent bat deflection and vibrations. Therefore, not only are improvements in comfort achieved, but the ball is also seen to travel further.

The changes in the length had a considerable influence on the mass of the bat, mainly due to the amount of material that is altered, when compared to the other variables. However, if the other variables were altered to the same extent the bat would become impractical to use. This

demonstrates how major alterations to the mass can be made following length changes, without altering the integrity of the structure to withstand impacts. As the length of the bat was reduced, the COM was moved towards the hands. This finding was mainly due to the portion of the bat between the hands and the handle being reduced. The location of the COM is associated with the rotational inertia and the position of the COP (chapter 3). Using Equation 3.6, it was calculated that following a reduction in length of 80mm, the COP would drop by 1.4mm from its current position. This shows that alterations to the length of the bat have limited influence on the location of the COM and subsequent COP location. However, if a larger section was removed from the bottom of the bat, the alterations to these factors may be more identifiable. If the position of preferred impact (as it is now) was much closer to the free end of the bat, the cricket bat would have a similar shape to a baseball bat and might also have a COP position further from the hands. Therefore, the player would be able to take advantage of the increased rotational velocity at this position, while experiencing reduced hand loads. However this design would not necessarily be advantageous, as the thickest section of the bat is currently raised from the bottom to impact a bouncing ball rather than impacting close to the end as during baseball. Therefore, it is unlikely that a player would actually impact this new lower COP position and even if they did, there would be a loss in the control and manoeuvrability.

It was not possible to make radical alterations to the width (maximum 18.5%) due to the restrictions of the laws of the game. The small changes that were made had limited influence on the results. A slight increase in the measured vibrational frequency was recorded and it was the third mode that increased the most (67Hz) from its original position. This finding is caused by the direction of the wave, as a reduction in the width enables the bat to vibrate more rapidly in the transverse direction. The alterations in the width had little influence on the measured deflection, therefore the changes in calculated frequency are purely due to the changes in dimensions and mass (although this was also relatively small). Drastic alterations to the width would be detrimental to performance due to difficulty in contacting the bat correctly, thus it is more advantageous to maintain the width to maximise the striking area.

When the thickness was enlarged by 40% from its current dimensions, the excited modes sharply increased when compared to other thickness changes. The second mode was found to increase by 145Hz following a 40% increase in blade thickness, which is caused by the direction of the wave. The second mode is a shear wave, thus if the blade thickness is increased, the stiffness in this direction will also increase, thus reducing the deflection and

increasing the frequency. As the blade thickness was increased, the COM moved away from the face and towards the free end of the bat. Moving the COM away from the face will improve the comfort and balance when lifting the bat in readiness for a shot. The COM moved closer to the free end with an increase in the thickness as the blade is not symmetrical in the longitudinal direction.

As the ridge size was increased the calculated frequencies of the three excited modes increased, which was associated with an increase in stiffness displayed as a reduction in the deflection (Figure 14.28). The third mode displayed the greatest alteration in the measured frequency as an increase in the size of the ridge decreases the ability of the third mode to rotate, increasing the vibrational frequency in this direction. Although there is not a considerable increase in this vibrational mode, any reduction in bat rotation during the impact period would be advantageous. A plateau in the recorded frequencies of the first and third mode were recorded until the ridge was reduced further than 40%, therefore this additional ridge height has little effect on the bat vibration. A 40% reduction in ridge height reduced the mass by 169grams, which would help with manoeuvrability and might increase swing velocity. As the deflection of the bat is not significantly affected by this reduction in ridge size, the post impact ball velocity would be increased. The COM also moved towards the hands (2mm), which is advantageous to a player as the bat is perceived to be lighter when it is lifted in preparation for impact. However, this movement is relatively insignificant when compared to the dimensions of the bat and therefore may not be noticed.

When the scoops were removed, the deflection was decreased as found during experimental analysis, when the bats with scoops were compared to those without. Although there will be differences in the construction and quality of the wood that will affect the experimental results, the trend of excluding scoops and decreasing deflection is comparable. Deflection reduction with the exclusion of scoops in the bat was also found by Grant & Nixon (1996). However, it should be noted that the relative changes that scoops make on the vibration, deflection, mass and COM position are smaller than any of the other variables investigated.

The structural alterations all raised the frequency of the fundamental mode, which could move the vibrational frequency away from the possibility of resonance, thus improving comfort. Using the data from the experimental impact tests, it was possible to calculate the mean impact

frequency of a ball at impact. Twenty force traces of the impact period between the ball and a load cell were analysed and a mean impact frequency of the ball of 18.2Hz was calculated. This finding highlights the frequency that the ball transfers into the bat during impact, thus if the bat naturally vibrates at or close to this frequency, resonance will occur. This will lead to an increase in the amplitude of the fundamental frequency and it would also reduce the energy transferred to the ball, decreasing the post impact ball velocity. When the dimensions of the bat were altered (especially reducing the length) the bat,s fundamental frequency was shifted away from the frequency of the ball, thus avoiding the possibility of bat resonance following impact.

14.4 Suggestions for improvements in bat performance.

A player can experience an improvement in feel and comfort during impact by reducing the bat length by 80mm (15%) from 563mm to 483mm as the third mode would be raised over 1kHz and outside a human's excitation spectrum. With a reduction in the length of the blade, the mass was also decreased by 0.137Kg. In tennis racket investigations, a lighter racket can improve comfort and control (Brody, 1987). A bat would also enable a player to swing it faster and make up for the loss of inertia following the reduction in mass. The deflection of the bat during the application of a load will be reduced by 2mm, thus reducing energy loss through this means. Therefore, it is considered that a reduction in the length of the bat would lead to an overall improvement in performance.

To maintain the current weight, which is preferred by players, it would be most beneficial to increase the edge thickness as this had the greatest effect on the modal frequencies and reductions in deflection. Therefore, to make up the 0.1374Kg lost through reducing the length, the thickness of the blade should be increased by 22.17%. The top scoops have also been removed to further improve performance due to the measured increase in deflection and the findings of previous literature (eg. Grant & Nixon, 1996).

14.4.1 Changes in bat dimensions.

Figure 14.31 illustrates the shape of the GN bat prior to structural alterations (original) and Figure 14.32 displays the modified GN bat shape.

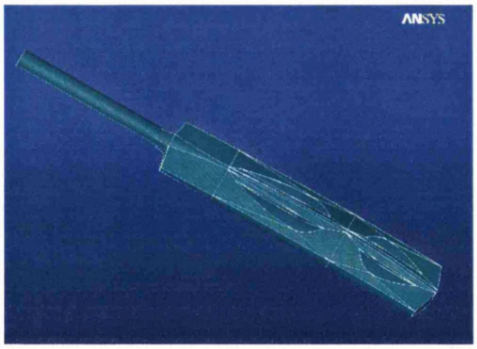

Figure 14.31: Original GN shape.

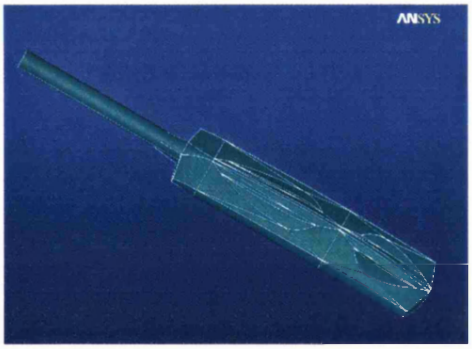

Figure 14.32: Modified GN shape.

Figure 14.32 shows how 80% of the length has been removed from below the handle in an attempt to keep the position of preferred impact at a similar distance from the bottom of the bat. The thicker edges of the new shape are also visible, especially at the position of preferred impact (0.16m from the free end).

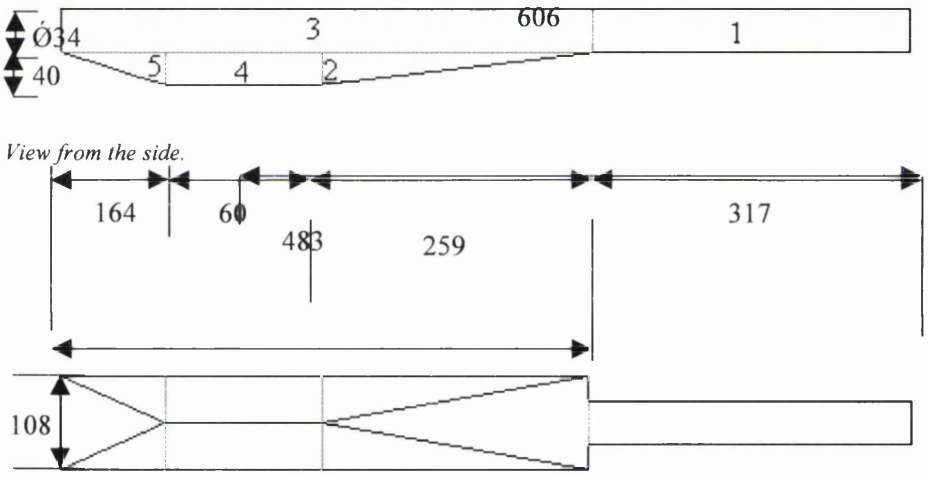

Figure 14.33: Simplified GN bat shape with numbered portions and new dimensions (mm).

Figure 14.33 illustrates the dimensions of the modified GN bat to aid the understanding of the location of the specific sweet spots. This figure also includes the five portions that make up the basic shape of the bat, which are used in the COP calculations (Chapter 3).

14.4.2 Calculation of performance.

Following the modifications to the bat, it is necessary to establish their influence on performance and player comfort. This section will outline the four main variables that have

been investigated during this thesis and apply them to the modified GN bat. Each variable will be calculated and then discussed to establish how each variable would influence the responses of the bat following impact.

14.4.2.1 Moment of inertia.

As reported in chapter 8, the moment of inertia is related to the feel of the implement during use. Lower moments enable the swing velocity to be increased thus maximising the post impact ball velocity. As it is not possible to experimentally calculate the moment of inertia of the modified GN bat, a mathematical equation outlined by Kreighbaum *et al.* (1996) will be employed (Equation 14.1).

$$I = mk^2$$

Equation 14.1

where, m is the mass, k is the radius of gyration and I indicates the rotational inertia.

As it is possible to experimentally measure the moment of inertia of the original GN bat (chapter 8) it is also possible to validate this equation. Using Ansys, it is possible to measure the radius of gyration (0.606m) and the mass (1.139Kg) of the modified GN bat.

Bat	**Original GN**	**Modified GN**
Experimental moment of inertia (Kg/m^2)	0.475	N/A
Calculated moment of inertia (Kg/m^2)	0.4736	0.4101

Table 14.7: Calculation of moments of inertia.

Primarily, it can be concluded that this equation can be applied to cricket bats as there are distinct similarities between the experimentally defined and calculated values of the original GN bat. Therefore, applying this equation to establish the moment of inertia of the modified GN bat is a viable method. From Table 14.7, the modified GN bat has a lower moment of inertia value by $0.063Kg/m^2$ compared to the original GN bat.

14.4.2.2 Deflection and stiffness.

As stated in section 11.2, the deflection and stiffness of the bat has a considerable influence on the measured COR of a cricket bat. By applying the load as before the deflection of the modified GN bat was measured and the associated stiffness was calculated.

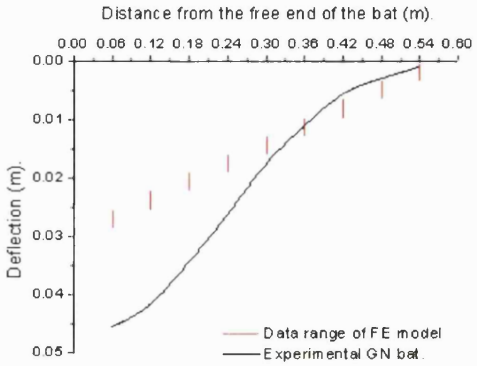

Figure 14.34: Deflection 0.06m from the free end of the modified GN bat.

Figure 14.34 shows that the peak deflection of the modified GN bat is 0.028m following the application of 1440N.

The stiffness of both GN bats (original and new) was also calculated along the length of the blade (Figure 14.35a and b).

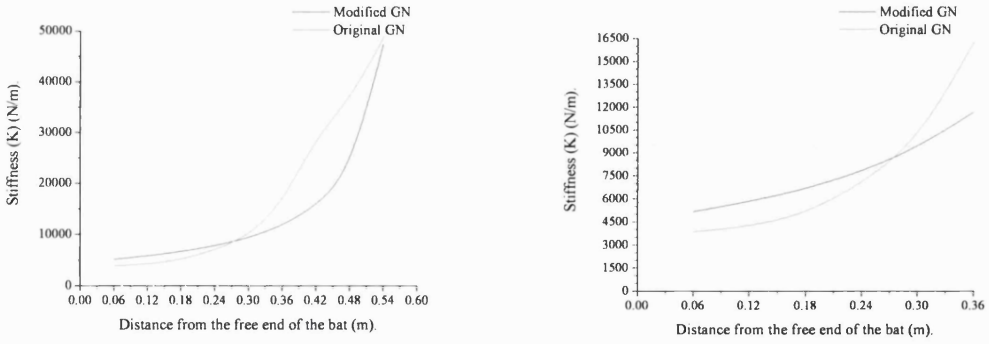

a, Comparison of bat stiffness. **b, Magnification of stiffness results.**

Figure 14.35: Experimental and theoretical stiffness of modified and original GN bats.

From Figure 14.35a, it is seen that the modified GN bat is stiffer than the original bat until approximately 0.3m from the free end, where the stiffness of the original bat increases considerably. The stiffness of the lower portion of the bat (below 0.36m) is of greatest interest

as this region is likely to be impacted regularly thus characterising the bats performance. Figure 14.35b shows that the stiffness of the modified GN bat is from 5174 to 11680N/m, where as the stiffness of the original bat ranges between 3862 and 16309N/m. The modified GN bat records the suggested optimum stiffness (section 11.2) of 6850N/m, 0.20m from the free end.

14.4.2.3 Vibrational frequencies.

The vibrational frequencies affect player comfort and so it was the aim of the modifications to increase the third mode above the excitation spectrum (1kHz) so the player would not perceive this mode. This would lead to improved comfort by eliminating some of the painful stinging associated with the higher frequencies of the excited modal vibrations.

	Mode 1 (Hz)	**Mode 2 (Hz)**	**Mode 3 (Hz)**
Original GN	15.51	346.82	881.61
Modified GN	31.272	623.43	1025.1
Difference	*15.762*	*276.61*	*143.49*

Table 14.8: Comparison of the excited modal frequencies.

From Table 14.8, there is a considerable difference between the measured vibrational frequencies of the bats. The first and second modes have doubled or almost doubled following the changes to the dimensions of the bat, while the third mode has been raised above 1kHz.

14.4.2.4 Nodal locations.

The nodes of vibration in the longitudinal direction have also been established. It is these locations that a player would wish to impact to minimise or not excite that associated mode.

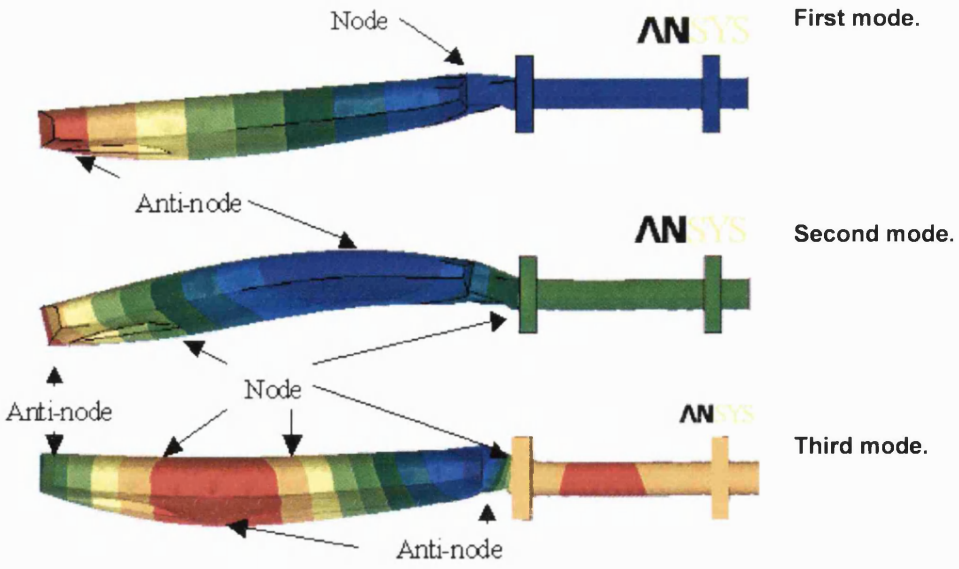

Figure 14.36: Modes in longitudinal direction.

Figure 14.36 shows the shape of the first three modes in the longitudinal direction. The location of the nodes have been indicated and they occur at the location where the colour matches the rigid clamps. The anti-nodes have also been included due to their association with player discomfort. An anti-node occurs at the thickest position of the bat during the third mode and a node is also found to occur at the location of the clamps for each of the modes as the motion at this point is restricted.

	Mode 1	Mode 2	Mode 3
Original FE GN bat	0.57	0.19, 0.59	0.13, 0.31, 0.6
Modified FE GN bat	0.46	0.15, 0.48	0.12, 0.26, 0.48

Table 14.9: Node locations (metres) for original and modified FE GN bats.

Table 14.9 shows the location of the nodes for each mode for the original and modified GN bats. The differences in node locations are initially due to the differences in the length of the blade. There is little difference (max 0.035m) in the location of the bottom node regardless of the mode, which is positioned closest the thickest region of the bat.

14.4.2.5 Location of the COP.

In chapter 3, an equation was proposed to establish the location of the COP by including the variations in the geometry of the bat. As a close correlation between the experimental results and those mathematically established was reported earlier, this method will be applied to the

modified GN bat. The location of the COP can now be established, along with whether the modifications to the dimensions of the bat have influenced its location (Table 14.10).

Portion	r (mm)	V (mm^3)	ρvr (mm^4)	ρvr^2
1	158.2	2.88E+05	1.61E+10	0.255E+13
2	478	4.20E+05	6.88E+10	3.29E+13
3	400	17.7E+05	27.6E+10	11.0E+13
4	606	1.46E+05	3.03E+10	1.84E+13
5	691	2.66E+05	6.30E+10	4.35E+13
Sum (Σ)		28.9E+05	45.4E+10	20.8E+13

Table 14.10: Calculated values for each variable of each portion of the modified cricket bat.

Therefore,

$$q = \frac{\Sigma vr^2}{\Sigma vr} = \frac{20.8E+13}{0.0454E+13}$$

q = 0.462m

Therefore, if the axis of rotation (centre of the handle) is 0.641m from the free end (due to the reduction in bat length), the location of the calculated COP is 0.179mm from the free end (0.641-0.462).

14.4.3 Discussion of performance improvements.

This section will discuss each of the examined variables, identifying which factors would have the greatest influence upon the performance of the bat and player comfort. It is important to remember that the bat was rigidly clamped, although as this method excludes the actions of the handle, the exact effects of structural alterations on bat responses can be established. However, it is not possible to suggest the exact effects that the dimension changes would have had on a hand held bat, although it can be proposed.

Initially the moment of inertia was calculated and verified using the experimental results from chapter 8. The modified GN bat had a lower moment of inertia than its original counterpart.

This is predominantly due to the reduction in length as the distance between the axis of rotation and the radius of gyration (thickest region) is reduced. Following this modification, a player would consider the bat to feel slightly lighter during the preparation for impact and might find improved control and manoeuvrability during the swing. Therefore, this should enable the player to impact the thickest region more regularly, thus maximising the potential to hit the ball further. A lower moment also enables a player to swing the bat faster as the resistance to acceleration is reduced, therefore maximising the post impact ball velocity.

The magnitude of deflection and the stiffness of individual positions along the length of the blade were calculated. The original GN bat deflected 0.0264m further than the modified GN bat. Primarily, this is due to the reduction in the length, as earlier in this chapter it was found that a bat of this length would deflect 0.0210m less than the original length. The remaining reduction in deflection (0.0054m) is mainly caused by the increase in the thickness, as the removal of the scoops were found to have little effect on the deflection. The modified GN bat maintained a higher stiffness than the experimental GN bat until 0.3m from the free end.

In chapter 11.2, a stiffness range of between 5000 and 12000N/m maintained the bat's COR above 4, while the optimum stiffness was 6850N/m, which increased the COR to approximately 4.4. The modified GN bat's stiffness is between these optimum boundaries until 0.36m from the free end, therefore the COR would be above 4 following impacts up to this position. As the stiffness is maintained and does not significantly decrease at 0.06m from the free end as found from the experimental analysis, it is unlikely that the modified GN bat would have a dead spot. Therefore, the COR would not be significantly reduced at this position and so the player would be able to take advantage of the greater velocity at this position, thus further maximising the post impact velocity. The position of maximum COR would occur 0.2m from the free end, which is above (0.04m) the position of preferred impact (0.16m), although this is within the thickest region of the bat. Due to the raised location, this position is less likely to be impacted by the player. However, as the COR remains above 4 for much of the bat, any improvements following an impact at the position of maximum COR would not be so noticeable. This is a considerable benefit as a player would no longer have to impact a specific position, they could almost maximise the post impact ball velocity as long as the impact was below 0.36m from the free end.

Using the previously solved FE models, it is possible to establish which of the three alterations (length, thickness and scoops) had the greatest influence on the vibrations of the modified GN bat. The first mode was found to increase by 15.7Hz following the changes to the dimensions. A rise of almost 7Hz is due to the reduction in the length of the blade, while an increase of 5Hz can be attributed to the increase in the blade thickness and the remaining is due to the removal of the scoops from the back of blade (approx 3.7Hz). The thickness had the greatest effect on the second mode as the frequency was found to rise by 150Hz, while an increase of 50Hz was caused by the reduction in length and an increase of 25Hz was due to the scoop's removal. The third mode was raised above the excitation spectrum of 1kHz following the structural changes. Therefore, a player would feel an improvement in the comfort following impact, as this mode would not be experienced. However, an increase in the frequency of the other modes may lead to a reduction in control and comfort as found during racket studies (eg. Brody, 1981). It has been found that the sound of a higher frequency vibration often gives a player the impression of improved comfort (Hocknell *et al.* 1996). It is also unclear whether a player would feel an improvement in comfort following this increase in the vibrational frequencies as the amplitude of the third mode is so small.

The node locations for each of the excited modes were also established, and a node was positioned at the clamps due to the handles being unable to move. This is an error caused by the clamping method, although the results are comparable within this FE study as the locations were maintained throughout the different structural modifications. Although the third mode would no longer be felt by the player, the node and anti nodes locations are important as they will affect the amount of energy transferred to the ball regardless of player comfort. An anti-node of the third mode is located at the thickest region, thus energy will be transferred to this mode. Even though the player would not feel any discomfort, they might notice a reduction in post impact ball velocity if this position is impacted.

An anti-node of the first mode occurs at the bottom of the bat, therefore it would be advisable for the player to avoid impacting this location as much of the energy would be transferred into propagating this mode rather than being transferred to the ball. Due to the constraints of the handle in the rigid clamps, the location of the first mode within the blade of the bat does not appear. However, there was a migration of the nodes towards the bottom of the bat with this new model when compared to the experimentally clamped GN bat. It can be hypothesised that the same would occur for the nodes during hand held conditions, with the node moving from

0.3m to between 0.27 and 0.28m from the free end, (based upon the movements from clamped FE and experimental results). If the node was relocated, it would increase the chances of a player impacting this position and experiencing the improved comfort and increased post impact ball velocity that would be associated with minimising this first mode. A node of the second mode occurred close (0.01m) to the thickest position of the bat. If an impact occurred at this location, this mode would also be reduced and thus further improvements to comfort and post impact ball velocity would be experienced as the energy is transferred to the ball. As the higher frequencies have been reported to cause increased discomfort, it may be beneficial for the player to impact the node of the second mode rather than the node of the first mode. Therefore under these bat conditions, the discomfort related to the high frequencies of the second and third modes would not be felt

It was also possible to locate the COP on the modified GN bat, which was 0.179m from the free end. The location of the COP during the experimental investigations was 0.18m from the free end. Therefore by shortening the length of the bat, the COP has only moved 0.001m away from the hands (clamps). Figure 14.37 illustrates this finding and also includes the location of maximum COR.

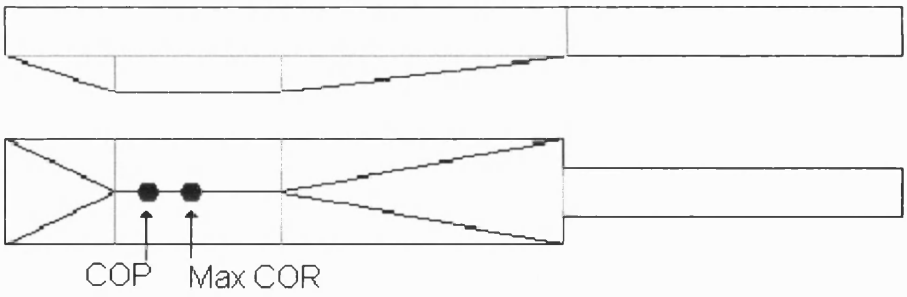

Figure 14.37: Location of COP and maximum COR on the modified GN bat.

From Figure 14.37 it can be seen that the COP is 0.021m below the location of estimated maximum COR (0.2m), although the COP is still within the thickest section of the bat. A player is more likely to impact this location as they aim for the position where the bat is the thickest. The location of the COP and COR have been separated compared to the experimental results, due to the dimension changes, thus losing the advantage of the convergence of these two points. However, the distance between the COP and COR is less than the width of a ball, therefore a player would still experience the benefits of both, although they are no longer at exactly the same location.

14.4.4 Conclusion.

This chapter constructed a representative model of an experimentally analysed cricket bat to establish the effects of dimension changes. Following the analysis of the results, a modified GN shape was established that took advantage of beneficial structural changes. It was proposed that using a modified bat shape, an increase in the post impact velocity and the vibrational frequencies would be achieved while the player would also feel an improvement in comfort. It was also found that the COP and COR were no longer at the same location, although the distance between them was such that a ball could still impact both sweet spot locations simultaneously. Therefore, it can be concluded that the selection of these variables and subsequent alterations to the dimensions produce an improved cricket bat.

15 CONCLUSIONS.

The main objectives of this thesis were to experimentally and theoretically analyse cricket bat responses, discover the locations of the sweet spots and establish how alterations to the design could improve performance and comfort. This has been achieved and has enabled certain conclusions to be drawn.

- Using material selection diagrams, willow was found to be the ideal material for cricket bat construction due to its overall superior material properties when compared to other wood species.

- Handle construction was found to have an influence on flexural stiffness and increased flexibility reduced hand loads and the vibrational frequency, thus improving perceived comfort.

- Static deflection was found to increase following the removal of sections from the back of the bat.

- The location of the COP was found to be 0.18m from the free end and was unaffected by structural design or impact speed. The benefits of the COP could be maximised following the use of a wide grip or with a bat of reduced stiffness.

- The position of maximum COR was located 0.2m from the free end and was not influenced by structural design or impact speed. The COR could be increased with a wide grip and a bat that exhibited limited deflection during ball contact.

- The lowest nodes of the first three excited modes were located 0.3m, 0.18m and 0.12m respectively from the free end. Only the third mode was found to be affected by the structural design, although clamping type had a considerable affect on node and anti-node positions for all of the excited modes.

- The location of the COP and COR were found to correlate and the position of the node of the first mode was proposed to cause the elongation of the high COR measured along the face of the bat.

- An FE model was constructed, which represented an experimentally analysed bat to establish the influence of structural design changes. It was proposed that a cricket bat

should be 0.08m shorter, 22% thicker and without scoops to maximise player comfort and post impact performance.

16 FUTURE WORK.

During this study there were various limitations and restrictions that inhibited a full analysis of the ball and bat interaction. It is the aim of this section to outline the areas that this study would prefer to investigate, in addition to and to substantiate the results that have been discussed.

16.1 Experimental analysis.

- Investigate the responses of the bats over a greater range of the ball impact speeds,
- Establish the influence of ball spin and off centre impacts on bat responses,
- Increase the number of human subjects to ensure representative data was displayed,
- Investigate other factors (including sound) that have an effect on subject perception,
- Calculate the distribution of the impact loads across the whole of the players hands to identify the exact COP location,
- Further develop the hand simulator.

16.2 Finite element analysis.

- Develop a computer model of the ball,
- Carry out dynamic modelling of the ball and bat interaction,
- Analyse handle responses during ball impacts,
- Develop a clamping method that replicates hand held impacts,
- Use orthotropic materials to closely represent the bat and balls properties.

17 REFERENCES.

Adair, R., K. (1998). Comment on "The sweet spot of a baseball bat", by Rod Cross. American Journal of Physics, 66, 9, 772-779.

Adair, R., K. (1995). The physics of baseball. Physics Today, 48, 26-31.

Annett, J. (2002). Subjective rating scales: science or art? Ergonomics, 45, 14, 966-987.

Ansell, M., P. (2004). Material selection lecture notes. Bath University.

Ansys (1997). Modelling and meshing guide. Second Edition. SAS; USA.

Ashby, M., F (1999). Materials selection in mechanical design. Second Edition. Butterworth Heinemann; Oxford.

Ashby, M., F & Jones, D., R. (1996). Engineering materials. Butterworth Heinemann; Oxford.

Baker, J., A., W., & Putnam, C., A. (1979). Tennis racket and ball responses during impact under clamped and freestanding conditions, Research Quarterly Exercise sport, 50, 164-170.

Bartlett, M. (2000). Game, set and match, without the crunch. Materials World, 8, 6, 15-16.

Barty-King, H. (1979). Quilt winders and pod shavers. MacDonald and James Publishers Ltd; London.

Beak, S., Davids, K., & Bennett, S. (2000). One size fits all? Sensitivity to moment of inertia information from tennis rackets in children and adults. In, Subic, A., and Haake, S., J. (Ed). The Engineering of Sport. Balkema; Rotterdam.

Borg, G. (1970). Perceived exertion as an indicator of somatic stress. Scandinavian Journal of Rehabilitation Medicine, 2, 92-98.

Britannica (2003). Online encyclopaedia. www.britannica.com.

British Standard (1967). BS 1902 : Part 1C, Section 10. Determination of Porosity and Density.

Brody, H. (2002). An overview of racket technology. Unpublished report courtesy of the International Tennis Federation Technical Centre Library.

Brody, H. (2000). Player sensitivity to the moments of inertia of a tennis racket. Sports Engineering, 3, 145-148.

Brody, H. (1997). The physics of tennis. III. The ball-racket interaction. American Journal of Physics, 65, 981-987.

Brody, H. (1995). How would a physicist design a tennis racket? Physics Today, 48, 26-31.

Brody, H. (1987). Tennis science for tennis players. University of Pennsylvania Press.

Brody, H. (1986). The sweet spot of a baseball bat. American Journal of Physics, 54, 640-643.

Brody, H. (1985). The moment of inertia of a tennis racket. The Physics Teacher, 23, 213-216.

Brody, H. (1981). Physics of the tennis racket II: The "sweet spot". American Journal of Physics, 49, 816-819.

Brody, H. (1979). Physics of the tennis racket. American Journal of Physics, 47, 482-487.

Bryant, F., O., Burkett, L., N., Chen., S., S., Krahenbuhl., G., S., & Lu.,P. (1977). Dynamic and performance characteristics of baseball bats. Research Quarterly, 48, 143-151.

Callister, W., D. (1994). Materials science and engineering, an introduction. Third Edition, John Wiley and Sons, Canada.

Casolo, F., & Ruggieri, G. (1991). Dynamic analysis of ball-racket impact in the game of tennis. Meccanica, 26, 67-73.

Chang, D., C., & Cutkosky, M., R (1995). Rolling with deformable fingertips. Presented at the IEEE/RSJ, International Conference in Intelligent Robots and Systems, Pittsburgh, PA, USA.

Clifford, N. (1957). Timber identification; for the builder and architect. Leonard Hill; London.

Cricket information. (2001). http://www.infoplease.com/ce6/sports/A0857624.html

Crisco, J., J., Greenwald, R., M., Penna, L., H., & Saul, K., R. (2000). On measuring the performance of wood baseball bats. In, Subic, A., and Haake, S., J. (Ed). The Engineering of Sport. Balkema; Rotterdam.

Cross, R. (2001a). Customising a tennis racket by adding weights. Sports Engineering, 4, 1-14.

Cross, R. (2001c). Response to "Comment on 'The sweet spot of a baseball bat'". American Journal of Physics, 69, 2, 229-230.

Cross, R. (1999b). Impact of a ball with a bat or racket. American Journal of Physics, 67, 692-702.

Cross, R. (1998a). The sweet spots of a tennis racquet. Sports Engineering, 1, 63-78.

Cross, R. (1998b). The sweet spot of a baseball bat. American Journal of Physics, 66, 772-779.

Cross, R. (1998c). Tennis Racquet Physics.

http://www.physics.usyd.edu.au/~cross/tennis.html

Cross, R. (1997). The dead spot of a tennis racket. American Journal of Physics, 65, 754-764.

Collyer, D. (1993). An engineering study of the cricket bat. Unpublished Final Year Project. Bolton Institute of Higher Education.

Daish, C., B. (1972). The physics of ball games. The English University Press Ltd, London.

Day, B. (1991). The Mail on Sunday, Ill-wind in the willows.

Den Hartog, J., P. (1985). Mechanical vibrations. Dover publications; New York.

Dinwoodie, J., M. (2000). Timber: Its nature and behaviour. Second Edition. E & FN Spon; London.

Dinwoodie, J., M. (1989). Wood, Nature's cellular, polymeric fibre-composite. The Institute of Metals; London.

Doren, V., G. (2003). Engineering material properties. www.apo.nmsu.edu.

Druschky, K., Lang, E., Hummel, C., Kalternhauser, M., Kohlloffle, L., Neundorfer, B., & Stefan, H. (2000). Pain-related somatosensory evoked magnetic fields induced by controlled ballistic mechanical impacts. Journal of Clinical Neurophysiology, 17, 6, 613-622.

ECB (2000). The laws of cricket, 2000 code.

http://www.cricket.org/link_to_database/NATIONAL/ENG

Edlin, H., L. (1973). Woodland crafts in Britain. Second Edition, Batsford Ltd; London.

Elliott, B. (1982). The influence of tennis racket flexibility and string tension on rebound velocity following a dynamic impact. Research Quarterly for Exercise and Sport, 53, 277-281.

Farmer, R., H. (Ed). (1981). Handbook of hardwoods. Second Edition. Her Majesty's Stationary Office; London.

Fertis, D., G. (1973). Dynamics and Vibration of Structures. Wiley & Sons; London.

Ferguson, D. (1992). Cricket, technique, tactics, training. The Crowood Press Ltd; London.

Findlay, W., P., K. (1975). Timber : Properties and uses. Crosby Lockwood Staples; London.

Fisher hand made cricket bats. (2001). http://www.fisherbats.com.

Fisher, S & Vogwell, J. (2003a). The effect of impact location on hand loads as experienced during ball and bat impact. Proceedings of the 2nd World Congress of Science and Medicine in Cricket, South Africa, 143-151.

Fisher, S & Vogwell, J. (2003b). The importance of grip pressure on vibrational frequency and nodal sweet spot location in cricket bats. Journal of Sports Engineering. Pending editorial changes.

Fisher, S. (2001). Soft tissue motion of the lower limb during drop landing of different impact severity. Masters Thesis. Liverpool John Moores University.

Fisher, S., Lake, M., J. and Coyles, V. R. (2001). Determining the presence of lower limb 'muscle tuning' during controlled drop landings of different impact severity. Proceedings of the First International Conference on Biomechanics of the Lower Limb in Health, Disease and Rehabilitation. Salford, UK, 14-15.

Fleisig, G.,S., Zheng, N., Stodden, D., F., & Andrews, J., R. (2002). Relationship between bat mass and ball properties and bat velocity. Sports Engineering, 5, 1-8.

Forest Products Society (1999). Wood Handbook, Wood as an Engineering Material. Forest Products Laboratory; USA.

Gere, J., M., & Timoshenko, S., P. (1997). Mechanics of materials. Fourth Edition, PWS Publishing; London.

Grabiner, M., Groppel, J., & Campbell, K. (1983). Resulting tennis ball velocity as a function of off-centre impact and grip firmness. Medicine Science Sports and Exercise, 15, 542-544.

Grant, C. (1998a). The role of materials in the design of an improved cricket bat. Materials Research Society Bulletin, 50-53.

Grant, C. (1998b). Design of a better cricket bat. Materials Research Society Bulletin: Advanced Materials in Sports & Leisure Equipment.

Grant, C., & Davidson, R., A. (1998). Design of a cricket bat test machine. In, Haake, S., J. (Ed). The Engineering of Sport. Balkema; Rotterdam.

Grant, C., Anderson, A., & Anderson, J., M. (1998). Cricket ball swing – the Cooke-Lyttleton theory revisited. In, Haake, S., J. (Ed). The Engineering of Sport. Balkema; Rotterdam.

Grant, C., & Paisley, P. (1997). Raising the game through modelling. Proceedings of the Fourth International Conference on Composite Engineering, Hawaii, USA.

Grant, C. (1996). Improved dynamic performance of a bat. Proceedings of the Third International Conference on Composites Engineering, New Orleans, LA.

Grant, C., & Nixon, S., A. (1996a). Parametric modelling of the dynamic performance of a cricket bat. In, Haake, S., J. (Ed). The Engineering of Sport. Balkema; Rotterdam.

Grant, C., & Nixon, S., A. (1996b). The effect of microstructure on the impact dynamics of a cricket bat. In, Haake, S., J. (Ed). The Engineering of Sport. Balkema; Rotterdam.

Grant, C., & Thethi, P. (1994). Impact mechanics of bat and ball. In, Recent Advances in Experimental Mechanics. Silva Gomes et al. (Eds). Balkema, Rotterdam.

Goldsmith, W. (1960 & 1991). Impact theory: Physical behaviour of colliding solids. Arnold Ltd; London

Gorman, D., J. (1975). Free vibration analysis of rectangular plates. John Wiley and Sons, USA.

Gough, W., Richards, J., P., G., & Williams, R., P. (1983). Vibrations and waves. John Wiley and Sons; USA.

Greenspan, J., D., & McGillis, S., L., B. (1990). Stimulus features relevant to the perception of sharpness and mechanical pain. Society for Neuroscience, 16, 1, 701.

Gunn & Moore. (2001). http://www.cricket.org/link_to_database/NATIONAL/ENG/

COMPETITIONS/GM/ BATMAKING.html

Harvey, K., Ansell, M., P., Mettem, C., J., Bainbridge, R., J., & Alexandre, N. (2000). Bonded-in pultrusions for moment-resisting timber connections. Proceedings from the International Council for Research and Innovation in Building and Construction. Working commission, W18 – Timber structures. Delft, Netherlands.

Hatze, H. (1998). The centre of percussion of tennis rackets: a concept of limited applicability. Sports Engineering, 1, 3-16.

Hatze, H. (1994). Impact probability distribution, sweet spot, and the concept of an effective power region in tennis rackets. Journal of Applied Biomechanics, 10, 1, 43-50.

Hatze, H. (1993). The relationship between the coefficient of restitution and energy losses in tennis rackets. Journal of Applied Biomechanics, 9, 124-142.

Hatze, H. (1992b). Objective biomechanical determination of tennis racket properties. International Journal of Sports Biomechanics, 8, 275-287.

Hatze, H. (1976). Forces and duration of impact and grip tightness during the tennis stroke. Medicine and Science in Sports, 8, 88-95.

Hearn, E., J. (1995). Mechanics of materials 1, an introduction to the mechanics of elastic and plastic deformation of solids and structural materials. Third Edition. Butterworth Heinemann; Oxford.

He, J., & Li, Y., Q. (1995). Relocation of anti-resonance of a vibratory system by local structural changes. Modal analysis: The International Journal of Analytical and Experimental Modal Analysis. 10, 4, 224-235.

Hennig, E., M., Valiant, G., A., & Liu, Q. (1996). Biomechanical variables and perception of cushioning for running in various types of footwear.

Hocknell, A., Jones, R., & Rothberg, S. (1996). Engineering 'feel' in the design of golf clubs. In, Haake, S., J. (Ed). The Engineering of Sport. Balkema; Rotterdam.

International Cricket Council (ICC) (2002).

http://www.cricket.org/link_to_database/NATIONAL/ICC/

Ivanov, A., P. (1995). The problem of the centre of percussion. PMM, Journal of Applied Mathematics and Mechanics, 59, 1, 151-153.

John, S., & Li, Z., B. (2002). Multi-directional vibration analysis of cricket bats. In, Subic, A., and Haake, S., J. (Ed). The Engineering of Sport. Balkema; Rotterdam.

Kandel, E., R., Schwartz, H., J., & Jessell, T., M. (2000). Principles of Neural Science. Fourth Edition. McGraw-Hill; London.

Kawazoe, Y. (1993). Coefficient of restitution between a ball and a tennis racket. Theoretical and Applied Mechanics, 42, 197-208.

Kimmeskamp, S., Milani, T., L., & Hennig, E., M. (1998). Relationships between perception scores and biomechanical variables for running in different footwear constructions. Proceedings of the North American Congress on Biomechanics (NACOB 98). University of Waterloo; Canada.

King Liu, Y. (1983). Mechanical analysis of racket and ball during impact. Medicine and Science in Sports and Exercise, 15, 5, 388-392.

Kirkpatrick, P. (1963). Batting the ball. American Journal of Physics, 31, 606-613.

Knowles, S., Mather, J., S., B., & Brooks, R. (1996). Cricket bat design and analysis through impact vibration modelling. In, Haake, S., J. (Ed). The Engineering of Sport. Balkema; Rotterdam.

Knudson, D., V. (1991a). Factors affecting force loading on the hand in the tennis forehand. The Journal of Sports Medicine and Physical Fitness, 31, 4, 527-531.

Knudson, D., V. (1991b). Forces on the hand in the tennis one-handed backhand. International Journal of Sport Biomechanics, 7, 282-292.

Knudson, D., V., & White, S.,C. (1989). Forces on the hand in the tennis forehand drive: Application of force sensing resistors. International Journal of Sport Biomechanics, 5, 324-331.

Koike, S., Fujii, N., Ae, M., Kobayashi, S., Kimura, H., & Takahashi, K. (2002). Estimation of forces and moments exerted on a baseball bat by hands using an instrumented bat. Proceedings of the International Sports Engineering Conference, Tokyo, Japan.

Kotze, J., Mitchell., S., R, & Rothberg, S., J. (2000). The role of the racket in high – speed tennis serves. Sports Engineering, 3, 67-84.

Kreifeldt, J., G., & Chuang, M., C. (1979). Moment of inertia: Psychophysical study of an overlooked sensation. Science, 206, 588-590.

Kreighbaum, E., F., & Smith, M., A. (1996). Sports & fitness equipment design. Human Kinetics; Champaign, USA.

Laver & Wood. Handmade cricket bats. (2001).

http://www.laverwood.co.nz

Lavers, G., M. (1969) & (1983). The strength properties of timbers. Her Majesty's Stationary Office; London.

Liu, Y. (1983). Mechanical analysis of racquet and ball during impact. Medicine and Science in Sports and Exercise, 15, 5, 388-392.

McCutchen, W. (2002). Coefficient of Restitution.

http://www.racquetresearch.com/coeffici.htm

Milani, T., L., Hennig, E., M., & Lafortune, M., A. (1998). Perceptual and biomechanical variables for running in identical shoe constructions with varying midsole hardness. Clinical Biomechanics, 12, 5, 294-300.

Mitchell, S., Jones, R., & Kotze, J. (2000a). The influence of racket moment of inertia during the tennis serve: 3-dimensional analysis. In, Subic, A., and Haake, S., J. (Ed). The Engineering of Sport. Balkema; Rotterdam.

Mitchell, S., Jones, R., & King, M. (2000b). Head speed vs racket inertia in the tennis serve. Sports Engineering, 3, 99-110.

MMS Sport. (2001). Composite cricket bats. http://www.mmsbats.co.za

Naß, D., Hennig, E., & Schnabel, G. (1998). Ball impact location on a tennis racket head and its influence on ball speed, arm shock and vibration. Proceedings of the XVI International Symposium on Biomechanics in Sport, Konstanz, Germany. Riehle, H., J., & Vieten, M., M. (Eds), 229-232.

Nash, W., A. (1972). Schaum's outline of theory and problems of strength of materials. McGraw-Hill; London.

Naruo, T., Sato, F. (1998). An experimental study of baseball bat performance. In, Haake, S., J. (Ed). The Engineering of Sport. Balkema; Rotterdam.

Noble, L., & Eck, J. (1985). Effects of selected softball bat loading strategies on impact reaction impulse. Medicine and Science in Sports and Exercise,18, 50-59.

Noble, L. (1985). Emperical determination of the centre of percussion axis of softball and baseball bats. In Winter, D.,A., Norman., R.,W., Wells., R., P., Hayes., K., C., & Patla., A., E (eds). Biomechanics ix-b, 561-520. Champaign, IL, Human Kinetics.

Penrose, J., M., & Hose, D., R. (1998). Finite element impact analysis of a flexible cricket bat for design optimisation. In, Haake, S., J. (Ed). The Engineering of Sport. Balkema; Rotterdam.

Plagenhoef, S. (1971). Patterns of human motion. 61-63, 71. Prentice-hall, Englewood Cliffs.

Plagenhoef, S. (1970). Fundamentals of tennis. Prentice- Hall, Englewood Cliffs, New Jersey.

Reynolds, D., D., Standlee, K., G., & Angevine, E., N. (1977). Hand-Arm Vibration, Part III: Subjective response characteristics of individuals to hand-induced vibration. Journal of Sound and Vibration, 51, 2, 267-282.

Robbins, S., E., & Gouw, G., J. (1991). Athletic footwear: unsafe due to perceptual illusions. Medicine and Science in Sports and Exercise, 23, 2, 217-224.

Roberts, J., R., Jones, R., & Rothberg, S., J. (2001). Measurement of contact time in short duration sports ball impacts: an experimental method and correlation with the perceptions of elite golfers. Sports Engineering, 4, 191-203.

Roberts, J., R., Jones, R., Mansfield, N., J., & Rothberg, S., J. (2005a). Evaluation of vibrotactile sensations in the 'feel' of a golf shot. Journal of Sound and Vibration, 285, 303-319.

Roberts, J., R., Jones, R., Mansfield, N., J., & Rothberg, S., J. (2005b). Evaluation of impact sound on the 'feel' of a golf shot. Journal of Sound and Vibration, 287, 651-666.

Salix cricket bat company. (2001).

http://www.cricketer.com/salix/index.html

Sayers, A., Koumarakis, T., & Sobey, S. (2000). Surface hardness of cricket bats following 'knocking-in'. In, Subic, A., and Haake, S., J. (Ed). The Engineering of Sport. Balkema; Rotterdam.

Slazenger cricket bat information. (2001).

http://www.Slazenger.co.uk

Smith, L., V. (2001). Evaluating baseball bat performance. Sports Engineering, 4, 205-214.

Sportsmans Warehouse (2001). Cricket bat care and maintenance.

http://www.Isw.co.za/h-crcare.htm

Steidel, R., F. (1980). An introduction to mechanical vibrations. Wiley & Sons; London.

Stevens, J., C., & Mack, J., D. (1959). Scales of apparent force. Journal of Experimental Psychology, 58, 5, 405-413.

Sykes, K., Scott, A., E., Kewllett, D., W. (1971). The centre of percussion and its implications for sport. Research Papers in Physical Education, 2, 2, 36-40. Carnegie.

Thomson, W., T. (1965). Vibration theory and applications. George Allen & Unwin; London.

Timber Research and Development Association (1980). Timbers of the world. Volume 2. TRADA/ The Construction Press; Lancaster.

Titmuss, F., H. (1971). Commercial timbers of the world. Second Edition CRC Press; Ohio, USA.

Watanabe, T., Ikegami, Y., Miyashita, M. (1979). Tennis: the effects of grip firmness on ball velocity after impact. Medicine and Science in Sports, 11, 359-361.

Weber, E., H., Schuchmann, J., A., Albers, J., H., & Ortiz, J. (2000). A prospective blinded evaluation of nerve conduction velocity versus pressure-specified sensory testing in carpal tunnel syndrome. Annals of Plastic Surgery, 45, 3, 252-257.

Wegst, U., G. (1996). The mechanical performance of natural materials. Ph.D thesis. University of Cambridge.

Wegst, U., G., & Ashby, M., F. (1996). Materials selection for sports equipment. In, Haake, S., J. (Ed). The Engineering of Sport. Balkema; Rotterdam.

Weyrich, A., S., Messier., S., P., Ruhmann, B., S., & Berry, M., J. (1989). Effects of bat composition, grip firmness, and impact location on post impact ball velocity. Medicine and Science in Sports and Exercise, 21, 199-205.

Wilson, J., F., & Davis, J., S. (1995). Tennis racket shock mitigation experiments. Journal of Biomechanical Engineering – Transactions of the ASME, 117, 4, 479-484.

Wood, G., A., & Dawson, M. (1977). Physical properties of cricket bats and their implications for hitting. Sports Coach, 1, 28-34.

Wynne-Thomas, P. (1997). The history of cricket; From the weald to the world. The Stationary Office; London.